The University Of Sheffield.

The Role and Regulation of Semaphorin 3B in Breast Cancer Progression

Nashwa Talaat Shesha

A thesis submitted in partial fulfilment of the requirements for the degree of Doctor of Philosophy
October 2019

The University of Sheffield
Faculty of Medicine, Dentistry and Health
School of Medicine

Academic Unit of Oncology & Metabolism

Dedication

Mr. Talaat Shesha (1951-2018)

A great father and a true leader

I will follow your steps through the road you have enlighten me until we meet.

Mrs. Ibtisam Zamzami

First teacher and beloved mother

I am strong woman because a strong woman raised me

Acknowledgments

First and Foremost praise is to **ALLAH**, the Almighty, the greatest of all, for giving me strength, determination and opportunity to undertake this research study.

I would like then to thank my supervisor *Dr. Carolyn Staton* I greatly appreciate her time, guidance, suggestions and patience in the scientific and editorial review during the entire period of my PhD.

I am obliged to my second supervisor *Professor. Nicola Brown* for her suggestions and help in manuscript review throughout my thesis.

I would like to thank *Dr. Daas Amdi* for his help in the proofreading during the writing up stage of this thesis. Thank you to my friends *Dr. Aisha Mukktar* for being very supportive and encouraging. She was a true friend with kind heart.

I also express my thanks to all people I worked with in our lab during the last four years. Thank you to *Dr. Mohammed Alfawaz* for his guidance and orientation in endnotes software and, technical advices and laboratory techniques support. Thank you to *Dr. Mohammed Ridha* and *Dr. Haider Aljanabi* for their help in qPCR settings. Thank you for *Dr. Mohammed Aldoghim* and *Dr. Tariq Abed* for their help in Western blot experimental setup and support. I've been lucky to make many friends over the course of my PhD and I want to thank them all for all their supports

Special thanks go to my Dad my one and only *Talaat Shesha* who passed away amid journey of my PhD. He was my inspirer, supporter and dream sharer. His supportive words will lead me along for the rest of my life and he will not be forgotten.

Thank you to my lovely Mum *Ebtisam Zamzami*, without your support, encouragement and prayers. I couldn't make it alone, her shoulder was my home in hard times and will be forever. Thank you to my brothers and sisters *Ghadeer, Rayan, Raaed, Renad* and *Remas*, for being exceptional family with true warm feelings and prayers and I am proud to have them around. Also, I would like to thank my nephews and niece *Anas, Diala, Tamem* and *Solaf* for being in my life.

Thank you to the department of oncology and metabolism in the University of Sheffield for providing a supportive and stimulating work environment. Thank you to the Ministry of health, Kingdom of Saudi Arabia for sponsoring me for the PhD.

Abstract

Semaphorin 3B (SEMA3B) is an 83 kDa secreted protein of the semaphorin family which has recently been shown to play an important role in angiogenesis and tumour progression and is thought to act as a tumour suppressor. SEMA3B is located at a site of frequent allele loss in the early pathogenesis of breast cancer, and the full-length form of SEMA3B is thought to be cleaved by furin-like pro-protein convertases (PPCs), into an inactive 51 kDa fragment. However, the role and expression of SEMA3B in breast cancer remain unclear. This project, therefore, tests the hypothesis that PPCs cleavage of SEMA3B results in inactivation of SEMA3B in invasive breast cancer. In order to test the hypothesis the project used a series of breast cell-lines consisting of normal breast epithelial cells, pre-malignant, pre-invasive, invasive and metastatic cell-lines, as a model of breast cancer progression. SEMA3B and PPCs mRNA and protein expression were investigated in these cell-lines using qPCR and Western blotting, respectively. Immunohistochemistry was then performed on tissue microarray slides in a panel representing different stages of breast disease. In addition, the effect of full-length recombinant SEMA3B was assessed in cell based functional assays. Finally, two PPC inhibitors, namely decRVKR-CMK and alpha-1 antitrypsin Portland variant (α1-PDX) were used to inhibit PPC activity and potentially restore the active full-length SEMA3B in breast cancer cells. The data in this thesis show that SEMA3B gene and protein expression was detected in all cell-lines tested, with the highest level of gene expression seen in the normal MCF-10A cells. These cells were the only ones to express the full-length SEMA3B with all other cells only expressing cleaved SEMA3B, which is likely to be inactive. Treatment with full-length recombinant SEMA3B showed that this protein inhibited breast cancer cell growth, migration and invasion. PPCs analysis did not show a significant relationship with increasing malignancy of cell-line for either mRNA or protein expression, although all cell-lines expressed at least some PPCs. Histological analysis showed that SEMA3B expression was significantly reduced with increasing malignancy of lesion and correlated closely with the expression of many of the PPCs. Although the CMK inhibitor did not prevent cleavage of SEMA3B, the α1-PDX inhibitor partially restored full-length SEMA3B. These data suggest that full-length SEMA3B is a tumour suppressor in breast cancer, and that the PPCs may be involved in cleavage of SEMA3B to allow breast cancer progression. Further work is required to confirm the hypothesis and to see whether α1-PDX may be a potential future therapy for breast cancer.

Table of Contents

List of Figures

List of Tables

List of Abbreviations

%	Percentage
°C	Degrees centigrade.
µM	Micrometre
A	Amber
aa	Amino acid
ABC	Avidin-biotinylated enzyme complex
ADH	Atypical ductal hyperplasia
APS	Ammonium Persulfate
Arg	Arginine
ASN	Asparagine
ASP	Aspartic acid
ATP	Adenosine triphosphate
BRCA1, BRCA2	Breast Cancer Antigen 1 and 2
BSA	Bovine serum albumin
Ca+	Calcium
CBA	Cytometric Bead Array assay
cDNA	Complementary DNA
CHRD	Cysteine-histidine rich domain
CM	Conditioned medium
CMK	Decanoyl-RVKR-cmk
CO2	Carbon Dioxide
CRD	Cysteine rich domain
CRMP	Collapse response mediator protein
Ct	Threshold cycle
CTBs	Cytotrophoblasts
Cu2+	Cupric
Cys	Cysteine
DAB	3,3-Diaminobenzidine substrate
DCIS	Ductal carcinoma *in situ*
dH_2O	Deionised Water
DMEM	Dulbecco's Modified Eagle's Medium
DMEM/F12	Dulbecco's Modified Eagle Medium; Nutrient Mixture F-12
DMSO	Dimethyl Sulphoxide
DNA	Deoxyribonucleic acid
dNTP -	Deoxyribonucleotide triphosphate
DPBS	Dulbecco's Phosphate Buffered Saline
ECGS/H	Endothelial cell growth Supplement/ Heparin
ECL -	Chemiluminescence
ECM	Extracellular matrix
EDTA	Ethylenediamine tetraacetic acid
EGF	Epidermal growth factor
EGFR	Epidermal growth factor receptor
EHS	Engelbreth-Holm-Swarm

EMT	Epithelial-to-mesenchymal transition
ER	Endoplasmic reticulum
ER	Oestrogen receptor
FBS	Foetal Bovine Serum
g	Times gravity
g	Gram
GAP	GTPase activity protein
GAPDH	Glyceraldehyde-3-phosphate dehydrogenase gene
G-CSF	Granulocyte-colony stimulating factor
Glu	Glutamic acid
GM-CSF	Granulocyte-macrophage colony-stimulating factor
gp	Glycoprotein
GPI	Ghycophosphatidylinositol anchor
H_2O	Water
Hep-G2	Hepatocellular carcinoma cell line
HER2	Human epidermal growth factor 2
His	Histidine
HRP	Horseradish peroxidase
HUVEC	Human Umbilical Vein Endothelial Cells
IDL	Invasive ductal carcinoma
IFN-γ	Interferon gamma
IgG	Immunoglobulin G
IG	immunoglobulin
IgM	Immunoglobulin M
IHC	Immunohistochemistry
IL-10	Interleukin 10
IL-11	Interleukin 11
IL8	Interleukin 8
ILC	Invasive lobular carcinoma
IMS	Industrial methylated spirit
IPT/GP	Immunoglobulin-plexin-transcription factor /glycine-proline
IU	International unit
kDa	Kilo dalton
L1cam,	L1 Cell Adhesion Molecule
LCIS	Lobular carcinoma *in situ*
LDLR	Low-density lipoprotein receptor
LIMK1 and LIMK2 kinases	LIM kinase 1 and LIM kinase 2
Log	Logarithm
Lys	Lysine
M	Molar
MAM	Meprin, A-5 protein, and receptor protein-tyrosine phosphatase mu
MBTPS1-	Membrane-bound transcription factor site-1 protease
MCF-7	Michigan Cancer Foundation-7
MDA-MB-231	M.D. Anderson- Metastasis Breast cancer".

Mg	Milligram
ML	Millilitre
mM	Milimolar
MM9	Matrix metalloproteinase 9
MMPS	Metalloproteinases
mRNA	Messenger RNA
MTS	Tetrazolium salt (3-(4,5-dimethyl-2-yl)-5-(3-carboxymethoxyphenyl)-2-(4-sulfophenyl)-2H-tetrazolium)
NARC-1-	Neura apoptosis-regulated convertase-1
NC	Negative control
Ng	Nanogram
NP1	Neuropilin 1
NP2	Neuropilin 2
Nrcam	Neuronal Cell Adhesion Molecule
NSCLC	Non-small cell lung cancer
P13K	Phosphatidylinositol-3 kinase
p21	Tumour suppressor gene
p38-MAPK	p38 mitogen-activated protein kinases
p53	Tumour suppressor gene
PACAP	Pituitary adenylate cyclase activating polypeptide
PACE4	Paired basic amino acid-cleaving enzyme 4
PBS	Phosphate Buffer Saline
PC	Positive control
PCSK1	Pro-protein convertase 1
PCSK2	Pro-protein convertase 2
PCSK4	Pro-protein convertase 4
PCSK5	Pro-protein convertase 5
PCSK6	Pro-protein convertase 6
PCSK7	Pro-protein convertase 7
PCSK8	Pro-protein convertase 8
PCSK9	Pro-protein convertase 9
pg/ml	Picogram/millilitre
PIGF2	Placental Growth Factor
PPCs	Pro-protein convertases
Pro	Proline
ProIGFs-I and II	Proinsulin like growth factor
ProNT/NN	Pro-neurotensin/neuromedin N
PR	progesterone receptor
PSI	semaphorin and integrins domain
PVDF	Polyvinylidene fluoride membrane
PX	Pixel
q-RT-PCR	Quantitative real-time PCR
RBD	Rho-GTPase binding domain
rSEMA3B	Recombinant Human Semaphorin 3B Fc Chimera Protein, CF
RNA	Ribonucleic acid

RPMI-1640	Roswell Park Memorial Institute
RT	Room temperature
SCLC	Small cell lung carcinoma
SD	Standard deviation
SDS	Sodium Dodecyl Sulfate
SDS-PAGE	Sodium Dodecyl Sulfate Polyacrylamide Gel Electrophoresis.
SEMA3A	Semaphorin 3A
SEMA3B	Semaphorin 3B
SEMA3F	Semaphorin 3F
Ser	Serine
SIP	Site-1 proteases
SKI-1	Subtilisin kexin isoenzyme-1
TBS	Tris-buffered saline
TBST	Tris-buffered saline-tween
TCGA	The cancer genome atlas
TEMED	N,N,N',N'tetramethylethylenediamine
TGN	Trans-Golgi Network
TMAs -	Tissue microarrays (TMAs)
UH	Usual hyperplasia
UV	Ultra Violet
V/V	Volume/Volume
V	Volt
Val,	Valine
$VEGF_{145}$	Vascular endothelial growth factor-145
$VEGF_{165}$	Vascular endothelial growth factor-165
VEGFB	Vascular endothelial growth factor-B
VEGFE	Vascular endothelial growth factor-E
VEGF	Vascular endothelial growth factor
VEGFR	Vascular endothelial growth factor receptor
WB	Western blot
α1-PDX	α1-antitrypsin Portland
µg	Microgram

Chapter 1: Introduction

1.1 Breast anatomy

The breast is made up of a large fatty area that is connected to the underlying ribs via the pectoralis major muscle and connected to the rest of the breast via connective tissue. The functional part of the breast is made of several mammary glands, which consist of lobules of glandular tissue; known as alveoli, as well as the milk ducts which come together forming a lobe. Each lobe consists of secretary cells specialized in milk production, which will be subsequently secreted through the breast ducts. Each breast has 15-25 lobes that are dividing into smaller lobules and acini ending with ducts which open individually into the nipple. These lobules and ducts are supported by stromal tissue, which has fat, ligaments, nerves, arteries, veins, and lymphatics embedded into it (figure 1.1) (Jesinger, 2014). Breast growth in females is initiated at puberty in response to oestrogen and progesterone secretion. Any changes in these hormonal levels could interfere with the development of breast.

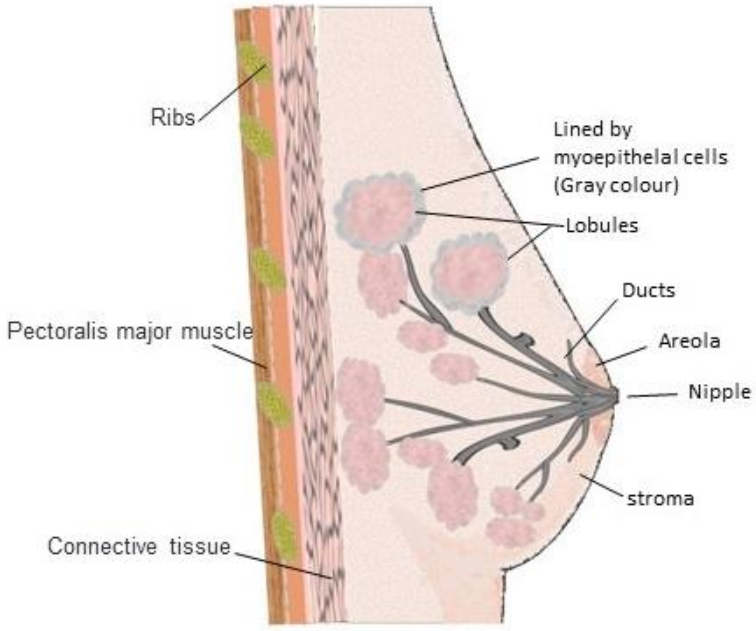

Figure 1.1: Schematic representation of the basic breast anatomy structure

1.2 Breast diseases

Breast disorders can be benign or malignant and it has been shown that benign changes in the breast may correlate with an increased risk for the development of breast cancer. Benign breast diseases are classified into non-proliferative changes, proliferative disease without atypia and proliferative disease with atypia (Guray and Sahin, 2006).

1.2.1. Non-proliferative epithelial lesions

Non-proliferative changes which are also known as fibrocystic changes and these include cysts, apocrine changes, adenosis which is characterised by increasing the number of small terminal ductules or acini that might be additionally associated with calcification, mild hyperplasia and fibroadenoma without complex features. The most frequently common change are cysts and fibrosis which are characterized by an increase in fibrous stroma due to dilatation of ducts and formation of cysts that vary in size. However, most of these lesions were not shown to have a link to subsequent development of breast cancer but in some rare cases they may be able to become malignant (Friedenreich et al., 2000, Guray and Sahin, 2006).

1.2.2 Proliferative disease without atypia

Proliferative breast diseases include florid hyperplasia, papilloma, radial scar and fibroadenoma with complex features (Schnitt, 2003). It has been found that proliferative change in the breast epithelial cells without atypia (atypia is abnormality in a cell structure), is associated with a 1.5 to 2 fold increase in risk of cancer development, particularly in the presence of other factors that could enhance it such as patient history, age and other environmental factors. As these cells did not show any signs of atypia but are characterized by faster growth rate than normal cells with a normal identical appearance to the normal cells and therefore they often described as usual hyperplasia of either the duct or lobule (Schnitt, 2003).

1.2.3 Proliferative disease with atypia

Similarly to usual hyperplasia, atypical hyperplasia shows increased growth of the epithelial cells and the cells look abnormal i.e. atypical. Atypical ductal hyperplasia and atypical lobular hyperplasia have been categorized as proliferative disease with atypia and show a 4-5 fold risk of becoming malignant. In spite of the wealth of studies suggesting an association between proliferative lesions with atypia and the risk of

development of breast cancer (Dupont et al., 1993), other studies, such as that by Fowble *et al* have found no significant influence of such risk factors for the later development of breast cancer (Fowble et al., 1998, Sasaki et al., 2018).

1.3 Morphology and progression of breast cancer

Normal human breast tissue consists of two layers of epithelial cells that line the lobules and ducts, the luminal epithelium and the myoepithelial layer. It is believed that the progression of breast cancer, which is a heterogeneous disease, is due to alterations in the luminal epithelial cells of the ducts and lobules. Cancer development is dependent on various factors, some of which also determine the type of breast cancer that the patient will present with. Breast cancer cells express a variety of different receptors and any alterations in their activity could cause changes in their progression (Allison, 2012). Oestrogen receptor (ER), progesterone receptor (PR), and human epidermal growth factor 2 receptor (HER2) are considered the most important receptors that correlate with breast cancer development. For instance, ER positive breast cancer is caused by an alteration in the expression of oestrogen receptors that induce a conformational change and uncontrolled binding to its ligand resulting in uncontrolled activation of the receptor and induced transcription of target genes resulting in uncontrolled proliferation. Just like ER, PR positive breast cancer results from uncontrolled activation of PR receptor and usually exists alongside ER positive breast cancer. HER2 positive breast cancer is caused by overexpression of HER2 receptor resulting in dysregulated HER2 signalling and target gene expression, again leading to increased proliferation of the cells. It is not uncommon to find patients exhibiting both PR and ER positive breast cancer and/or HER2 negative or positive receptor expression, however, a patient can develop breast cancer that is not related to these three receptors resulting in a triple negative breast cancer, giving rise to a disease with a complex genetic background (Eroles et al., 2012). Based on this, it is clear that not all breast cancers evolve in the same way and some types of breast cancer are more aggressive than others. So understanding the histopathological alterations and the different characteristics of breast cancer is important to develop strategies to prevent development and progression of breast cancer.

1.4 Breast cancer risk factors

Although the majority of breast cancers are sporadic and multifactorial, numerous breast cancer risk factors have been identified. Mutation in *BRCA1* and *BRCA2* genes are the most common factors that are strongly associated with a family history for developing breast cancer. These factors are involved in repair of DNA damage and when they are mutated increased mutations in the breast DNA result in the development of cancer (Balmana et al., 2011). Breast cancer is also attributed to other risk factors including reproductive factors, which are associated with the ER status. These factors included late menopause, early menarche, nulliparity and late age at first pregnancy, all of which increase the length of exposure to oestrogen (Sun et al., 2017). Furthermore, environmental and lifestyle factors also contribute to the incidence of breast cancer. For example, alcohol consumption can increase the risk of breast cancer by increasing the level of oestrogen-related hormones in the blood and stimulate the oestrogen receptor pathways (Jung et al., 2016). Obesity and too much dietary fat intake, smoking and environmental contaminations can also enhance the risk of DNA mutations and therefore increase the risk of breast cancer (Sun et al., 2017).

1.5 Epidemiology of breast cancer

Breast cancer is the most common form of cancer in the UK, even though it is rare in men due to smaller amounts of breast tissue. It therefore highly affects women, with a total of 55,122 cases reported in 2015, which accounts for about 30% of all recently diagnosed cancer cases (CRUK, 2015). Breast cancer is considered the second most common cause of cancer death in females in the UK with about 11,500 deaths in 2016, while in males with breast cancer there were 80 deaths in the same year (CRUK,2018). It is considered the leading cause of death among women globally. According to the world health organization, in 2018, the worldwide estimation of the number of breast cancer cases is about 11.6% of all cancers with breast cancer causing 6.6% of all deaths worldwide (WHO, 2019). Despite the fact that there are a large variety of different treatment measures, if not detected early, the prognosis of breast cancer remains poor and correlates with tumour metastasis (Rakha et al., 2007). That said, there has been an improvement in breast cancer mortality, which is attributable to a combination of improved screening programmes that facilitate early detection and availability of effective systemic adjuvant therapy. Recent improvement in the

knowledge of the molecular pathogenesis of breast cancer and its progression have led to the understanding of novel molecular pathways involved in the development of breast cancer resulting in development of target specific therapeutics. Since each patient has a varying genetic background, this necessitates the development of patient specific treatment and that could help to aid further reduction in breast cancer mortality.

1.6 Breast cancer histopathologic classification

Normal breast epithelial cells are surrounded by different proteins in the extracellular matrix which consists of proteins such as glycoproteins and collagen, which regulate cell-cell adhesion. Several factors, such as those described earlier in section 1.4, could directly or indirectly derail the normal processes and result in increased cell production of the normal breast epithelia resulting in hyperplasia (Koukoulis et al., 1991). As stated earlier, hyperplasia has been graded histologically into two types; usual hyperplasia (UH) which the duct filled with proliferating epithelial cells but with no atypia present and the cells look normal, and atypical ductal hyperplasia (ADH) which could become localized in the duct with distorted, abnormal cells. There is no evidence of neoplasia detected in UH (Page and Dupont, 1990). However, ADH is characterized by increasing nuclear pleomorphism, hyperchromatism and a uniformity arrangement and organization of cells within the breast duct, and some studies have suggested this could be considered as an indicator for developing breast cancer in the future (Page and Dupont, 1990). Indeed, one study found that patients with ADH had 5.3 times increased relative risk for developing breast cancer than patients with non-proliferative lesions. In addition, the family history and other risk factors may contribute to the development of breast cancer (Dupont and Page, 1985).

In a stepwise manner, ADH also have the potential to become ductal carcinoma *in situ* (DCIS), which is a non-invasive but premalignant type of breast cancer. DCIS can occur due to an abnormal proliferation of neoplastic epithelial cells. These cells are contained within the breast ducts and have not yet spread beyond the basement membrane (Simpson, 2009). DCIS may exhibit some tumour characteristics such as nuclear atypia and is also found to have carcinoma precursor cells which share similar genetic features with invasive carcinoma (Carraro et al., 2014). These could enhance the development of pre-invasive and pre-malignant lesions with subsequent progression of invasive breast cancer potential (Wellings and Jensen, 1973). ADH is

sometimes difficult to differentiate from DCIS. DCIS is characterised by a high nuclear grade with necrosis and debris. However, ADH can sometimes be distinguished from DCIS by cellular variability or clonality and nuclear overlap as ADH is usually made up of cells with low grade nuclei which are uniform and small (Lakhani et al., 1995, Pinder and Ellis, 2003).

The alteration in growth regulating pathways leading to an imbalance of proliferation and therefore increased cell growth are the major causes of developing DCIS and subsequently invasive breast cancer. The level of ER is found to be higher in many DCIS cells suggesting a role for this growth factor in breast cancer progression (Arpino et al., 2005). In addition to DCIS*,* other *in situ* carcinomas are also found such as lobular carcinoma *in situ* (LCIS), which refers to cancerous epithelial cells that accumulate within the lobules, and are contained within the lobular basement membrane. Importantly, when DCIS develops it can increase the risk of progression to invasive breast cancer, as one study found that 43% of the invasive breast cancers studied had been diagnosed earlier as DCIS by mammography (Leonard and Swain, 2004). Therefore, strategies to control DCIS by surgery or selective oestrogen modulation by Tamoxifen are used and can work effectively to prevent the subsequent development of aggressive breast cancer. However, not all DCIS cases will progress to invasive breast cancer leading to possible over treatment of patients, something that has become a major concern nowadays.

Invasive ductal carcinoma (IDC) accounts for about 86% of breast cancer cases, which is the highest percentage of all breast cancers and in this form, the cancer cells have developed in the milk ducts (as DCIS) and progressed to invade through the basement membrane into nearby tissues to become IDC (Arpino et al., 2004). It is characterized by the dissemination of cancer cells beyond the basement membrane of the ducts. In addition to IDC, invasive lobular carcinoma (ILC) accounts about 10% of invasive breast tumours (Arpino et al., 2004). ILC formation is often predicted by its risk factors, lobular neoplasia, which is comprised of LCIS, a monomorphic population of non-adhesive cells in the lobular duct and atypical lobular hyperplasia, in which there is accumulation of abnormal cells that can develop to form cancer cells.

Clinical investigations have illustrated that there are major differences between IDC and ILC. ILC are known to have a “single-file” growth pattern rather than forming a mass, are larger in size and less aggressive compared to IDC, and often ER and PR

positive (Tazaki et al., 2013, Engels et al., 2014). However, treatment modalities employed in both cases are similar with respect to systemic adjuvant therapy that considers histological grade, size of tumour, and hormone and growth factor receptor status (Engels et al., 2014). Thus, understanding the molecular pathways involved in breast cancer progression may be of more importance than histopathological studies, for development of effective therapeutic strategies (figure 1.2).

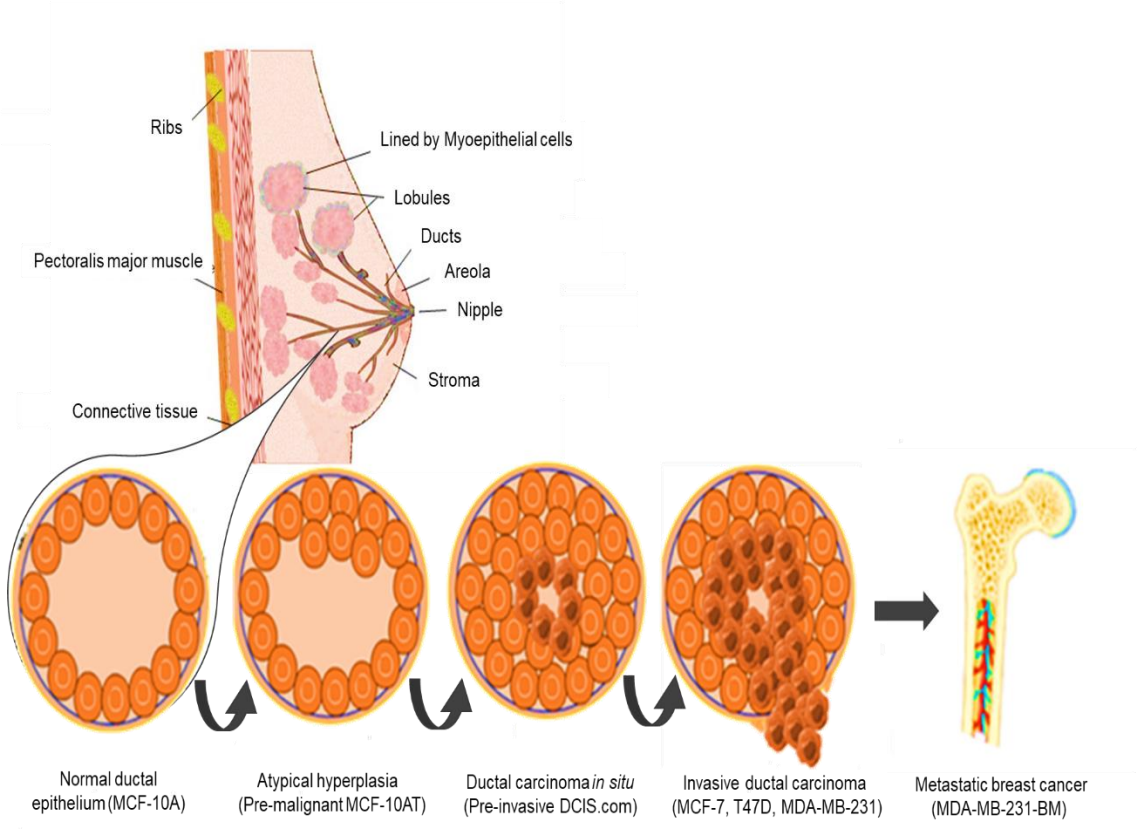

Figure 1.2: Model of breast cancer stages. The drawing shows a schematic illustration of the model of breast cancer evolution and cell-lines that reflect the different breast cancer stages. The terminal normal duct epithelium (MCF-10A represent the normal cells in this project) enlarges to form hyperplastic epithelial lobular units which alter to more complex lesions including ADH (MCF-10AT represents the ADH stage). ADH lesions may then progress and differentiate into DCIS (DCIS.com cells represent the DCIS stage). The DCIS can then progress and break through the basement membrane to become invasive breast cancer (MCF-7 and T47D cells represent the invasive cell lines with variable receptor status) and MDA-MB-231 cells represent metastatic cells. The invasive cells then metastasise and one of the most common sites for breast cancer metastasis is the bone; this stage is represented by the fully bone-homed cells called MDA-MB-231-(BM). Elements of this figure were produced using Servier Medical Art: http://www.servier.com/Powerpoint-image-bank).

1.7 Breast cancer molecular subtypes

Multiple molecular changes occur during the progression of breast cancer including the oestrogen and progesterone receptors, proliferation markers, and the HER2 receptor expression. The expression of these markers differs between different breast cancer subtypes including luminal A, luminal B, HER2 positive, basal-like and claudin-low. Knowing the receptor status of the breast cancer is very important in determining the best strategies for treating and targeting the disease. For example, high levels of Ki-67, which is a nuclear antigen detected in cells in the proliferative phases of the cell cycle (G1, S, G2, and M) and helps in maintaining the growth rate, has been associated with increased risk of breast cancer recurrence (Rivenbark et al., 2013).

Luminal A subtype is characterized as hormone receptor positive ER and/or PR positive and HER-2 negative with low Ki-67 expression. The proliferation rate and the histological grade of luminal A are low. This subtype accounts for 50%-60% of the cases and considered the most common type of breast cancer. Luminal A subtype shows a good prognosis in response to chemotherapy (Yersal and Barutca, 2014).

Luminal B subtype is characterized as hormone receptor positive ER and/or PR positive in addition to a positive HER-2 expression. The expression of Ki-67 is high and the proliferation rate of this type is slightly faster than the luminal A cancer with poorer prognosis compared to luminal A. However, both luminal subtypes have an excellent long-term survival of about 80% to 85% at 5-years. The luminal B cancer represents about 15% to 20% of all breast cancers. Both luminal A and B can be treated by hormonal therapy as both showed ER-dependent growth phenotype with a varying response (Rivenbark et al., 2013, Yersal and Barutca, 2014).

HER2 positive cancer represents 15-20% of breast cancer subtypes. It is characterized by high expression of HER2 gene with negative ER and PR. The expression of Ki-67 is usually high in HER2 positive cancer. The proliferation rate of HER-2 positive is faster than luminal cancers and therefore it has a slightly lower prognosis which about 71% 5-year survival but the HER2 can be targeted and the cells are responsive to Herceptin (an antibody to HER2), which is a common treatment for this subtype (Dias et al., 2017).

Basal-like cancer is characterized by cancers that do not express ER, PR and HER-2 hence it is often referred to as triple-negative causes. It is more common in patients

with *BRCA1* gene mutation and accounts for 15% of all breast cancers. Triple negative cancer has a high rate of cell proliferation with an extremely poor prognosis. The Ki-67 level is high in triple negative cancers and this type of cancer is positive for EGFR (Rivenbark et al., 2013). It has a survival rate of 73% at 5-years survival (Dias et al., 2017). Claudin-low breast cancer is somewhat similar to the triple negative type. It accounts for 10% of all breast cancers. As in triple negative, claudin-low is receptor negative for ER, PR and HER-2. It is enriched in epithelial-to-mesenchymal transition and has reduced expression of Claudin with a survival rate of 79% at 5-years (Prat et al., 2010, Yersal and Barutca, 2014, Dias et al., 2017).

Normal breast-like cancer is poorly characterized and is usually classified as a fibroadenoma. It represents 5-10% of all breast cancer and does not express any of ER, PR and HER-2 receptors and has an intermediate prognosis between luminal and basal-like. It expresses gene characteristics of adipose tissues and it does not respond to neoadjuvant chemotherapy. Normal breast-like cancer are not characterised as basal-like as they are negative for basal myoepithelial markers such as CK5 and epidermal growth factor receptor which make it different from triple negative cancer (Yersal and Barutca, 2014).

Despite the differences between the molecular subtypes of breast cancer, the development and pattern of metastasis is considered the most important risk factor for cancer prognosis, and has important implications for the clinical management of the disease (Gupta and Massague, 2006). The ability of aggressive malignant cells to spread beyond the breast and nearby lymph nodes to distant organs is known as tumour metastasis, and occurs as a late event in tumour progression. Tumour cells may travel into blood vessels, lymphatic vessels, or spread within body cavities. The distant metastatic spread is the most common cause of death among patients with breast cancer. Depending on the breast cancer subtypes, it primarily metastasizes to bone, lung, liver and brain; the last two sites occur less frequently but are seen more in triple negative tumours. Overall bone is considered the main site for breast cancer metastasis especially for oestrogen receptor positive tumours (Scully et al., 2012, Jin and Mu, 2015).

In order for cancer cells to be able to metastasize they must have some fundamental properties and gain certain tumorigenic features and functions to complete the multistep metastatic cascade. The metastatic cascade can be divided into different

steps (Scully et al., 2012) including invasion and intravasation, dissemination into the circulation, arrest and extravasation at the distant site, and micrometastasis and colonization of target organs (Hunter et al., 2008).

Tumour invasion is one of the first steps that cells must fulfil in order to be able to metastasise. Malignant cells undergo the process of epithelial-to-mesenchymal transition (EMT) by down-regulation of E-cadherin and up-regulation of vimentin giving them a migratory phenotype. This enables them to move through the extracellular matrix (ECM) and basement membrane of the vasculature and intravasate into blood or lymphatic vessels (Hunter et al., 2008). Invasion is preceded by break down of the ECM to allow the penetration of tissue boundaries. This degradation is carried out via the release of metalloproteinases (MMPs) which are a family of endopeptidases that are able to break down most known extracellular matrix components. Cells squeeze through spaces in the matrix and move into the circulation. Once in the circulation they have to survive a hostile environment, which they do via aggregation in clumps with each other and platelets. The cells travel to the secondary sites, mainly bone in breast cancer, where they arrest in the microvessels and extravasate out again. The cells then initiate growth in the secondary site which is directly enhanced by the recruitment of the tumour metastasis-associated macrophages, and over time, cancer cells can establish full colonization of secondary organs (Hunter et al., 2008, Scully et al., 2012).

Therefore, the development and progression of breast cancer is regulated by a variety of different genetic factors resulting in changing expression of different proteins. There are a number of proteins that are considered to be tumour suppressor proteins that are down-regulated or switched off in breast cancer and these include the semaphorins.

1.8 Breast cancer and semaphorins

The development and pathogenesis of breast cancer is not fully elucidated due to diversity and complex genetic background. However, emerging evidence suggests that semaphorins have an important role in some tumours types by affecting their progression either by activation or inhibition (Nasarre et al., 2005, Segarra et al., 2012). The differences in gene and protein expression of semaphorins among normal and different grades of breast cancer suggest their role as important prognostic factors for evaluating breast cancer progress (Butti et al., 2018), and therefore could be useful

for the diagnosis and prognosis of breast cancer and indeed for targeted therapy to prevent cancer in the early stages of the disease.

1.8.1 Semaphorins

Semaphorins (collapsins) are a family of secreted and transmembrane proteins, which have a substantial impact on axon guidance, the development of the renal, respiratory systems and on the immune system. In recent years, they have been shown to play an important role in angiogenesis, regulation of cell-cell interactions and cell differentiation, immune responses and tumour progression, where some semaphorins are thought to act as tumour suppressors (Luo et al., 1993, Yazdani and Terman, 2006, Capparuccia and Tamagnone, 2009). Importantly, some semaphorins are overexpressed and others are under expressed in different cancers (Rehman and Tamagnone, 2013). Semaphorins are mostly expressed during nervous system development, however, this is not exclusive with expression in many organ systems including the cardiovascular, endocrine, gastrointestinal, hepatic, immune, renal, reproductive, and respiratory systems. Notably, the expression of semaphorins has been shown to be reduced with cellular maturity in neuronal tissue. During adulthood the expression of semaphorins was notably altered during tissue damage associated with certain pathological conditions. One of the common functions of semaphorins is their direct effect on of tissue morphogenesis and the other critical cellular processes. The alteration of semaphorin function has been associated with some neural disorders such as epilepsy, Alzheimer's and Parkinson's disease (Eastwood et al., 2003). The proteolytic processing of semaphorins by cleavage of furin-like proprotein convertases helps to activate the function of some semaphorins and therefore mediate axon guidance, migration, invasiveness and metastasis of cancer cells (Adams et al., 1997).

One of the cancer hallmarks is that cancer cells must gain some tumorigenic features in order to metastasize and persist (Seyfried and Huysentruyt, 2013). The metastatic tumour cells must be supplied with nutrients to enhance the growth of tumours and this is via the process of developing new blood vessels called angiogenesis. Angiogenesis is one of the multisteps in the development of human cancers and directly contributes to tumour progression. Semaphorins play critical roles in angiogenesis by regulating vascular endothelial growth factor VEGF/VEGFR, considered to be the main player in this scenario (Castro-Rivera et al., 2004). A previous study suggests that semaphorins regulate angiogenesis by competing with

VEGF for neuropilin binding which acts as a co-receptor for some types of semaphorins as well as for the VEGF family of proteins (Castro-Rivera et al., 2004). Other semaphorin members promote tumour function by enhancing cell proliferation and migration in breast cancer. However, some members function as suppressor genes and anti-angiogenic factors that lead to decrease of metastatic ability and reduced aggressiveness of breast tumours (Varshavsky et al., 2008). It has been reported that breast cancer development and progression is associated with inactivation of SEMA3F as the knockdown of SEMA3F promotes tumour invasion (Xiong et al., 2012). Based on the evident relationship between semaphorin expression and cancer, attention has focused on the possibility of targeting semaphorin expression as a potential strategy for treating breast cancer, as some members have been shown to be effective in some types of cancer (Joseph et al., 2010, Loginov et al., 2015). This evidence strongly suggests a critical role of semaphorins in breast cancer and highlight the importance of their expression on cancer progression, which needs to be thoroughly investigated to clarify how modification of the semaphorin family could be used in cancer therapeutics as novel factors to regulate tumour development.

1.8.2 Classification of semaphorins

Based on their structure and the phylogenetic characteristics, semaphorins are classified into eight subclasses. Class 1 and 2 are found in invertebrates only, whereas classes 3 to 7 are expressed in vertebrates, class 5 is found in both vertebrates and invertebrates, and class 8 is only found in viruses. Each subclass consists of several individual semaphorin proteins; each assigned a different letter (table 1.1). The structure of semaphorins consists of a highly conserved region of 500 amino acids at the amino-terminal end –the sema domain– which contains 17 highly conserved cysteine residues folded into a seven blade β-propeller structure. In addition, semaphorins comprise of at least one plexin, semaphorin and integrin (PSI) domain which is a cysteine-rich domain. Other aspects of semaphorins differ from each other. For example, SEMA4 and SEMA6 commonly have PDZ binding motifs at the C-terminal of their intracellular domain, which can be cleaved proteolytically to generate soluble proteins (Artigiani et al., 2003, Kruger et al., 2005). In contrast, SEMA7 proteins have a ghycophosphatidylinositol anchor (GPI) in their structure to help them remain linked to the plasma membrane and therefore they can interact with β integrins

in order to mediate the inflammatory response (Suzuki et al., 2007). Some classes of semaphorins, including SEMA 2, 3, 4, 7 also have a single immunoglobulin IG-like domain in their structure, while SEMA5 has seven thrombospondin domains (figure. 1.3).

Table 1.1: Semaphorins receptors and their locations (Law and Lee, 2012, Sabag et al., 2014).

Semaphorin	Receptor	Location
Class 1		Invertebrate
SEMA1A	PlexinA	
SEMA1B	PlexinA	
Class 2		Invertebrate
SEMA2A	PlexinB	
Class 3		Vertebrate
SEMA3A	NP1; Plexin-A4	
SEMA3B	**NP1, -2, Plexin-A1, -A2, -A4**	
SEMA3C	NP1, -2; Plexin-A2, -D1	
SEMA3D	NP1	
SEMA3E	Plexin-D1	
SEMA3F	NP1, -2; Plexin-A1, -A2	
SEMA3G	NP2	
Class 4		Vertebrate
SEMA4A	Plexin-B1, -B2, -B3, -D1	
SEMA4B	Plexin-B1	
SEMA4C	Plexin-B2	
SEMA4D	Plexin-B1, -B2	
SEMA4G	Plexin-B2	
Class 5		Vertebrate and Invertebrate
SEMA5A	Plexin-B3, -A1, -A3	
SEMA5B	Plexin-A1, -A3	
Class 6		Vertebrate
SEMA6A	Plexin-A4	
SEMA6B	Plexin-A4	
SEMA6C	Plexin-A1	
SEMA6D	Plexin-A1	
Class 7		Vertebrate
SEMA7A	Plexin-C1	
Class 8		In virus only

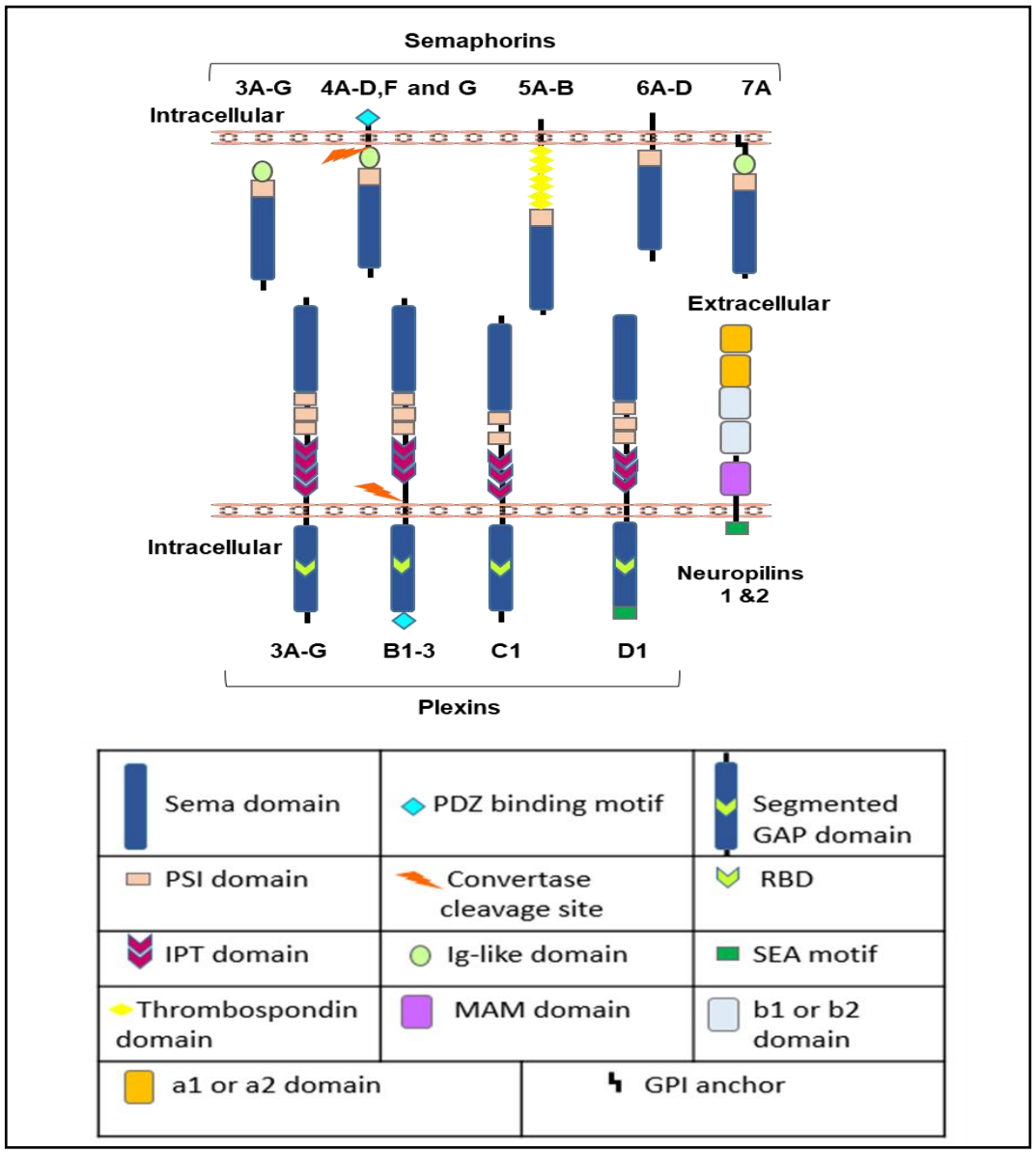

Figure 1.3: Vertebrate semaphorin structure and their binding partners, plexins and neuropilins. Semaphorin protein family members are classified into 8 classes based on their domain structure. Class 3 semaphorins are secreted, semaphorins of other classes are attached to the membrane. Class 3 semaphorin members are grouped into 7 classes including 3A, 3B, 3C, 3D, 3E, 3F and 3G. Class 3 semas are found in vertebrates. Plexin receptors, the main receptors for semas, are classified into 4 classes (3A–G), (B1-3), (C1) and D1. Each plexin receptor class interacts with a certain semaphorin class to initiate signaling. Neuropilins receptors (NP1 and NP2) act as ligand binding co-receptors. Reproduced from (Worzfeld and Offermanns, 2014).

1.8.3 Semaphorin signalling and biological implications

The plexins, a group of transmembrane receptors, are utilized by semaphorins for their signalling and these receptors are expressed in a wide range of cell types such as in the bone marrow progenitors, endothelial cells and cancer cells. For instance, plexin A, a neuronal semaphorin receptor, controls axon guidance through binding to class 1 semaphorins (Winberg et al., 1998). Plexin receptors play a critical role in the recognition and mediation of semaphorins as the majority of semaphorins work through these receptors (Tamagnone et al., 1999). However, some classes of semaphorins, including SEMA3s, also utilize co-receptors such as the neuropilins (NP1& NP2), which exist in a complex with plexin for plexin activation and cell signalling to occur (Takahashi et al., 1999). The affinities of the binding between class 3 semaphorins and neuropilin-plexin complexes are variable depending on each specific SEMA3 protein (Gaur et al., 2009). The plexin-semaphorin ligand binding results in activation of downstream signalling pathways and this is known to have a significant function in many disorders including the development of inflammation, lung and renal disorders and most importantly, cancer development or regression (Capparuccia and Tamagnone, 2009). Different members of the semaphorin family have different signalling pathways and interactions in cancer in general, and in breast cancer in particular. However, the signal transduction cascades of each semaphorin are not yet clearly identified (Butti et al., 2018).

Class 3 semaphorins are secreted proteins that in general, with SEMA3B and SEMA3F specifically, are thought to play an important role in cancer development as they act as tumour inhibitors and potential anti-angiogenic factors in some lung and breast cancers (Neufeld et al., 2005, Gaur et al., 2009, Staton et al., 2011). In fact, SEMA3B and SEMA3F are both regarded as tumour suppressors as the expression of both genes are found to be lost in some lung cancers (Xiang et al., 1996), and re-expression of these genes in a mesothelioma cell-line inhibited lung cancer cell growth (Tomizawa et al., 2001).

In contrast, other classes of semaphorins could aid cancer development by stimulating crosstalk between intracellular and extracellular signals, enhancing cell migration and invasion into adjacent tissues, both of which are hallmarks of cancer. Indeed, semaphorins act as pleiotropic factors by controlling multiple signalling pathways involving cell survival and apoptosis. Semaphorins may be released in the tumour

microenvironment by infiltrating leukocytes or cancer cells where they can exhibit an autocrine regulatory loop (Rehman and Tamagnone, 2013). Hence, changes in expression pattern of semaphorins may be responsible for their different functions in varying pathological conditions. For instance, loss of heterozygosity of SEMA3B and SEMA3F has been observed in different cancers and mRNA overexpression of these proteins induces apoptosis and inhibits cell proliferation (Castro-Rivera et al., 2004). In contrast, expression of SEMA3B has been correlated with poor prognosis for cases of glioblastoma because even though it inhibits tumour growth, the cancer cells were found to retain their metastatic potential in a number of cases, which is consistent with p38-MAPK dependent activation of p21 and induction of interleukin 8 (Rolny et al., 2008).

1.9 Class 3 semaphorins

Class 3 semaphorins are a subfamily of semaphorins, and are secreted proteins which are expressed in numerous cells including neurons, epithelial cells and some tumour cells (Worzfeld and Offermanns, 2014). They consist of seven soluble proteins (A, B, C, D, E, F and G) and are found in vertebrates. Like most semaphorins, Class 3 semaphorins consist of a 500 amino acid sema domain and PSI domain, in addition to an immunoglobulin-like domain, and a C-terminal basic-rich domain (Yazdani and Terman, 2006, Staton, 2011, Nasarre et al., 2014). As previously stated, SEMA3 signalling is activated through binding to plexin receptors in the presence of NP1 and NP2 which act as co-receptors. The main receptors for the class 3 semaphorins are the Plexin A subgroup, however, additional receptors/co-receptors are also known to contribute to class 3 semaphorin signalling such as L1cam, Nrcam, Plexin B1 and PlexinD1 (Takahashi et al., 1999, Gu et al., 2005, Julien et al., 2005).

Neuropilin co-receptors are essential to stimulate cell signalling and to stabilize the semaphorin–plexin interactions. The resultant signalling is dependent on the affinity of class 3 semaphorins to these co-receptors, which varies between members of the class, with SEMA3A binding to NP1 while SEMA3F and SEMA3G bind to NP2. Some, like SEMA3B, SEMA3C and SEMA3D bind to both NP1 and NP2, whereas SEMA3E is the exception as it binds directly to Plexin D1 without the need for a neuropilin co-receptor (Nasarre et al., 2014). It has been shown previously that class 3 semaphorins play an important role in axon guidance and cell-cell signalling. They are also known to reduce endothelial cell adhesion and migration, thereby acting as anti-angiogenic

agents preventing vascularization of tumours. The majority of SEMA3 members including SEMA3A, 3B, 3D, 3F and 3G all act as anti-angiogenic factors, however, SEMA3C and SEMA3E have the potential to activate angiogenesis and tumour growth (Martín-Satué and Blanco, 1999). Class 3 semaphorins are also thought to act as tumour suppressors by inhibiting tumour growth in some types of cancers, in addition to inducing programmed cell death (Rolny et al., 2008).

1.9.1 Class 3 semaphorin receptors and their cell signalling

1.9.1.1 Plexins

Plexins are large transmembrane cell surface receptors that act as the main receptors for semaphorins. They are expressed in both embryonic and adult tissues and act as signal transduction molecules. They are classified into four classes, namely plexin A, B, C and D, and each class has a number of different subclasses consisting of plexin A1-4, B1-3, C1 and D1 (Tamagnone et al., 1999, Shim et al., 2012). The extracellular structure of plexins consists of a 500 amino acid sema domain, which does not dimerize, a PSI domain and Immunoglobulin-plexin-transcription factor (IPT)/glycine-proline (G-P), which are proline rich motifs that interact with the sema domain of semaphorins. The intracellular portion of plexins contains a split GTPase activity protein (GAP) domain which comprises of C1 and C2 domains separated by Rho-GTPase binding domain (RBD). However, not all plexins are identical in their structure. For instance, plexin class B1-3 contain intracellular PDZ binding motifs and extracellular convertase cleavage sites whereas plexin D1 contains SEA motifs composed of the amino acids Ser, Glu and Ala in their extracellular region (Worzfeld and Offermanns, 2014).

Plexins are known to have a role in the regulation of Rho-family GTPases and in stimulation of R-Ras/M-Ras family, which are involved in semaphorin signaling (Nasarre et al., 2014). To be activated, plexin receptors are bound to semaphorins after which they are phosphorylated on a tyrosine residue in the cytoplasmic domain. Otherwise, they remain in their inactive forms. Semaphorin binding to plexins stimulates different intracellular signaling cascades that eventually effect semaphorin biological function. For instance, the GAP domain of plexins are activated in the presence of Rho-GTPase binding domain, which interact with the Rnd family of proteins, a multidrug efflux pump. Rnd proteins are a distinct subclass of Rho-

GTPases and the interaction with plexin GAP domain requires GDP-GTP exchange in a reaction that also require Ras-related proteins RRas and MRas to form RRas-GAP or MRas-GAP (Saito et al., 2009, Worzfeld and Offermanns, 2014).

Dependent upon their location plexins function as axon guidance receptors, although they also have a significant role in cellular migration, tumour growth, metastasis and angiogenesis whether by overexpression or downregulation dependent on the plexin class and cancer types (Hota and Buck, 2012). It has been shown that plexin A1-4 are the main receptors for SEMA3s, when they form complexes with neuropilins in initiating SEMAs biological function (Worzfeld and Offermanns, 2014) (figure 1.4). Class A plexins regulate tyrosine kinases Fes and Fyn which modify the interaction of SEMA3A with plexin A1. Plexin A1 is phosphorylated by Fes, collapse response mediator protein (CRMP) and CRMP associated protein (CRAM) (Mitsui et al., 2002). In this way, Fes promotes collapse of growth cones of COS-7 cells by SEMA3A and this kinase activity of Fes on plexin A1 is required for collapse of dorsal root ganglion neuronal cells (Mitsui et al., 2002). In addition, an upregulated expression of plexinA1 is observed in some cancers, such as colorectal carcinoma and gastric cancer, where the upregulation correlates with increased vascularisation through angiogenesis (Zhao et al., 2007, Carrer et al., 2008). However, in invasive breast cancer, the expression of plexin A1 and A3, in addition to class 3 semaphorins has been shown to be downregulated and this correlates with an increase in angiogenesis (Staton et al., 2011). This suggests that plexin As are important contributors in cancer development.

Although Plexin A1-4 are the main receptors for SEMA3 proteins, there is a suggestion that Plexin D1 may interact with one member of the family. Indeed, in many cancer cells where there is elevated expression of SEMA3E, elevated levels of plexinD1 are also observed and this correlates with the aggressiveness of the tumour. It is therefore not surprising that knockdown of plexinD1 and/or SEMA3E inhibited metastasis in a xenograft mouse model (Tseng et al., 2011, Luchino et al., 2013) suggesting an interaction between the two proteins.

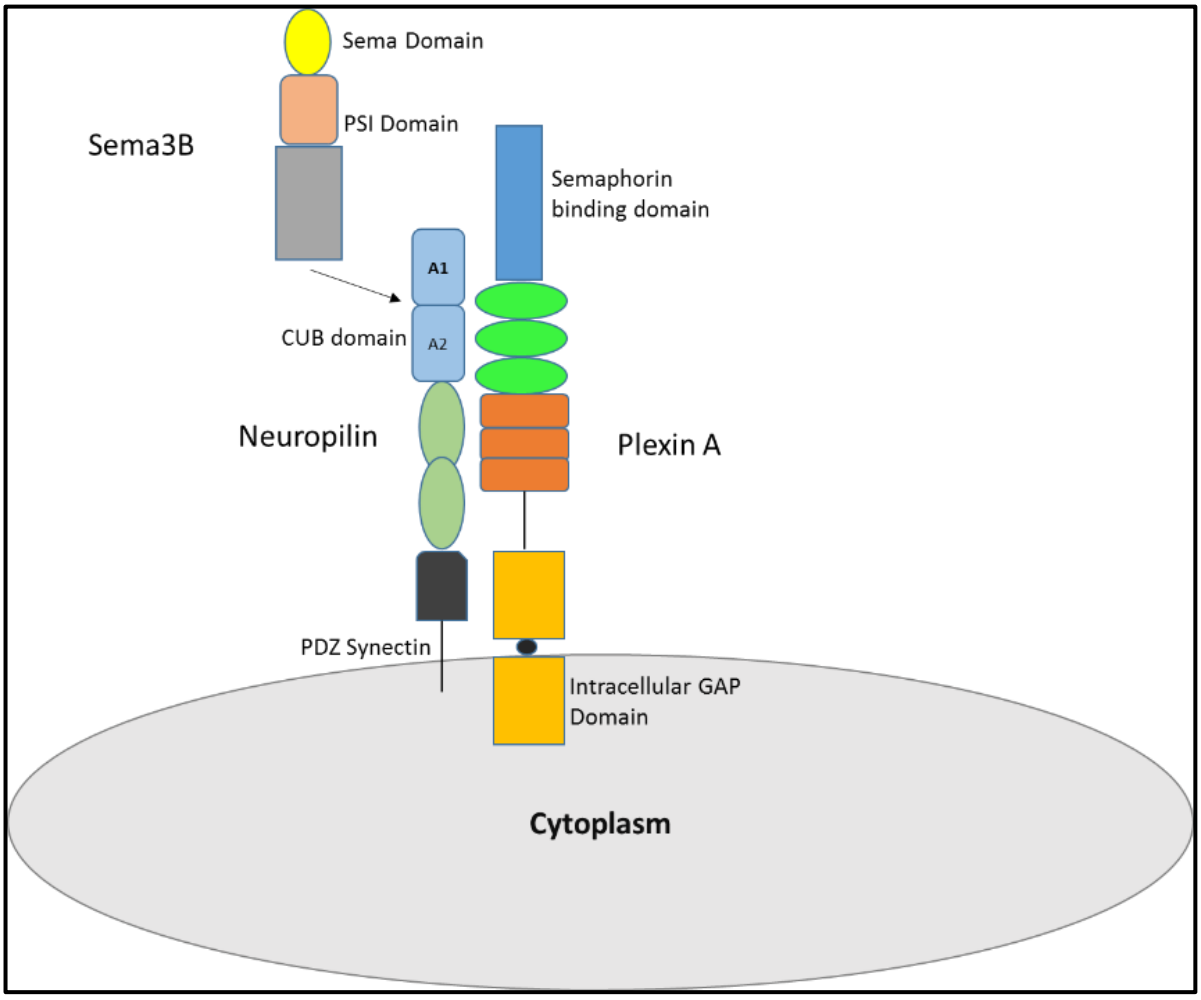

Figure 1.4: Class 3 semaphorins and their interaction with neuropilin and plexin. Class 3 semaphorins such as SEMA3B signal through neuropilins like NP1 or NP2 in the presence of a receptor known as plexin (Plexins A1, A2 and A4 in case of SEMA3B). This interaction results in a cytoplasmic signaling cascade, in some oncogenic pathways through the GAP domain of plexinA for instance. SEMA3B is characterized by a large sema domain, one PSI domain and a C-terminal basic that is required for neuropilin binding. Neuropilins receptors are transmembrane receptors that act as a co-receptor for SEMA3B and consisting of CUB (a1 and a2) domains, two coagulation factor V/VIII domains (b1/b2) and a MAM domain (c domain). Plexins receptors are transmembrane receptors consisting of sema domain, three PSI domains, three Ig-like folds in their extracellular portion, and GAP domain in their cytoplasmic portion. Reproduced from (Ellis, 2006).

1.9.1.2 Neuropilins

Neuropilins are transmembrane glycoproteins with a molecular mass of 120 to 130 kDa and classified into NP1 and NP2, which are encoded by genes located at 10p12 and 2q34, respectively (Nakamura and Goshima, 2002, Ellis, 2006). They are expressed by different cells including neuronal, dendritic, inflammatory, endothelial, vascular smooth muscle, and tumour cells (Herzog et al., 2001). NP1 and NP2 have a similar protein structure but NP2 shares only about 44% sequence homology with NP1. The extracellular part of the neuropilins consists of five domains; two N-terminal CUB (a1 and a2) domains, Bone Morphogenetic Protein 1 (BMP1), and Tolloid proteins. Neuropilins also have two coagulation factor V/VIII domains (b1/b2) which bind to several ligands including VEGF and a MAM domain (meprin, A-5 protein, and receptor protein-tyrosine phosphatase mu), which is found in many receptors and mediates the dimerization of neuropilins. However, the intracellular part of neuropilins is only 20 amino acids in length and consists of SEA motifs which bind to different proteins, one of which is the PDZ synectin known to confer the VEGFR specific interaction to NP1 (figure 1.4). This interaction is essential for VEGF-dependent migration of endothelial cells (Wang et al., 2003, Worzfeld and Offermanns, 2014). Despite this ability to bind intracellular proteins, the small cytoplasmic domain of neuropilins leads them to mostly depend on molecules like plexins to transduce signals (Rohm et al., 2000, Prahst et al., 2008).

Neuropilins comprise of a small family of co-receptors, which form a complex formation with plexins in the presence of semaphorins, by providing a high affinity-binding site for the semaphorin ligand. Neuropilins also bind to VEGF, thus playing an important role in angiogenesis (Gaur et al., 2009). Interestingly, neuropilins have been implicated in vascularization within the tumour microenvironment, due to their interactions with semaphorins and VEGFs affecting cell proliferation, migration and survival (Rizzolio and Tamagnone, 2011). NP1 is observed to be mainly expressed in carcinomas while NP2 is found to be expressed in tumour cells derived from neural crest cells (Ellis, 2006). Increased expression of NP1 often correlates with poor prognosis due to accelerated cancer progression. Interestingly, growth factors such as epidermal growth factor (EGF) can induce NP1 expression (Akagi et al., 2003).

Neuropilin binding to VEGF is important for vascularisation in tumour cells by forming receptor complexes (Gluzman-Poltorak et al., 2000). NP1 appears to bind specifically

to $VEGF_{165}$ while NP2 binds both $VEGF_{145}$ and $VEGF_{165}$, and both NP1 and NP2 can bind additional VEGF family members such as VEGFB, VEGFE or Placental Growth Factor (PlGF2) (Migdal et al., 1998, Makinen et al., 1999). NP1 has been shown to enhance VEGFR2 signaling and it has been proposed that enhanced ligand binding to VEGFR2 in the presence of NP1 is responsible for enhanced potency of VEGF (Whitaker et al., 2001). It is worth noting that binding of VEGFR2 to NP1 occurs through the PDZ domain and this domain is known to confer angiogenic properties to neuropilins. This was confirmed in PDZ deficient cells which showed reduced NP1/VEGFR2 complex formation (Prahst et al., 2008).

The activity of VEGF is inhibited by semaphorins which was originally thought to be due to the competition between VEGF and semaphorins for the neuropilin binding site (Appleton et al., 2007). This fact was strengthened by the study carried out by Pan et al. (2007) where blocking of the NP1 VEGF binding motif resulted in additional inhibition of NP1 angiogenic properties. However a new line of evidence from a mutagenesis study has shown that even though both $VEGF_{165}$ and SEMA3 proteins bind to the b1b2 subdomain of NP1, the amino acids of NP1 that bind $VEGF_{165}$ are different from those binding the SEMA3 proteins (Geretti et al., 2008), thus suggesting the possibility of another mechanism of angiogenesis inhibition rather than competitive binding. For example, Geretti *et al* (2008) found that $VEGF_{165}$ can bind to the B (b1b2) domain of NP2, and this interaction can be altered by the reduction of the electronegative potential of B-NP2 which can decrease the affinity of binding between $VEGF_{165}$ and NP2 without affecting SEMA3F affinity (Geretti et al., 2008). Thereby, this knowledge could play a potential role in developing effective anti-angiogenic therapies.

1.10 Semaphorin 3B (SEMA3B)

Semaphorin 3B (SEMA3B) is an 83 kDa protein member of the class 3 semaphorins, and its gene is located on the 3p21.3 LUCA region, which is found to exhibit a high loss of heterozygosity in lung and ovarian cancers (Tse et al., 2002). In fact, up to 40% of SEMA3B allele losses on chromosome 3 contribute to the progression of some types of cancers like lung, renal, breast and cervical carcinomas. These allele losses of SEMAB gene impaired different cellular processes such as stimulation of apoptosis and inhibition of angiogenesis (Senchenko et al., 2004). SEMA3B shares the same

structure as all semaphorins including the NH_2-terminal highly conserved sema domain and has a basic domain at the COOH terminal (Roskies, 1998).

SEMA3B has a recognition site for pro-protein convertases (PPCs) which is susceptible to cleavage by proteolytic activity. Cleavage at this site generates a 51-60 kDa of SEMA3B protein which has been suggested to be an inactive form of SEMA3B (Varshavsky et al., 2008).

1.10.1 SEMA3B receptors and signaling

The main receptors for SEMA3B are plexins A1, A2 and A4, and neuropilins (NP1 and NP2), which serve as mediators for its biological function through receptor complex formation (Gaur et al., 2009, Sabag et al., 2014). NP1 and NP2 both interact with SEMA3B by providing a binding site for the semaphorin while plexins are required for enhancement of signal transduction such as stimulating kinase activities (Nakamura and Goshima, 2002). By forming a receptor complex with neuropilins, SEMA3B is able to induce apoptosis in cancer cells, and is thought to be able to regulate their survival, migration and cell proliferation (Castro-Rivera et al., 2008). This is thought to be through inhibiting P13K and therefore inactivating AKT signaling leading to decrease cell survival and cell proliferation (Butti et al., 2018). SEMA3B also inhibits $VEGF_{165}$ angiogenic activity, although whether it is through competition for NP1/2 binding or through stimulating different signalling pathways remains to be elucidated. NP1 also serves as a co-receptor for SEMA3B for axonal guidance during development of embryos (Tse et al., 2002, Bielenberg et al., 2006).

However, the role of specific plexins in SEMA3B signalling is not fully understood. Previous studies have shown that plexin A1 is required alongside NRCAM, an adhesion molecule, for the transduction of SEMA3B signals for commissural axon guidance in vertebrates during nervous system development (Nawabi et al., 2010). Interestingly there is now some data suggesting plexin A4 is required for SEMA3B complexes and inhibition of plexin A4 expression nullifies SEMA3B signalling in endothelial and glioblastoma cells (Sabag et al., 2014). Unlike SEMA3A that signals through NP1 alone, SEMA3B signals through NP2 as well and this interaction appears to require plexin A2 (Sabag et al., 2014). Interestingly, a transcription factor of GATA3, which can be used as a marker of breast cancer as it helps to increase the maturation of precursor cells into breast epithelial cells, was found to be targeted by SEMA3B

resulting in suppression of breast cancer metastasis by phosphorylation and activation of LIMK1 and LIMK2 kinases (Shahi et al., 2017). Therefore, although the signaling pathways are not entirely clear it is evident that the specific plexin involved confers the specificity of the resultant SEMA3B signaling pathway.

1.10.2 Regulation of SEMA3B

Regulation of SEMA3B gene expression occurs in many different ways. Several studies have found that in different types of cancer such as neuroblastoma, lung cancer, renal cell carcinoma and oral squamous cell carcinoma there is methylation or hypermethylation of the CpG island/promoter region of SEMA3B resulting in loss of function of the gene (Grote et al., 2005, Nair et al., 2007, Loginov et al., 2009, Wang et al., 2013). Indeed, Nair *et al*.,2007 discovered that CpG islands in the promoter region of SEMA3B were highly methylated in neuroblastoma cell-lines that exhibit a 3q loss (about 95%) or in tumours without 3q loss (52%), suggesting a two hit mechanism for loss of function i.e. deletion and hypermethylation. Loss of function due to methylation was confirmed by treating the neuroblastoma cells with demethylating agents which resulted in some level of SEMA3B expression (Nair et al., 2007). Loginov *et al*. (2009) also discovered a high frequency of methylation in the SEMA3B CpG island which inversely correlates with the expression level of SEMA3B mRNA in clear cell renal cell carcinoma.

In addition to 3q deletion and hypermethylation which both lead to loss of function or inactivation, SEMA3B is also regulated through cleavage by furin, a pro-protein convertase which is a calcium-dependent serine endoprotease (Ito et al., 2005, Varshavsky et al., 2008). Importantly, processing of some SEMA3 proteins, namely SEMA3A and SEMA3E, by furin resulted in about a 40% reduction in their effectiveness to inhibit VEGF function (Parker et al., 2013) and therefore reduced their functional activity. Normally furin as a pro-protein convertase facilitates the conversion of inactive proteins such as some metalloproteinases to the active form (Tellier et al., 2007), however, it appears that here furin generally converts active SEMA proteins to inactive forms depending on the cleavage site, thereby suggesting an alternative pathway for regulation of semaphorins by furin. Furin and the family of furin-like pro-protein convertases will be discussed in more detail later in this chapter.

1.10.3 SEMA3B effect on normal cells

Semaphorins such as SEMA3B are expressed in many normal cells such as endothelial and neuronal cells, as well as cancer cells as previously stated. The ubiquitous expression of this protein suggests it plays a cellular role that is critical to the survival of certain normal cells. Indeed, SEMA3B is implicated in physiological functions including endothelial development and control of the immune system (Kruger et al., 2005). SEMA3B is expressed by endothelial cells, suggesting that SEMA3B can regulate endothelial cell functions in an autocrine manner by transducing signals that compromise endothelial cell survival (Kruger et al., 2005, Guttmann-Raviv et al., 2007, Staton et al., 2011). Moreover, the expression of SEMA3B is high in normal breast epithelium compared to invasive breast cancer (Staton et al., 2011). It remains unclear whether or not SEMA3B is maintaining mammary gland homeostasis in these circumstances. However, SEMA3B has a potential autocrine function by promoting luminal epithelial cell differentiation and could therefore function as a safeguard for cellular function (Shahi et al., 2017).

In addition, SEMA3B is expressed in the floor plate region of the spinal cord in rat embryos and it has been found to play a critical role in commissural axon directional growth (Zou et al., 2000). Because of the lack of decussated commissural axons in the floor plate at the embryo stage, it was suggested that SEMA3B could be playing a role in directing axons into appropriate tracts. In fact, *in vitro* explant assays have shown that commissural axons become sensitive to floor plate secreted factors as mimicked by COS7 cells secreting SEMA3B (Zou et al., 2000). Recently it has been demonstrated that mice lacking SEMA3B presents commissural defects where the axons fail to cross the midline and turn prematurely, further reinforcing its role in axon guidance (Nawabi et al., 2010).

Villous cytotrophoblasts (CTBs) are present in the placenta and they differentiate to establish the maternal interface. They also differentiate into aggressive endothelial–like cells invading the uterus and surrounding vasculature so as to re-route a blood supply to the placenta (Zhou et al., 2013). CTBs have been found to express high levels of *SEMA3B* in pre-eclampsia and this has been corroborated in a study by Zhou *et al*. (2013) where they discovered that adding exogenous SEMA3B to CTB reduces the invasiveness of the cells to create a pre-eclampsic phenotype. In addition to this, they discovered downregulation of VEGF signaling via PI3K/AKT signaling as

discussed earlier. Like endothelial cells, CTBs express VEGFRs and other cell surface receptors and the downregulation of VEGF signaling by SEMA3B could result in SEMA3B-neuropillin mediated internalization of VEGFR resulting in reduced vascular processes that cause pre-eclampsia. Here, SEMA3B expression seems to play a negative role thereby causing the development of preeclampsia and a reduced expression may be required for normal VEGF signaling to prevent pre-eclampsia.

1.10.4 Cellular and tissue expression of SEMA3B and its effect in cancer

Expression of SEMA3B mRNA in different cancer cells and tissues have been analyzed. Chen et al. (2014) demonstrated that the expression level of SEMA3B mRNA was higher and the methylation status was lower in normal gastric cells than in gastric tumour cells. Interestingly, of all the semaphorins, only SEMA3B is predominantly expressed in normal ovarian tissue and this expression goes down in invasive ovarian cancer (Sekido et al., 1996, Joseph et al., 2010). In addition to this, it was found that the majority of SEMA3B expression in breast cancer is high in the duct of normal breast tissues but significantly reduced in invasive breast cancer (Staton, 2011). Likewise, similar studies have found that SEMA3B expression was higher in normal lung tissue compared to invasive forms of lung cancer (Castro-Rivera et al., 2004). SEMA3B mRNA levels are decreased in many cancer cell-lines, for instance in small and non-small cell lung cancer (NSCLC) and it has been shown that SEMA3B suppresses the growth of a NSCLC cell-line and tumour development in an immunodeficient mouse model (Pronina et al., 2009). An *in vitro* study carried out on four different gastric cancer cell-lines showed that mRNA expression of SEMA3B was lower than in the normal cell-lines utilized (Chen et al., 2014). This low expression level may be linked to the high methylation of SEMA3B promoter found through bisulphite sequencing in the same study, since high methylation of promoters results in low mRNA expression. From all indications, expression of SEMA3B seem to be significantly reduced in cancer cells when compared with normal cells.

1.10.5 SEMA3B in breast cancer

There are relatively few studies investigating the role and expression of SEMA3B in breast cancer. Staton *et al*.,(2011) found a significantly higher cytoplasmic expression of SEMA3B protein in normal breast epithelial cells compared to invasive breast cancer cells. This is supported by the findings of the study by Pronina *et al*.,(2009),

where they found reduced SEMA3B mRNA expression in breast cancer cell-lines and primary breast tumour cells. However, comparing SEMA3B mRNA expression in normal cells and six different breast cancer cell-lines used in their study, shows SEMA3B mRNA level was significantly decreased in breast cancer cell lines by 10-250 fold compared to normal cells (Pronina et al., 2009).

In a study by Castro-Rivera et al. (2004), using conditioned medium containing full length SEMA3B, growth inhibition of a breast cancer cell-line was observed. They also demonstrated that SEMA3B inhibits VEGF-dependent cell growth in a VEGFR-independent manner using an MDA-MB-231 breast cancer cell-line that does not express VEGFR. This pattern is in agreement with a recent study that demonstrated an angiogenic signature of low expression of SEMA3B with high expression of VEGFA in MDA-MB-231 cells, suggesting an important role of the angiogenic factors in the triple negative breast cancer cell-line (Bender and Mac Gabhann, 2013). Given that SEMA3B may compete with VEGF for binding to NP co-receptors, this pattern of gene expression may promote tumour progression. Indeed, patients that exhibit this type of VEGF-SEMA3B signature have poor prognosis irrespective of their triple negative status (Bender and Mac Gabhann, 2013).

Akt is a critical factor in the regulation of phosphatidyl inositol 3-kinase (PI3K) pathway of cell survival in cancer cells. Recent evidence showed that the Akt signaling pathway which promotes tumour cell proliferation in lung and breast cancers is inactivated by SEMA3B through NP1 (Castro-Rivera et al., 2008). In this study, breast cancer cell-lines knocked down in NP1 and expressing active Akt were found to be insensitive to SEMA3B while they became sensitive to SEMA3B when NP1 was exogenously expressed. This suggests that the NP1-SEMA3B complex formation is essential for SEMA3B activity in inhibiting Akt signaling pathway to induce apoptosis in cancer cells. These findings also highlight the role of SEMA3B in tumour-inhibitory function and inhibition of proliferation.

However, in contrast to this, another study found that even though SEMA3B could suppress tumour growth, it could trigger prometastatic signaling by releasing interleukin 8 (IL8) via the activation of p38-MAPK pathway on NP1-dependent manner in breast cancer cell-lines (Rolny et al., 2008). As such if SEMA3B is expressed in cancer cells, it may interact with proinflammatory cytokines to cause relapse in cancer development.

A role for SEMA3B in the p53-dependent apoptotic pathway has also been highlighted as SEMA3B seems to function as a tumour growth suppressor by inducing apoptosis of premalignant and malignant cells via Akt inhibition. A study showed increased SEMA3B expression in breast cancer cells deficient in p53 when the cells were treated with UV and doxorubicin (Ochi et al., 2002). These studies suggest SEMA3B may be mediating a p53 independent DNA damage response since p53 is normally upregulated during DNA damage. Even though most of these studies were descriptive analysing expression of SEMA3B without investigating the in-depth mechanism, evidence from these studies further suggests that SEMA3B may be involved in breast cancer pathogenesis.

1.10.6 SEMA3B regulation in breast cancer pathogenesis

One of the first lines of evidence that SEMA3B may play a crucial role in the pathogenesis of breast cancer is the detection of frequent deletion of the 3p21.3 chromosomal location through genetic mapping of breast tumours, premalignant lesions and breast cancer cell-lines (Lerman and Minna, 2000). In a later study using genetic mapping with polymorphic microsatellites that are specific to the 3p location, there was allelic imbalance due to loss of a section of the chromosome that may likely house some tumour suppressors (Ingvarsson et al., 2015). Several earlier studies confirmed this observation (Ji et al., 2002, Hesson et al., 2004, Senchenko et al., 2004). In addition to allele deletion, hypermethylation of the SEMA3B promoter correlates with the progression of different cancers (da Costa Prando et al., 2011) and this may also be the case for breast cancer. Promoter methylation in breast cancer has not been widely studied but one *in vitro* methylation study using seventeen different breast cancer cell-lines and three other non-tumourigenic breast cell-lines including 184A1, 184B5 and MCF-10A, showed that hypermethylation of CpG Island gene cluster containing SEMA3B results in reduced expression of SEMA3B (da Costa Prando et al., 2011). As a consequence of this, the hypermethylation of the CpG Island is regarded as a potential factor for altering SEMA3B expression, and hence, a cancer progression marker in breast cancer. These data suggest that SEMA3B expression is down-regulated in breast cancer via two mechanisms, allelic loss and promoter hyermethylation. Despite this some breast cancers do express SEMA3B (Staton et al., 2011). However, other work has suggested that SEMA3B can also be cleaved by furin

(Varshavsky et al., 2008), and potentially other proteases and it is not clear whether, when SEMA3B is expressed in breast cancer, it is cleaved and therefore inactive.

1.11 Proteases

Proteases, commonly called peptidases, are a family of enzymes that regulate proteolytic events in cellular mechanisms. They have an important role in the post-translational processing of various inactive proteins to bioactive molecules by hydrolysis of peptide bonds producing new, active, protein products. Proteases are categorised based on the mechanism of catalysis and the nucleophilic amino acid in the active site involved in proteolysis, into six main families including serine, cysteine, threonine, aspartic, glutamic and metallo-proteases (Lopez-Otin and Bond, 2008). Serine proteases contain a serine residue in the active site and this plays the nucleophilic role of attacking the bound peptide/protein thereby catalysing the hydrolysis reaction. Similarly, cysteine proteases have cysteine residues in their active site and have been known to be involved in programmed cell death and immunity. Aspartic proteases have a pair of aspartic acids in the active site that work together to catalyse the cleavage of peptide bonds. Examples of aspartic proteases are renin, which is known to control blood pressure, and pepsin that is found in the digestive system. Metallo-proteases have metal residue in their active site, which are responsible for increasing the nucleophilic capability of the enzyme. Importantly, most proteases are synthesised as an inactive form (zymogen) and by the mechanism of proteolysis they are activated through removal of a small peptide (Lopez-Otin and Bond, 2008) (figure 1.5).

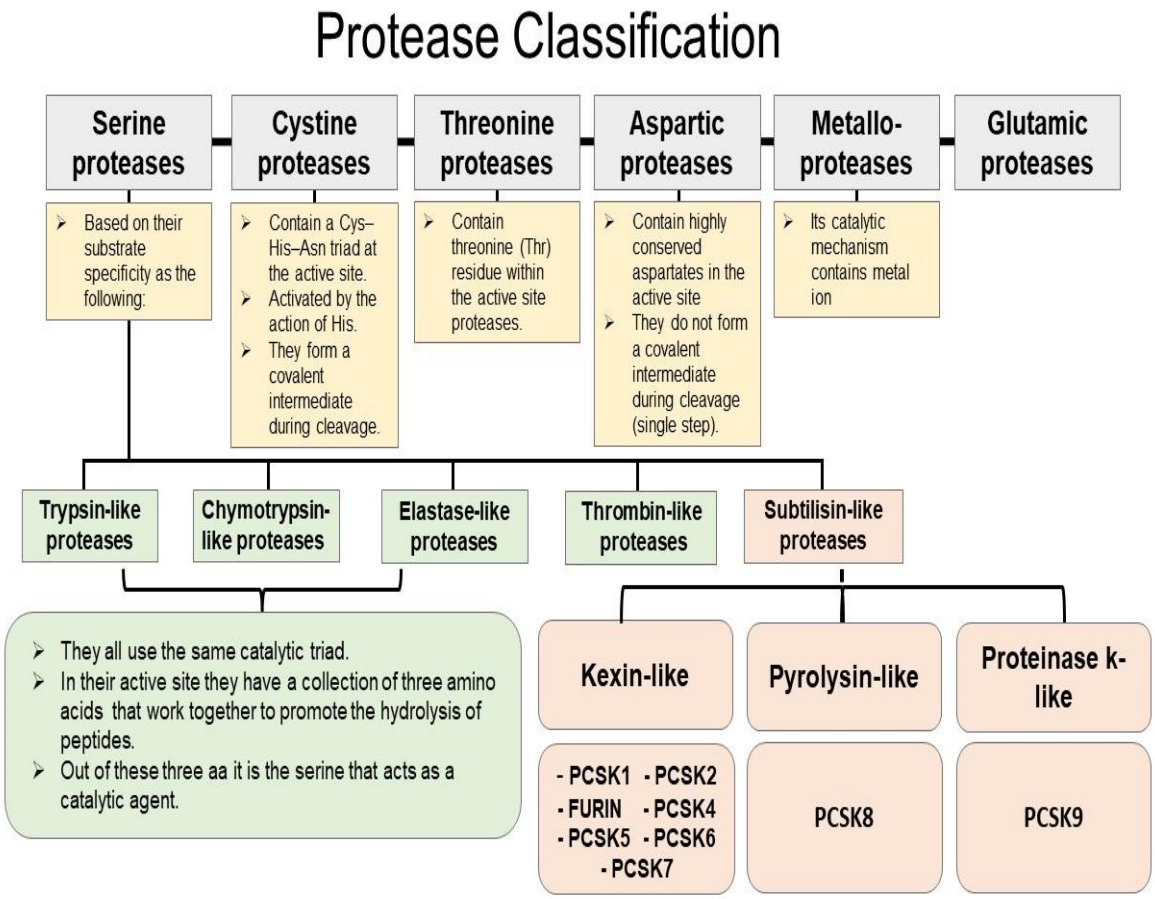

Figure 1.5: Classification of proteases. Proteases are classified based on the chemical structure of their active site. Each class has a chemical structure of the core residue in their active site. Six known distinct classes are described: serine, cysteine, threonine, aspartic and metallo proteases. Serine proteases are grouped into five classes, Trypsin-like, Chymotrypsin-like, Elastase-like, Thrombin-like and Subtilisin-like proteases. Subtilisin-like proteases are also classified into three main groups, Kexin-like, including PCSK1, PCSK2, Furin, PCSK4, PCSK5, PCSK6 and PCSK7, Pyrolysin-like, including PCSK8 and Proteinase K-like, including PCSK9.

1.11.1 Proteases mechanism of action

Serine proteases are included in biological processes such as digestion, blood coagulation and immunity and are the most common type of protease. They are characterised based on their substrate specificity into different classes including trypsin-like proteases, chymotrypsin-like, thrombin-like, elastase-like and subtilisin-like etc. All of these classes cleave peptides by a similar mechanism of action but their differences are in their regulation and specificity (Lopez-Otin and Bond, 2008, Page and Di Cera, 2008).

Serine protease enzymes are able to cleave peptide bonds in a protein to activate it, to increase the rate of chemical reactions without being consumed by the reaction, as well as helping to breakdown large proteins into small fragments. The active site of the enzyme contains three different residues that act together to promote and catalyse the cleavage of peptide bonds, and this collection of three amino acids is known as a catalytic triad. The catalytic triad is considered the main player in the serine proteases catalytic mechanism and consists of serine 195, histidine 57 and aspartate 102 that are essential for the active site of enzyme (Polgar, 2005). These amino acids are located distant from each other on the sequence but due to protein folding are held in close proximity; this closeness and the flexibility of the enzyme play an important role in the catalytic action (figure 1.6, step 1 and 2). The binding of the substrate to the enzyme occurs in the S1 pocket of the enzyme, which is known to give enzyme specificity and is responsible for holding the protein that is going to be cut (figure 1.6, step 3). There are two different phases taking place in this action, first is the positioning step in which a polypeptide chain aligns itself in the active site of the enzyme that contains serine, histidine and aspartic acid. By this binding, the structure of the enzyme will slightly change altering the proximity of the aspartic acid and histidine side chains (Polgar, 2005) (figure 1.6, step 4). The negative charge on oxygen molecule of aspartic acid will make it closely move to histidine, changing the electron configuration of nitrogen molecule of histidine and grabbing the hydrogen from serine, enabling the catalytic mechanism to start. Consequently, the –OH proton of serine is binding to nitrogen molecules of histidine ring, leading the oxygen of serine to have a negative charge and that called alkoxide ion (figure 1.6, step 5). Alkoxide ion is generating nuclephilic attack on carbonyl carbon of peptide bond, leading to rearrangement of

molecules, which make these molecules unstable due to having a single bond between carbon and oxygen molecules (figure 1.6, step 6).

In order to deal with this instability, the oxyanion hole in the enzyme helps the molecules to fall apart easily (figure 1.6, step 7). At this stage, the hydrogen of histidine will take the nitrogen of the substrate, yielding a tetrahedral intermediate resulting in the bond between the carbon and nitrogen of the substrate breaking, and therefore part of this protein will be free to do its business while the other part will be attached to serine by a covalent bond (figure 1,6, step 8). The covalent bond then has to be broken in order for the original protein to be released. In order to do this, H_2O comes into the active site and the nitrogen of histidine will attack the proton of the water, leading to activated hydroxide which will attack carbonyl carbon and rearrange the electronic environment generating tetrahedral intermediate again (figure 1.6, step 9). This results in breaking bonds between the protein and serine and completing the process (Polgar, 2005, Page and Di Cera, 2008).

Most protease classes such as cysteine, asparatic acid and metallo-protease function in a similar way with slightly different nucleophilic agents present in the active site. Cysteine proteases use cysteine as a nucleophilic residue to cleave the peptide bond. As the cysteine nucleophile is not strong enough on its own, it is activated by the action of histidine. On the other hand, aspartic acid proteases contain a highly conserved pair of aspartic acid residues that work together to transform the water into a good nucleophilic agent that can hydrolyse peptide bonds. Metallo-proteinases have a metal atom in the active site to bind the water and transform it into a more capable nucleophile so the water can hydrolyse the peptide bonds. Importantly, metallo-proteinases and asparatic acid proteases use water as the nucleophile to break peptide bonds while the others use their own collection of amino acids to hydrolyze peptide bonds (Page and Di Cera, 2008).

As serine proteases are the most abundant proteases and furin, which is thought to cleave SEMA3B is a serine protease, this project will focus on the family of serine proteases that furin belongs to, namely the subtilisin-like pro-protein convertases.

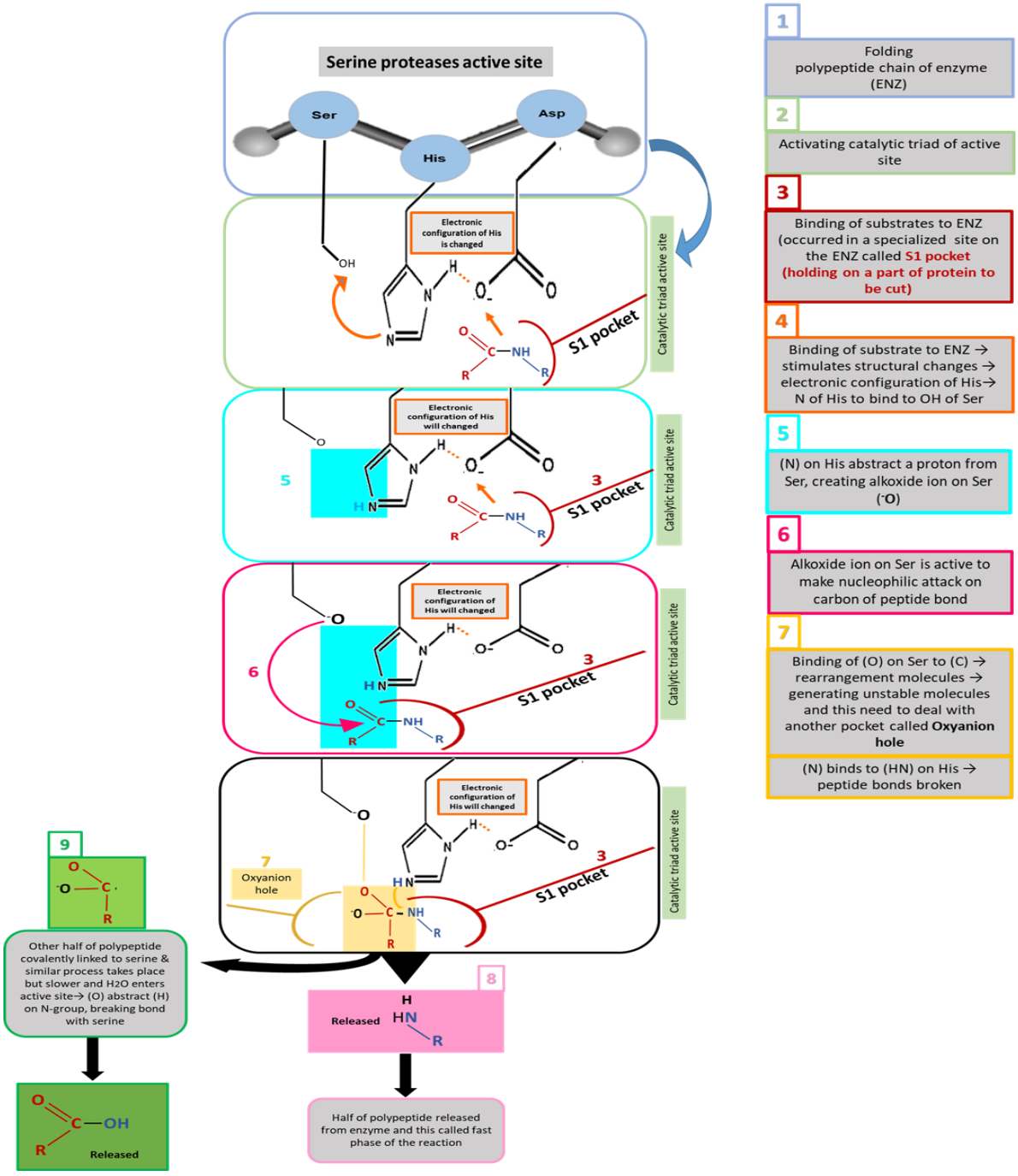

Figure 1.6: Catalytic mechanism. Steps of the catalytic reaction by the catalytic triad of serine protease. The nucleophile residues Ser, His and Asp are shown in step 1 where folding of polypepties chain of enzyme takes place. The initial step of activation of catalytic triad is shown in step 2. During the catalytic reaction process, S pocket is holding on a substrate to be cut is shown in step 3. Binding of substrate to enzyme, leading electronic configuration of His as shown in step 4. These changes creating alkoxide ion on Ser, resulting in negatively charged oxygen ion of the tetrahedral intermediate generated in steps 5, 6 and 7, which are stabilized by the oxyanion hole, releasing half of polypeptide shown in step 8. The other half link to Ser to complete the process as shown in step 9. See details in the text.

1.11.2 Subtilisin-like pro-protein convertases

The subtilisin-like pro-protein convertases are a family of calcium and pH-dependent serine endoproteases that are responsible for protein cleavage and maturation. Subtilisin-like pro-protein convertases function via autocatalytic cleavage of their N-terminal region, which they activate to mediate their functionality. The abnormal activation and production of pro-protein convertases has been associated with tumour progression. PPCs are inhibited by some inhibitors that can bind to the active site of enzymes and this is usually an irreversible inhibition. Several strategies aiming at inhibiting the activity of pro-protein convertase rely on competitive inhibition of PPCs activity using various protein-based inhibitors. α1-PDX, CMK, and the pro-segments are some examples of these inhibitors (Basak, 2005). Most of the precursor proteins bind and cleave at a general consensus motif at paired basic residues Lys(K)-Arg(R) or Arg(R)-Arg(R) to generate a mature form such as growth factors, certain receptors, bacterial toxins and viral surface glycoproteins such as gp160 (Seidah et al., 1998).

The Pro-protein convertase (PPC) family comprises nine members that were identified according to their structure and cleavage motifs (Seidah and Chrétien, 1999). Seven of these PPCs have been identified to cleave their substrates at single or paired basic residues at (RK)-(X)n-(KR)↓, where X= any amino acids and n = the number of amino acids 0,1,2,4 or 6 and the downward arrow emphasises the cleavage position. These seven PPCs are PCSK1 (also known as PC1/3), PCSK2 (also referred to as PC2), Furin (also known as PC3), PCSK4 (also referred to as PC4), PCSK5 (also known as PC5/6), PCSK6 (also called PACE4) and PCSK7 (also called PC7). PCSK8 (also called subtilisin kexin isoenzyme-1 “SKI-1” and also known as site-1 proteases “SIP”) is a pyrolysin-like protease and cleaves its substrate at a non–basic residue sequence (R/K)X(V/L/I)Z↓, where Z is any amino acid except Val, Pro, Cys, Glu, or Asp, and the spacer X is often a basic residue (Seidah et al., 2013). The final family member is PCSK9, which also belongs to the proteinase K family (also known as neura apoptosis-regulated convertase-1 NARC-1). This protein cleaves itself once in the endoplasmic reticulum at the sequence Val-Phe-Ala-Gln152↓ (VFAQ^{152}↓) within its pro-segment (Seidah et al., 2014). Importantly, all of these PPCs are responsible for orchestration of a series of events involving proteolytic cleavage that is a crucial step in the activation of many secreted proteins (Seidah and Chrétien, 1999, Seidah et al., 2008, Seidah et al., 2013).

1.11.3 Tissue distribution and cellular localisation of pro-protein convertases

PPCs are expressed in most mammalian cells where they play an important role in cleavage of their substrates within the constitutive or regulated pathways (Seidah and Prat, 2012) (table 1.2).

Table1.2: Expression and subcellular localization of pro-protein convertases

PPCs name	Tissue distribution	Cellular localization	Clinical significance
PCSK1	Neuroendocrine	Secretion granules	Implicated in diabetes and obesity (Creemers et al., 2012).
PCSK2	Neuroendocrine	Secretion granules	Diabetes (Leak et al., 2007).
Furin	Ubiquitous in many tissues	TGN, cell surface & endosomes	Responsible for activation of some viral infections e.g. HIV (Hallenberger et al., 1992) and has a role in tumour progression (Jaaks and Bernasconi, 2017).
PCSK4	Expressed in germ cells, testis, placenta, and ovary	Cell surface	Linked with infertility in male and has a role in fertilization, and embryonic development (Gyamera-Acheampong and Mbikay, 2009).
PCSK5	Intestine, ovary, kidney	PCSK5 a: secreted through the regulated secretory pathway. PCSK5 b: active at cell surface and extracellular matrix	Implicated in cancer including lung, head and neck cancer and viral infection (Bassi et al., 2005, Sun et al., 2009).
PCSK6	Widespread: muscle, heart, kidney, intestine, cerebellum	Cell surface and extracellular matrix	Implicated in arthritis pain (Malfait et al., 2012) and cancer (Couture et al., 2017).
PCSK7	Ubiquitous	TGN, cell surface, endosomes	Implicated in cancer (Demidyuk et al., 2013) and in iron metabolism (Guillemot et al., 2013).
PCSK8	Ubiquitous	cis- and medial-Golgi	Implicated in viral infection and cholesterol metabolism (Seidah et al., 2013).
PCSK9	Liver, intestine, kidney	TGN, extracellular	Implicated in lipid and cholesterol metabolism (Dubuc et al., 2004) and cancer (Sun et al., 2012).

1.11.4 Pro-protein convertases structure

All PPCs have multiple domains and share a similar N-terminal structure with a slightly variable C-terminal resulting in differing biological function. Each protease has an N-terminal pro-peptide that consists of a signal peptide that is necessary to direct the precursors to the appropriate cellular compartment, and for entry of PPCs into the endoplasmic reticulum where these enzymes are processed for releasing within the secretory pathway. This signal peptide is followed by a pro-domain or pro-segment domain consisting of 80-90 residues, which acts to mediate correct folding of the proteins as well as acting as a competitive inhibitor for the enzymatic activity until it is released by cleavage (Artenstein and Opal, 2011). Subsequently the first cleavage is usually after the pro-domain. Downstream of the pro-domain, the catalytic domain is located including the catalytic triad of serine, histidine and aspartic acid. Following the catalytic domain, all the PPCs, except for PCSK9, have a P-domain that helps the correct folding and stability of the enzyme in the endoplasmic reticulum and regulates Ca+ and pH. Following these largely conserved domains, the carboxyl terminal (C-terminal) of each PPC is less conserved and they have unique sequences controlling their subcellular routing and trafficking, in addition to its role in substrate binding (figure 1.7) (Gensberg et al., 1998, Page and Di Cera, 2008).

Some PPCs like furin, PCSK5 and PCSK6 contain a cysteine rich domain (CRD) consisting of repeats of a cysteine rich domain containing multiple cysteine residues. which is involved in regulating the activity of the PPCs. Moreover, furin, PCSK5, PCSK7 and PCSK8 have a transmembrane domain and cytosolic domain which both are involved in directing PPCs sorting and transit control within cell compartments in addition to direct cell surface tethering, while some PPCs such as PCSK1, PCSK2, PCSK4 and PCSK7 contain a ser/thr rich region, which is highly glycosylated and this domain is important for cell surface exposure, instead of the CRD. PCSK9 is unique as it possesses a cysteine-histidine rich domain (CHRD), which was found to be important for binding of the protein to low-density lipoprotein receptor (LDLR) and the trafficking of LDLR (figure 1.7) (Benjannet et al., 2004, Page and Di Cera, 2008).

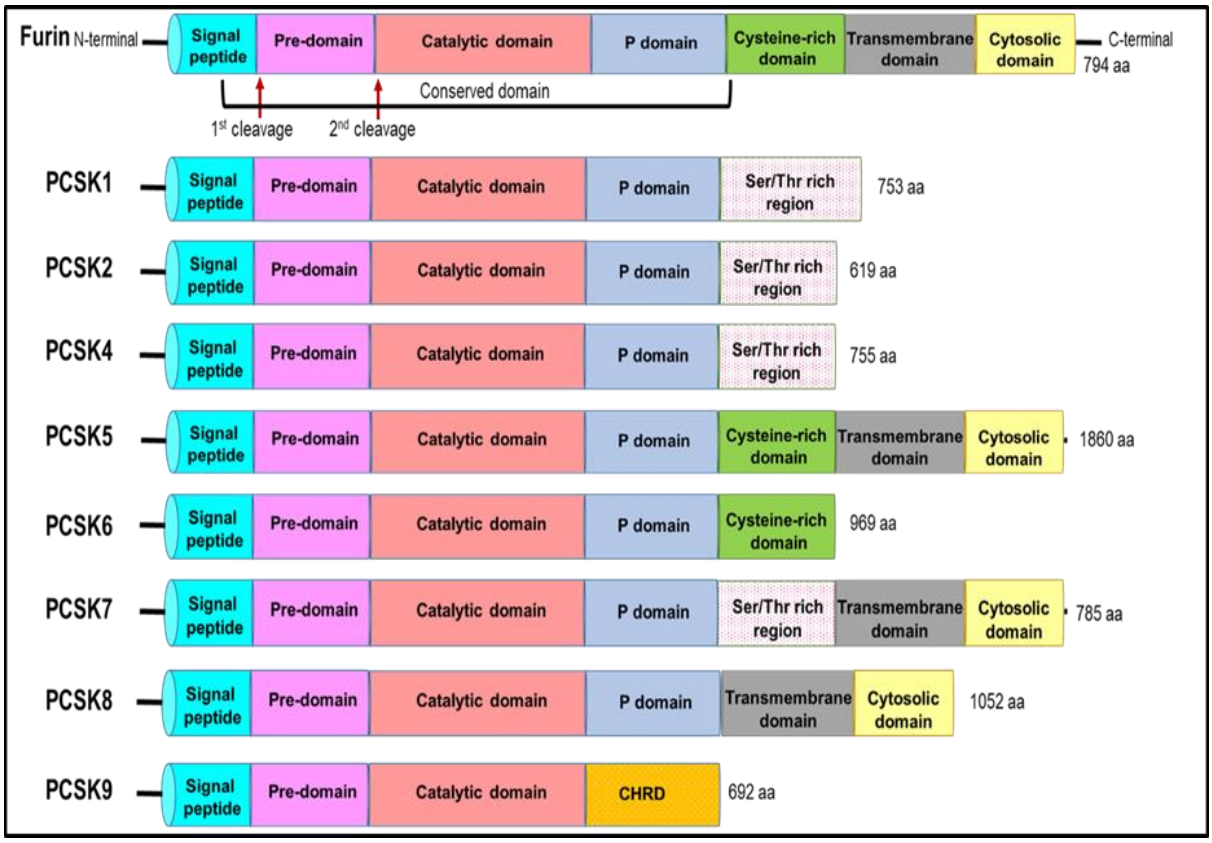

Figure 1.7: Schematic representation of the pro-protein convertases structure. All PPCs are kexin-like basic amino acid (aa) except PCSK8, which is pyrolysin-like and PCSK9, which is proteinase-like. The presence of a signal peptide, a pro-domain and catalytic domain is conserved in all convertases that display where the catalytic triad occurs. The C-terminal domain of each PPC has unique sequences regulating their cellular localization and trafficking. CHRD = Cys-His-rich domain. Reproduced from (Seidah and Prat, 2012).

1.11.5 Pro-protein convertases activation

Most proteases are synthesized as an inactive form and these inactive enzyme precursors are known as zymogen or proenzymes. These proenzymes are present in endoplasmic reticulum (ER) as full-length proteins, and two cleavages need to take place in order for the PPCs to be fully activated. The first cleavage occurs between the pro-domain and the catalytic domain and takes place in the ER. However, the enzyme will not be activated by this event, as the pro-domain will remain attached to the catalytic domain thereby acting like an inhibitor. The complex of pro-domain and the rest of the molecule then exit the ER moving to the Golgi apparatus to be processed by a second cleavage in order to generate the active enzyme. The second cleavage is Ca+ and pH dependent, and occurs in the trans Golgi network, completely removing the pro-domain thereby activating the catalytic domain (Polgar, 2005, Page and Di Cera, 2008). Following this, PPCs transport to either the plasma membrane for secretion, lysosomes (for endocytosis) or return to the ER using the KDEL sequence (figure 1.8). KDEL sequence contain four amino acids located at the C-terminal of proteins that acts as a signal for localization of proteins to the lumen of the ER. Most PPCs are activated similarly to each other, but some have slight differences. For example, PCSK2 needs 7B2 binding protein as a chaperone for activation, with the complex of PCSK2 and 7B2 undergoing an autocatalytic cleavage in the trans-Gogli after they exit from ER. Furthermore, PCSK1 and PCSK2 are generated and activated late in the secretory granules due to replacement of the oxyanion hole ASN residue with ASP in their structure (Seidah et al., 2008).

PPCs are secreted via two different pathways, and in both types of secretory pathways, all proteins exit from the trans-Golgi network and are then secreted via the constitutive or regulated pathways. In the constitutive pathway, the protein is contained in a vesicle, which will fuse to the cell membrane in order to release the protein molecules outside the cells. This pathway is considered to be the default pathway for the secretion of proteins (Gensberg et al., 1998). In contrast, the regulated pathway usually involves the protein being sorted and held in vesicles until an extracellular signal triggers and stimulates their secretion. In the PPC family, PCSK1, PCSK2 and PCSK5a are secreted from the cell in a regulated manner whereas furin, PCSK4, PCSK5b, PCSK6, PCSK7 and PCSK8 are active in TGN and secreted via constitutive vesicles, with the exception of PCSK9 as the inhibitory pro-domain remains attached

tightly with the catalytic domain, indicating that the circulating PCSK9 is enzymatically inactive due to this association, and only in an acidic compartment, PCSK9 can enhance degradation of its substrate (Zhou et al., 1999, Dikeakos et al., 2007, Seidah, 2017).

To summarise, the PPC family are serine proteases, which are released from cells to cleave proteins at specific sites to activate or inactivate them. Many of them are up-regulated in cancer and may therefore have a specific role in cancer. Furthermore, furin is thought to potentially cleave SEMA3B thereby inhibiting its activity as a tumour suppressor, so the expression and action of the PPCs will now be discussed in more detail.

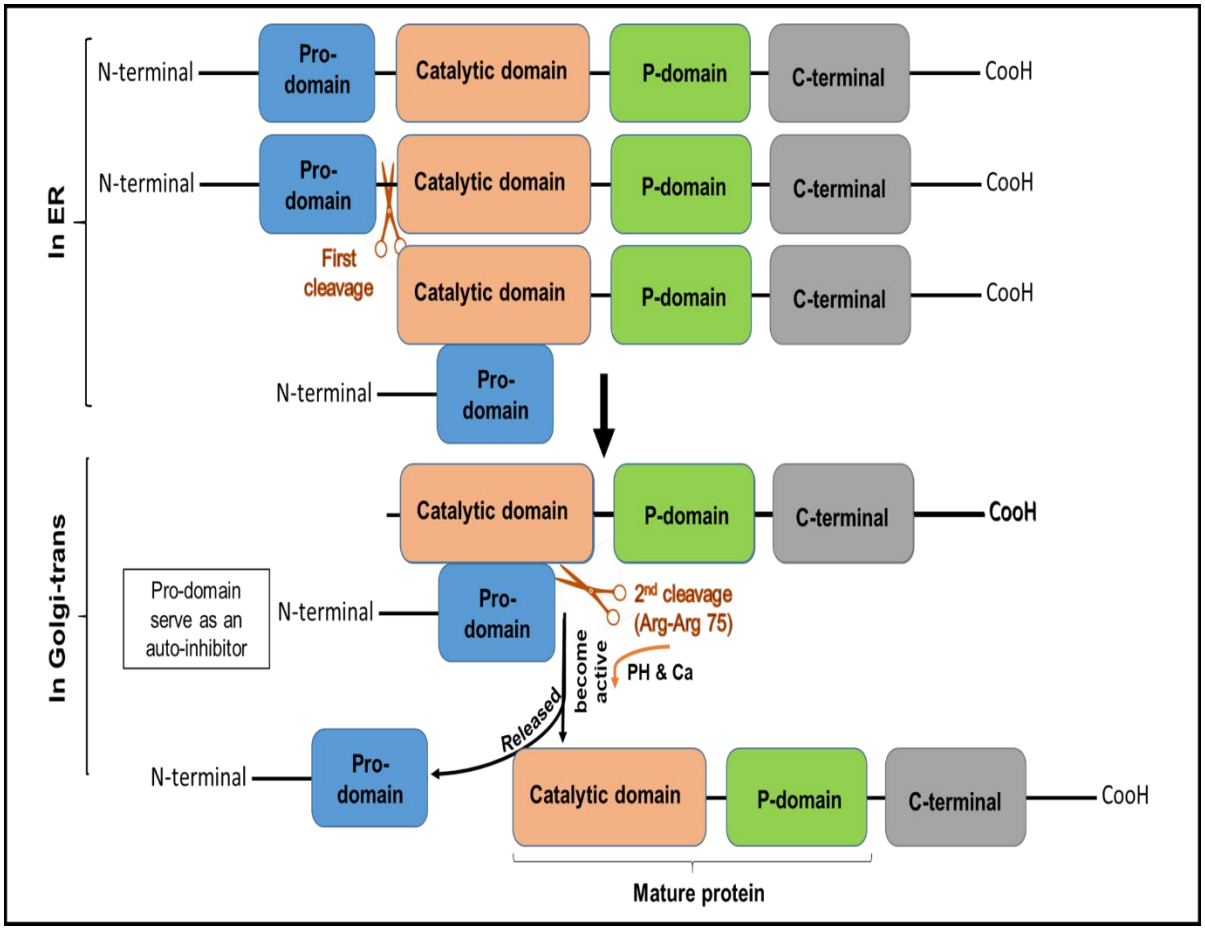

Figure 1.8: Activation of pro-protein convertases. Different processes are used by the pro-protein convertases to be activated. PPCs are initially synthesised as inactive precursors, and specific processing is required to convert these pro-proteins into active forms. All the maturation steps of PPCs start in the ER, where the first autocatalytic cleavage occurs. The zymogen of PPCs contains a signal peptide, a pro-domain, a catalytic domain, a P domain and a cytoplasmic tail. After the first cleavage, the pro-domain remains attached to the catalytic domain and act as an inhibitor. PPCs require proteolytic removal of the inhibitory pro-domain to become proteolytically active enzymes. The second cleavage takes place in Golgi in Ca+ and pH-dependent to release the pro-domain thereby activating the catalytic domain generating mature protein.

1.12 Furin an essential convertase

Furin is a calcium-dependent serine endoprotease, which needs approximately 1mM of calcium for full activity, and it is considered a key member of the pro-protein convertase family as it is expressed in many tissues throughout the body in both vertebrates and invertebrates. Its name, furin, refers to the encoded gene, which is known as *fur.* It is located on chromosome 15q26.1 and the protein is 794 aa in length (Paleyanda et al., 1997) (figure 1.7). Furin is initially synthesised as an immature inactive 100 kDa protein, which is cleaved to 98 kDa by removing the pro-domain at the Arg-Ala-Lys-Arg site (residues 104–107), and this is inactive due to the remainder of the pro-domain attached to the catalytic domain. The second cleavage takes place after Leu at the C-terminal of furin, generating two fragments with different molecular weights at 84 kDa and 60-70 kDa. Both forms are active, however the 84 kDa fragment is considered less active due to the lack of the transmembrane domain whilst the fragment detected at 60-70 kDa arises from additional cleavage(s) in the cysteine-rich region and indicates an active mature form of furin (Paleyanda et al., 1997). The way furin processes the proteins and cycles between the trans Golgi network and the cell surface via the constitutive secretion pathway makes it important and has a role in the maturation of bioactive peptides and proteins in both the exocytic and endocytic pathways (Plaimauer et al., 2001).

Several studies have demonstrated high furin activity in different cancers correlating with cancer aggressiveness and malignancy (Bassi et al., 2003, Siegfried et al., 2003). In addition, furin is expressed at low levels in normal tissues and at higher levels in cancers including lung and breast (Cheng et al., 1997). In agreement with a potential role of furin in cancer progression, other studies have suggested that inhibition of furin expression correlates with reduced cancer growth (Bassi et al., 2001a, Coppola et al., 2008). Varshavsky *et al*. (2008) showed that furin cleaves SEMA3B into 61 kDa and 20 kDa inactive fragments, which resulted in inhibition of the SEMA3B antiangiogenic effects. Treating the cancer cells with furin like pro-protein convertase inhibitor resulted in restoring the full-length form of SEMA3B (83 kDa-active form). This group suggested that furin was responsible for cleavage of SEMA3B (Varshavsky et al., 2008), however, the inhibitor used could inhibit other PPCs so it may not be furin that is responsible for SEMA3B cleavage.

1.13 Pro-protein convertase 1 (PCSK1)

PCSK1 which is also called prohormone convertase PC1/3, is encoded by the Pcsk1 gene which is located on chromosome 5q15 and is expressed as a 753 aa zymogen. PCSK1 undergoes cleavage in the ER like other PPCs to become active. It is released to the cell surface via the regulated secretory pathway and stored in secretory granules. PCSK1 is expressed in most of the neuroendocrine tissues and has a role in the activation of brain functions as it has been demonstrated that the expression of PCSK1 mRNA is high in the anterior subdivisions of the thalamus (Seidah and Chrétien, 1999, Podvin et al., 2018). However, it is mostly found in endocrine and neural tissue as well as in pituitary (Seidah and Chrétien, 1999).

In addition to the normal structure of PPCs, PCSK1 has Serine/Threonine-rich region at its C-terminal, which helps in sorting of PCSK1 into secretory granules (figure 1.7). The cleavage of the 94 kDa proPCSK1 generates two forms of proteins, 87 kDa which represents an enzymatically active form and a more completely cleaved 74-66 kDa form, which is much more functionally active than the 87 kDa form, but is less stable (Zhou and Lindberg, 1994, Seidah and Chrétien, 1999). PCSK1 is known to cleave several important substrates like pro-insulin, pro-opiomelanocortin, pro-renin, pro-enkephalin, so it is not surprising that it is linked to various human diseases. For example, the expression of PCSK1 has been associated with early onset of obesity, as a PCSK1 mutation resulting in loss of PCSK1 activity increases the risk of obesity (Creemers et al., 2012).

High expression of PCSK1 mRNA was found in small cell lung carcinoma (SCLC) with no expression found in non-SCLCs and normal lung (Creemers et al., 1992), suggesting a role in SCLC progression. Similarly, another study demonstrated increased PCSK1 protein expression in colon cancer and liver metastasis compared to the normal liver (Tzimas et al., 2005). As of yet the expression of PCSK1 has not been investigated in breast cancer progression.

1.14 Pro-protein convertase 2 (PCSK2)

PCSK2 (also known as prohormone convertases PC2) is localized on chromosome 20p12.1. The PCSK2 mRNA is translated into 619 aa and undergoes autocatalytic cleavage steps before it becomes fully active. PCSK2 is initially synthesised as an immature 75 kDa protein, which is then cleaved to mature PCSK2 (64-68 kDa) (Mbikay et al., 1997, Tzimas et al., 2005). However, this maturation process is extremely slow compared with other member of PPCs. For the intercellular maturation of PCSK2, it needs to bind to another protein namely 7B2 to be activated and is considered the only one member of PPCs that requires the presence of this protein for proper folding and maturation (Zhu and Lindberg, 1995). Despite the need for 7B2 for the activation of proPCSK2, 7B2 has also an inhibitory effect on PCSK2 function. Removal of the C-terminal peptide of 7B2 leads to disable the PCSK2 processing and therefore inhibition of activity (Zhu and Lindberg, 1995).

The expression of PCSK2 is largely limited to neuroendocrine tissues including the pancreatic islets (Mbikay et al., 1997). Since this protein is found mostly expressed in neuronal and endocrine cells, it is not surprising that it is associated with a neuroendocrine phenotype in some cancers. For example, PCSK2 mRNA was detected at high level in SCLCs, which show neuroendocrine features, more than in adenocarcinoma and squamous cell carcinoma (Mbikay et al., 1997). PCSK2 is also known to influence glucose homeostasis, and it has been involved in the cleavage of proinsulin to insulin. Any defect in this pro-hormone processing could lead to metabolic disorders and obesity, so it is not surprising the PCSK2 is linked to obesity (Anini et al., 2010, Leak et al., 2007).

PCSK2 protein expression also was detected in much higher levels in 85% of pheochromocytomas tumours, a neuroendocrine tumour of the medulla of the adrenal glands, than in normal adrenal human tissue (Konoshita et al., 1994). However, in contrast, one previous study has shown that PCSK2 mRNA is not present in human breast cancer (Cheng et al., 1997).

1.15 Pro-protein convertase 4 (PCSK4)

PCSK4 also known as PC4, SPC5 is located on human chromosome 19 and is translated into 755 aa. The lack of the secondary cleavage site in the pro-domain of PCSK4 makes it unclear how this protein becomes fully activated. Like other PPCs, PCSK4 cleaves its substrate at paired basic residues at (KR↓ and RR↓), however, it appears to cleave better at a monobasic site usually at a single R↓ residue (Gyamera-Acheampong and Mbikay, 2009). PCSK4 is synthesised as a proPCSK4 82 kDa, which is then cleaved to different fragments ~62 and 38 kDa. The fragment of 62 kDa is an enzymatically active protein with a high degree of efficiency. The fragment of 38 kDa is also active but with less stability (Basak et al., 2008). The PCSK4 substrates are limited with only two substrates that have been shown to be processed by PCSK4. One of these is pituitary adenylate cyclase activating polypeptide (PACAP) which is produced during spermiogenesis and has a role in the reproductive system, where PCSK4 is known to be most highly expressed (Thomas et al., 2013). The other is proinsulin like growth factor (proIGFs-I and II), which is also thought to be processed by PCSK4, in part due to its role in localization in the testis (Basak et al., 1999).

PCSK4 expression has been linked to fertility as its expression is limited to testicular cells in males, and ovarian and placenta cells in females (Gyamera-Acheampong and Mbikay, 2009). Indeed, a decrease in its expression in mice has been found to interfere with the ability of sperm to fertilize oocytes by reducing its ability to bind to the zone pellucide. Also in female mice, decreases in PCSK4 expression resulted in impaired folliculogenesis. All these findings suggest a role in reproductive physiology and in embryonic development. In contrast, the role of PCSK4 in the pathogenesis of cancer has not been clearly identified. To our knowledge there is only one study investigating this, which demonstrated that a defect in PCSK4 expression could be responsible for unprocessed insulin-like-growth factor II which is secreted from the tumour in a case of pleural solitary fibrous tumour. This, caused non-islet tumour hypoglycaemia, so it is possible that the low expression of PCSK4 could enhance pleural solitary fibrous tumour growth (Tani et al., 2008).

1.16 Pro-protein convertase 5 (PCSK5)

PCSK5 also known as PC5/6 is ubiquitously expressed in adrenal gland, uterus, brain, intestine, liver and lung and it is important for mammalian development. It is located on chromosome 9q21.13 and is translated into a 1860 aa protein. It has two identified alternatively spliced forms that are soluble PC5/6A (1860 aa) which is thought to regulate secretory granules, and membrane-bound PC5/6B (913 aa) which moves between the trans-Golgi network and the cell surface. Both transcripts share similar structures they both have a signal peptide, pro-segment, catalytic domain, P-domain and a cysteine rich domain (figure 1.7). In addition, PC5/6B has also a transmembrane domain and cytosolic domain that are important for sorting and direct cell surface tethering. PCSK5 is mainly active at the cell surface after the second auto-cleavage event in the Golgi apparatus (Artenstein and Opal, 2011).

However, the role of PCSK5 in cancer has not been fully investigated. In colon cancer, the expression of PCSK5 was detected in three different colon cancer cell-lines HCT8, LS174T and ColoDM320 suggesting it may have a role in colon cancer (Rovere et al., 1998). The study suggests that this role is via processing pro-neurotensin/neuromedin N (proNT/NN) which is a regulatory peptide known to promote carcinogenesis and stimulate the growth of human colon cancer cell-lines (Rovere et al., 1998). Moreover, high PCSK5 expression was also found in very aggressive lung cancer cell-lines as well as in head and neck cancer cells suggesting that PCSK5 might have a role in cancer development as its expression correlated with the aggressiveness of the cancer (Bassi et al., 2005). In contrast, one study showed that expression of PCSK5 was decreased in endometrial cancer, perhaps suggesting that the role of PCSK5 in cancer progression is dependent on the cancer type (Singh et al., 2012). However, only one study has investigated the expression of PCSK5 in breast cancer where its expression was not detected (Cheng et al., 1997).

1.17 Pro-protein convertase 6 (PCSK6)

PCSK6, also called paired basic amino acid-cleaving enzyme 4 (PACE4) is the only member of the pro-protein convertase family to share a chromosome with furin as they are both located on chromosome 15. PCSK6 is highly expressed in the anterior pituitary, liver, kidney and pancreas (Nour et al., 2005). PCSK6 is a 969 aa protein, which is made up of a single peptide followed by pro-domain, the subtilisin-like catalytic domain, p-domain and cysteine-rich domain (figure 1.7). Its activity is found at the cell surface and it is constitutively secreted into the extracellular milieu (Nour et al., 2005). As most of PPCs, PCSK6 is initially synthesised as inactive zymogen (106 KDa) that undergoes autocatalytic processing in the ER. Then, it undergoes a second cleavage to be active in the TGN at the cell surface as approximately 97 kDa (Mains et al., 1997, Nour et al., 2005). The mature protein of PCSK6 is found in a monomer form while in ER, it is found as a dimer suggesting an association between its cleavage and the tertiary or quaternary structure of the protein (Nagahama et al., 1998). PSCK6 was shown to be overexpressed in non-small cell lung cancer (NSCLC) and their expression correlates with disease prognosis (Lin et al., 2015). Interestingly, the expression of PCSK6 was also shown to be involved in increasing invasiveness in breast and prostate cancer (Lapierre et al., 2007). Silencing of PCSK6 gene reduced proliferation of prostate cancer cells indicating the importance of this gene in the progression of this cancer (D'Anjou et al., 2011). Similarly, knockdown of PCSK6 in MDA-MB-231 breast cancer cells was associated with decreasing proliferation, migration and invasion of these cells suggesting its role in cancer progression (Wang et al., 2015). Furthermore, in oestrogen-receptor-positive breast cancer, inhibition of PCSK6 showed delayed tumour progression with a decrease in cell proliferation (Panet et al., 2017).

PCSK6 can play an opposing role to furin in cancer development depending on the expression of other factors. For instance, expression of PCSK6 in a breast cancer cell-line resulted in increased expression of matrix metalloproteinase 9 (MM9), a member of a group of proteins responsible for the turnover of protein in the extracellular matrix, and subsequent increase in the metastatic potential of the cell-lines. The effect of PCSK6 was abolished in the presence of furin expression in the same breast cancer cell-line (Lapierre et al., 2007, Seidah and Prat, 2012). The expression of PCSK6 mRNA was detected in MCF-7, T47D and MDA-MB-231 cell-lines in similar

concentrations but undetectable in normal breast tissues suggesting the role that PCSK6 may have in inducing the pathobiology and progression of breast cancer (Cheng et al., 1997).

1.18 Pro-protein convertase 7 (PCSK7)

PCSK7 is a type-I membrane-bound protease, which is ubiquitously expressed in various tissues including neuroendocrine, liver and brain. It is located on chromosome 11 and is translated into 785 aa. As with all other PPCs, the protein sequence has different domains including signal peptide, predomain, catalytic domain, P-domain and in addition to that, PCSK7 has a Ser/Thr rich region, transmembrane domain and cytosolic tail (figure 1.7). PCSK7 is activated in the trans-Golgi network and it reaches the cell surface by the constitutive pathway (Rousselet et al., 2011). PCSK7 plays an important role in in iron homeostasis and metabolism which may influence its regulation (Guillemot et al., 2013). PCSK7 has multiple physiological functions as it has the ability to process certain precursor proteins by activating growth factors such as EGF which suggests that PCSK7 may have implications in cancer growth by enhancing the activity of EGF receptor. The role of PCSK7 has been also identified in prostate cancer, knockdown of PCSK7 in the prostate cancer DU145 cell-line resulted in decreased tumour cell proliferation *in vitro* (Couture et al., 2012). Moreover, the inhibition of PCSK7 resulted in decreased progression of hepatocellular carcinoma (Declercq et al., 2015). In contrast, PCSK7 mRNA expression was decreased in human lung cancer suggesting different pathways of tumour development and progression could be involved (Demidyuk et al., 2013). In breast cancer, PCSK7 mRNA was higher in cancer cell-lines than in normal breast tissues (Cheng et al., 1997). Similarly, the expression of PCSK7 mRNA in MDA-MB-231 breast cancer cells was increased compared to an oestrogen-receptor-positive breast cancer cell-line MCF-7 (Panet et al., 2017).

.

1.19 Pro-protein convertase 8 (PCSK8)

PCSK8 is called subtilisin/kexin-isozyme-1 (SKI-1) and also known as membrane-bound transcription factor site-1 protease (MBTPS1), or site-1 protease (S1P) and it belongs to pyrolysin-like of subtilisin-like proteases. PCSK8 is encoded by the *MBTPS1* gene, located on16q23.3 and translated into 1052 amino acids. PCSK8 is synthesised as a 148 kDa zymogen that is processed into a 120 kDa (inactive form) and 106 kDa protein form in the ER and then secreted as a 98 kDa form (active form) (Seidah et al., 1999). It is widely expressed and found abundantly in the anterior pituitary, thyroid, and adrenal glands (Seidah et al., 1999). PCSK8 is the only member of pro-protein convertases known to cleave its substrates at non-basic residues in the Golgi. The PCSK8 protein sequence shares the same conserved domain structure of other pro-protein convertases members. It comprises of a signal peptide, pro-domain, and a catalytic domain that contains Arg-Arg-Gly-Ser-Leu which differs to other members. In addition, the PCSK8 has no p-domain however, its C-terminal has a transmembrane domain and a cytosolic tail (Seidah et al., 1999). PCSK8 undergoes initial autocatalytic processing in the ER, and then a second autocatalytic event for maturation in the Golgi, where the catalytic activity takes place (Seidah et al., 1999). It has been implicated in viral infections and cholesterol and lipid metabolism. However*, in vivo,* the loss of PCSK8 expression is associated with embryonic development, as deficiency of PCSK8 enhanced early embryonic death by reducing axonal growth (Seidah et al., 2013).

A previous study revealed that in lung tumour tissue, the expression of PCSK8 mRNA is decreased compared to furin, which was increased, suggesting different pathways of different pro-protein convertases members may contribute differently in tumour progression and development (Demidyuk et al., 2013). However, in human metastatic melanoma there was a significant increase of PCSK8 mRNA compared to normal skin signifying the crucial role that PCSK8 might have on melanoma cell (Weiss et al., 2014). The role of PCSK8 in breast cancer is not yet identified.

1.20 Pro-protein convertase 9 (PCSK9)

PCSK9 is also known as neural apoptosis-regulated convertase 1 (NARC-1), it is the most recently discovered pro-protein convertase. It belongs to the proteinase K-like subfamily of subtilisin-like proteases. It cleaves itself at VFAQ152↓motif and it has only one substrate, which is the low-density lipoprotein receptor. It is located on chromosome 1p32.3 and translated into 692 amino acids. It is synthesised as a 74 kDa zymogen which is inactive and this processed to 62 kDa (active form) (Wicinski et al., 2017). PCSK9 is highly expressed in liver, kidney, cerebellum, and small intestine (Seidah et al., 2003). The protein sequence of PCSK9 shares similar domains as other PPCs members, in addition, it has a CHRD in its C-terminal that helps for the internalization and lysosomal trafficking of the PCSK9 (figure 1.7). However, PCSK9 is the only member of protein convertases that does not undergo a second cleavage. It is secreted as an inactive form in complex with the inhibitory prosegment which does not release from it (Seidah et al., 2003). PCSK9 has a role in regulating cellular apoptosis and proliferation. In some tissues such as in primary cerebellar neurons, PCSK9 induces an apoptotic effect (Dubuc et al., 2004). PCSK9 also acts as a key regulator for lipid metabolism which has been associated with cholesterol homeostasis and hypercholesterolemia (Schulz and Schlüter, 2017). The new strategy to reduce the high cholesterol level is by inhibiting the function of protein PCSK9 which disrupts binding to the LDL receptor, leading to a decrease in the cholesterol level. Moreover, in melanoma, PCSK9 decreased liver metastasis progression by sustaining high cholesterol levels (Sun et al., 2012). PCSK9 has been positively correlated with some cancers such as brain cancer, colon cancer and prostate cancer (Sun et al., 2012). However, surprisingly, the expression of PCSK9 was significantly decreased in hepatocellular carcinoma, with PCSK9 mRNA expression released compared with the normal liver cells (Bhat et al., 2015). As it has been shown that the elevation of cholesterol levels is strongly associated with an increase risk of breast cancer (Nelson et al., 2014), this could suggest a link between PCSK9 expression and breast cancer progression. However, its role in breast cancer is not yet been elucidated.

Based on the above studies, each member of pro protein convertases has a unique function, some of them have shared similar functions whilst others do not, and are implicated in a variety of diseases (figure 1.9).

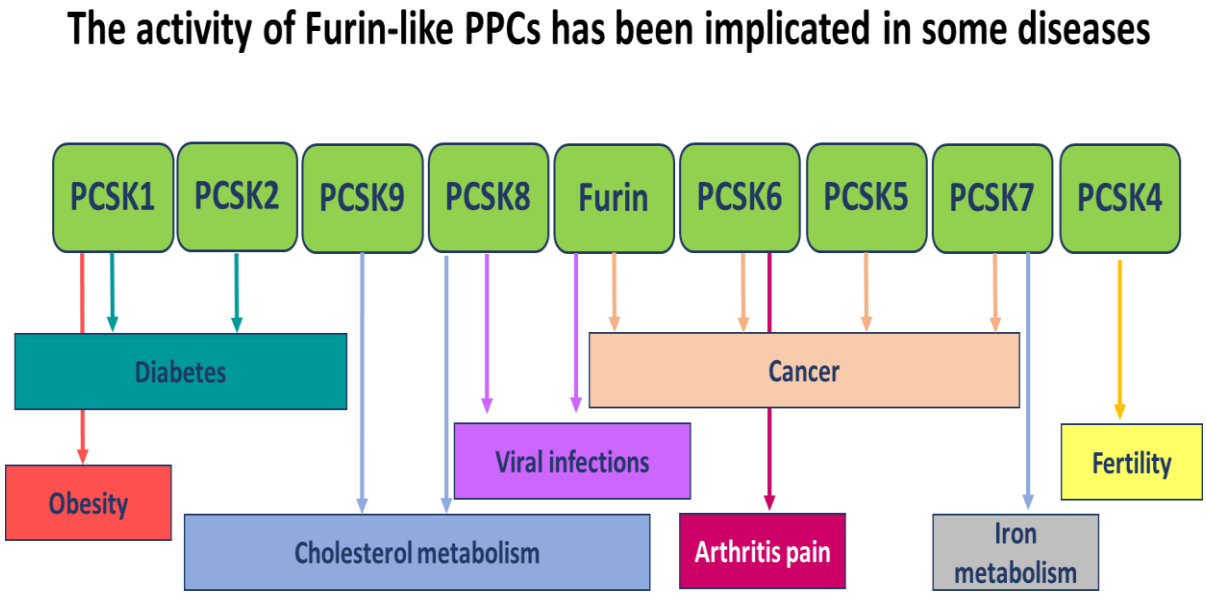

Figure 1.9: Physiological and pathological conditions linked to pro-protein convertases.

1.21 Inhibition of pro-protein convertases as a potential treatment for cancer

Many cancers appear to progress when there is an overproduction of one of the PPCs resulting in activation of their substrates or cleavage of a tumour suppressor (Basak, 2005, Bassi et al., 2005). Therefore suppression of PPCs activity may result in decreasing tumour growth. As a result, several approaches have been established to inhibit the activity of PPCs. These methods include silencing gene expression, which has been implemented for targeting the PPCs activity, or by using small molecules inhibitors that are directed against the proteases by blocking their active site from being occupied by substrates (Basak, 2005, Klein-Szanto and Bassi, 2017). The most attractive method as a potential therapy is using the small molecule compounds because of their metabolic and proteolytic stability. Various PPCs inhibitors have been reported in the literature, with differences in these inhibitors dependent on their chemical structure and their competitive binding for inhibition of PPCs activity (Basak, 2005). As furin is the most commonly studied PPCs most studies have attempted to inhibit this PPC using a peptidyl chloromethyl ketone called decanoyl-RVKR-cmk (CMK) (Basak, 2005) and/or a protein-based inhibitor called α1-antitrypsin Portland (α1-PDX). However, both of these inhibitors are limited as they do not demonstrate good selectivity between PPCs.

CMK is an irreversible competitive inhibitor of furin and other pro-protein convertases, but is a pan-PPC inhibitor (Basak, 2005). The drawback of using this inhibitor is its cytotoxicity and instability. CMK has been shown to successfully inhibit PPC-mediated cleavage of MT1-MMP, which is associated with the invasive and metastatic potential of tumour cells, thereby resulting in decreased MT1-MMP maturation, and a decreased invasive ability of the cells (Maquoi et al., 1998). Another study, showed that treating head and neck squamous carcinoma cells with CMK reduced their proliferation rate and invasive potential, suggesting a key role of the PPC family in these processes at least *in vivo,* although which PCC family member is not clear as it is a pan-inhibitor (Bassi et al., 2003). A previous study found that CMK-dependent blockage of furin-like pro-protein convertase activity in breast cancer cell-lines resulted in impaired SEMA3B cleavage, diminished the activity of PPCs, and therefore restored the suppression ability of SEMA3B, suggesting a key role of the PPC family in these processes, although which PPC family member is not clear due to pan-inhibition (Varshavsky et al., 2008).

In contrast, α1-PDX has been shown to be a potent inhibitor of furin and it contains a single minimal furin consensus motif in its reactive site Arg-Ile-Pro-Arg (Tsuji et al., 1999). Despite evidence of furin selectivity, some studies argue that α1-PDX is a general inhibitor of PPCs family members (Benjannet et al., 1997). α1-PDX showed potent inhibition of the processing of the furin substrates HIV-1 gp160 and gp120 by inhibiting the catalytic activity of PPCs. The study demonstrated that furin is the most efficient convertase and to a lesser extent PCSK6, PCK5-B and PCSK1 are involved in the intracellular processing of gp160 into gp120/gp41 in addition to the capability of furin to produce gp70 gp50-like proteins, suggesting that these are the most likely candidates to be involved in this process. However, this study found that α1-PDX is a potent inhibitor for both furin and PCSK6 (PACE4)-mediated processing of gp160 and gp120 (Vollenweider et al., 1996). *In vitro* experiments showed that the inhibition by α1-PDX of furin-expressing invasive HNSCC cell-lines also resulted in decreased the invasion of head and neck squamous cell carcinoma cells (Bassi et al., 2001a). Moreover, α1-PDX decreased the cell growth, proliferation and invasive ability of two transfected tumorigenic astrocytoma cell-lines of brain tumours by blocking furin function. The inhibition effect of α1-PDX on furin was confirmed by studying the effect of α1-PDX on a specific furin substrate called insulin-like growth factor which was not activated in PDX-expressing astrocytoma cells (Mercapide et al., 2002). *In vivo* experiments using animals injected with HT-29 cells and the α1-PDX inhibitor demonstrated reduced tumour growth (Khatib et al., 2001). Although there is limited evidence of using these inhibitors in breast cancer, it is clear that PPCs actively contribute to the malignant phenotypes of some cancers, so inhibiting their activity by using one of these inhibitors could reduce the progression of cancer.

.

1.22 Aim and hypothesis

In conclusion, previous studies suggest that SEMA3B acts as a tumour suppressor and that SEMA3B can be cleaved and rendered inactive by PPCs. However, there has been little investigation into the active role of SEMA3B and its relationship with other factors in the development of breast cancer. Furthermore, it is not clear whether SEMA3B inactivation by furin or other pro-protein convertase family members is responsible for cancer cells invasiveness or progression.

Thus, we hypothesize that PPC cleavage of SEMA3B results in inactivation of SEMA3B in invasive breast cancer (figure 1. 10)

To test our hypothesis, this project aimed to determine whether or not cleavage by furin-like pro-protein convertase leads to inactivation of SEMA3B in a spectrum of normal to metastatic breast cell-lines by assessing both mRNA and protein expression of SEMA3B and Furin like pro-protein convertases using qPCR, western blot and immunohistochemistry.

1.22.1 objectives

1- To establish and characterise an *in vitro* model of breast cancer progression.

- Proliferation, migration and invasion of different cell-lines representing the stages of breast cancer
- Investigate the expression of SEMA3B in breast cancer cell-lines and tissues representing various stages of breast cancer development.

2- To assess whether any factors/proteins are produced by the cells which cleave the full-length SEMA3B, and then determine the effect of full-length SEMA3B on proliferation, migration and invasion of the normal breast and cancer cell-lines.

3- To investigate furin-like pro-protein convertase gene and protein expression in the model.

4- To assess the expression of furin-like pro-protein convertases in human tissue samples.

5- To determine the effects of PPC inhibitors on SEMA3B cleavage.

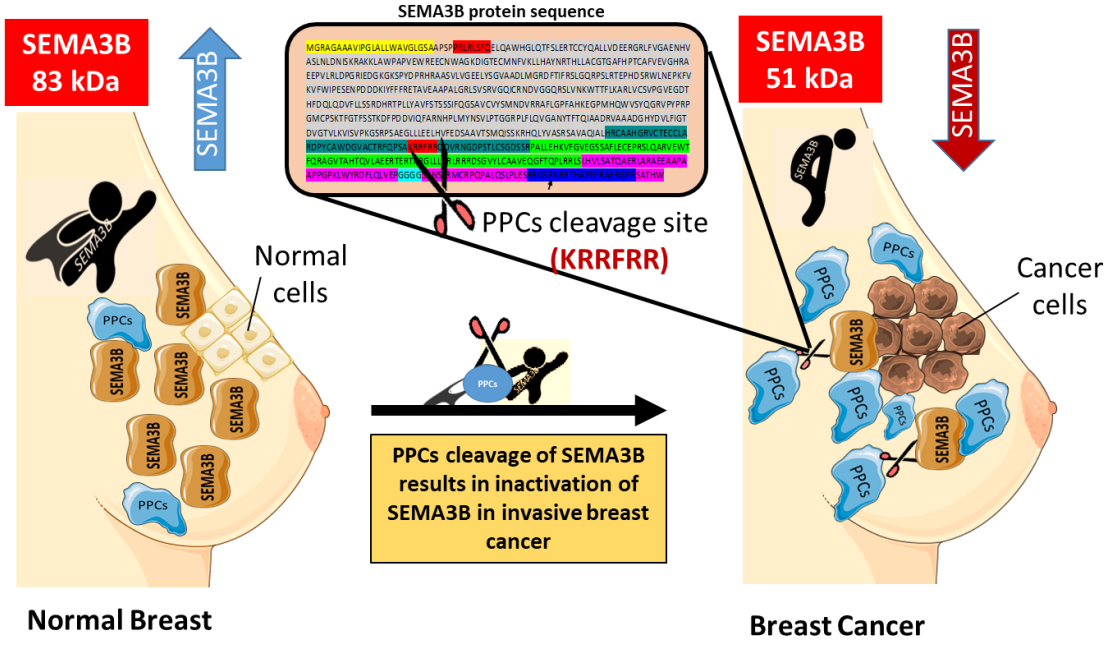

Figure 1.10: Hypothesis of the project. In normal breast cells, the expression of full-length SEMA3B (83 kDa, active fragment) is increased whilst in breast cancer cells, the expression of SEMA3B is decreased with tumour progression as SEMA3B undergoes proteolytic cleavage by PPCs at KRRFRR cleavage site present in the SEMA3B protein sequence by generating a 51 kDa SEMA3B (inactive fragment) with released tumour suppressor activity.

Chapter 2: Materials and Methods

2.1. General materials and suppliers

Materials	Catalogue number	Storage	supplier
1,4-Dithiothreitol (DTT)	NP0009	4 °C	Sigma-Aldrich, UK
1.5M Tris-HCL /PH8.8	EC-892	RT	Sigma-Aldrich, UK
10 % SDS	101685031	RT	Sigma-Aldrich, UK
100% isopropyl alcohol	-	RT	Fisher Scientific, UK
3,3-Diaminobenzidine substrate (DAB)		4 °C	Vector Laboratories, Peterborough, UK
30% acrylamide	EC-890	RT	Sigma-Aldrich, UK
70% ethanol		RT	Fisher Scientific, UK
Ammonium Persulfate (APS)	A3678-25G	RT	Sigma-Aldrich, UK
Antigen Retrieval Solution		4 °C	Dako, Spain
Breast common disease array of 102 cases	ab178113	4 °C	Abcam ,UK
Casein		4 °C	Vector Laboratories, Peterborough, UK
Chemiluminescent substrate	34077	RT	ThermoFisher scientific, UK
Corning matrigel basement membrane matrix growth factor reduced 5 ml.	(cat.356230)	-20 °C	Corning ,USA
Deionised Water (dH_2O)	-	RT	Millipore-QTM Water Purification system
Developing Solution		RT	AGFA, Mortsel, Belgium
Dimethyl Sulphoxide (DMSO)	D5879-500ML	RT	Sigma-Aldrich, UK
Films Hyperfilm™ ECL		RT	Sigma-Aldrich, UK
Filter Paper		RT	Sigma-Aldrich, UK
Fixing Solution		RT	AGFA, Mortsel, Belgium
Goat serum		4 °C	Vector Laboratories, Peterborough, UK
Haematoxylin		RT	Fisher Scientific, Loughborough, UK
Invasive breast tissues slides	-	RT	Obtained from patients attending the Royal Hallamshire Hospital from 1995-2003 (Research Ethics: SSREC 98/137).
Laemmli Sample Buffer	NP0007	4 °C	Sigma-Aldrich, UK
Marvel dried skimmed milk		RT	UK
Methanol		RT	Fisher Scientific, Loughborough, UK
Mitomycin C		4 °C	Sigma-Aldrich, UK
Phosphate Buffer Saline (PBS)	BE17-512F	RT	Lonza, Slough, UK
Pierce™ 20X TBST	28358	RT	ThermoFisher scientific, UK
Polyvinylidene fluoride (PVDF) membrane	1620177	RT	BIO-RAD,UK

Precision Plus ProteinTM Standard	1610374	-20 °C	Bio-Rad Laboratories Ltd., UK
Pre-invasive (DCIS.com) breast tissues slides	-	RT	Obtained from patients attending the Royal Hallamshire Hospital from 1995-2003 (Research Ethics: SSREC 98/137).
Protease Phosphatase Inhibitor Cocktail	1862209	4 °C	Sigma-Aldrich, UK
Rabbit serum		4 °C	Vector Laboratories, Peterborough, UK
RIPA Buffer, Cell Lysis Buffer	89900	4 °C	Fisher Scientific, UK
Running Buffer	EC-870	RT	Flowgen bioscience, UK
Stripping Buffer	21059	RT	Fisher Scientific, UK
TBS-Tween 20x	28360	RT	Fisher Scientific, UK
TEMED	101199677	RT	Sigma-Aldrich, UK
Transfer buffer	EC-880	RT	Sigma-Aldrich, UK
Trypan Blue		RT	Life Technologies, UK
Trypsin (0.05%)/EDTA (0.02%)		4 °C	Sigma-Aldrich, UK
Tween20		RT	Sigma-Aldrich, UK
Wax pen	-		Vector
Xylene	470045-580	RT	VWR,UK

2.1.1 Equipment and suppliers

Equipment	Catalogue number	Storage	Suppliers
25, 75 And 175 Cm2 Tissue Culture Flasks	156367 156499 159910	RT	ThermoFisher Scientific, Denmark
348 PCR Plate	Z374911-1PAK	RT	Sigma-Aldrich,UK
6, 12 and 24 wells plates (Nunclon tm Delta surface)	3516	RT	ThermoFisher Scientific, Denmark
96 well cell culture	3595	RT	Life science ,USA
ABI Prism 7900HT Sequence Detection System	-	-	Applied Biosystems, Life Technologies, UK
Cell culture inserts, Falcon®	734-0038	RT	VWR International Ltd.UK
Centrifuges - Harrier 18/80	-	-	Sanyo , Electric Biomedical Co, Japan
CO_2 incubator	-	-	SANYO Electric Biomedical Co, Japan
Counting slides dual chambers	1450003	RT	Bio-Rad, UK
CryoPure Tube 1.8 ml	72.379	RT	Sarstedt, Leicester, UK
Disposable pipets 10 ml		RT	Thermo fisher scientific, Denmark
Falcon® 24 Well Treated Cell Polystyrene Permeable Support Companion Plate	353504	RT	Corning ,USA
FLUOstar® Galaxy microplate reader	-	-	BMG LABTECH, London, UK
Freezer (-20 °C and -80 °C)	-	-	Sanyo , Electric Biomedical Co, Japan
Grant JB Series Water Bath	-	-	Wolflabs, UK

Heat Block	-	-	Hybride Thermal Reactor, UK
Laminar Flow Hood (Class II)	-	-	Walker Safety Cabinet Ltd., UK
Mr. Frosty™ Freezing Container	5100-0001	-80 °C	ThermoFisher Scientific, Denmark
Nanodrop©Lite Spectrophotometer	-	-	Nanodrop Technologies, USA
Nikon Eclipse TS 100 Inverted Microscope	-	-	Nikon UK Ltd, UK
Pipettes Tips (P2-P1000)		RT	Sarstedt, Leicester, UK
Shaker	-	-	Stuart, Staffordshire, UK
TC20™ Automated Cell Counter	-	-	Bio-Rad, UK
Trans-Blot® Turbo™ Transfer System	-	-	BIO-RAD, UK
Tubes 50 ml	352070	RT	Sarstedt, Leicester, UK
Universal tubes 25-50 ml		RT	Sarstedt, Leicester, UK
Vortex	-	-	VWR , Lutterworth, UK

2.1.2 Commercial kits and suppliers

Commercial Kits	Catalogue number	Storage	suppliers
CellTiter96 Aqueous One Solution cell viability assay	G3582	-20 °C	Promega, UK
Ez-PCR Mycoplasma Test Kit	1721460	-20 °C	Geneflow Ltd, Litchfield, UK
High Capacity RNA-To-cDNA Kit	4368814	-20 °C	Applied Biosystems, Life Technologies, UK
Micro BCA Protein Assay Kit-500 ml)	23235	RT	Thermo-Scientific, UK
Nuclease-Free Water	AM9937	RT	Ambion™,
Qiagen RNeasy mini kit	74104		Qiagen, Germany
SYBR® Green qPCR Mastermix (Precision 2X q-PCR Mastermix)	PP00508	-20 °C	PrimerDesign, UK

2.1.3 Cell culture media

All media were stored at 4 °C.

Cell culture media		Supplier	
Dulbecco's Modified Eagle's Medium (DMEM)		Lonza, Slough, UK	
Roswell Park Memorial Institute 1640 (RPMI 1640) Medium without L-Glutamine (1x)		Lonza, Slough, UK	
Supplements for cell culture media of DMEM and RPMI 1640:			
Component	**Growth medium**	**Storage**	**Suppliers**
Foetal Bovine Serum (FBS)	50 ml (10% final)	Aliquoted and stored at -20 °C until required	Biosera, Ringmer, UK
Glutamine (G)	5 ml (2 mM final)	Aliquoted and stored at -20 °C until required	Sigma-Aldrich,UK
Penicillin/Streptomycin	5 ml (100 IU/ml penicillin and 100 µg/ml streptomycin)	Aliquoted and stored at -20 °C until required	Invitrogen, Paisley, UK
Dulbecco's Modified Eagle Medium; Nutrient Mixture F-12 (DMEM/F12)		Lonza, Slough, UK	
Supplements for cell culture media of DMEM/F12:			

Cholera Toxin	50 µl (100 ng/ml final)	Aliquoted and stored at 4 ^{0}C until required	Sigma-Aldrich, Poole, Dorset, UK
Bovine Insulin	500 µl (10 µg/ml final)	Aliquoted and stored at -20 °C until required	Sigma-Aldrich, Poole, Dorset, UK
Epidermal Growth Factor (EGF)	100 µl (20 ng/ml final)	Aliquoted and stored at -20 °C until required	Pepro.Tech EC Ltd., London, UK
Horse Serum	25 ml (5% final)	Aliquoted and stored at -20 °C until required	Sigma-Aldrich, Poole, Dorset, UK
Hydrocortisone	250 µl (0.5 µg/ml final)	Re-suspended in absolute ethanol and aliquoted and stored at -20 °C until required	Sigma-Aldrich, Poole, Dorset, UK
Penicillin/ Streptomycin	5 ml (100 IU/ml penicillin and 100 µg/ml streptomycin)	Aliquoted and stored at -20 °C until required	Invitrogen, Paisley, UK
Human endothelial cell growth medium (C-22010)		Promocell, UK	
Endothelial cell growth medium supplementMix (C-39210)		Promocell, UK	

2.1.4 Quantitative polymerase chain reaction (qPCR) primers

Primers		
Forward	**Reverse**	**Suppliers**
SEMA3B primer (cat .HQP070437)		
GCGGCAAGACGTAAGGAATG	CTGGAAAGTCCACTCCACGC	GeneCopoeia, USA
Furin primer (cat. HQP012121)		
GCATTGTGGTCTCCATTCTG	CGTGCCTGTTGTCATTCATC	GeneCopoeia, USA
GAPDH primer (housekeeping gene)		
TGCACCACCAACTGCTTAGC	GGCATGGACTGTGGTCATGAG	GeneCopoeia, USA
PCSK1 primer (cat.HQP012539)		
TCACACATGGGGAGAGAACC	GGCTGCTTCATATGCTCTGG	GeneCopoeia, USA
PCSK2 primer (Accession No.NM_00120152)		
CCTGTACGACGAGAGCTGC	CCCAGAATGCCTCAGAGTGC	Primer design ,UK
PCSK4 primer (cat.HQP013677)		
GACCTGGAGATCTCGCTCAC	GGTTCTCATCCCAGAAGTGG	GeneCopoeia, USA
PCSK5 primer (cat.HQP059944-01)		
CCTGCCCCATGACAAGGATT	ACTTCCTTGGCATCTCTGGC	GeneCopoeia, USA
PCSK6 primer (cat.HQP070611)		
CGCAGGCCCTTTACTTCAAC	CGGCAGCGACTGTTCTTGT	GeneCopoeia, USA
PCSK7 primer (cat.HQP02211)		
CTTCAGCCATAGCCACCAG	CGGAATCGCCTTGTTTTC	GeneCopoeia, USA
PCSK8 primer (cat.no. SY-hu-600)		
TGCCACAGAACGGAGACAAC	GCCGCTTTCTTGGTCACAGA	Primer design ,UK
PCSK9 primer (Cat.no. SY-hu-600)		
AAGTTGCCCCATGTGGAGTA	AGCGGTCTTCCTCTGTCTG	Primer design ,UK
***Forward and reverse primers have different directions in which they initiate the replication.**		

2.1.5 Western blot primary antibodies

Primary Antibodies	Catalogue Number	Dilution	Suppliers
SEMA3B antibody (Rabbit polyclonal)	ab48197	1:1000	Abcam ,UK
Furin antibody (Rabbit polyclonal)	H-220-20801	1:1000	Santa Cruz,UK
PCSK1 antibody (Rabbit polyclonal)	Ab55543	1:1000	Abcam, UK
PCSK2 antibody (Rabbit polyclonal)	ab135808	1:1000	Abcam, UK
PCSK4 antibody (mouse polyclonal,)	ab169708	1:1000	Abcam, UK
PCSK5 antibody (Rabbit polyclonal)	LS-C408843	1:500	Lifespan BioSciencesInc, UK
PCSK6 antibody (Rabbit monoclonal)	ab151562	1:1000	Abcam, UK
PCSK7 antibody (rabbit polyclonal)	ab116567	1:1000	Abcam, UK
PCSK8 antibody (Rabbit polyclonal)	.ab140592	1:500	Abcam, UK
PCSK9 antibody (Rabbit polyclonal)	ab135647	1:1000	Abcam, UK
Anti-beta actin (Rabbit polyclonal).	ab16039	1:2000	Abcam, UK
Recombinant protein			
Recombinant Human Semaphorin 3B Fc Chimera Protein, CF	9518-S3-025	0.5,1 and 2 µg	R&D system
PPCs Inhibitors			
Decanoyl-RVKR-CMK inhibitor	3501	135 and 200 µM	Biotechne
Human alpha-1 PDX Recombinant Protein	RP-070	8.0-20µM	Thermo Fisher Scientific

2.1.6 Commercial human tissue slides for IHC

Tissue slides	Storage	Supplier
Breast common disease array of 102 cases (cat.ab178113)	4^{o}C	Abcam ,UK

2.1.7 Immunohistochemistry primary antibodies

Primary Antibodies	Catalogue number	Suppliers
SEMA3B antibody (Rabbit polyclonal)	ab48197	Abcam,UK
Furin antibody (Rabbit polyclonal)	H-220-20801	Santa Cruz,UK
PCSK1 antibody (Rabbit polyclonal)	ab55543	Abcam,UK
PCSK2 antibody (Rabbit polyclonal)	ab135808	Abcam,UK
PCSK4 antibody (Rabbit polyclonal)	HPA005572	Sigma-Aldrich, UK
PCSK5 antibody (Rabbit polyclonal)	LS-C408843	Lifespan Bioscience,UK
PCSK6 antibody (Rabbit monoclonal)	ab151562	Abcam,UK
PCSK7 antibody (Rabbit polyclonal)	12044-1-AP	Proteintech, UK
PCSK8 antibody (SKI-1 Antibody mouse monoclonal)	A-11-sc-271916	Santa Cruz,UK
PCSK9 antibody (Rabbit polyclonal)	ab135647	Abcam,UK

2.1.8 Secondary antibodies

Secondary antibodies	Catalogue number	Dilution	Technique	Suppliers
Polyclonal anti-mouse Immunoglobulins	P0260	1/2000	WB	Dako
Polyclonal anti-mouse biotinylated IgM	NA931V	1/2000	IHC	GE Healthcare
Polyclonal anti-rabbit IgG-horseradish Peroxidase (HRP)	P0448	1/2000	WB	Dako
Polyclonal anti-rabbit biotinylated IgM	BA-1000	1/2000	IHC	Vector Labs
Polyclonal anti-goat biotinylated secondary antibody	BA-5000	1/2000	IHC	Vector Laboratories, Peterborough, UK

2.2. Cell-lines and cell culture

2.2.1. Cell-lines

Cell-lines were selected to represent a range of breast cancer subtypes and aggressiveness. Human breast cell-lines: MCF-10A, MCF-10AT, DCIS.com, MCF-7, T47D and MDA-MB-231 and MDA-MB-231-BM were used in all the experiments**.**

Table 2.1: Cell Lines

Cell-lines		Catalogue number and suppliers
MCF-10A	Epithelial cells derived from a patient with fibrocystic disease	(ATCC® CRL-10317™).
MCF-10AT	Atypical ductal hyperplasia cell -line	Obtained from Ann Arbor institute. USA
DCIS.com	Ductal carcinoma *in situ* cell-line	Provided by Karmanos Cancer Institute, USA.
MCF-7	Invasive ductal carcinoma with low metastatic potential	(ATCC® HTB-22™).
T47D	Invasive ductal carcinoma with low metastatic potential	(ATCC® HTB-133™).
MDA-MB-231	Metastatic adenocarcinoma with pleural effusion	(ATCC® HTB-26™).
MDA-MB-231-BM	Bone homing metastatic cell-line	Obtained from Professor Janet Brown. University of Sheffield
Hep-G2	Hepatocellular carcinoma cell-line	Obtained from Dr Karen Sisley. University of Sheffield
HUVEC	HUVE-c pooled -Human Umbilical Vein Endothelial Cells	C-12203, Promocell, UK

The **MCF-10A cell-line** was derived from a patient with fibrocystic disease and is a non-tumorigenic normal breast epithelial cell. It is used as a model for the *in vitro* study of normal breast cell function and transformation. These cells do not express the oestrogen receptor. Cells were immortalised after proliferating for more than four years and maintained in a medium with low calcium concentration so as to increase their longevity (Soule et al., 1990).

The **MCF-10AT cell-line** is an atypical ductal hyperplasia that represents the pre-malignant stage of breast cancer. These cells were implanted in mice for a 12-16 week period which generated lesions similar to ductal hyperplasia. MCF-10A was transfected by T24 c-Ha-ras oncogene for a period of one year, during which time the cells sporadically transformed into carcinomas. These cells are therefore used as a model for the conversion of normal breast ductal epithelial cells into malignant cells (Dawson et al., 1996).

The **Ductal carcinoma *in situ* (DCIS) cell-line** is a non-invasive model that originated from premalignant MCF10AT cells. MCF-10AT cells were injected as xenografts into severe combined immune deficient mice in order to generate DCIS (Miller et al., 2000).

The **MCF-7 cell-line** is derived from a metastatic adenoma patient with a pleural effusion. It is a widely studied model for a hormone-dependent human breast cancer. It represents an invasive ductal carcinoma with low metastatic potential, is luminal type A, oestrogen and progesterone receptor positive and HER2 negative, with a wild type p53 (Lim et al., 2009).

The **T47D cell-line** is derived from a metastatic ductal carcinoma patient with pleural effusion. It represents an invasive breast carcinoma with low metastatic potential, and is classified as luminal type A, oestrogen receptor positive, progesterone receptor negative and HER2 negative, with a mutant p53 (Lim et al., 2009).

The **MDA-MB-231 cell-line** is derived from a metastatic patient with metastatic adenocarcinoma with pleural effusion. It represents an invasive breast carcinoma with high metastatic potential. It is classified as basal type, claudin-low, triple negative receptor (ER, PR and HER2) and has mutant p53 (Lim et al., 2009)

The **MDA-MB-231-BM cell-line** is a specific bone homing metastatic cell-line. In order to establish bone metastatic cell-lines, MDA-MB-231 cells were injected into the tail vein of nude mice and then the cells were collected, cultured and re-injected several times into the mice. The cells were passaged seven times and, once injected into the tail, they were able to make their way to the bone (Nutter et al., 2014).

The **Hep-G2 cell-line** was isolated from a patient with hepatocellular carcinoma. It was used as a positive control for pro-protein convertases since it known that the expression of furin-like pro-protein convertases is abundant in these types of cells (Nutter et al., 2014).

Human umbilical vascular endothelial (**HUVEC**) cell-lines are isolated from large umbilical veins. The cells were supplied from pooled donors and each cryovial contained more than 500,000 viable cells after thawing. HUVEC were used as a positive control as it has previously been known that SEMA3B inhibits migration and angiogenesis of HUVEC cells.

All cell culture work was carried out in a class II safety cabinet under sterile conditions**.** **MCF-10A cells** were cultured in Dulbecco's Modified Eagle Medium (DMEM-F12),

which is a mixture of DMEM medium and Ham's F-12 medium, containing a high amount of glucose, amino acids and vitamins. It is supplemented with horse serum, penicillin and streptomycin, insulin, hydrocortisone, EGF and cholera toxin (in order to promote cell growth by increasing the intracellular cAMP level in the mammary epithelial cells) to a total volume of 500 ml, and at the concentrations stated in table 2.1.3.

MCF-10AT and DCIS.com cell-lines were used to culture in the same medium as MCF-10A. Following advice from internal examiners of the initial stages of this project, however, the same culture medium was used for all cell-lines in order to minimise the variables and ensure that comparisons could be made based on the same conditions. Accordingly, cells were re-cultured in RPMI-1640 and both MCF-10AT and DCIS.com cells grew normally, except for MCF-10A cells which died. Since it was evident that these could not survive in RPMI medium they were kept in their normal culture medium. The **MCF-10AT, DCIS.com, MCF7, T47D and MDA-MB-231 cell-lines** were cultured in supplemented RPMI-1640 as stated in table 2.1.3. The **MDA-MB-231-BM cell-line** was cultured in supplemented DMEM medium (table 2.1.3). All cells were incubated at 37 °C with 5% CO_2 until use, and all the prepared media were stored at 4 °C. The cells were kept in exponential growth by re-culturing of stock cultures two to three times a week. The morphology of the cells used throughout this thesis is shown in figure 2.1.

HUVEC cell-line was cultured in supplemented human endothelial cell growth medium, containing a low foetal calf serum (2% v/v), EGF, hydrocortisone and endothelial cell growth Supplement/ Heparin (ECGS/H) to a total volume of 500 ml. HUVEC cells were incubated at 37 °C with 5% CO_2.

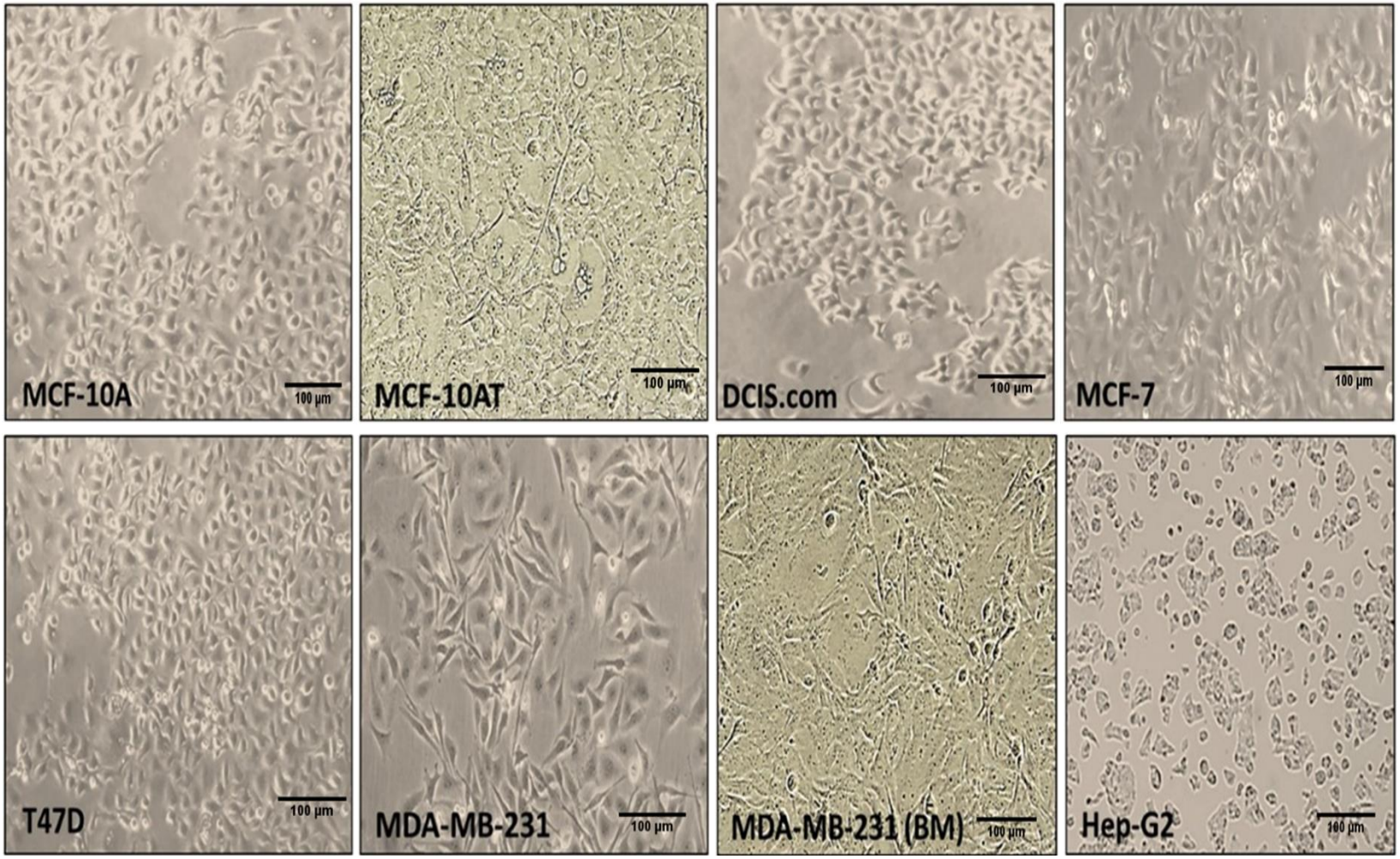

Figure 2.1: Microscopic appearance of the cell-lines used. Objective 10x. All are 70-80% confluent. Scale bar =100 µm.

2.2.2 Cell culture

All the culture work was done in a sterile class II laminar flow hood using aseptic techniques. The cabinet was switched on and left for 30 minutes before use to allow the air to circulate. The cabinet and all the equipment was cleaned with industrial methylated spirit (IMS) before use. All cell-lines were grown in T75 or T25 flasks in complete medium and incubated in a humidified atmosphere at 37 °C and 5% CO_2. The cells were monitored daily to make sure that they were growing well and were free of contamination. They were fed with the full growth medium every 48 hours until they reached 70-80% confluence and were ready for sub-culturing.

2.2.2.1 Passaging of mammalian cells

All cell-lines were grown in T75 flasks in complete medium as described above in section 2.2.2. After reaching 70% confluency, cells were washed twice with 10 ml Dulbecco's Phosphate Buffered Saline (DPBS) without calcium and magnesium in order to remove any residual serum that could interfere with the trypsin action. The cells were then trypsinised with 0.05% (v/v) trypsin in 0.02% EDTA solution and incubated at 37 °C and 5% CO_2 for about 2-5 minutes to allow complete detachment from the surface of the flask. This mixture of trypsin and EDTA was added in order to remove the calcium and magnesium from the cell surface, which allows trypsin to hydrolyse specific peptide bonds and therefore release the cells adhering to the culture vessel. Cells that are difficult to detach may be left longer at 37 °C in order to facilitate dispersal. Some cells, like MCF-10A, DCIS.com and T47D, were incubated for up to ten minutes in the trypsin to ensure that they had all detached from the surface of the flask. The flask was checked under the microscope and tapped sharply to release the cells. Long exposure to trypsin, leads to cell death, which can often be recognised by aberrant morphology. The trypsin was deactivated by adding 7.5 ml of complete medium containing 10% FBS serum, in addition to protease inhibitors, particularly α1-antitrypsin, which inhibits the trypsin activity. This step was followed by extensive pipetting up and down and then centrifugation at 1000 x g for five minutes. The supernatant was removed, and the cell pellet was re-suspended in 5 ml of the appropriate complete medium. Depending on the growth rate of each cell-line, 0.5-1 ml of the cell suspension was added to 10 ml of complete medium in a T75 flask so as to generate a split ratio of 1:2 - 1:10 (table 2.2.). When it was important to generate cells at 70% confluent by a specific date, however, they were seeded at a particular

number per flask rather than using the split ratio depends on the set up of the experiment.

For HUVEC cells, an appropriate volume of growth medium was filled in T25 cell culture flask and placed in an incubator (37°C, 5% CO_2) for 30 minutes to adjust the temperature of the medium. HUVEC cells were grown in T25 flask in complete medium as described above in section 2.1.3 and 2.2.1. After reaching 70% confluency, cells were washed twice with 5 ml DPBS to wash the cells and the flask was agitated carefully for 15 seconds. The DPBS was aspirated from the flask and trypsin/EDTA was added and the flask was kept at room temperature for 2-3 minutes, allowing cell detaching. The cells were examined under a microscope and when they started to detach, the flask was tapped gently to loosen the remaining cells. Medium containing 10% serum was added for neutralization and the flask was gently agitated. The cell suspension was aspirated and transferred to a centrifugation tube and then centrifuged at 220 x g for three minutes. The supernatant was discarded and the cell pellet was re-suspended in 1 ml of the appropriate HUVEC complete growth medium in new cell culture flask containing prewarmed growth medium. The flask was then placed in an incubator (37°C, 5% CO_2) and the media was changed every two to three days (table 2.2.). The cells were used between passages 2 to 6.

Table 2.2: Split ratio for the cell used:

Cell-lines	Split ratio	Medium Renewal
MCF-10A	1:3 to 1:4	2 to 3 times/week
MCF-10AT	1:4	2 to 3 times/week
DCIS.com	1:4	2 to 3 times/week
MCF-7	1:3 to 1:6	2 to 3 times/week
T47D	1:3 to 1:5	2 to 3 times/week
MDA-MB-231	1:2 to 1:4	2 to 3 times/week
MDA-MB-231-BM	1:10	2 to 3 times/week
HUVEC	1:3	2 to 3 times/week

2.2.2.2 Cryopreservation and retrieval of cells

In order to keep the cells for a long period of time, they were cryopreserved and kept in liquid nitrogen until use. Cells were re-suspended at $1x10^6$ cells/ml in medium containing 90% FBS and 10% dimethyl sulphoxide (DMSO) so as to prevent the formation of ice crystals during the freezing process. Then, the cryovials containing 1 ml cells were placed in cell freezing containers (Mr Frosty) to allow the cells to be slowly frozen at -80 °C for 24 hours before transfer to liquid nitrogen. When it was necessary to retrieve these cells from liquid nitrogen, the cryovials were defrosted rapidly in a 37 °C water bath, and the cells were then spun down at 1000 x g for five minutes to remove DMSO from the media. The cells were re-suspended in 5 ml of fresh growth medium that had been warmed to 37 °C and transferred into a T25 flask and incubated at 37 °C with 5% CO_2. The following day, the media was changed to fresh growth medium and the cells were monitored as they grew to confluence before passaging as required.

2.2.2.3 Mycoplasma testing of cell-lines

A regular mycoplasma testing schedule across the department was carried out shortly after the cell-lines arrival into the laboratory. The cells were checked every six months to ensure that the used cells were free of mycoplasma, especially after reviving the cells from frozen stocks. 5 ml of conditioned medium of the samples was collected and placed in a universal container for testing. The EZ PCR Mycoplasma Detection Kit was used to perform this test. The screening was carried out by the laboratory technicians using PCR techniques, and the results were as shown in figure 2.2.

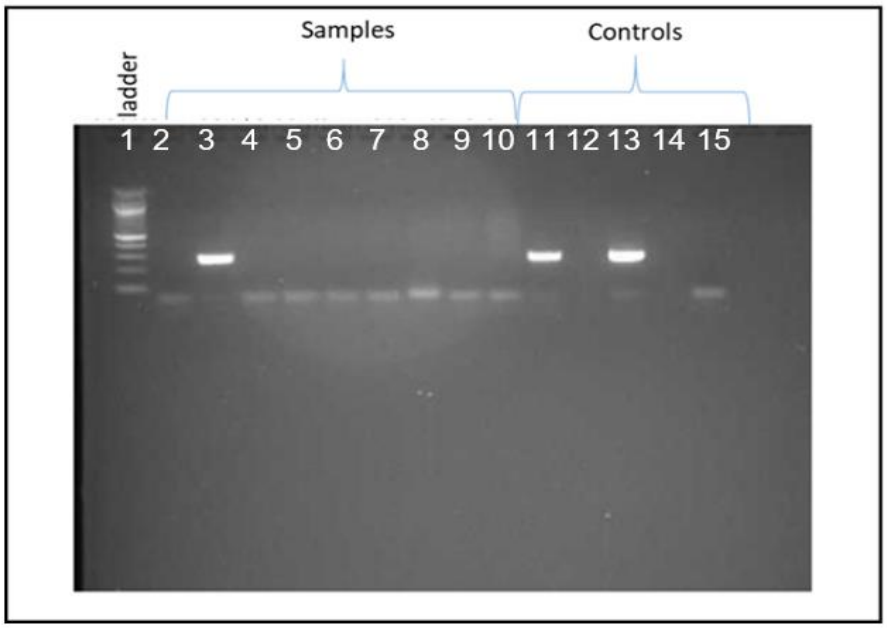

Figure 2.2: Example of mycoplasma test results. Lane 1 = 100 bp ladder, samples from lane 2 to 10, lane 2 and 3 unrelated samples, lane 4 (MCF-10A), lane 5 (MCF-10AT), lane 6 (DCIS.com), lane 7 (MCF-7), lane 8 (T47D), lane 9 (MDA-MB-231) and lane 10 (MDA-MB-231-BM) represent the related samples. Lane 11 = In-house positive control for mycoplasma test, Lane 12 = Gap, Lane 13 = Kit Positive Control, Lane 14 = Gap and Lane 15 = Negative control (sterile endotoxin-free water).

2.2.2.4 Cell counting

In order to seed the correct number of cells, they were counted using a TC20™ automated cell counter by mixing 10 µl of re-suspended cells with 0.4% (v/v) of trypan blue (1:1) and then adding 10 µl of the mixture onto a counting slide. The cell counter machine detects the viability, the number of viable cells and the total number of cells.

The principle for this is based on the fact that live cells possess intact cell membranes that exclude certain dyes, whereas dead cells do not, and this allows dead cells to take up trypan blue. This trypan blue cell exclusion assay is widely used with an automated cell counter, since this approach is more rapid, reliable and accurate. The potential weaknesses of this assay, however, are that the dye can be fused by live cells after a short exposure time (Avelar-Freitas et al., 2014).

2.3 Assessment of cell proliferation and survival

Cell proliferation was assessed by two different methods, cell counting, including viability, and measuring the cellular metabolic activity using the MTS assay (Kroemer and Pouyssegur, 2008).

2.3.1 Cell counting

Initially, cell counting was used in order to generate a growth curve for each cell-line. The seeding density of this experiment was optimised to avoid any cellular over-confluence during the assay. Initially, all cell-lines were seeded at different densities ($5x10^3$, $1x10^4$ and $2x10^4$ cell/well) in a 12-well plate in order to determine the most appropriate seeding density for the experiment to ensure that there was a change in the number of cells across the duration of the experiment and that the cells did not become too confluent with slow of growth during this time.

At $5x10^3$ and $1x10^4$ cell/well, counting the number of cells led to large errors in some cell types, especially for those with a low growth rate e.g T47D and DCIS.com. At $2x10^4$ cell/well the growth rate was steady and appropriate for all cell-lines. This was important to minimise the variability between cells. Cells were therefore seeded at 2 x 10^4 cells into 12-well plates and then incubated at 37 °C before monitoring proliferation at 24, 48, 72 and 96-hour time points using trypsinisation and cell counting as follows. At the relevant time point, all conditioned media were collected and then cells were washed with 1 ml of DPBS (without calcium and magnesium) and the washes were added to the conditioned media. This ensures that all dead cells were collected. Cells were then trypsinised by adding 500 µl of trypsin and incubated for 2 to10 minutes at 37 °C. Then, 1.5 ml of medium was added to the cells and all cell suspensions were collected and added to the wash and conditioned medium to ensure that all cells within each well were collected. The cells were then centrifuged at 1000 x g for five minutes and then cell counting was carried out as described previously in section 2.2.2. For each individual experiment, there were three wells/time point and the experiment was repeated as three independent experiments.

The length of time that cells took to double in number was measured using a doubling time computing tool (available from http://www.doubling-time.com/compute.php) (Roth, 2006) in order to assess the difference in growth rate between the cell-lines. The doubling time was calculated using the following equation:

$$Doubling\ time = \frac{\text{duration} \times \log 2}{\log(\text{Final concentration}) - \log(\text{Initial concentration})}$$

* "log" is the logarithm to base 10 (as automatically calculated).

2.3.2 Cell counting in response to Semaphorin 3B treatment

In order to assess the effect of recombinant semaphorin 3B on cell growth and proliferation, DCIS.com and MDA-MB-231 cells were seeded at 2 x 10^4 cells in 12-well plates. The recombinant semaphorin 3B was added at different concentrations 0, 0.5, 1 and 2 µg at the same time as the cells were seeded in media containing 1% serum. The cells were incubated at 37 °C before monitoring proliferation at 24, 48 and 72 hour time points using trypsinisation and cell counting as previously described in 2.2.2.

2.3.3 MTS cell proliferation/ viability

The MTS assay was performed in order to measure the metabolic activity and the viability of the cells over a 96h period using the CellTiter96 AQueous One Solution cell viability assay. MTS is a colorimetric assay which is based on the ability of viable cells to reduce the MTS tetrazolium salt (3-(4,5-dimethyl-2-yl)-5-(3- carboxymethoxyphenyl) -2-(4-sulfophenyl)-2H-tetrazolium) to a formazan product, a process mediated by NAD(P)H-dependent dehydrogenase enzymes and therefore measuring the mitochondrial function (Dunigan et al., 1995). The amount of the formazan product is measured by reading the absorbance of the solution at 490 nm. In order to perform the experiment, when cells reached 70% confluent they were trypsinised, counted and seeded into four 96-well plates at a seeding density of 5x10^3 cells in 100 µl of culture medium/ well. Optimisation of the assay was previously performed by other members of our group.

DPBS (100 µl) was added to wells at the edges of the 96-well plate to avoid evaporation of the medium over the duration of the assay. At each time point (24, 48, 72 and 96 hour), a plate was removed from the incubator and 20 µl of CellTiter Aqueous One solution reagent was added into each well. The plates were incubated for an additional three hours in the dark at 37 °C. Then, the absorbance was measured at 490 nm using a microtitre plate reader. The experiments were repeated three times for each cell-line, with six wells per cell-line per repeat. Wells seeded with media alone were used as the absorbance control. The background absorbance of the media was subtracted from each value and the results were graphically presented using Prism 7 software.

2.3.4 Effect of recombinant Semaphorin 3B (rSEMA3B) on metabolic activity of the cells

In order to assess the potential effect of recombinant SEMA3B on actively proliferating cells, the cell-lines of interest, DCIS.com and MDA-MB-231 cells, were seeded into a 96-well plate and incubated overnight. The following day, the media was removed and replaced with media containing 1% serum and a range of rSEMA3B concentrations (0, 0.5, 1, 2 µg/ml) in the total volume 100 µl in each corresponding well. Plates were incubated at 37 °C for 24, 48, 72 hours and the protocol followed as described in section 2.3.3.

2.4 Scratch (wound healing) assay

The scratch assay was carried out to assess the ability of cells to migrate, since this assay can mimic the behaviour of tumour cells during migration *in vivo.* This is a straightforward, convenient and cost-effective method for analysis of cell migration *in vitro*. The limitation of this method, however, is that it takes longer to perform since the cells need to be confluent and the scratch should be done by wounding the surface of a confluent monolayer of cells which can lead to damage of the extracellular matrix components of cells (Liang et al., 2007). The gap closure is measured over time, thereby quantifying both the migration and proliferation of the cells. In order to reduce the proliferation and ensure that only the migration is measured, mitomycin C was used in this experiment, as described below in 2.4.1.3.

2.4.1 Optimisation of the scratch assay

2.4.1.1 Seeding densities

Different seeding densities were used to optimise a consistent migration assay ($2x10^4$, $5x10^4$ and $1X10^5$ cells/well) (figure 2.3). This experiment was intended to choose an appropriate seeding density at which the cells became confluent having formed a monolayer of cells. This was achieved at cell density of $1x10^5$ in 24-well plates after 48 hours.

2.4.1.2 Starvation period

Cell serum starvation is a necessary step in this assay in order to minimise the cell proliferation by synchronising the cells to arrest at the G0 phase of the cell cycle. The period of serum starvation was established and the cells were starved for 48 hours prior to the scratch, at which point they were compared to the cells without serum

starvation. Adherent cells were not affected after this time. To ensure that cells were not actively proliferating at the start of the experiment, cells were starved for 48 hours.

2.4.1.3 Mitomycin C optimisation

Mitomycin C is a DNA synthesis inhibitor which is known to inhibit proliferation and this was therefore used to prevent proliferation in the migration assay and to ensure that the gap closure measured is due to cell migration only. Studies have shown, however, that mitomycin C can cause cell death and disruption of the cell monolayer (Verweij and Pinedo, 1990). Therefore it was necessary to establish an appropriate concentration of mitomycin C, sufficient to stop proliferation but not so much as to kill the cells or disrupt the cell monolayer. In order to identify a mitomycin C concentration that would inhibit cell proliferation without killing the cells, the MTS assay was performed. Previous studies in the lab have shown that breast cancer cell-lines are sensitive to mitomycin C so a low dose range was tested (from 0.5 to 10 µg/ml). As previously described in section 2.3.3, cells were seeded at $5x10^3$ in 96-well plates and incubated overnight at 37 °C. The following day, the cells were treated with different concentrations of mitomycin C (0, 0.5, 1, 2, 5 and 10 µg/ml) for one hour (figure 2.4) and then cells were washed and the cell proliferation was assessed at different time points (24, 48 and 72 hours). The cellular proliferation was measured by MTS assay (section 2.3.3) and the absorbance was measured at 490 nm (figure 2. 5.). As seen in figure 2.4, after one hour of adding the higher doses of mitomycin C into the cells (5 and 10 µg), some cells had detached from the flask and died. The lower doses (1 and 2 µg/ml) showed less cytotoxic effect on cells with no cell detachment.

Nonetheless, proliferation was initially measured by MTS so as to confirm the effectiveness of the above process. The results showed that the mitomycin C-treated cells did not proliferate over the course of the assay (72 hours) compared to the untreated cells and that proliferation reduced in a dose-dependent manner (figure 2.5). Accordingly, the scratch assay was performed using 2 µg/ml to ensure that the confluent monolayer would not be disrupted and to guarantee that the majority of the scratch closure would be due to the migration and not the proliferation of the cells.

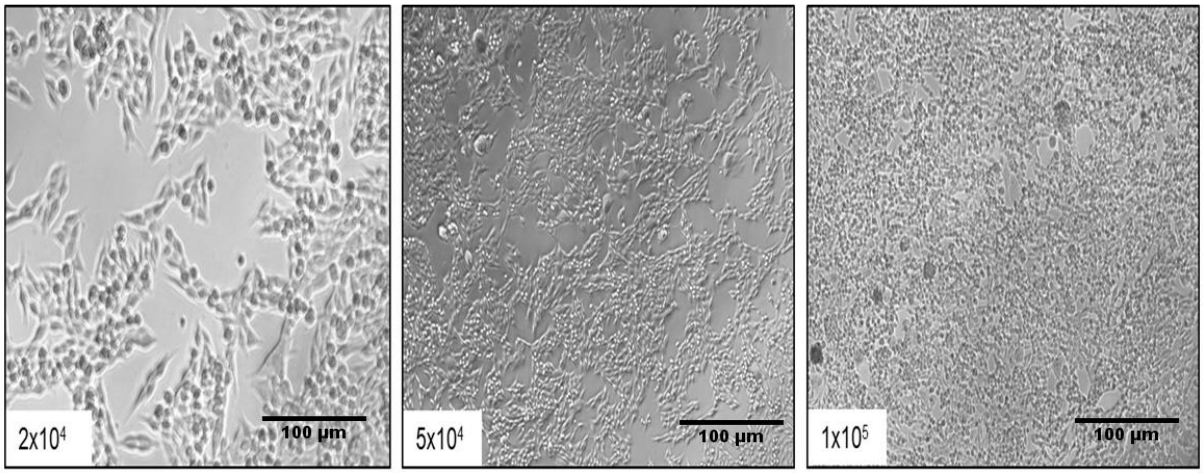

Figure 2.3: Examples of optimisation of different seeding densities. Scale bar = 100 µm

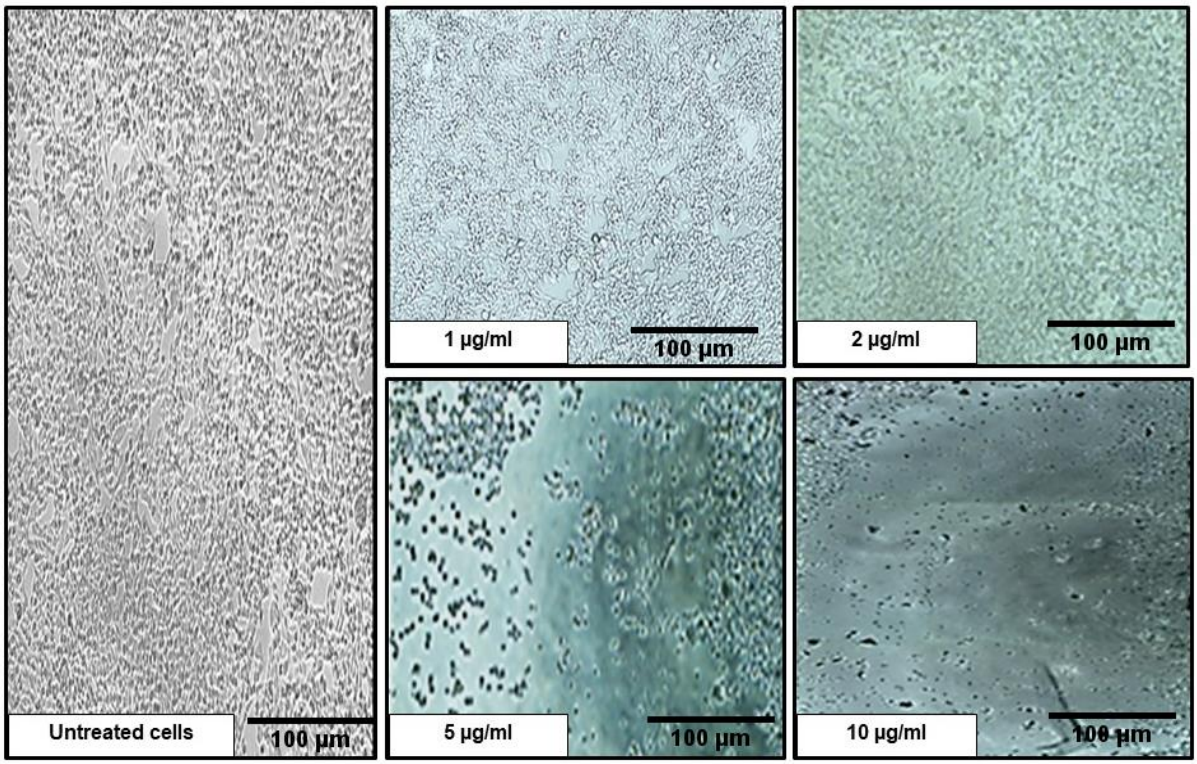

Figure 2.4: A representative image of the effect of different doses of mitomycin C on MDA-MB-231 monolayers. Cells were treated with different doses of mitomycin C (0,1, 2, 5 and 10 µg/ml). Cells were less confluent and cell death occurred after 1 hour with increased doses of mitomycin C. Scale bar = 100 µm.

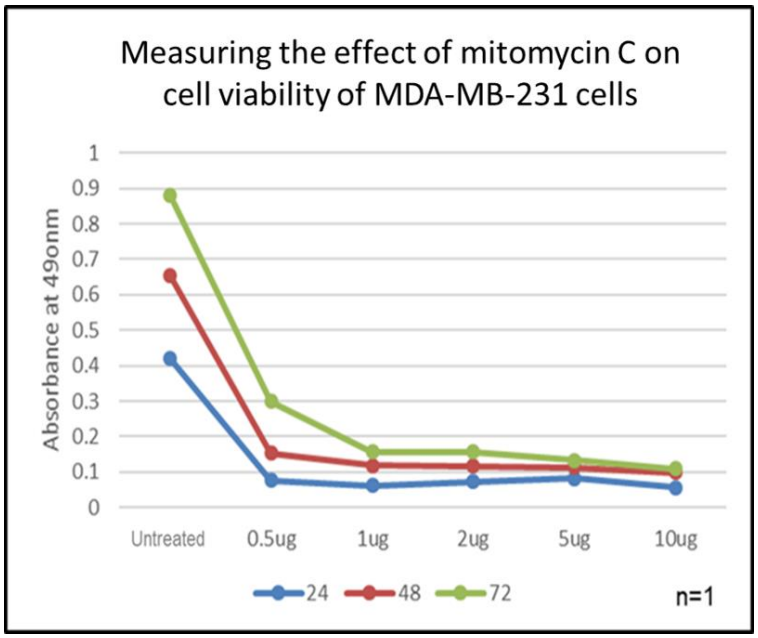

Figure 2.5: The effect of different doses of mitomycin C on cell viability of MDA-MB-231. Cells were seeded into 96-well plates and treated with different doses of mitomycin C (0, 0.5, 1, 2, 5 and 10 µg/ml) for an hour and then washed. The cell viability was then measured at different time points (24, 48 and 72 hours) using the MTS assay and expressed as absorbance at 490 nm. The viability of the MDA-MB-231 cells decreased with increased doses after 72 hours (n=1).

2.4.2 Protocol

All cell-lines were seeded into a 24-well plate ($1x10^5$ cells/well) to a final volume of 500 µl in full medium and incubated for 48 hours to obtain a confluent monolayer, and then the media was replaced with serum free medium so as to starve the cells for a further 48 hours. Mitomycin C was then added to the medium for an hour prior to making a straight line scratch using a p200 pipette tip. Cells were washed once with 500 µl DPBS in order to remove debris and floating cells, and the wells were then filled with 500 µl serum free medium and the plate incubated for a further 30 minutes to allow the stressed cells to equilibrate. After that, the medium was aspirated off and replaced with 500 µl of medium containing 1% serum. Images were taken under a microscope at 10x magnification for each well before and after scratching. The plates were placed in a tissue culture incubator at 37 °C and images were captured after 0, 24, 36 hours. ImageJ software was used to measure the gap closure and to calculate the remaining clear area after each time point compared to the control time zero hour. About 20 horizontal lines were drawn across the edge of the scratch, the measurements of the length of the drawn lines were obtained and the percentage of the closed area was calculated (figure 2.6). These steps were repeated for each cell-line. The percentage of wound closure was calculated using the following equation:

$$\text{Wound closure (\%)} = \frac{\text{width of initial scratch - width of scratch at 0, 24 or 36h)} \times 100}{\text{width of initial scratch}}$$

The experiments were repeated three times for each cell-line, with three wells per cell-line per repeat.

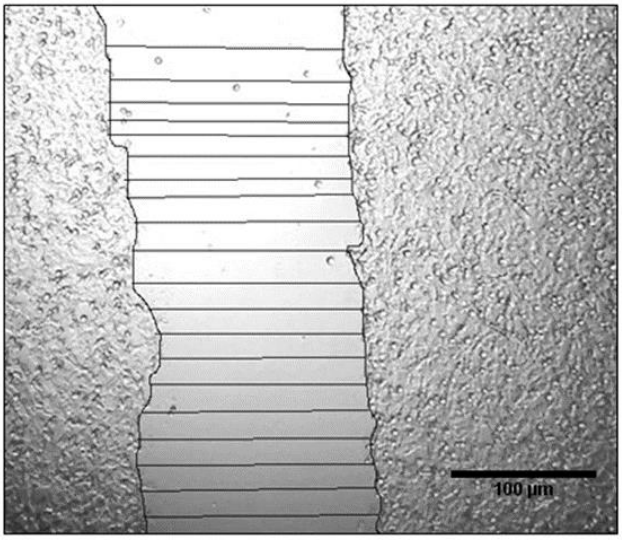

Figure 2.6: Analysis of cell migration by scratch assay using ImageJ software. Twenty lines were drawn randomly across the entire length of the scratch in the well and quantified using Image J. The percentage of the closed area was calculated for each scratch. Scale bar = 100 µm.

2.5 Effect of recombinant Semaphorin 3B on cell migration

In order to assess the potential effect of recombinant SEMA3B on cells migration, the cell-lines of interest, MDA-MB-231 and HUVEC cells, were seeded into a 24-well plate and incubated for 48 hours to obtain a confluent monolayer as described in section 2.4.2. HUVEC cells were used as a positive control in this assay. Then, the medium was removed and replaced with serum free medium and cells were starved for 48 hours except for HUVEC cells which could not survive in the absence of serum therefore they were kept in 2% serum. The cells were treated with Mitomycin C as described in section 2.4.2 and then a straight line scratch was applied using a p200 pipette tip. Cells were washed and then the media containing 1% serum and differing concentrations of rSEMA3B (0, 0.5, 1, 2 µg/ml) in the total volume 500 µl was added in each corresponding well. Plates were incubated at 37 °C for 24, 36 hours and the protocol followed as described in section 2.4.2. The results were analysed by drawing twenty horizontal lines across the edge of the scratch, the measurements of the length of the drawn lines were obtained and the percentage of the closed area was calculated as decribed in section 2.4.2.

2.6 Invasion assay

One of the major characteristics of tumour metastasis is the ability of tumour cells to invade through the basement membrane. An invasion assay was therefore performed in order to study this characteristic of each cell-line toward a chemoattractant gradient (10% FBS as chemoattractant in medium). Matrigel is a solubilised basement membrane protein mixture extracted from Engelbreth-Holm-Swarm (EHS) mouse sarcomas that represents the basement membrane found in many tissues, and can therefore be used to study the invasion of cells.

2.6.1 Preparation of Matrigel for membrane coating

Matrigel was aliquoted upon receipt and thawed on ice at 4 °C overnight before use. Then, it was swirled gently to ensure homogeneity and kept on ice continually until use, at which point it was dissolved in pre-cooled serum-free medium to 9.5 mg/ml (protein concentration).

2.6.2 Preparation of transwell invasion assay plates

The required number of transwell inserts were placed into a 24-well cluster plate using sterile tweezers. 20 µl of Matrigel (30 µg/insert) was applied to coat each transwell

insert, making sure that the entire surface was evenly coated. The plate was then incubated for two hours at 37 °C to allow the Matrigel to set.

2.6.3 Principle of invasion assay

Two chambers were used in this assay, separated by a filter coated with Matrigel components. The cell suspension containing serum free medium was placed in the top chamber and incubated for a specific time in the presence of medium containing chemoattractants (10% FBS in medium) in the bottom chamber. The invasive cells migrate from the top chamber through the coated filter pores to the bottom underside of the filter (figure 2.7).

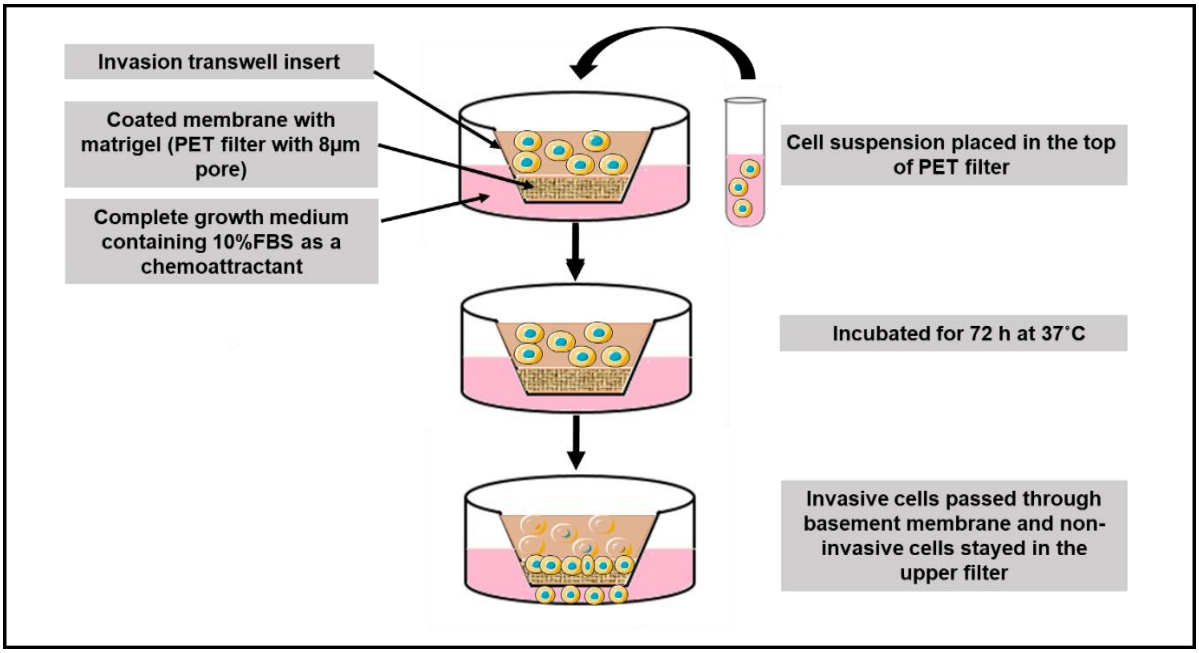

Figure 2.7: Principle of invasion assay. The steps of the invasion are illustrated in the diagram.

2.6.4 Optimisation of seeding density and time for invasion

In order to optimise the assay, MCF-10A, MCF-10AT, DCIS.com, MCF-7, T47D, MDA-MB-231 and MDA-MB-231-BM cells were seeded at $1x10^4$, $2x10^4$ and $3x10^4$ cell/well in the appropriate assay media (figure 2.8). MCF-10A, MCF-10AT, DCIS.com cells did not invade over the course of the 72 hours experiment and so were excluded from further experimentation.

To establish how long the cells took to penetrate through the Matrigel-coated cell culture insert the extent of invasion at a range of time points was investigated, and cells were seeded at different densities for 48 and 72 hours. MCF-10A, MCF-10AT and DCIS.com cells did not invade over a period of three days. MCF-7, T47D, MDA-MB-231 and MDA-MB-231-BM did invade, but the number of invaded cells were few after 48 hours, although after 72 hours the cells did have better invasion (figure 2.8). Based on this investigation, a cell density of $3x10^4$ and a duration of 72 hours were used in subsequent experiments.

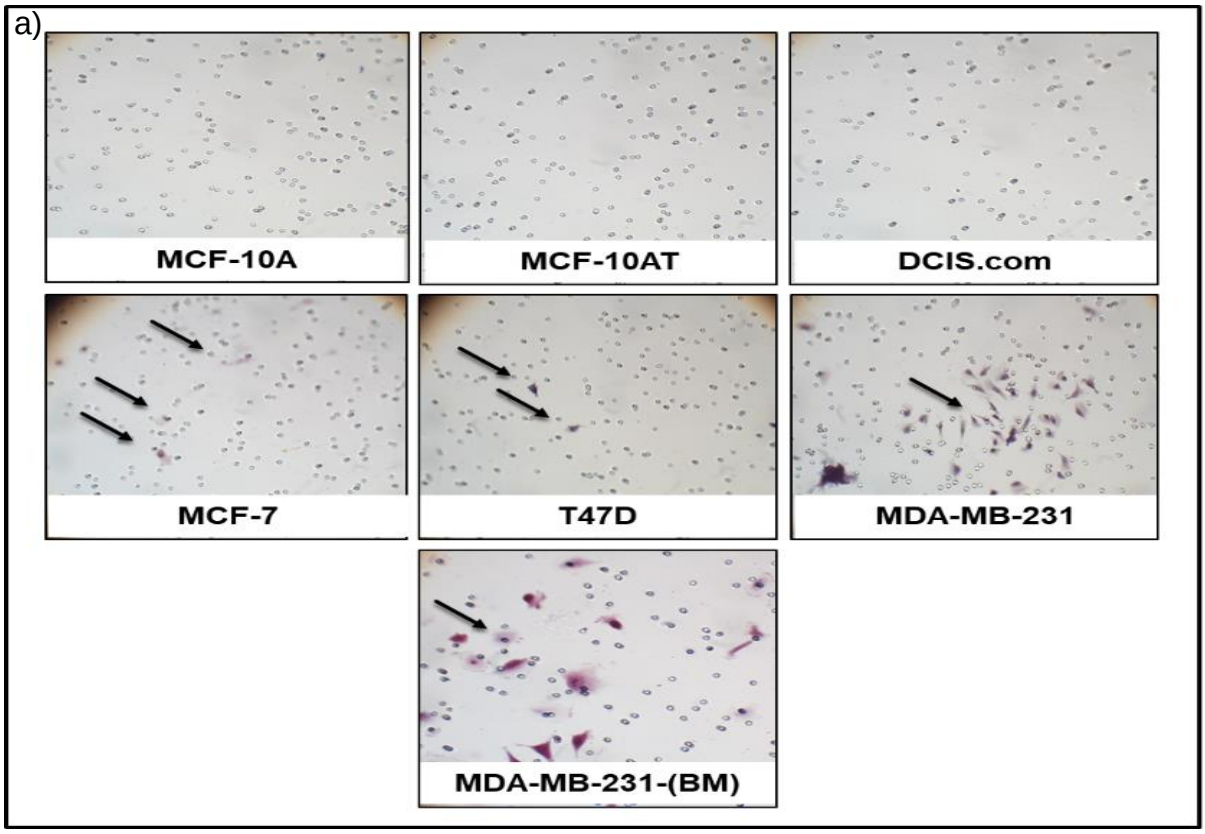

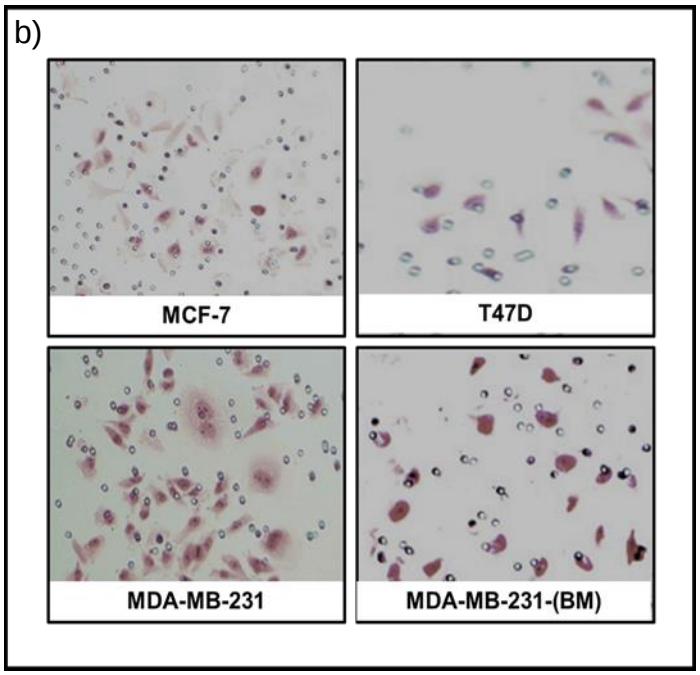

Figure 2.8: Optimisation of the seeding density and the time-period of the invasion assay. Images were taken after 48 and 72 hours of untreated cells. The number of invaded cells were measured/10 fields of view at x20 magnification. Pre-invasive, pre-malignant and invasive cell-lines were optimised at different concentrations. The representative images show examples of seeding densities at **(a)** $1x10^4$ cells/insert for 48 hour. **(b)** $2x10^4$ cells/insert for 72 hours. The arrows indicate the invaded cells.

2.6.5 Protocol of the invasion assay

The cells were starved overnight by replacing the complete medium with serum free medium. The media was removed, and the cells were washed twice with 1X PBS and trypsinised, re-suspended in serum-free medium, counted and seeded at $2x10^4$ cell/200 µl medium /insert in 24-well plates (figure 2.8). Cells were seeded onto coated inserts in triplicate under sterile conditions. The outer wells were filled with 500 µl of complete growth medium containing 10% FBS and the plate was incubated for 72 hours at 37 °C. After incubation, each insert was fixed by being placed into 100% ethanol for ten minutes followed by washing with PBS for two minutes. The coated chambers were stained with haematoxylin (300 µl) for 30 minutes and then the inserts were washed twice with distilled water (500 µl) in order to remove excess stain. They were then allowed to dry at room temperature. The following day, the non-invading cells were removed by repeatedly “scrubbing” the membrane with a cotton swab (moistened with PBS) inside the bottom of the membrane, applying firm pressure to rub the top surface. This was repeated twice. Then, the membrane was cut and mounted onto glass slides. It was expected that the invasive cells would penetrate through the Matrigel basement membrane while the non-invasive cells remain in the upper filter on the top of the Matrigel and hence removed with the swab. Images were taken in ten random fields by phase contrast and the number of invaded cells were quantified using a 20X objective. The number of cells was counted, both by eye and using the cell counter in ImageJ software, which allows cells to be counted by clicking on the cell image and thus provides the total number of cells in the field

2.7 The effect of recombinant SEMA3B on cell invasion

In order to assess the effect of rSEMA3B on invasion, cells were seeded at $2x10^4$ in 200 µl of total serum free medium into the upper chamber of the 24-well transwell plate. Various concentrations of rSEMA3B (0, 0.5, 1, 2 µg/ml) were added to the medium containing full serum in the lower chamber. After incubation for 72 hours at 37 °C under 5% CO_2, each insert was fixed and stained as previously described in 2.6.5. Images were taken and the invaded cells counted in ten random fields/slide by phase contrast microscopy and the number of invaded cells quantified by using a 20X objective. Then the cell number was counted by both eye and ImageJ software. The number of invaded cells in the presence of rSEMA3B was compared to the negative control (untreated cells).

2.8 Cytometric Bead Array assay

The aim of this experiment was to identify which cytokines are released by the different cell-lines and to assess their expression levels by a Cytometric Bead Array assay (CBA). This assay works by coating multiplex beads with antibodies to specific cytokines. The antibodies then bind to and pull out the cytokines from the cell supernatants. The amount of cytokine in each sample can then be quantified using an Attune Autosampler to measure the concentration of cytokines in the samples.

Cells were seeded at $2x10^6$ cells/ml in T75 flask in medium containing full serum as described in section 2.2.2. After reaching 70-80 % confluency, the media was replaced with serum free medium and after 24 hours the medium was collected and centrifuged at 1000 x g for five minutes. The supernatants were then collected to be investigated by CBA. Different cytokines were purchased from BD Biosciences, including IL-8, IL-11, G-CSF, GM-CSF, IFN-Y and IL-10. The BD CBA Flex set used the range of fluorescence detection offered by the Attune Autosampler and antibody-coated beads to capture analytes. The CBA Flex Set contained two vials of standard and one vial each of Capture Bead and PE Detection Reagent (reporter). The standard component was reconstituted in 4.0 ml assay diluent, the standard contained a protein concentration of 10,000 pg/ml. The prepared components were stored at 4 °C in order to protect them from exposure to light. The binding complex between antibody and cytokine provides a fluorescent signal which reflects the concentration of the analyte in the test matrix. Standard curves were generated to determine the concentration of each analyte in the test sample (figure 2.9). The CBA assay was performed by staff of the flow cytometry facility of the Medical School.

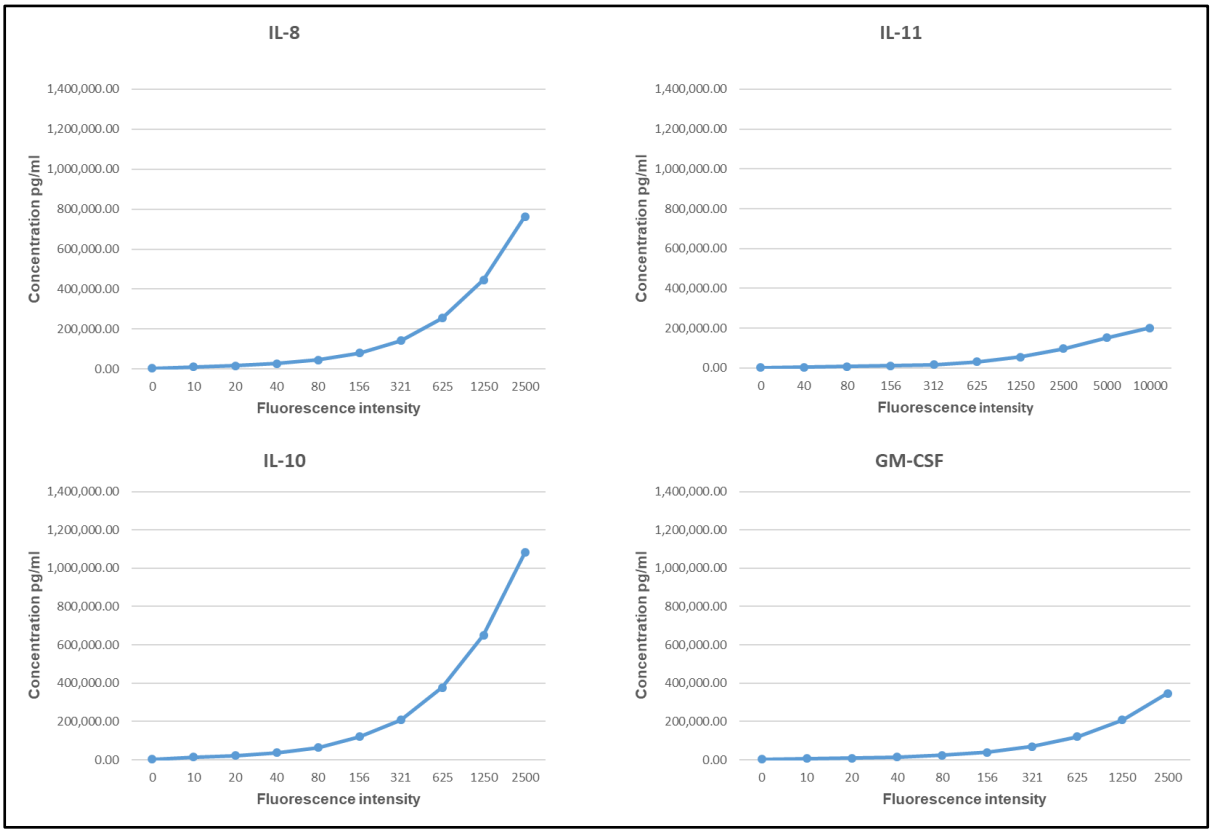

Figure 2.9 Example of standard curves of CBA assay

2.9 RNA extraction and quantitative real-time reverse transcription PCR

Quantitative real-time PCR (q-RT-PCR) was performed to determine the gene expression levels of SEMA3B and furin-like pro-protein convertases in all the breast tumour and non-tumour cell-lines. The mRNA expression of all genes of interest were analysed by q-RT-PCR. The qRT-PCR assay is based on measuring the fluorescence using SYBR Green as a fluorescent reporter molecule. In this technique, RNA is transcribed into complementary DNA (cDNA) by reverse transcriptase from mRNA and then used as the template for the q-RT-PCR reaction.

2.9.1 RNA extraction

Total RNA was isolated from cultured cells using the Qiagen RNeasy mini kit and following the manufacturer's instructions. Once cells reached 80-90% confluence, they were detached from the bottom of the flask using trypsin, centrifuged, and then the cell pellet was re-suspended in 1 ml of fresh media and counted as described in 2.2.2. A minimum of 1 x 10^6 cells/ml were then lysed as follows. 350 µl of RLT buffer was added to the pellet, containing guanidine isothiocycanate and lysis buffer, which deactivated RNAses and bind RNA to the silica membrane in order to extract cell

nucleic acid. The sample was then homogenised using a 21-gauge needle and a 1 ml syringe. Then, 350 µl of 70% (v/v) ethanol was added and mixed thoroughly to provide optimal RNA-binding conditions, and the lysate was transferred to a silica-based RNeasy Mini spin column. The silica membrane selectively helps to exclude short RNA molecules of <200 nucleotides, enriching the mRNA. The column was centrifuged at 8000 x g for 15 seconds. After centrifugation, 700 µl of a guanidine salt-containing buffer (RW1) was added to the spin column and used as a washing buffer in order to remove proteins and debris, and the column was again centrifuged at 8000 x g for 15 seconds. The flow through from the column was discarded and 500 µl of RPE buffer was added to the top of the column to remove any excess traces of salts, and the centrifugation step was repeated. This step was performed twice to ensure thorough washing. The spin-column containing sample was then transferred into new collection tubes and 50 µl of RNase-free water was loaded directly into the spin column, which was then centrifuged for one minute at 8000 x g, releasing the RNA into the water. The eluted RNA was collected and was stored at -80 °C until required.

In order to remove unwanted DNA from the cell lysate, and to treat RNA samples with DNase in order to minimise genomic DNA carryover, which has the potential to affect the result, an RNAse-free DNAse kit was used. 50 µl of RNA sample was incubated with 1 µl DNAse I and 5 µl of the RNAse-free DNAse 10x reaction buffer for 30 minutes at 37 °C. The DNAse reaction was terminated by the addition of 5 µl of the stop solution (inactivation enzyme) and left for 5-10 minutes at room temperature to be centrifuged for two minutes at 14000 x g, at which point the supernatant was collected.

2.9.2. Assessment of RNA yield and quality

The purity and the quantity of nucleic acid were measured using the NanoDrop spectrophotometer machine. 1 µl of RNase-free water was placed into the NanoDrop machine for the blank measurement and stored as a reference spectrum; then, 1 µl of sample was added and the ratio of absorbance measured at 260 and 280 nm, used to calculate the purity of the extracted RNA, determined from the ratio 260/280 and the concentration of the RNA. A ratio of ~1.9 - 2.1 is considered to be pure RNA. As determined from the NanoDrop measurement, the concentration of the extracted nucleic acid was calculated and 100 ng/µl was used for all cell-lines.

2.9.3 Reverse transcription polymerase chain reaction (RT-PCR)

cDNA was synthesised from the extracted RNA using a High-Capacity cDNA Reverse Transcription Kit and following the supplier's instructions. cDNA was prepared according to the table 2.3, No-RT control (no reverse transcriptase) was included in each experiment to ensure that the run had no contamination. The RNA template (50 ng in 10 µl) was add to a 20 µl reaction mixture of MultiScribe reverse transcriptase, reverse transcriptase buffer, random hexamer primers and dNTP mix, as described in table 2.3. The mixtures were added into 0.5 ml reaction tubes on ice. The tubes were then placed in a thermal cycler and the RT-PCR programme started using the following conditions listed in table 2.4 to generate complementary DNA.

Table 2.3: Component of Reverse Transcription Master Mix

Reagents	Final volume (Per 20-µL reaction)	Description
Nuclease-free H2O	4.2 µl	For dilutions
MultiScribe™ Reverse Transcriptase, 50 U/µL	1 µl	RNA–dependent DNA polymerase which uses single-stranded RNA as a template to generate a cDNA strand
10×RT Buffer, 1.0mL	2 µl	Obtains higher yield of cDNA
10×RT Random Primers, 1.0mL	2 µl (0.5 µg/µl)	Produces short cDNA fragments that would convert mRNA to cDNA
25×dNTP Mix (100mM)	0.8 µl (0.5 µg/µl)	Contains premixed aqueous solutions of dATP, dCTP, dGTP and dTTP
Extracted RNA	X µl	-
Total	20 µl	

Table 2.4: Thermocycler parameters for cDNA synthesis

Step	Temperature	Time
Pre-denaturation	25 °C	10 minutes
Primer extension	37 °C	120 minutes
cDNA synthesis	85 °C	5 minutes
Reaction termination	4 °C	Hold

2.9.4 Quantitative polymerase chain reaction (qPCR)

Quantitative real-time PCR was performed using the SYBR® Green qPCR Master Mix and following the manufacturer's instructions. The components of the Master Mix are described in table 2.5, a total volume of 9 µl containing SYBR green mastermix, nuclease-free H_2O, and the primers for the gene of interest (section 2.1.4) were loaded into each well of the qPCR 384 well plates and 1 µl of cDNA was added to the corresponding wells. Each sample was run in triplicate. Glyceraldehyde-3-phosphate dehydrogenase gene GAPDH (a reference housekeeping gene) was used as an endogenous control in each run. The qPCR plate was sealed with an optical adhesive film and then centrifuged at 2000 x g for two minutes using a Sorvall Legend X1 centrifuge before being placed into the PCR machine.

Table 2.5: Components of qPCR Master Mix

Reagents	Final volume (per 10µl reaction)
Nuclease-free H_2O	3 µl
SYBR Green	5 µl
Gene of interest primer/ reference gene primer	1 µl (0.2 µM)
cDNA sample	1 µl
Total	10 µl

Then, the plate was placed into the 7900HT Applied Biosystem and the machine was set up according to the supplier's protocol, as in the following table 2.6:

Table 2.6: Parameters for qPCR

Cycles	Reaction Step	Cycle length	Temperature
x 1 cycle	Enzyme Activation	10 minutes	95 °C
x 40 cycles	Denaturation (to separate the DNA strands)	15 seconds	95 °C
	Data Collection (annealing step to allow the primers to anneal to the template of interest	1 minute	60 °C
	Extension step	15 seconds	72 °C
	Melt curve	15 seconds	95 °C
	Cooling	15 seconds	60 °C

All the primers used (All-in-One™ qPCR Primers) were experimentally validated by the manufacturer and a single amplification curve of the correct size for the targeted gene was generated. The primers were therefore not further validated.

2.9.5 Data analysis

The Ct values were retrieved automatically from the PCR system. The first cycle at which the amplification curve is generated is called the Ct or threshold cycle, which is the first point at which the target amplification is detected. This reflects the amount and the concentration of the target in the reaction, where lower Ct values indicate high target concentrations. Melting curves were generated for each run in order to verify the specificity of each PCR reaction. The GAPDH reference gene was used to calculate the relative amount between each target gene and GAPDH. GAPDH was used as an endogenous control because its expression does not change between the different cell-lines. In order to calculate the change in Ct, relative quantification was used to normalise each respective gene to the GAPDH reference. The mean of each gene Ct, was subtracted from the mean of the reference gene Ct, according to the following equation: ΔCT= Ct [target gene] - Ct [reference gene]. These values were compared between the samples being analysed. The experiments were repeated three times for each gene, with three wells per gene per repeat.

2.10 Western blot analysis

Western blot analysis was carried out to determine the expression of SEMA3B and Furin-like pro-protein convertases proteins in all the cell-lines. This technique relies on the separation of proteins extracted from cells or in conditioned media, according to their molecular weight, on SDS-PAGE. These are then transferred to a membrane and the specific proteins of interest detected using specific antibodies. A secondary antibody can then identify the primary antibody and in the presence of a soluble enzyme substrate, the reaction can be detected by the emitted chemiluminescent light, producing a band (figure 2.10) (Mahmood and Yang, 2012).

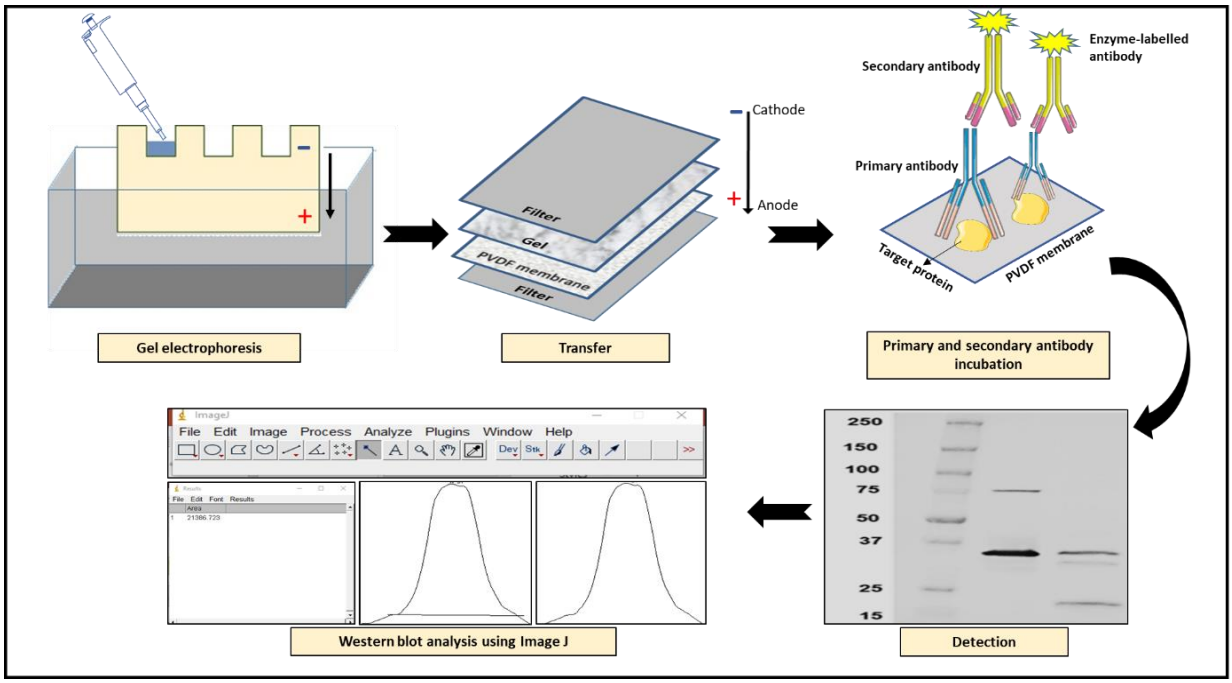

Figure 2.10: Western blotting procedure. The samples are loaded onto the gel and separated by SDS-PAGE according to their molecular weights, and then transferred to a PVDF membrane. The membrane is blocked and the target protein is incubated with a highly selective primary antibody and a secondary antibody. The reaction can be detected by the chemiluminescent light emitted in the presence of a soluble enzyme substrate.

2.10.1 Sample preparation and extraction

Once cells reached 80-90% confluence, they were washed twice with 10 ml cold DPBS. Then, 1 ml of RIPA lysis buffer, which contains (25 mM Tris-HCl pH 7.6, 150 mM NaCl, 1% NP-40, 1% sodium deoxycholate, 0.1% SDS), mixed with 10 µl halt protease phosphatase cocktail inhibitors (leupeptin which targets serine and cysteine proteases), was added to the cells to extract the proteins. The function of these inhibitors is to block or inactivate endogenous proteolytic and phospholytic enzymes that are released during cell lysis, so to avoid any protein degradation. It should be mentioned that the protease inhibitors were used when lysates were extracted for analysis of rSEMA3B stability (see section 2.10.10) to prevent excessive proteolytic degradation. Cells were then incubated with the lysis buffer for five minutes, with continuous movement and on ice so as to avoid protein degradation, before they were scraped and collected into Eppendorf tubes and were passed through a 25-G needle ten times to rupture the cell wall and release the proteins into the solution. Lysed cells were incubated for 30 minutes on ice to allow full lysis, followed by centrifugation at

13000 ×g for 15 minutes at 4 °C to remove cell debris. The supernatants containing the proteins were collected, a small aliquot was used in the protein quantification assay, and the remaining sample stored at -80 °C until use.

2.10.1.1 Collection and concentration of conditioned medium

Since cells are known to release proteins into the culture medium it was important to study the protein expression of SEMA3B and other pro-protein convertases in conditioned medium in parallel with protein lysates. Once cells reached 70% confluence, the medium was then changed to a serum-free medium for a further 24 hours and the conditioned medium was then collected and concentrated by 10 or 20 fold by centrifuging it using a swinging-bucket rotor at 4000 x g for 30 minutes using Amicon® Ultra-4 Centrifugal Filter Units. The retained concentrated medium was collected and stored at -80 °C until needed. Proteins were quantified in conditioned media as described below for cell lysates.

2.10.2 Protein quantification

Protein quantification was measured using a Micro™ BCA Protein Assay Kit to ensure equal protein loading onto the Western blotting (SDS-PAGE) wells. The principle of this assay is that Cu^{2+} is reduced to Cu^{1+} by proteins under alkaline conditions and the cuprous cation (Cu^{1+}) can be detected by bicinchoninic acid, which is highly sensitive and specific. The relationship between absorbance and protein concentration is close to linear, allowing determination of unknown protein concentrations from a standard curve. That standard curve was generated by diluting bovine serum albumin (BSA) stock to a final concentration of 0.2 mg/ml (w/v) (100 µl stock to 900 µl of the sample diluent, RIPA buffer), after which standard dilutions, which ranged from (0-20 µg/ml) were prepared, as shown in table 2.7. Samples were then prepared at different concentrations, 1:50, 1:100, 1:200 (table 2.8), to confirm that the absorbance of samples will fall within the range of the prepared BSA standard curve.

Table 2.7: BSA preparation

No.	Standard (µg/ml)	BSA µl of 0.2mg/ml working stock	µl of dH_2O
1	0	0	1000
2	2.5	12.5	987.5
3	5	25	975
4	7.5	37.5	962.5
5	10	50	950
6	15	75	925
7	20	100	900

Table 2.8: Sample preparation for BCA assay

Concentration	Sample (Cell lysate)	RIPA buffer
1:50	20 µl	980 µl
1:100	10 µl	990 µl
1:200	5 µl	995 µl

150 µl of the BSA standard, blank and unknown protein samples were pipetted into 96-well plates in triplicate. The BCA working stock solution contained 25 parts of reagent A (containing alkaline tartrate-carbonate buffer) and 24 parts of reagent B (containing bicinchoninic acid solution) and 1 part of solution C (copper sulphate solution) (2.5 ml, 2.4 ml and 0.1 ml, respectively), mixed until light green in colour. Then 150 µl of this working solution was added to each well. The plate was then incubated at 37 °C for two hours and the absorbance was measured at 562 nm (Fluostar Galaxy Reader). The standard curve was used to calculate the protein concentration of each cell-line by linear regression analysis using GraphPad prism (figure 2.11).

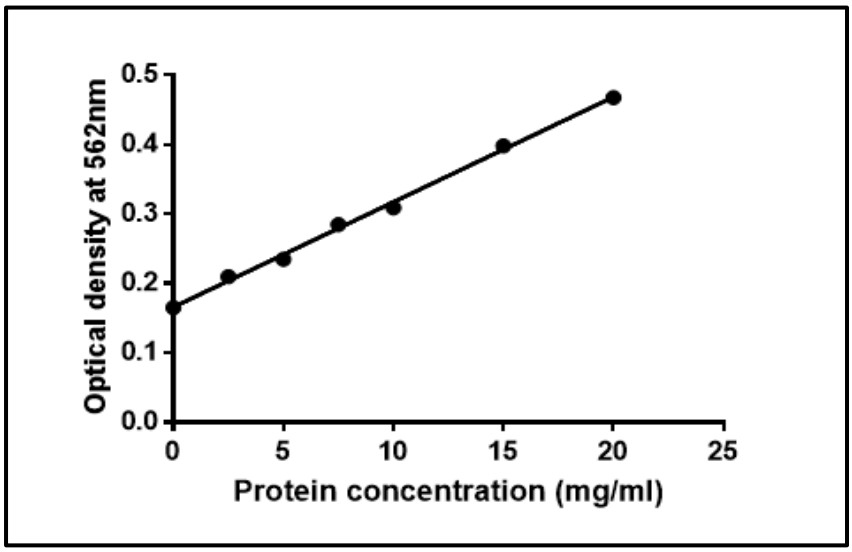

Figure 2.11: BCA standard curve example. The line is the linear regression curve for the entire set of standard BSA points. This was generated automatically using GraphPad Prism 7 software.

2.10.3 SDS-PAGE and gel preparation

Gels containing 10% sulphate-polyacrylamide, which were 1.5 mm thick, were prepared as below (table 2.9).

Table 2.9: Gel preparation

Resolving gel		Reason	Stacking gel	
Reagents	**Quantity**		**Reagents**	**Quantity**
dH_2O	8.1ml	To make a reagent dilution	dH_2O	6.1 ml
1.5M Tris-HCL /PH8.8	5ml	To maintain the pH within a relatively narrow range.	0.5 M Tris-HCL /PH6.8	2.5 ml
10% (w/v) SDS	200µl	Sodium dodecyl sulphate is a detergent that has been known to denature proteins. It has a negative charge so it can apply large negative charges to all proteins to help them migrate toward the positive pole of an electrophoresis electronic field	10% (w/v) SDS	100 µl
30% (w/v) acrylamide	6.6ml	To complete removal of oxygen from the solution leading to rapid polymerisation.	30% (w/v) acrylamide	1.5 ml
10% (w/v) APS	100µl	Ammonium Persulfate (APS) is an oxidising agent that was used to catalyse the polymerization of acrylamide.	10% (w/v) APS	100 µl
TEMED	25µl	N,N,N',N'tetramethylethylenediamine is a free radical stabiliser which is generally included to promote polymerisation by catalysing acrylamide.	TEMED	25 µl

*** 10% (w/v) APS was freshly prepared by dissolving 100 mg of APS in 1 ml of dH_2O.**

After the resolving gel was prepared, it was poured into the gel cast and a small volume of ethanol was added to remove air bubbles and generate a flat surface. The gel was then left for about 30 minutes to set at room temperature. After which the excess ethanol was removed and the gel was washed with deionised water and then dried using filter paper. The prepared stacking gel solution was added and the comb was placed and left to set for 30 minutes. Both layers of stacking and resolving gels were arranged to ensure that all of the proteins reached the running gel at the same time, regardless of their molecular weight, allowing them to migrate smoothly as tight bands.

2.10.4 Sample preparation and loading

1x volume of cell lysate, diluted to a final concentration of 20-50 µg protein in dH_2O, was incubated at 95 °C for ten minutes with 1x volume of 2X Laemmli. Laemmli buffer contains 4% (w/v) SDS to denature the proteins and make them linear molecules, 10% 2-mercaptoethanol to reduce disulphide bonds, 20% (v/v) Glycerol to increase the density of the sample, 1% (v/v) Bromophonol blue used as a track dye, and 0.125 M Tris-HCl (pH 6.8) and dH_2O.

2.10.5 Electrophoresis and protein transfer

5 µl of precision plus protein dual colour standards (MW range: 10-250 kDa) was loaded into the first lane in order to track the molecular weight of each band. Prepared cell lysates were loaded into the 10% SDS-PAGE gel and the gel was run in a tank containing 1x running buffer (25 mM Tris, 190 mM glycine and 0.01% (w/v) SDS) to generate an electric connection between gel and electrodes. Gels were run at 100 V for 30 minutes until the samples had passed through the stacking gel. Then the voltage was increased until the blue dye ran off the bottom of the gel. The casting plates were separated, the stacking gel removed and the proteins were then transferred to polyvinylidene fluoride (PVDF) membrane using a semi-dry transfer machine. In order to create the transfer sandwich, the PVDF membrane was soaked in methanol for five minutes to activate it and then washed with dH_2O for five minutes. After that, it was placed into 1x transfer buffer (containing 25 Mm Tris, 190 glycine and 20% (v/v) methanol) for five minutes. At the same time, filter papers were also soaked in the transfer buffer. The transfer sandwich was generated by placing the pre-soaked filter paper, then membrane, then gel and then a final layer of pre-soaked filter paper, rolling out the layers to ensure removal of air bubbles, which could disturb the transfer of the

proteins (Figure 2.12). The transfer machine was run for seven minutes at 1.3 A and 25 V. After confirming that the proteins were transferred to the membrane successfully, by checking the transfer of pre-stained standards visually, the membrane was washed once with 1X TBST. This was prepared by mixing 100 ml of 10X TBS with 900 ml of dH_2O and 500 µl of Tween-20 0.05% (v/v) and mixed well. The membrane was incubated in blocking solution (5% (w/v) non-fat milk in 0.05% TBS-Tween) at room temperature for one hour on a shaker to prevent non-specific binding of the antibodies.

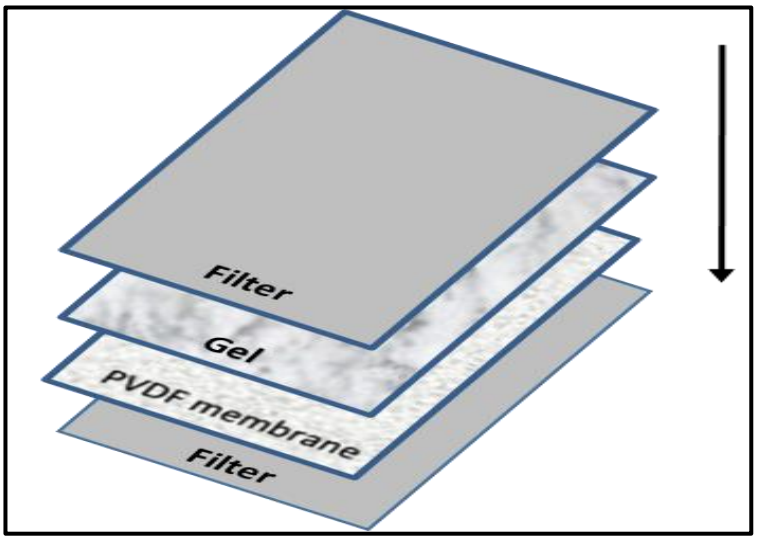

Figure 2.12: Semi dry elecroblotting arrangement: The membrane was placed on soaked filter papers with the transfer buffer followed by placing the gel on the membrane. A further layer of soaked filter was placed on top, as seen in the figure.

2.10.6 Antibody probing and blot development

After blocking, the membrane was incubated with optimised primary antibodies of interest. The desired concentrations of antibodies were diluted in the blocking solution and were incubated on a shaker overnight at 4 °C. On the following day, the membrane was incubated for one hour at room temperature on the shaker and was then washed with TBST three times for five minutes each time in order to remove all unbound antibodies. Then, 10 ml blocking solution containing an appropriate dilution of the relevant horseradish peroxidase (HRP) secondary antibody, was placed on the membrane and incubated for one hour on the shaker at room temperature. After the incubation, the membrane was again washed with TBST five times for five minutes each time.

2.10.7 Chemiluminescence development

In the dark room under red light, the enhanced chemiluminescence (ECL) substrate was added to the membrane and was left for five minutes to react. After removing excess substrate from the membrane, it was wrapped in plastic and placed in a hypercassette and exposed to X-ray film for a time ranging between 30 seconds and one hour depending on the band intensity. Afterwards, the film was placed in a developing solution until the bands developed (1-2 minutes), and then was washed with tap water before transferring into the fixing solution for 1-2 minutes and then washing again with running water and left to dry. The film was then scanned and saved for analysis.

2.10.8 Stripping and re-probing of membranes

Loading controls were performed in order to check that protein quantities had been loaded equally and efficiently, and to compare the expression level between different samples. Since ß-actin is involved in the cytoskeletal structure of cells and is therefore present in all human cells, its expression level is similar in almost all cells, meaning that it can be used as a loading control. In order to assess the levels of ß-actin, the initial antibodies needed to be removed from the membrane and this was done using a stripping solution. The membrane was washed with TBST for five minutes and then 5 ml of stripping buffer was added to the membrane and kept for 15 minutes at room temperature to allow the release of the first set of probes of the primary and secondary antibodies from the membrane. After the incubation, the stripping buffer was removed and the membrane was washed with TBST three times for five minutes each and incubated in 10 ml of blocking buffer for an hour at room temperature with shaking. The blocking buffer was removed and the membrane was washed twice with TBST for five minutes each time. The TBST was discarded and 10 ml of the blocking solution containing 1:10000 of anti-β-actin antibody was added and incubated overnight at 4 °C. On the following day, the membrane was incubated for 60 minutes on a shaker at room temperature before washing with TBST three times for five minutes each time, and then 10 ml of the blocking solution containing 1:2000 -1:10000 of secondary antibody was added and incubated for 60 minutes. The membrane was then washed five times with 1X TBST before developing in the darkroom, using the technique described earlier in 2.10.7.

2.10.9 Analysis of Western blot

In order to compare the level of protein expression in the different cell-lines compared to the house-keeping β-actin, the intensity of the detected bands were calculated as a proportion of the relevant β-actin band using a densitometer programme in the ImageJ software. This ensures that the protein loaded was equal and that any differences between the amounts of protein seen are not just due to loading differences. Each of the detected protein bands was represented as a peak, the signal of which was proportional to the amount of the protein loaded. The exposure time was optimised to avoid overexposure which can provide inaccurate quantification, if the Western blot bands are overexposed the band density will not be different.

2.10.10 Analysis of rSEMA3B protein

Two different protocols were used to examine the stability of rSEMA3B when exposed to cells or their conditioned media or cell lysates.

The first protocol was performed in order to test the effect of cell lysates and cell conditioned media on rSEMA3B stability. DCIS.com and MDA-MB-231 cell-lines were seeded at $10x10^5$ cells per well in 12-wells plate and incubated for 24 hours. The medium was then changed to a serum-free medium for a further 24 hours. Lysates were extracted as described in section 2.10.1 and conditioned media were collected and concentrated 10 to 20 fold to be transferred into Eppendorf tubes. The lysates and conditioned media were treated with rSEMA3B (2 µg/ml) and then incubated for three hours at 37°C. After incubation, a BCA protein assay was done and 20 µg of protein was used for analysing the samples by Western blot (figure 2.13). The concentration of protein started to decrease after three hours so we decided to incubate the treated and untreated lysates and conditioned media for no longer than three hours.

The second protocol was performed to test the effect of intact cells on rSEMA3B. DCIS.com and MDA-MB-231 cell-lines were seeded at 10x105 cells per well in 12-wells plate and incubated for 24 hours as above. The medium was then changed with serum-free medium for a further 24 hours. The medium was then changed to medium containing 1% FCS and cell cultures were treated for 24 and 48 hours with rSEMA3B (2 µg/ml). After the incubation, the conditioned media were collected and the cell proteins were extracted and collected,a BCA protein assay was done and 20 µg of protein was used for analysis by Western blot (figure 2.13).

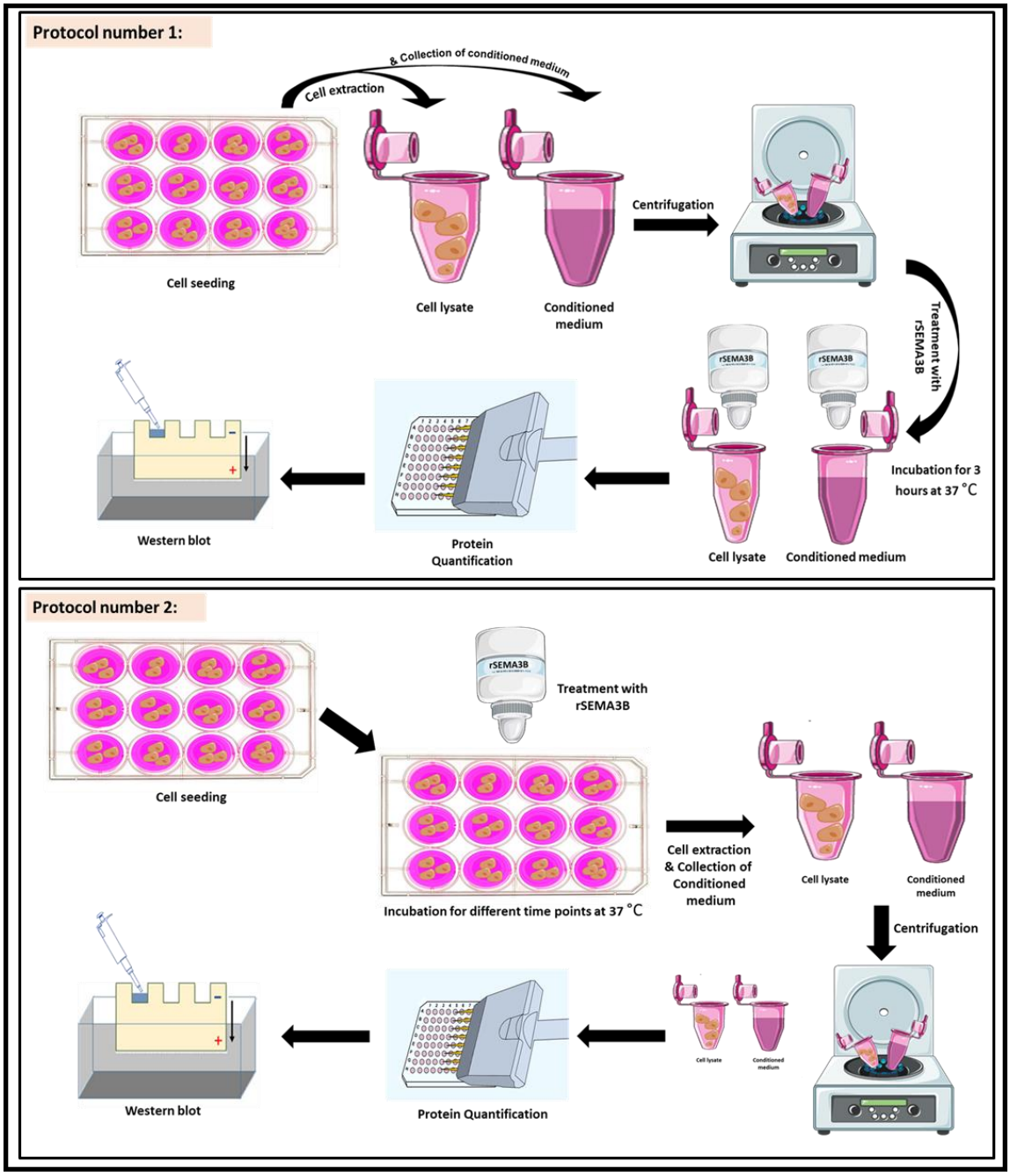

Figure 2.13: Protocols for Western blot treatment by rSEMA3B protein.

2.11 Immunohistochemistry of a breast tissue microarray

Immunohistochemistry was carried out to assess the expression pattern of SEMA3B and furin-like other pro-protein convertases in human tissue breast microarrays (TMAs) which included a spectrum of tissue from normal, premalignant and cancer tissues (table 2.10).

This technique is the process of using antibodies to detect specific proteins (antigens) in cells in the tissue sections of interest. Briefly, the unlabelled primary antibody binds to the antigen of interest and then a labelled reporter secondary antibody will bind to the primary one. The antibody-antigen binding can be visualised by using an enzyme such as HRP, which is commonly used to catalyse a colour-producing reaction.

Table 2.10: Human tissue breast microarrays slides

Tissue type	Number of cases	supplier
Normal Tissue	27	Abcam Uk
Atypical Ductal Hyperplasia (ADH)	8	
Ductal Carcinoma *in situ* (DCIS)	9	
Invasive Ductal Carcinoma	31	

2.11.1 Protocol

The protocol was optimised on tissue sections of pre-invasive (DCIS) and invasive breast tissues which were obtained from patients attending the Royal Hallamshire Hospital between 1995 and 2003 (Research Ethics: SSREC 98/137).

All the TMAs slides were baked at 60 °C for 30 minutes in an oven, deparaffinised in order to remove the embedding wax and then rehydrated. They were then dewaxed using Xylene for ten minutes and transferred into fresh Xylene to ensure that no residue of wax was present on the slides which could interfere with the quality of staining. Slides were placed into 100% (v/v) absolute alcohol for five minutes, and then into a second bath of 100% absolute alcohol for three minutes, transferred into 95% (v/v) absolute alcohol for three minutes before incubating for 30 minutes at room temperature in a mixture 30 ml (v/v) of hydrogen peroxide and 270 ml of methanol in order to block endogenous peroxidase activity and to avoid background staining. After incubation, all slides were washed with gently running water for five minutes.

Heat-induced target retrieval was performed in order to unmask the antigenic epitope and enable an antibody to access the target protein within the tissue and therefore

recover the antigen. The target retrieval solution 10x (citrate buffer containing 10 mM citric acid, 0.05% (v/v) tween 20, pH 6.1) was diluted in dH_2O (1:10) and then was heated in a microwave for three minutes on high power. The slides were then immersed in the solution and heated for seven minutes on low power to avoid boiling and damaging tissues. This step helps to increase the staining intensity as well. Slides were left to cool for ten minutes and then were rinsed with phosphate-buffered saline with 1% (v/v) tween (PBST) once for a few seconds and then washed three times with PBST for ten minutes at room temperature on a rocker. Following that, the slides were tapped off and tissue paper was used to remove any excess PBST carefully without disturbing the tissue. A wax pen was used to draw a circle to minimise the area and ensure that the antibodies cover the entire tissue surface on the slides.

All slides were then placed on a slide tray and a 10% (v/v) blocking solution containing 300 µl of goat/rabbit serum and 30 µl of casein in 3 ml of PBS, was added to each slide to block non-specific antibody binding. The blocking buffer was incubated for 30 minutes and then the slides were tapped off and the primary antibodies SEMA3B, furin and other pro-protein convertases were diluted at different concentrations in 2% (v/v) serum as described in table 2.11 and 200 µl was added to each relevant slide. The controls for the experiment were as follows, the negative control was incubated with only the 2% (v/v) serum blocking solution not containing any antibodies. Positive controls were generated by using tissues that were known to express the protein of interest (table 2.12), and isotype controls (IgG or IgM) were used to ensure that the antibody was specific (table 2.13). All slides were incubated overnight at 4 °C.

On the following day, slides were washed once with PBST for a few seconds and then washed three times for five minutes each on a rocker, and then the relevant secondary antibody was diluted at 1:200 in 2% (v/v) serum and 200 µl added to the slides and incubated for one hour. At the same time, avidin-biotinylated enzyme complex (ABC) containing 2.5 ml of PBS, one drop of A reagent and one drop of B reagent was prepared immediately before use and incubated for one hour. Then, the secondary antibody was washed off the slides with PBST twice for five minutes each and then ABC was applied to the slides and incubated for 30 minutes at room temperature. ABC is commonly used to visualise the antibody-antigen complex. The primary antibody binds to the antigen to form the first complex and then a biotin conjugated secondary antibody is added that is raised against the species in which the primary antibody was

made. The secondary antibody is biotinylated and binds to the primary antibody forming a large complex. The ABC contains HRP that has a high affinity for biotin and which will therefore bind to the biotin on the secondary antibody. The slides were then washed with PBST twice for five minutes each and 3-diaminobenzidene tetrahydrochloride (DAB) was added as a substrate. The peroxidase enzyme of ABC catalyses a colour change in DAB which results in the formation of an insoluble brown-coloured product.

Within ten minutes of adding DAB, the slides were checked under the microscope at 4x magnification to assess the development of any brown colour. Once the brown staining could clearly be seen, slides were washed with running water for five minutes and then were stained with Gill's haematoxylin for one minute to visualise the cell nuclei. After that, they were washed with running tap water until the run off was clear, before incubating in 70% (v/v) alcohol for three minutes to start the dehydration process. Then, slides were placed into 90% (v/v) alcohol for three minutes, 95% (v/v) for three minutes, and then 100% (v/v) for two lots of three minutes. In order to mount the slides to allow examination under the microscope, the slides were placed in xylene for a further two minutes before adding DPX in order to preserve the stain and tissue. The mounted slides were then stored at room temperature.

Table 2.11: IHC Primary Antibodies

Antibodies	Dilution
SEMA3B antibody (Rabbit polyclonal)	1:100
Furin antibody (Rabbit polyclonal)	1:100
PCSK1 antibody (Rabbit polyclonal)	1:100
PCSK2 antibody (Rabbit polyclonal)	1:50
PCSK4 antibody (Rabbit polyclonal)	1:50
PCSK5 antibody (Rabbit polyclonal)	1:100
PCSK6 antibody (Rabbit monoclonal)	1:100
PCSK7 antibody (Rabbit polyclonal)	1:50
PCSK8 antibody (SKI-1 Antibody mouse monoclonal)	1:50
PCSK9 antibody (Rabbit polyclonal)	1:50

Table 2.12: Positive tissue controls used for optimisation of the IHC assay

Protein of interest	Positive control (human tissue sections)	Dilution
SEMA3B	Mouse brain	1:100
Furin	Placenta	1:100
PCSK1	Mouse brain	1:100
PCSK2	Mouse brain	1:50
PCSK4	Prostate tissue	1:50
PCSK5	Colon tissue	1:100
PCSK6	Placenta	1:100
PCSK7	Colon tissue	1:50
PCSK8	Colon tissue	1:50
PCSK9	Colon tissue	1:50

Table 2.13: Isotype controls for IHC

Primary Antibody	Clonality	Isotype
SEMA3B antibody	Rabbit polyclonal	IgG
Furin antibody	Rabbit polyclonal	IgG
PCSK1 antibody	Mouse monoclonal	IgG
PCSK2 antibody	Rabbit polyclonal	IgG
PCSK4 antibody	Rabbit polyclonal	IgG
PCSK5 antibody	Rabbit polyclonal	IgG
PCSK6 antibody	Rabbit monoclonal	IgG
PCSK7 antibody	Rabbit polyclonal	IgG
PCSK8 antibody	Mouse monoclonal	IgM
PCSK9 antibody	Rabbit polyclonal	IgG

2.11.2 Analysis of immunohistochemical staining

The quality of the staining was approved by a consultant histopathologist Dr. P. Vergani Royal Hallamshire Hospital. The staining was assessed in all breast epithelium and tumour tissues and scored using semi-quantitative grading systems.

- The intensity of staining and the scores were given as follows:
- 0= no staining
- 1= weak staining
- 2= moderate staining
- 3= strong staining

All sections were grouped according to lesion type including normal, atypical hyperplasia, DCIS and invasive cancer. Then the percentage was used to determine any changes in expression between each type. Each tissue was compared to the intensity of the staining in normal breast tissue, and the positive and negative controls were used to confirm the validity of the results. The scoring was double assessed by another scorer (Aesha Mukktar), showing a high level of agreement.

2.12 Cytospin

Cytospin is a technique that is used to concentrate cells in a defined area by using a special centrifuge in order to deposit cells evenly onto slides. Since some antibodies did not work in the Western blots, despite attempts at optimisation, cytospins were generated to establish whether the protein expression of these specific proteins could be identified in the cell-lines. The cytospins were followed by immunocytochemistry for detection of the protein expression. Positive controls of cells known to express the protein of interest were included.

2.12.1 Protocol

Once cells reached 70% confluence, cells were washed twice with 10 ml DPBS and trypsnised as described in 2.2.2. In order to optimise the ideal number of cells that would give an even spread in a cytospin, different cell concentrations of $1x10^4$, $2x10^4$, $5x10^4$ and $1x10^5$ cell/ml were spun with $5x10^4$ cells/ml being identified as the optimal concentration where the cells were not too condensed and were distributed evenly on the slides when 200 µl of the cell suspension was used (figure 2.14). Labelled slides, chambers and blotter for each sample were prepared and 200 µl of each cell suspension was added to each slide chamber. Then the slides were centrifuged at 800 x g for two minutes. The slides were removed from the cytocentrifuge and were left to dry prior to staining. All slides were then processed by immunocytochemistry in a similar way to immunohistochemistry.

The slides were fixed with absolute methanol for 30 minutes at room temperature and then incubated in permeabilisation solution, which consists of 0.5% (v/v) Triton 100 and PBS (5 ml Triton 100 in 1 litre PBS) for five minutes in order to permeabilise the membranes of cells. The slides were then washed with PBS three times for two minutes each, hydrated in 95% (v/v) ethanol for five minutes and 70% (v/v) ethanol for five minutes. Thereafter, the same protocol as described in 2.11.1 was followed.

2.12.2 Analysis of cytospin slides

Slides were analysed based on the intensity of staining and the scores were given as follows: 0= no staining, 1= weak staining, 2= moderate staining, 3= strong staining. Each slide was compared with the normal cell-line slide. The controls for the experiment included a negative control, which was incubated with only the 2% serum blocking solution not containing any antibodies, and positive controls which was generated by using cells that were known to express the protein of interest. The scoring was double assessed by another scorer (Aesha Mukktar), showing a high level of agreement.

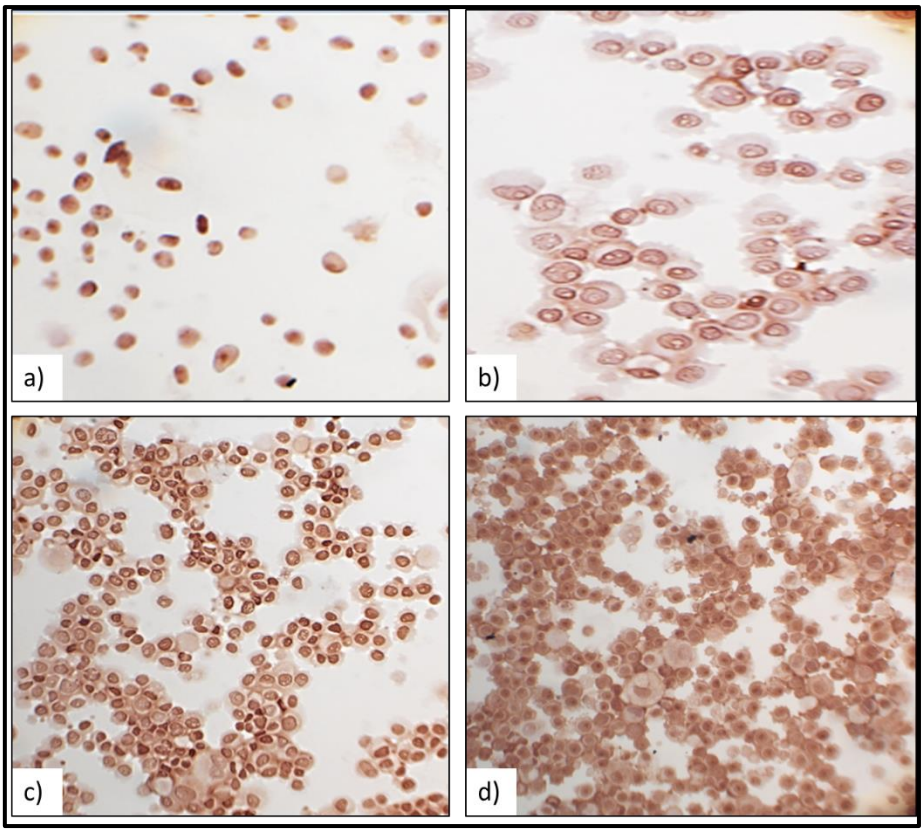

Figure 2.14: an example of the determination of optimal cell density for cytospin slides. **a)** $1x10^4$ cell/ml **b)** $2x10^4$ cell//ml **c)** $5x10^4$ cell/ml **d)**$1x10^5$ cell/ml.

2.13 Statistical analysis

Statistical analysis were carried out using GraphPad Prism software 7 for Windows. All data are presented as the mean ± standard deviation (SD) in all graphs. The data were analysed using one-way ANOVA test followed by Dunnett's post hoc test for multiple comparison/ two way ANOVA to compare the means of data between groups, followed by Tukeys test for multiple comparison. All cell-lines and tissue experiments were compared with the normal non-tumorigenic cells. The criterion for statistical significance was set at $P< 0.05$.

Chapter 3: Development of an *in-vitro* Breast Cancer Model for Studying SEMA3B

3.1 Introduction

SEMA3B is a secreted protein that has been known to be expressed in many normal cells such as endothelial and neuronal cells, but the expression tends to be downregulated in cancer cells such as the breast cancer progresses (Yazdani and Terman, 2006, Varshavsky et al., 2008). Although a previous study from our laboratory has suggested that SEMA3B expression is reduced in human breast cancer compared to normal breast tissue (Staton et al., 2011), there are only minimal studies investigating the expression of SEMA3B or response to recombinant SEMA3B in a few breast cancer cell-lines *in vitro* such as MDA-MB-231 and MCF-7 cells (Varshavsky et al., 2008, Pronina et al., 2009). It has been found previously that SEMA3B mRNA is downregulated in breast cancer MDA-MB-321 cells more than MCF-7 cells (Pronina et al., 2009). To date, the SEMA3B expression in breast cancer cell-lines and its relevance in tumour progression has not been studied in any detail.

Epigenetic alterations are frequent events in human cancers. Abnormalities in DNA methylation and post-translational modifications of histones, which includes some modifications like methylation and phosphorylation are examples of some molecular defects in cancer that can affect gene expression. Hypermethylation one of the common cancer-related disruptions of the DNA methylome, has been observed in breast cancer and found likely to be linked with promotors of tumour suppressor genes, causing transcriptional silencing (Kuroki et al., 2003, Loginov et al., 2015). However, previously published studies have suggested that downregulation of SEMA3B mRNA may be due to the methylation of CpG-islands of the SEMA3B gene and contributes to the tumour suppressor function of the *SEMA3B* gene (Pronina et al., 2016).

SEMA3B is deleted in some types of cancer and decreased in the majority of cancer cell-lines due to either allele loss or methylation (Ito et al., 2005). However, SEMA3B protein is highly susceptible to degradation by pro-protein convertases, upstream of C-terminal it is highly conserved and has been shown to be a cleavage site for the pro-protein convertases, which therefore may also result in inactivation of SEMA3B (Varshavsky et al., 2008). Since it has been shown that furin-like pro-protein

convertase processing of SEMA3B can inactivate the anti-angiogenic activity of this protein, therefore, it is likely that SEMA3B is a tumour suppressor gene which is switched off or mutated during breast cancer development. In order to investigate these further, a range of breast cancer cell-lines were used representing the different malignancy of breast disease, to study the growth-suppressive and the anti-proliferative effect of SEMA3B in breast cancer.

Breast cancers arise in different areas of the breast, therefore, distinguishing between each subtype is important as each has different diagnoses and treatment options and responses. Based on molecular biology and invasiveness, breast cancers are divided into three main groups, including non-invasive, invasive, and metastatic breast cancers (see section 2.2.1). Breast cancer is initiated in normal breast epithelium, and due to some neoplastic evolution, it progresses to atypical ductal hyperplasia which is considered as a pre-malignant stage which develops to ductal carcinoma *in situ*. Whilst a cancer is still confined within the breast and not spread beyond the cell membrane this known as non-invasive cancer and this reflects a pre-invasive stage. Once cancer cells breach the duct or lobule wall and access to the circulation and lymph system they are then classified as invasive cancer. Cancers cells with the ability to travel or move to other parts of the body may be highly invasive and have the metastatic capacity, are classified as metastatic breast cancers (Bombonati and Sgroi, 2011).

However, there is no guarantee that the progression of breast cancer is likely to progress in sequence from pre-malignant or pre-invasive stage to the invasive stage. There is evidence that *in situ* disease is more likely to progress to invasive breast cancer if not treated. The DCIS cells may have bipotential progenitor properties, generating heterogeneous cell populations with tumour-initiating features (Hu et al., 2008, Cowell et al., 2013). It has not been yet identified how to predict the most likely patients to develop invasive disease following a diagnosis of DCIS. However, it has been observed that 20 to 50% of DCIS patients have developed invasive breast cancer later. (Cowell et al., 2013). Therefore, in this chapter, a panel of different cell-lines were used to represent each stage of breast cancer progression to mimic the development and diversity of breast disease. The MCF-10A cell-line was used as an example of non-transformed breast ductal epithelial cells, MCF-10AT cells were used to represent pre-malignant hyperplastic ductal epithelial cells, and the DCIS.com cells was used to represent pre-invasive ductal carcinoma *in situ*. The invasive breast

cancer cell-lines were chosen to represent a diversity of hormone receptors status and metastatic potential. MCF7 have wild-type p53, and T47D have mutant p53, and both are hormone-dependent breast cancer cell-lines exhibiting luminal A subtypes (ER and PR positive) with non-invasive and low to moderate metastatic potential, respectively (Aka and Lin, 2012). Interestingly, T47D cells are more responsive to progesterone than the MCF-7 cells, suggesting the susceptibility of T47D cell-lines to be targeted and treated with specific progesterone therapy (Yu et al., 2017). MDA-MB-231 cells, which are less differentiated and have a more mesenchymal-like appearance, were used to represent triple-negative tumours (ER-, PR-, HER2-) with a highly invasive and metastatic potential capacity. Finally, as bone is the most common site of metastasis, we used the fully bone homed MDA-MB-231-BM cell-line.

Hence, this chapter aimed to assess the *in vitro* behaviour of this model of breast cancer development, and then to study the expression of SEMA3B in breast cancer progression. Specific aims were to:

1. Investigate the proliferation and metabolic activity of the normal, pre-malignant, pre-invasive, invasive, and fully bone homed breast cell-lines.
2. Investigate the migration and invasion of the normal, pre-malignant, pre-invasive, invasive, and fully bone homed breast cell-lines.
3. To measure the expression of cytokines in all cell-lines.
4. To measure the expression of *SEMA3B* mRNA and protein in these cell-lines and see whether it correlated with protein expression in human breast tissues also representing breast cancer progression.

3.2 Methods

The cell-lines representing different severities of breast lesion used in this project were maintained in sterile culture conditions as previously described in section 2.2.2.

3.2.1 Cell counting assay

The assay was used to investigate the growth pattern of cell-lines used and the viability and total cell count of the breast cells. The cell number was counted using an automated cell counter machine and the proliferation rate was calibrated based on the relative increase in cell number versus the number of days. Untreated tumour and non-tumour cell-lines were seeded at $2x10^4$ in 12-well plates of three replicates and incubated over a 96 hour period in their normal growth medium, and the viable cells were counted as described in section 2.3.1.

3.2.2 MTS assay

The assay was used to assess the metabolic activity of each cell-line. The untreated cells were seeded at $5x10^3$ in 96-well plate for 24, 48, 72 and 96 hours and the optical densities were measured at the absorbance of 490nm following the protocol described in section 2.3.3.

3.2.3 Scratch (wound healing) assay

The assay was used to assess the ability of cells to migrate. The images were taken at 0, 24 and 36 hours using a cell imaging system microscope (10X phase objective). The rate of wound closure was measured as described in section 2.4.

3.2.4 Invasion assay

The assay was used to assess the invasive ability of each cell-line using a pre-coated Matrigel invasion chamber. Photomicrographs were taken using a microscope and the invaded cells were counted as described in section 2.6.

3.2.5 CBA assay

The assay was used to measure different cytokines that have been linked to cancer progression following the protocol in section 2.8.

3.2.6 qPCR analysis

The technique was performed to investigate the mRNA expression of SEMA3B in all the cell-lines by extracting mRNA from the cells, converting to cDNA for use in the

quantitative real-time PCR as detailed in section 2.9. The validated SEMA3B qPCR primer ID and sequence is listed in table 2.1.4.

3.2.7 Western blot analysis

The analysis was used to assess SEMA3B protein expression in all cell-lines by preparing 20 µg protein samples, which were resolved by SDS-PAGE, transferred to a membrane and probed with the corresponding primary and secondary antibodies for visualization by chemiluminscence. β-actin was used as a housekeeping protein to normalise protein expression and semi-quantification was performed using Image-J software as described in section 2.10.

3.2.8 Immunohistochemical staining

This method was performed to characterize SEMA3B expression in human tissue microarray sections representing a model of breast cancer progression as detailed in table 2.10 along with the positive control tissue for SEMA3B, mouse brain tissue. Immunohistochemical staining was performed and analysed as described in sections 2.11. The total sample size of 75 specimens comprised

- Normal breast (n=27)
- Pre-malignant atypical ductal hyperplasia (ADH, n=8)
- Pre-invasive ductal carcinoma *in situ* (DCIS, n=9)
- Invasive breast carcinoma (IC, n=31)

All data were analysed using GraphPad Prism 7 software, with all statistical analyses performed by comparing each cell-line/tumour tissue to the non-tumorigenic MCF10A cells/normal tissue. The tests used were one-way ANOVA test with Dunnett's multiple comparisons test. Data expressed as mean ± SD from at least three independent experiments. P-value of <0.05 was taken to be significant.

3.3 Results

3.3.1 Cell growth of breast cell-lines

Cell growth curves for all breast cells lines were established to compare the growth patterns and rates across the spectrum of breast disease. As shown in the figure.3.1, the human mammary epithelial cell-line MCF-10A had the highest cell growth compared with all other cells. The pre-malignant MCF-10AT and the pre-invasive DCIS.com cells had a slower cell growth compared with the invasive cells except with T47D cells as they grew at the slowest growth rate. The cell growth of the invasive cells MDA-MB-231 (highly metastatic, triple-negative) and MDA-MB-231-BM (highly metastatic, triple-negative, bone homing) were much higher than other pre-malignant, pre-invasive and invasive cells (figure 3.1). The exception was the MCF-10A cells that proliferated very fast. This could be due to the fact that a different growth medium was used to sustain the growth of these cells that included insulin, EGF and hydrocortisone and cholera toxin

The doubling times of all cell-lines were determined by counting the viable cells at different time points (24, 48, 72 and 96 hours) and then the doubling time of each cell-line was calculated by doubling time computing tool from Roth (2006) used the following equation:

$$Doubling\ Time = \frac{Duration * \log 2}{\log(final\ concentration) - \log(initial\ concentration)}$$

There are three phases of the growth curve. These include the lag phase which represents the first day of the seeding, the exponential phase is the period when the cells start proliferating until they reach the plateau phase when the cell growth is inhibited. However, MCF-10A cells had the shortest doubling time (20.83 hours) with the highest cell growth. The doubling time for the rest of the cell-lines was in the following order: MDA-MB-231 (23.22 hours), MDA.MB.231-BM (25.34 hours), MCF-7 (30.96 hours), MCF-10AT (32.39 hours), DCIS.com (33.05 hours) and T47D (48.10 hours) which showed the longest doubling time. The differences in cell growth are based on the population doubling time, as summarized in table 3.1.

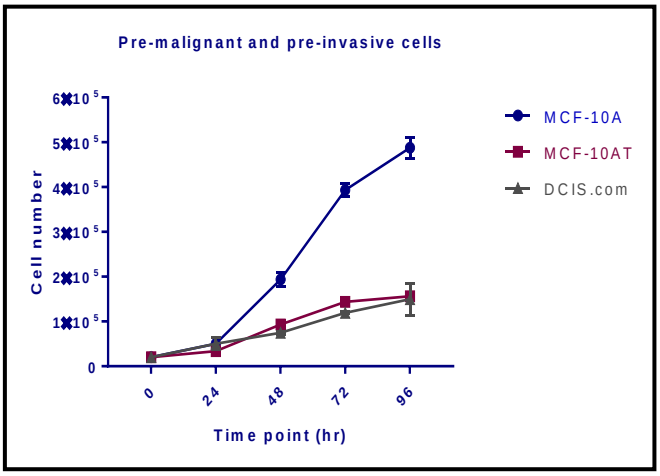

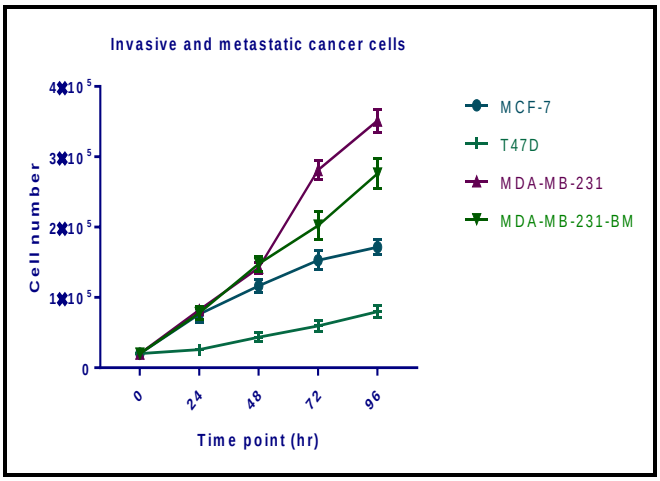

Figure 3.1: The cellular growth rate and population doubling time for each cell-line calculated using doubling time computing software. Cells were seeded at $2x10^4$ in 12- well plates and incubated for 24, 48.72 and 96 hours after which the cells were monitored under the microscope to observe the cell growth and measuring the cell number using cell counting chamber. These data are presented as mean ± SD from three independent experiments.

Table 3.1: The doubling time of the cell-lines

Cell type	Doubling time	ATCC datasheet
MCF-10A	20.83 hour	20 hours
MCF-10AT	32.39 hour	Not available
DCIS.com	33.05 hour	Not available
MCF-7	30.96 hour	29 hours
T47D	48.10 hour	32 hours
MDA-MB-231	23.22 hour	36 hours
MDA-MB-231-(BM)	25.34 hour	Not available

3.3.2 Metabolic activity of breast epithelial and tumour cell-lines

Since differences in cellular metabolic activity may contribute to the tumour cell phenotype (Kroemer and Pouyssegur, 2008) and targeting the mitochondrial metabolism can help to slow or inhibit the growth and proliferation of cancer cells, therefore, the metabolic activity and cell viability across the spectrum of breast cell-lines were investigated by MTS assay. The cells were seeded at $5x10^3$ in 96-well plates for 24, 48, 72 and 96 hours, and the optical densities were measured at the absorbance of 490 nm as described in section 2.3.3. As shown in figure 3.2, the pre-malignant MCF-10AT, normal epithelial MCF-10A and pre-invasive DCIS.com cells had higher metabolic activity than other cells. In contrast, invasive breast cancer cells demonstrated a lower metabolic activity compared to the non-tumour cells. The invasive cells showed a different pattern of metabolic activity, with highly metastatic cells showing lower metabolic activity than the low metastatic potential cells with the exception of T47D, which demonstrated the lowest metabolic activity (figure 3.2). However, the deficiency of mitochondrial activity in aggressive tumours may play a role in these findings, resulting in dysfunction of the NADH-oxidizing mitochondrial enzymes and therefore altered metabolism in tumours (Zancan et al., 2010). There is a positive correlation between glycolytic efficiency, and cell aggressiveness suggesting that cells with lower glycolytic efficiency compensate with higher mitochondrial metabolism. Therefore, the lack of mitochondrial activity in invasive MCF-7, MDA-MB-231 and MDA-MB-231-BM cells, make these cells highly dependent on glycolytic flux for energy and consequently have high a glycolytic efficiency with a lower mitochondrial metabolism which may result in a lower metabolic activity (Zancan et al., 2010).

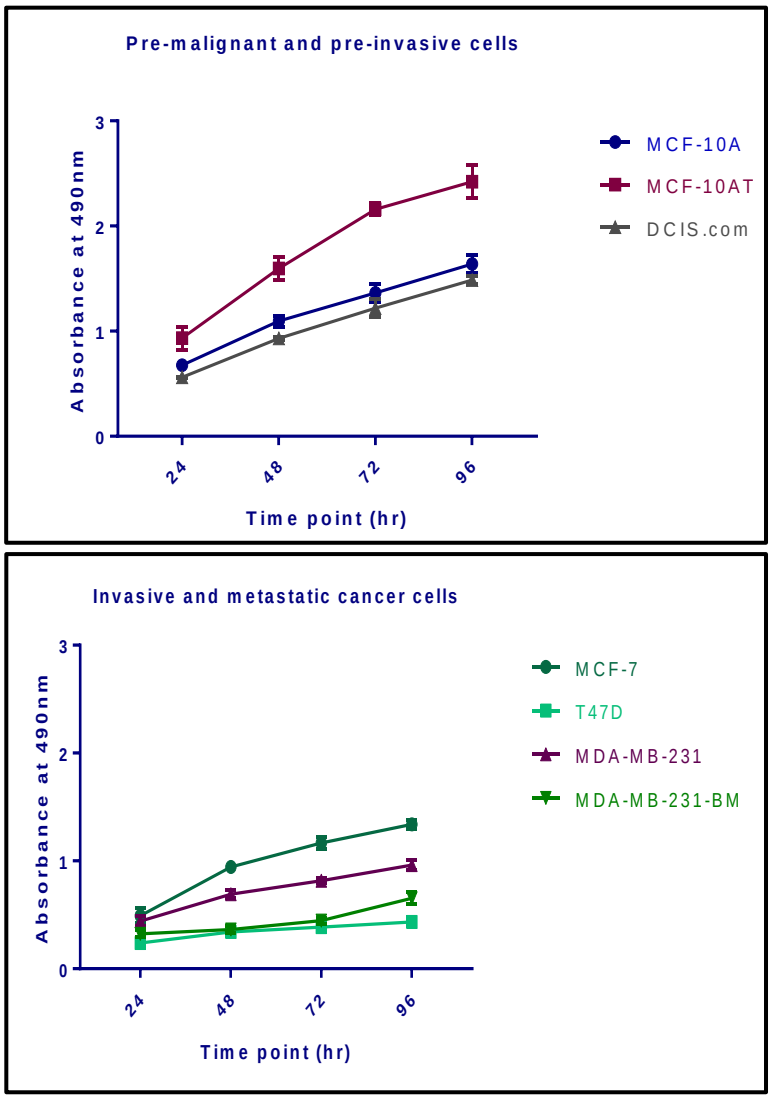

Figure 3.2: Metabolic activity of the non-tumour and tumour breast cell-lines. Cells were seeded at $5x10^3$ in 96-well plate and incubated for 24, 48, 72 and 96 hours after which MTS reagent (20 µl) was added and incubated for three hours before the absorbance was measured by spectrophotometer at 490 nm in order to assess the metabolic activity of each cell-line. These data are presented as mean ± SD of three independent experiments.

3.3.3 Migration of breast epithelial and tumour cell-lines

A migratory phenotype is required for the development of metastasis, therefore the scratch assay was performed to assess the cell migration rates of the different cell-lines. Cells were seeded at $1x10^5$ in 24-well plate to obtain a confluent monolayer after 48 hours, then subjected to a scratch, with images captured at 0, 24 and 36 hours post wounding as described in section 2.4.2. The cells were treated with mitomycin C to inhibit cell proliferation one hour prior to the scratch assay, thus ensuring only migration is assessed. The rate of migration was measured by quantifying the total distance across the scratch at each time point compared to the zero-hour time point.

As shown in figure 3.3, the results indicated that the normal, the pre-malignant and the pre-invasive cells did not migrate over the 36 hours time point of the assay. However, the invasive cell-lines did migrate, the fastest rate of migration by MDA-MB-231-BM > MDA-MB-231> MCF-7> T47D at 24 hours (100% ±, 60% ±, 49.34% ±, 30 % ±, respectively). By 36 hours, both MDA-MB-231-BM and MDA-MB-231 cells had 100%± wound closure with MCF-7 at 60% ± and T47D at 37.42% ±.

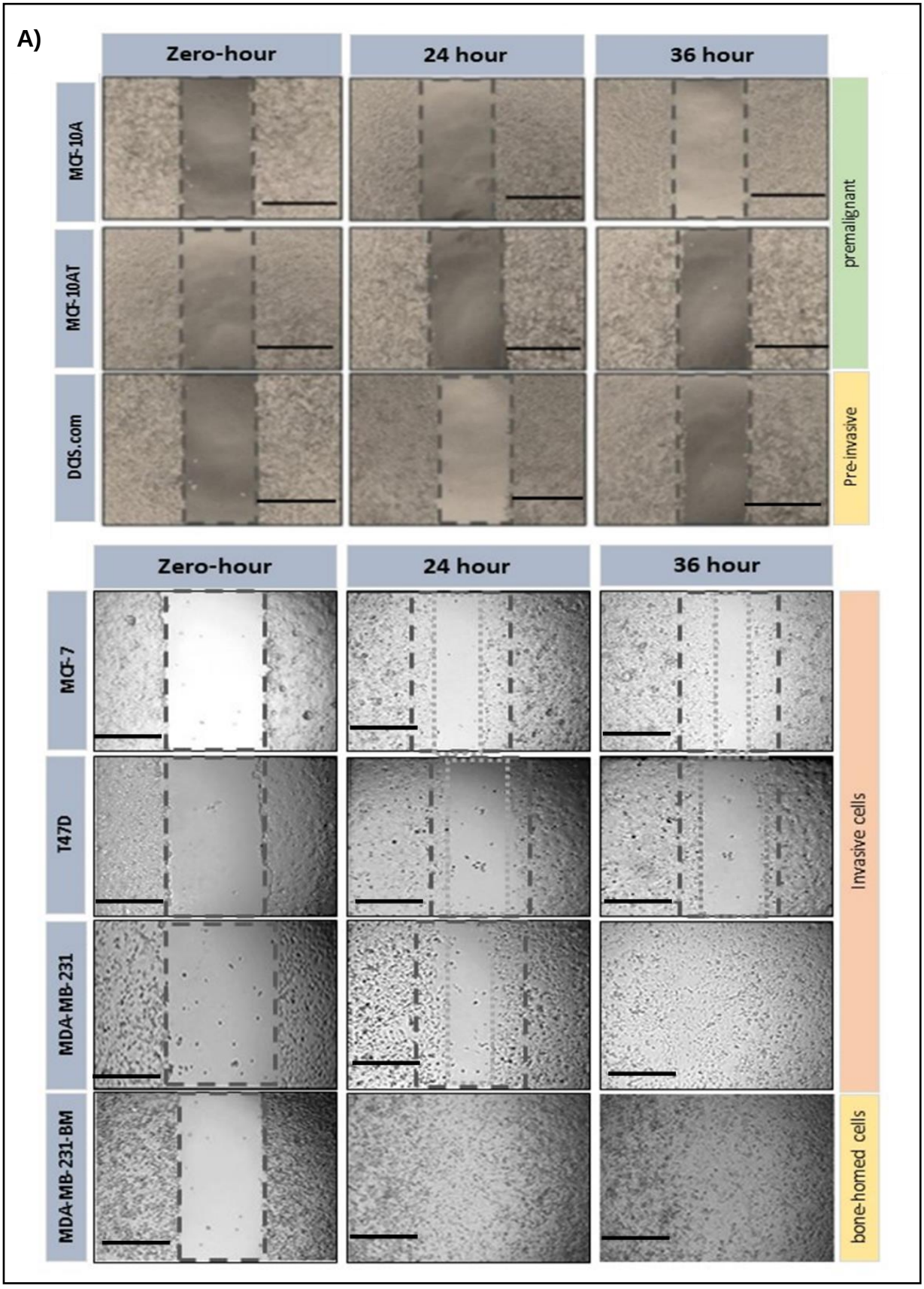
A)
Zero-hour
24 hour
36 hour
MCF-10A
MCF-10AT
DCIS.com
premalignant
Pre-invasive
Zero-hour
24 hour
36 hour
MCF-7
T47D
MDA-MB-231
MDA-MB-231-BM
Invasive cells
bone-homed cells

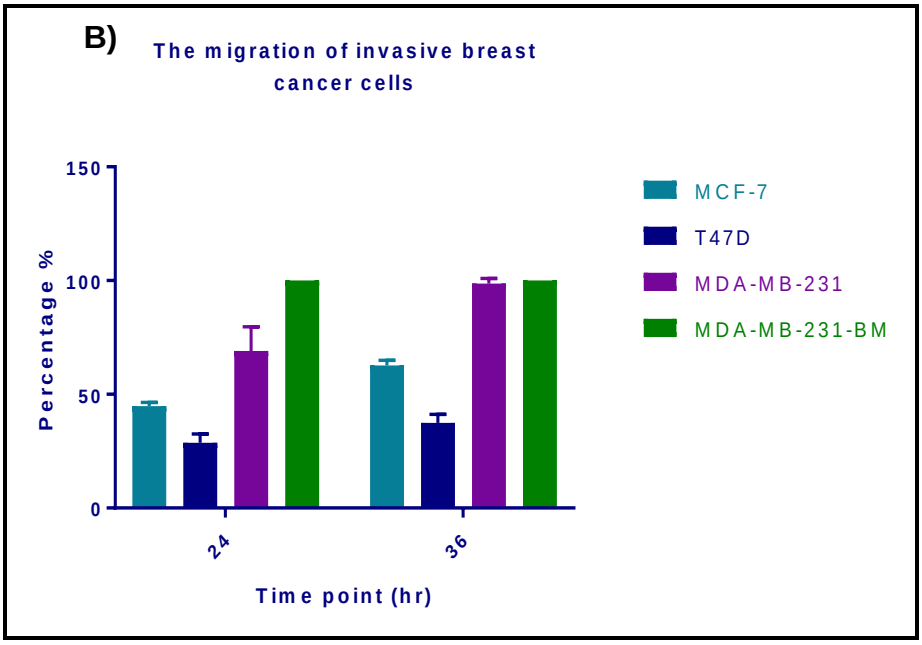

Figure 3.3: The migration of breast cancer cells. A) Representative photograph images. Scale bar = 100 µm. **B)** Percentage of wound closure at two time points. Cell migration was captured at 0, 24, and 36 hours on the EVOS® Cell Imaging System. The data are representative of three independent experiments. Error bars represent mean ± SD.

3.3.4 Invasion of breast epithelial and tumour cell-lines

As migration and invasion involve different mechanisms, with invasion requiring the ability to degrade and migrate through a basement membrane and/or extracellular matrix, the invasion assay was carried out to understand the behaviour and the ability of normal and cancer cells to invade through Matrigel pre-coated transwell chambers representing invasion through the basement membrane. In order to encourage the cells to invade a chemo-attractant gradient was established by using complete growth medium containing 10% FBS, to measure the capacity of the cells motility and invasiveness toward a chemo-attractant gradient as described in section 2.6.

As shown in figure 3.4, the non-malignant MCF-10A, pre-malignant MCF-10AT or pre-invasive DCIS.com cell-lines did not invade as demonstrated by the absence of cells on the underside of the membrane. However, the invasive tumour cells were able to cross the basement chambers. The highest number of invaded cells were observed in MDA-MB-231 (246 ±), MDA-MB-231-MB (234.68 ±) then MCF-7 (217.5 ±), whilst T47D cells (11.7 ±) had the lowest invasion by the cells over 72 hours.

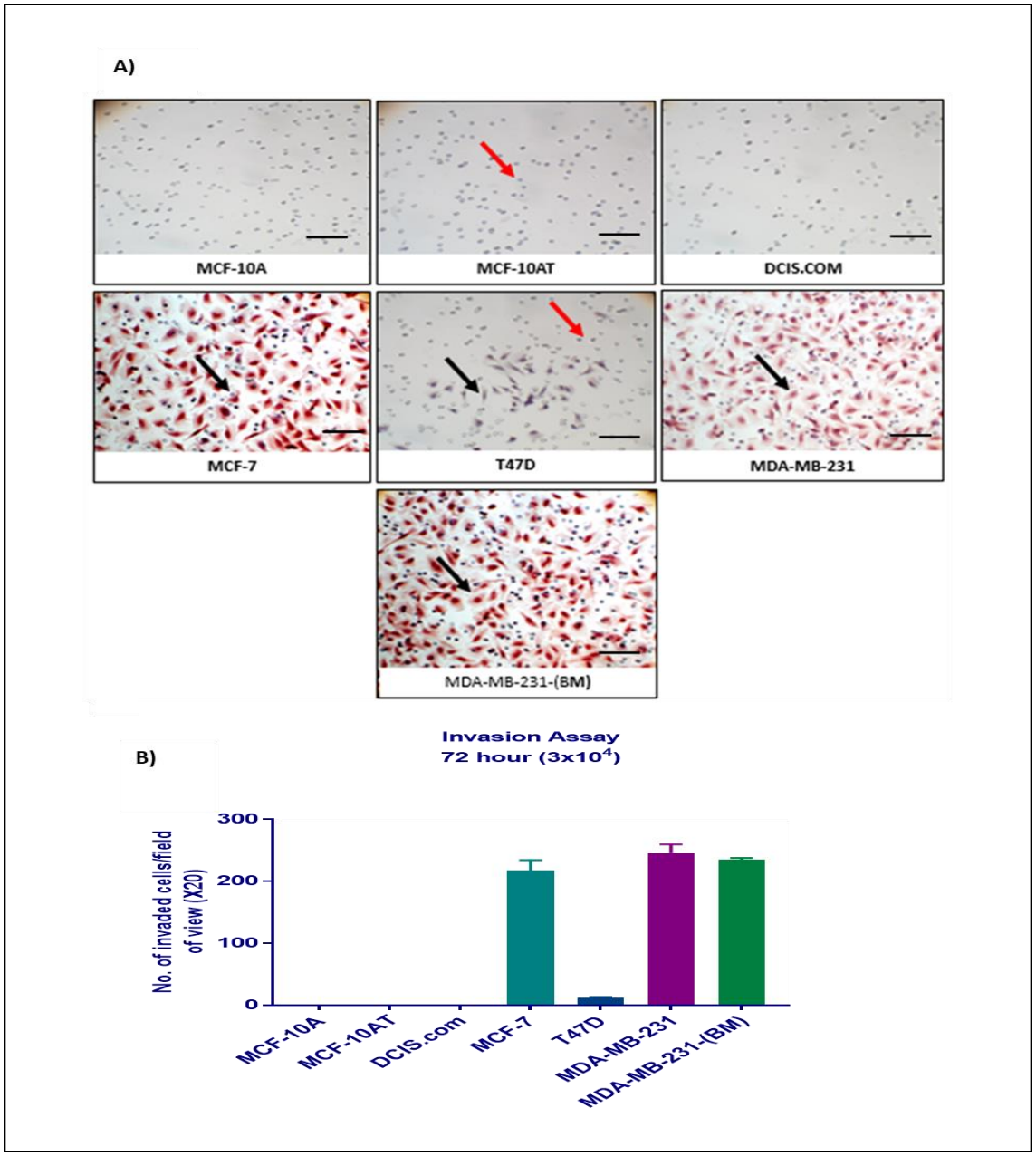

Figure 3.4: Invasion of breast epithelial/tumour cell-lines. A) Representative image of a randomly selected field of invasion. The cells were stained with haematoxylin and the invaded cells were counted by eye and using the cell counter in Image J software. The images show no invaded cells in normal, pre-malignant, and pre-invasive cells compared to the invasive cells. Scale bar = 100 µm. **B)** The data are representative of three independent experiments. Error bars represented mean ± SD. The black arrow indicates the invaded cells, and the red arrow indicates the membrane pores.

3.3.5 Cytokine expression of breast epithelial and tumour cell conditioned media

Breast cancer progression is linked to a change in the expression of cytokines, including IL-11 and IL-8. Therefore, to validate this cell-line model as a good model of breast cancer progression for use in investigating SEMA3B expression, it was essential to establish the changing expression of common key cytokines in the model. The data from the CBA assay measured the expression of six critical cytokines in the conditioned medium, and the data is presented in figure 3.5.

IL-8 is a chemoattractant cytokine that induces chemotaxis in target cells. It is found to be a potent mediator of angiogenesis. IL-8 secretion is increased in inflammation and has been implied to have a role in cancer development (Waugh and Wilson, 2008). Our findings demonstrated a high expression of IL-8 in all the cell-lines with the highest expression found in MCF-10A and the lowest expression in T47D cells ($P < 0.0001$).

IFN-Y has the ability to inhibit the growth of several types of a tumour; however, recently it was found that IFN-Y also has a stimulating effect on tumour progression (Xu et al., 2009, Mojic et al., 2017). Our result showed that the expression of IFN-Y was very low or non-existent in all the cell-lines.

IL-10 is a pleiotropic anti-inflammatory cytokine and has been known to have a variety of roles in breast cancer progression. Although IL-10 is demonstrated to have an anti-tumour effect, IL-10 also decreases the immune response. IL-10 has been shown able to suppress the production of other cytokines such as IL-8, IFN-Y, IL-12 and GM-CSF. The secretion level of IL-10 has been found more in tumour than in normal cells e.g. in supernatant of breast cancer cell, the secretion of IL-10 found able to stimulate angiogenesis of breast cancer (Sabat et al., 2010, Hamidullah et al., 2012). However, our results showed that IL-10 was minimally expressed in all the cell-lines, with no significant differences between the cell-lines.

In contrast, **IL-11** is a member of the IL-6 family of cytokines, and its overexpression is associated with tumorigenesis and inflammation (Johnstone et al., 2015). However, our data showed low expression of IL-11 in MCF-10A and T47D cells but had significantly high expression of IL-11 in invasive cells including MCF-7 ($P<0.0001$), MDA-MB-231 ($P<0.0001$), and MDA-MB-231-BM ($P<0.0001$) compared with the normal epithelial MCF-10A cells.

G-CSF (Granulocyte-colony stimulating factor) has been known to stimulate neutrophil proliferation and maturation. It, therefore, helps to fight infection by inducing the production of cytokines (Xu et al., 2000). Our findings showed that G-CSF expression was low in the breast epithelial cell-line MCF10A, pre-malignant MCF10AT and pre-invasive DCIS.com and T47D cell-lines, but was significantly increased in MCF-7 ($P<0.0001$) and MDA-MB-231 invasive cell-lines ($P<0.0001$) compared with the normal MCF-10A cells, but reduced again in the fully bone homed MDA-MB-231-BM cell-line.

GM-CSF (Granulocyte-macrophage colony-stimulating factor) that functions as a cytokine and has a vital role in the inactivation of VEGF. It helps decrease the progression of angiogenesis and metastasis of cancers (Eubank et al., 2004). However, our data found that the expression of GM-CSF showed an almost identical pattern to G-CSF, with significantly increased expression in MCF-7 ($P<0.0001$) and MDA-MB-231 invasive cell-lines ($P<0.0001$) compared to normal cells.

It should be noted that the number of cells in the collected supernatant was not quantified, which may account for some of the differences seen.

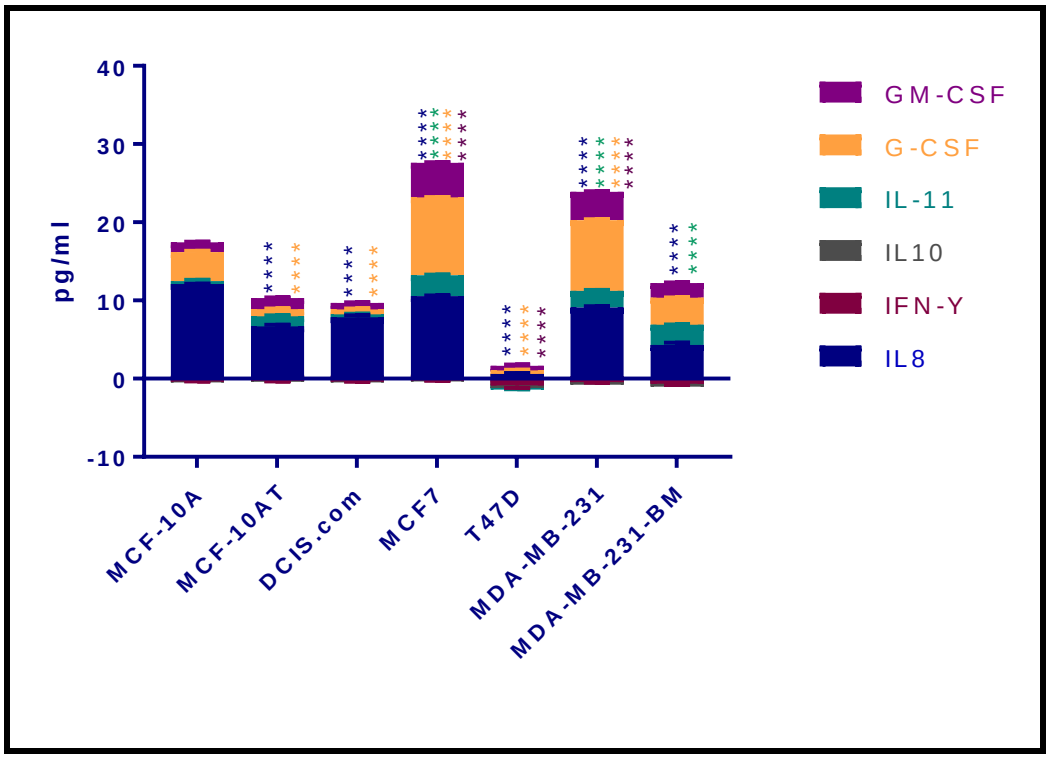

Figure 3.5: Concentration of cytokines (pg/ml) in different cell-lines supernatants measured by CBA. Cells were seeded at $2x10^6$ cells/ml in T75 flask in complete medium. After reaching 70-80 % confluency, the media was replaced with serum free medium and after 24 hours the medium was collected and centrifuged at 1000 x g for five minutes. The supernatants were then collected to be investigated by CBA.These data are the mean ± SD of three independent experiments. Data was analysed statistically by two-way ANOVA followed by Tukey's multiple comparisons test, with comparisons to the normal MCF-10A cells. ****P<0.0001 with respect to relevant MCF-10A expression (control).

3.3.6 *SEMA3B* mRNA expression in breast epithelial and cancer cell-lines

As some studies have indicated, the expression of SEMA3B may be lost in tumour cells, (Tse et al., 2002, Castro-Rivera, 2005) we therefore investigated the expression of *SEMA3B* mRNA in our cell-lines representing breast cancer progression to confirm whether or not the *SEMA3B* gene is expressed. *SEMA3B* mRNA was determined by qPCR as described in 2.9. *GAPDH* gene was used as a housekeeping gene for all qPCR experiments. The relative expression of *SEMA3B* was quantified to determine the changes in steady-state mRNA levels among all the selected cell-lines and expressed relative to the expression level of *GAPDH*. As shown in figure 3.6, the highest *SEMA3B* mRNA expression was found in MCF-10A cells compared to other cell-lines with a gradual decrease in gene expression seen with increasing malignant and invasive potential of the cell-lines with the lowest expression found in MDA-MB-231-BM ($P<0.0001$) cells compared to MCF-10A cells.

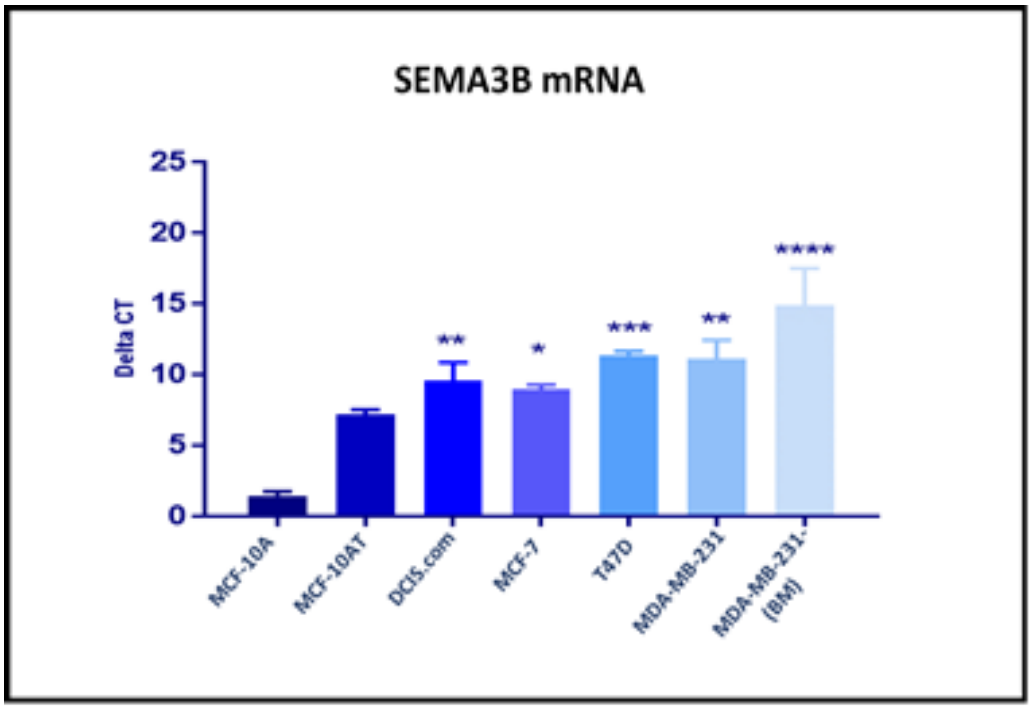

Figure 3.6: qPCR analysis of *SEMA3B* mRNA expression in breast normal /cancer cells lines: RNA was extracted from cells and cDNA was synthesised and was analysed by qPCR. GAPDH was used to confirm the integrity of RNA. Data are presented as a ratio to GAPDH. Y-axis represented the Delta Ct which was calculated by subtracting the mean of cell Ct from the mean of the reference gene. Data presented the mean +/- SD of three independent experiments. The lower the Ct level the higher the amount of target nucleic acid. Data was analysed statistically by one-way ANOVA with Dunnett's multiple comparisons and P values were generated * indicates P<0.05, ** indicates P<0.01, *** indicates P<0.001 and **** indicates P<0.0001.

3.3.7 SEMA3B protein expression in normal breast and cancer cell-lines

Since the expression of *SEMA3B* mRNA was detected in all the cell-lines, but with reduced expression with increasing malignancy of the cells, it was important to determine whether this related to final protein expression of SEMA3B in these cells. The protein expression of SEMA3B was evaluated by Western blotting in the cell lysates and conditioned media from the cells.

As shown in figure 3.7, in the cell extracts, only the normal breast epithelial (MCF-10A) cells expressed full-length SEMA3B (83 kDa). In all other cell-lines, the only band present was at 51 kDa, which was a proteolytically cleaved form of the protein. In contrast to the reduced mRNA expression with increasing cell malignancy, levels of cleaved SEMA3B protein increased with increasing malignancy with MDA-MB-231 and MDA-MB-231-BM expressing the highest level of cleaved SEMA3B (P=0.0001). Interestingly additional bands were observed at ~37 kDa present in MCF-7 and T47D cells and are thought to represent an additional proteolytic cleavage product.

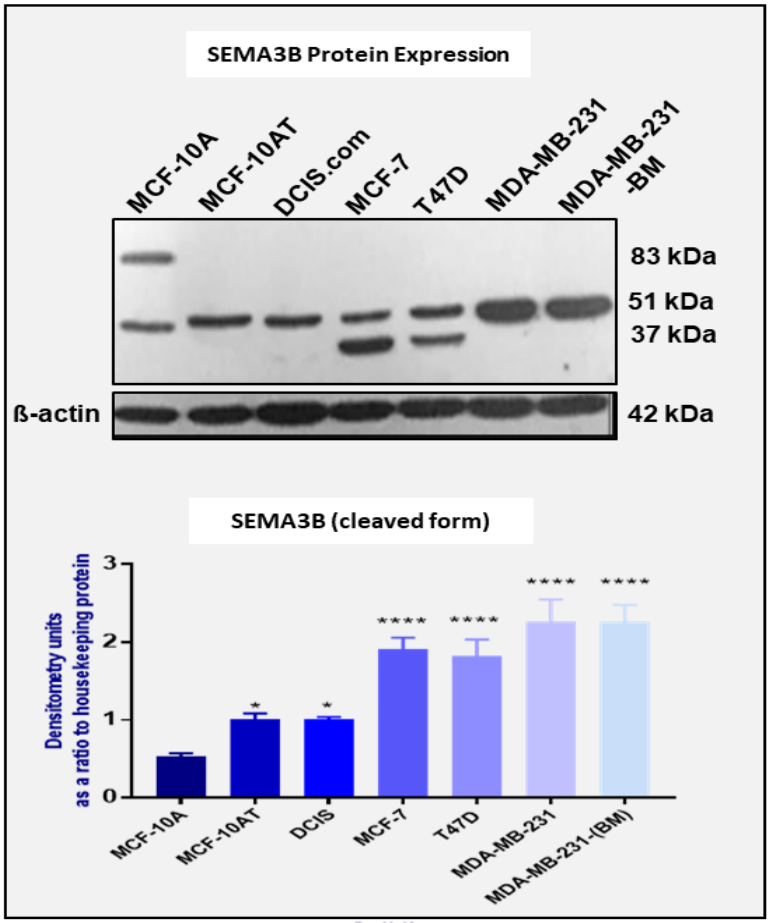

Figure 3.7: Representative immunoblot of the expression of cleaved SEMA3B protein in breast tumour and non-tumour cell-lines. Cell lysates were separated on a 10% SDS-PAGE gel, and then blotted onto PVDF and probed with the anti-SEMA3B antibody. To confirm that the amount of protein in each lane was equal, the membrane was stripped and re-probed with anti-β-actin housekeeping protein as a loading control. Densitometry analysis was performed for all cells using ImageJ software to assess relative band densities. Data are the mean ± SD of three independent experiments. Data was analysed statistically by ordinary one-way ANOVA followed by a post hoc Dunnett's test (* represent $P<0.05$ and **** represent $P<0.0001$ in comparison to the normal epithelial MCF-10A cells). The sizes of molecular weight markers are indicated in kDa. The bottom graph refers only to the cleaved form of SEMA3B. Representative immunoblot shown of n=3.

3.3.8 SEMA3B protein detection in conditioned medium of normal breast and cancer cell-lines

SEMA3B is a secreted protein, we therefore examined the expression of SEMA3B in conditioned medium in all selected cells. This result showed a similar pattern of expression with MCF-10A cells being the only cell-line to secrete the full-length (83 kDa) protein, and all others secreting the 51 kDa cleavage product (figure 3.8).

Compared with the conditioned medium of normal epithelial MCF-10A cell, the highest level of cleaved SEMA3B expression was found in MDA-MB-231-BM ($P=0.0001$) and then in DCIS.com then MDA-MB-231 condtioned medium ($P<0.05$) respectively. However, the lowest expression of cleaved SEMA3B was found in MCF-10A conditioned medium (figure 3.8).

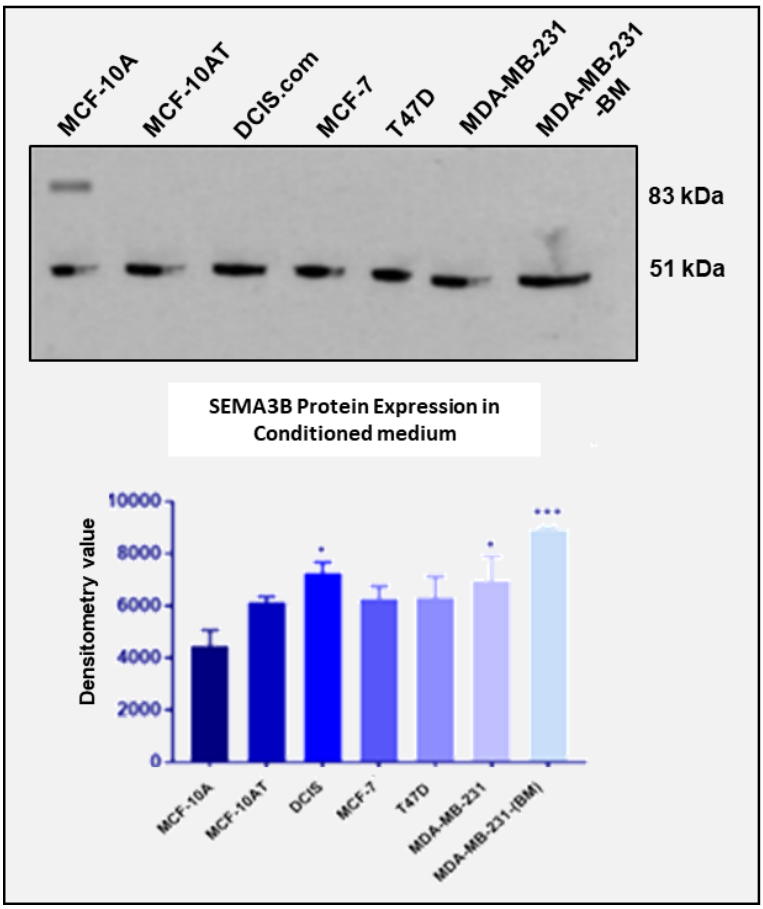

Figure 3.8: Representative immunoblot of the detection of SEMA3B in conditioned medium of breast tumour and non-tumour cells. Conditioned medium was collected from cells, and was quantified by BCA and then was separated on a 10% SDS-PAGE gel, and then blotted onto PVDF and probed with an anti-SEMA3B antibody. The sizes of molecular weight markers are indicated in kDa. Densitometry analysis was performed for all cells using ImageJ software to assess band densities and presented as densitometry value. Data are the mean ± SD of three independent experiments. Data was analysed statistically by ordinary one-way ANOVA followed by a post hoc Dunnett's test (* represent $P<0.05$ and **** represent $P<0.0001$ in comparison to normal MCF-10A cells). Representative immunoblot shown of n=3.

3.3.9 Assessment of SEMA3B protein expression in human breast tissue

Since there are limited studies on the protein expression of SEMA3B in breast cancer tissues we aimed to determine whether there is any correlation between protein expression in cell-lines and with those obtained from human tissue microarray slides, which included different breast tissue stages (normal, atypical hyperplasia, DCIS and invasive tissues). The histological analysis revealed that there was a moderate to strong cytoplasmic expression of SEMA3B (71.42%) in normal tissue and this decreased to 62.5% in atypical ductal hyperplasia and then 28.12% in the invasive tissue. The DCIS tissue had surprisingly high expression 75%, but there were only nine DCIS samples which may account for this. SEMA3B expression was identified in the majority of normal, pre-malignant and pre-invasive tissues, however the expression of lower intensity and less extensive was in invasive tissue compared with the other tissues.

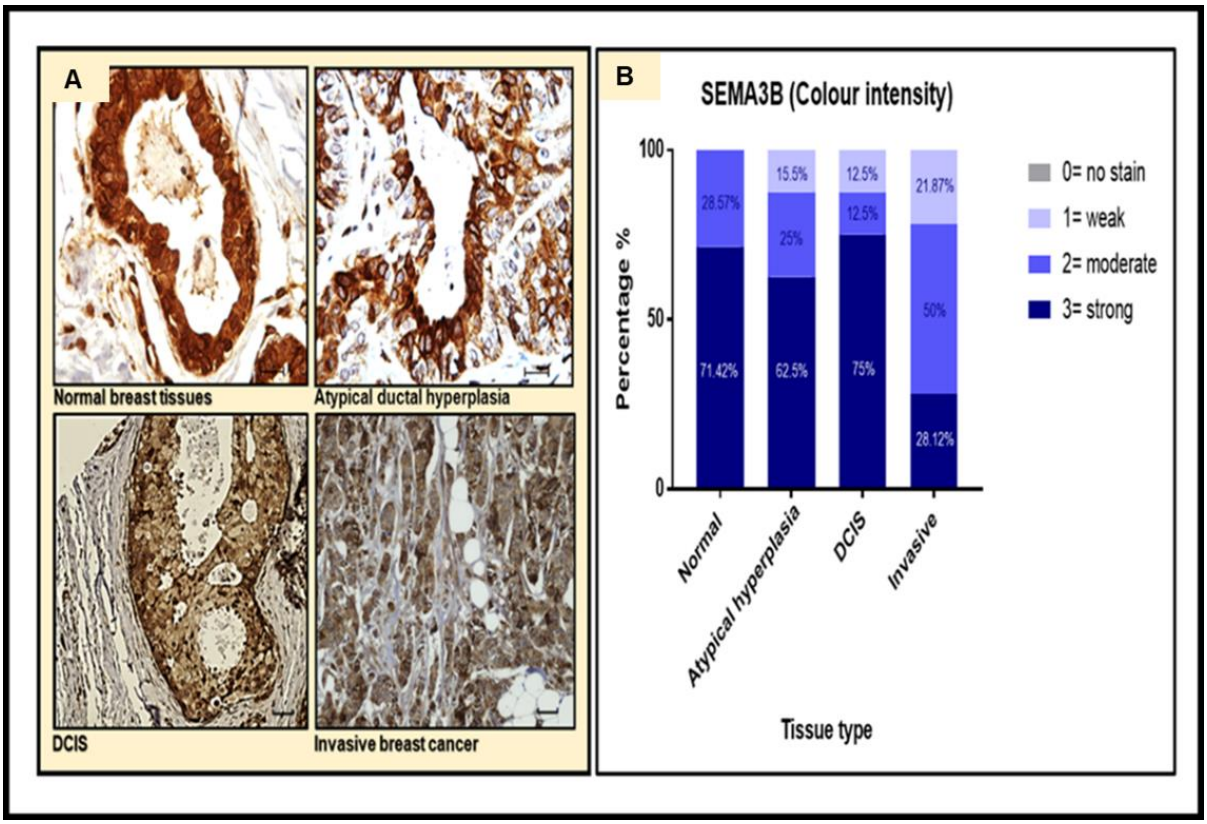

Figure 3.9: A representative image of the immunohistochemical staining of SEMA3B in breast lesions. A) SEMA3B expression in normal breast duct (n=27), atypical ductal hyperplasia (n=8), DCIS.com (n=9) and invasive breast cancer tissue (n=31). **B)** The analysis of the expression of SEMA3B based on the colour intensity. All photographs were taken using a x20 objective. Scale bar = 10 µm.

3.4 Discussion

The rationale behind this study was to determine the putative role of SEMA3B expression in breast cancer progression. Understanding the behaviour of cells is essential to determine the mechanism of the response we are investigating. Since we hypothesised that PPCs cleavage of SEMA3B results in inactivation of SEMA3B in invasive breast cancer, characterisation of cell-lines models of breast cancer development and determining the expression of SEMA3B in these models were important to our study before testing the hypothesis using different cell-based functional assays. Therefore, the determination of the growth characteristics, metabolic activity, migration and invasion of cell-lines are an important first step.

When cell growth and metabolic activity of breast tumours and non-tumour cells was investigated it was found that the different human breast cell-lines demonstrate variability in cell growth depending on the cell behaviour and cell invasiveness. To minimize the variability in cell culture, all cell-lines were cultured and assayed in the same medium RPMI-1640 except for the normal epithelial MCF-10A cells as they require specific nutrients to grow. The addition of hydrocortisone, cholera toxin and EGF in the MCF-10A medium were used to stimulate the growth and proliferation of MCF-10A cells by inducing the intracellular level of cyclic adenosine monophosphate, which has a growth stimulatory effect and therefore increases DNA synthesis (Yang et al., 1981). However, the immortalized mammary epithelial cell-line, MCF-10A, which is non-tumorigenic, shows a significantly high cell growth compared with the other cells, with an increased doubling time of 16-20 hours compared to the other cell-lines (Osborne et al., 1987, Bessette et al., 2015). The addition of a numbers of growth factors to the media may play a role in this finding, however the cells do not grow or have a slow growth rate in the absence of the growth factors. The pre-malignant MCF-10AT and pre-invasive DCIS.com demonstrated a longer doubling time than the MCF-10A cells, 32.39 hours and 33.05 hours, respectively. As the growth characteristics of human breast cancer is also important in this study, the cell growth of invasive breast cancer cells was also established. The highly metastatic MDA-MB-231 and MDA-MB-231-BM cells showed the fastest cell growth (23.22 and 25.34 hours, respectively) after the normal epithelial MCF-10A cells. The absence of the hormone receptors ER, PR and HER2 may result in the increased proliferation rate and could help them to proliferate faster (Holliday and Speirs, 2011). However, the low metastatic MCF-7 cells

which have been isolated from pleural effusions derived from two ER+/PR+ breast carcinomas showed a lower cell growth compared to normal epithelial MCF-10A and other invasive cells. The exception was the T47D cells as they had the slowest cell growth among all cell-lines. Despite the tumorigenic cell behaviour, the differences of the doubling time of the cells may have an impact on the cells behaviour as the doubling time of MDA-MB-231, MDA-MB-231-BM, MCF-7 and T47D are 23.22, 25.34, 30.96 and 48.10 hours respectively as this is an index of proliferations behaved. These data suggest that the cell doubling time maybe contributes to the cell metabolic activity and the cell growth.

Our findings observed that the invasive T47D cells were slower growing than other malignant and non-malignant cells used in this study. This was unexpected as according to ATCC datasheet, the doubling time of these cells is 32 hours while our results showed longer doubling time 48.10 hours. However, these findings are consistent with a previous study showing that growth rate assessment of a panel of breast cancer cells demonstrated that T47D had the slowest doubling time 47.4 hours (Risinger et al., 2015). Interestingly, although MCF-7 and MDA-MB-231 are the most commonly studied cell-lines in experimental cancer research, a previous study showed that T47D showed a closer correlation to human tumours in protein level and molecular analysis when compared to MCF-7. In addition, proteins involved in cell growth and carcinogenesis are highly expressed in T47D when compared to MCF-7 cells, and this could explain why T47D is considered to be more invasive than MCF-7 (Aka and Lin, 2012).

The metabolic activity relies on the mitochondrial dehydrogenase enzyme in viable cells and shows a different pattern in the cell-lines used in the current study. MCF-10A was found to have higher metabolic activity than the majority of other cells, but it was a slightly lower than that of MCF-10AT. This suggests mitochondrial dysfunction of the cancer cells used (DeBerardinis, 2008). However, when MCF-10A has been used as an *in vitro* model for normal breast cells, it was found to be karyotypically slightly abnormal therefore entirely could not reflecting the identical phenotype of normal breast cells (Soule et al., 1990, Qu et al., 2015). MCF-10AT, which is a non-tumorigenic cell-line that was generated from transfecting MCF-10A with T24 RAS (Dawson et al., 1996), showed the highest metabolic activity of all the cells. These could be due to an alteration in the energy metabolism of MCF-10AT where these cells

have been transformed with RAS oncogene resulting in a high glycolytic activity and greater glucose uptake (Zheng et al., 2015). DCIS cell-line which is one of the derivatives of the MCF10A panel representing ductal carcinoma *in situ* (Miller et al., 2000) had a slightly higher metabolic activity than invasive cell-lines but lower than premalignant cells. However, there is no previous literature with which to compare these results directly, but the metabolic activity does affect the glycolytic efficiency, as a previous study showed that aggressive tumours have a deficiency in mitochondrial activity and which leads a high depending on glycolytic flux for energy (DeBerardinis and Chandel, 2016). These cancerous cells with a high glycolytic efficiency have a lower metabolic activity and therefore, the lowest level of intracellular ATP. Moreover, the cell doubling time may also contribute to the cell metabolic activity.

Our data also suggest that the acidification of the culture media due to glycolysis throughout the assay, may affect the metabolic activity of the cancers cells resulting in more metabolic activity in non-tumorigenic cells than in invasive cells (DeBerardinis, 2008). Surprisingly, the bone homing metastatic cells MDA-MB-231-BM exhibited an increased metabolic activity when compared to the T47D invasive cells. This may suggest, that tumour cells may exhibit a different metabolic phenotype by having a different level of dehydrogenase activity. However, there are some limitations to the MTS assay which is used to assess metabolic activity, as cell-lines may demonstrate different levels of absorbance even if they have similar seeding densities and degree of cell confluency (Staton et al., 2009). In addition, pipetting errors could affect the accuracy of the results. Prolonged incubation of cells resulting in an acidic culture condition can affect the production of the formazan product. Also the high cellular density could lead to ambiguous results (Johno et al., 2010).

In terms of cell migration and invasion the scratch (wound healing) assay was then performed to assess breast cancer cell migration, a process required for metastasis formation that is associated with dysfunction in cell adhesion. Metastasis requires increased cancer cell migration as well as invasion. Despite the simplicity of this assay and its cost-effectiveness, the scratch is generated by a pipette and the gap width is dependent on the pressure applied to the pipette tips. In addition, the process of scratching can damage the cells along the edge of the scratch, affecting the migration rates of cells (Liang et al., 2007). Care needs to be taken to ensure an even scratch (Hulkower and Herber, 2011). Moreover, the proliferation of cells can overtake the

migration speed, and therefore, we used mitomycin C to present cell migration (Liang et al., 2007).

When the migration rate was evaluated using the scratch assay, the non-tumorigenic epithelial cells MCF-10A, the pre-malignant MCF-10AT and the pre-invasive DCIS.com cells did not migrate in the time frame of the assay and likely because they lack the invasive and metastatic capacity. These cells are characterized by high expression of E-cadherin, which plays an essential role in the adhesion of cells and is useful as a phenotypic marker in breast cancer and has been found downregulated in tumour cells (Pecina-Slaus, 2003). The findings of the current study are in agreement with a previous study that demonstrated that switching off E-cadherin mediates the migration of MCF-10A cells (Hirohashi, 1998, Park et al., 2015). However, our findings of a non-migratory phenotype of DCIS.com cells are not directly comparable with a previous published study which revealed that the untreated DCIS.com cells showed some migration after 16 hours. This data may be attributed to the difference in the protocol as the cells did not appear to be serum starved or have been treated with mitomycin C (Kim et al., 2016).

In contrast, the migration rate of MCF-7 and T47D cells were reduced in comparison to the highly invasive and metastatic cell-lines MDA-MB-231 and MDA-MB-231-BM. Furthermore, we showed that T47D cells had a low level of migration, which was in agreement with a study using an alternative method, the Boyden chamber technique (Neve et al., 2006). These data are in agreement with the literature, showing that luminal cells MCF-7 and T47D are more differentiated and have tight cell-cell adhesion when compared to basal cells MDA-MB-231 and MDA-MB-231-BM, which are less differentiated, leading to the promotion of their migratory and invasive ability (Neve et al., 2006). Moreover, the loss of E-cadherin expression in the highly invasive and metastatic cell-lines may be implicated in the rate of cell migration and may correlate with these findings (Singhai et al., 2011). The ability of bone homing cells to migrate was inconsistent with a previous study showing that MDA-MB-231-BM cells demonstrated significantly decreased migration of cells in a wound-healing assay as it found that at 24 hours, the gap closure of MDA-MB-231-BM cells was 74.4% while our findings showed a 100% gap closure by 24 hours. However, this variation in the results may be attributed to the difference in the protocol as they seeded the cells onto

0.2% gelatin which was absent in our study and this could contribute to this small variation (Nutter et al., 2014).

Despite differences in cell migration being observed between cells, the cell invasion was also investigated. The initial step of tumour cell invasion is characterized by the breakdown of the basement membrane and followed by the invasion by the cells. The Matrigel chamber invasion assay was used to mimic this process. Our findings showed that the non-tumorigenic epithelial cells MCF-10A, the pre-malignant MCF-10AT and the pre-invasive DCIS.com cells did not invade, whereas the cancer cells did. However, the lack of invasive and metastatic capability in non-malignant cells, in addition, the non-tumorigenic epithelial cells MCF-10A do not support anchorage-independent growth, are all factors which could explain our findings (Neve et al., 2006).

A high number of malignant cells invaded through the transwell membrane. We cannot disregard the fact that differences in invasive capacity of MCF-7, T47D, MDA-MB-231 and MDA-MB-231-BM cell-lines to invade are due to the presence and absence of ER and PR expression on these cells. The absence of these receptors is associated with the highly invasive phenotype of invasive and metastatic potential cell-lines. Moreover, our result in MCF-7 and T47D are consistent with a previous study that has shown a similar number of invaded cells after 24 hours (Zhao et al., 2011, Zheng et al., 2017). Interestingly, T47D does appear to be less invasive than the other invasive cell-lines. However, since most cell-lines were derived from distant metastatic sites or pleural effusions and not from primary breast tumours, this suggests that these cells could be more aggressive and may not reflect the behaviour of cells derived from the primary tumour. Despite the high cost of this assay, one limitation of conducting the invasion assay is that the Matrigel may not set evenly across the membrane, which can result in false high-invasion rates as tumour cells pass through the poorly coated area of the membrane (Justus et al., 2014). It is also an expensive assay to perform.

In regards with the cytokine expression of breast epithelial/tumour cell conditioned media the previous studies provide convincing evidence that cytokines act as a regulator of inflammation and tumour progression by either promoting or inhibiting the development of diseases (Esquivel-Velazquez et al., 2015). However, the critical role of cytokines in tumour progression cannot be neglected. In response to tissue damage, a cascade of events take place to fight infection. Chemotactic signals, which

include cytokines, activate leucocytes which migrate to the site of tissue injury. It has been proposed that inflammation is implicated in tumour initiation and has a role in angiogenesis and metastasis (Esquivel-Velazquez et al., 2015). Since, cytokines are an essential player in tumour progression, as they play a role in the regulation of both induction and protection in breast cancer quantification of the expression of cytokines in all cell-lines would provide evidence of a possible association between their expression and breast cancer progression.

The current study investigated the expression of cytokine variation in breast tumour and non-tumour cell-lines, including IL-8, IFN-Y, IL-10, IL-11, G-CSF and GM-CSF. Our data showed that the expression of IL-8, which is known to contribute to tumorigenesis, showed at a high level in all the cell-lines with the highest level found the normal epithelial MCF-10A cells. However, our findings were not in agreement with the previous study that showed the expression of IL-8 was significantly higher in breast cancer patients compared with healthy controls as we observed a high level of IL-8 in non-tumorigenic normal epithelial cells (Benoy et al., 2004). These could suggest that the changes in IL-8 levels in cells *in vitro* may not reflect the serum level *in vivo*.

There are inconsistences in laboratory studies since Yao *et al*. showed suppression of IL-8 had no effects on cell proliferation *in vitro* while it did promote tumour growth in nude mice *in vivo* (Yao et al., 2007). Moreover, in a review that set to determine the potential influence of IL-8 in cancer progression, studies showed highly elevated IL-8 expression in oestrogen receptor-negative breast cancer and found enhanced invasiveness and metastatic potential of both ER- and ER+ breast cancer cells. IL8 is used to identify an early stage of breast cancer and as a marker of progression (Todorovic-Rakovic and Milovanovic, 2013).

Another study conducted to identify the role of IL-8 in ER-negative breast cancer cell-lines MDA-MB-231, revealed that inhibition of IL-8 expression, results in significant reductions in cell invasion ($P<0.001$) and decreases in neutrophil infiltration into the tumours ($P<0.05$) suggesting a potent effect of IL-8 in the regulation of breast cancer progression (Yao et al., 2007). Taken together, ER-positive breast cancer, expresses a low level of IL-8, which was in agreement with our finding in T47D cells of IL-8 showed the lowest in these cells suggesting an inverse relationship between IL-8 expression and oestrogen receptor status (Yao et al., 2007). Consistent with previous

studies using tumour cell-lines, we observed significant high expression of IL-8 in all invasive cell-lines.

IFN-γ which has been known to act as an anti-tumor agent by inhibiting the growth of some tumours has been found to have an anti-proliferative effect on breast cancer by up-regulating the apoptotic members of the bcl-2 family that are essential regulators of controlling cell death (Garcia-Tunon et al., 2007). Previous studies indicate the importance of IFN-γ in homeostasis by controlling and eradicating the infections and some types of cancers (Gooch et al., 2000). It has been shown that IFN-γ expression significantly inhibited the growth of normal mammary epithelial cells, resulting in irreversible growth arrest of G1, however the growth of MCF-7 and MDA-MB-231 breast cancer cells was only minimally inhibited. Harvat *et al*. showed that the difference in response to IFN-γ between normal epithelial cells and breast cancer cells might be due to defects in the IFN-γ signal transduction pathway in breast cancer cells (Harvat and Jetten, 1996). Work of Gooch *et al*. reported inhibition of the growth of MCF-7 and MDA-MB-231cells by the expression of IFN-γ (Gooch et al., 2000). However, our data showed that the expression of IFN-γ was deficient in non-tumorigenic normal epithelial MCF-10A, pre-malignant MCF-10AT, pre-invasive DCIS.com and low in all the invasive cell-lines. These results are in agreement with a previous study suggesting that the defect in IFN- γ signalling in breast cancer cells (Gooch et al., 2000). In addition, our data were consistent with a previous study reporting decreased IFN-γ in the plasma of cancer patients (Niwa et al., 2001).

However, it is known that IL-10 suppresses the production of IL-8, IL-12 & GM.CSF and regulates the tumour angiogenesis (Huang et al., 1999). The level of IL-10 in oestrogen receptor positive patients is significantly linked with breast cancer disease free survival (Bhattacharjee et al., 2016). Moreover, a previous study showed that IL-10 mRNA expression was detected in more than 50% of the breast tumours tissue analysed suggesting a potential role for IL-10 in suppressing tumour activity by inhibiting T-cell activation, and the antigen presentation by macrophages and the presentation of tumour-associated antigens by tumour cells (Venetsanakos et al., 1997). In addition, the concentration of serum IL-10 was significantly higher in breast cancer patients than in the normal serum and was correlated directly with the clinical stage of the disease (Kozlowski et al., 2003). Conversely, our results showed that the expression of IL-10 was very low in all cells tested with no differences observed

between the normal and invasive cells. Interestingly, there is further evidence suggesting that an inverse association between IL-10 expression and ER-positive breast cancer, demonstrating that low IL-10 expression is associated with poor survival rates, which might explain our findings (Ahmad et al., 2018). However, another study showed that the IL-10 was decreased in the plasma of cancer patients (Niwa et al., 2001). Moreover, IL-10 expression has been shown to decrease the migration of MCF-7 and MDA-MB-231 cells when used as a chemoattractant in Boyden Chamber-based assays, suggesting an anti-metastatic effect on tumour invasion (Ahmad et al., 2018). However, collectively the data from all of these studies is conflicting so further studies are required to determine the relevance of these cytokines.

Likewise, IL-11 expression is increased in breast cancer compared to normal breast tissue and significantly higher in patients with bone metastasis compared to those without distant metastasis (Ren et al., 2013). It has been shown that IL-11 stimulates breast cancer proliferation and/or invasion *in vitro* (Nicolini et al., 2006). In agreement with this study, we found that the expression of IL-11 was at the highest level in invasive cells compared with the non-tumorigenic normal epithelial MCF-10A.

In contrast, it has been demonstrated that breast tumours express higher levels of G-CSF cytokines than normal tissues do (Chavey et al., 2007). Our data showed that the expression of G-CSF was significantly lower in pre-malignant MCF-10AT and pre-invasive DCIS.com cells and T47D compared with the non-tumorigenic epithelial MCF-10A cells. However, a significantly high level of G-CSF expression was detected in MCF-7 and MDA-MB-231 cells compared with the control cell-lines. Our data was inconsistent with a previous report which detected very low levels of G-CSF in normal breast tissue whereas the G-CSF was overexpressed in breast carcinoma with no correlation between the expression of G-CSF and ER status, but correlation with PR-negative tumours (Chavey et al., 2007). This study could explain why we had a lower level of G-CSF expression in T47D cells compared with MDA-MB-231 and MDA-MB-231-BM cells.

Nonetheless, GM-CSF expression was also investigated in all the cell-lines and our data showed that the expression of GM-CSF was significantly increased in both MCF-7 and MDA-MB-231 invasive cell-lines compared to normal cells. Chavey *et al*, observed no detection of GM-CSF in the serum of the normal breast sample, however, in breast cancer tissue there was significantly overexpressing of GM-CSF, which is in

agreement with our findings as the expression of GM-CSF was significantly lower in MCF-10A compared with invasive cells (except for T47D cells) (Chavey et al., 2007).

Overall, in the present study, seven cell-lines including MCF-10A, MCF-10AT, DCIS.com cell type and MCF-7, T47D, MDA-MB-231 and MDA-MB-231-BM cancer cells have been tested and characterised. Breast cancer subtype can be easily distinguished in the cell-lines used in this project. However, the variability in cell culture medium should be considered as some like the normal epithelial MCF-10A cells were cultured in DMEM/F12 medium with special supplementation for supporting their growth while all other cell-lines were cultured in RPMI-1640. The fast growing and the shorter doubling time of the normal epithelial MCF-10A cells may appear surprising, as these cells should grow much slower than the others but this is a limitation to be aware of going forward. However, observations from previous studies have shown similar results suggested that the increasing growth potential is likely due to the addition of EGF, cholera toxin and hydrocortisone to the medium (Yang et al., 1981, Bessette et al., 2015).

It is important to mention that T47D cells findings are unexpected as they had the slowest growth rate among all other cells. It was therefore decided that T47D cells would be excluded from further investigations, as the behaviour of these cells is not a worthy target for the SEMA3B studies planned in the following chapter. Despite this limitation of these cells, it is important to note that the majority of cells were bought fresh from ATCC at the beginning of this project and so are unlikely to be contaminated. Despite the obvious advantages of using these different cell-lines, the continual culture of cell-lines may result in changes in their phenotype and genotype (Brodaczewska et al., 2016). In order to minimize these possible changes, low passage number have been used throughout the studies.

In consideration of gene and protein expression of SEMA3B, it was important to assess the expression of SEMA3B in these cell-lines used, qPCR was performed to determine the gene expression of SEMA3B. qPCR is a highly reproducible and sensitive approach (Smith and Osborn, 2009) however, an appropriate internal control should be used to allow accurate quantification of the mRNA level (Smith and Osborn, 2009). We used SYBR green which binds to all double-stranded DNA, thus in order to avoid the generation of non-specific binding products, it was important to use primer pairs that are highly specific to our target sequence. Therefore, the optimized primer

concentrations (see section 2.1.5) were used to minimize this limitation. The primers were validated by melt-curve analysis and performing a standard curve analysis to assess efficiency, and the primers had been validated by company (GeneCopoeia and Primer design).

Our data revealed that the cell-lines demonstrated different expression of SEMA3B mRNA with significantly lower levels in MCF-10A and moderate expression in the rest of the cells. This result is in agreement with a previous study that determined the levels of SEMA3B mRNA in different cells lines of breast cancer, ovarian carcinoma and renal cell carcinoma. However, out of six breast cancer cell-lines including MDA-MB231, MDA-MB435S, MDA-436, MCF7, BT 20, BT 474, only MDA-MB-231 cells showed a reduction of SEMA3B expression which may correlate with increasing the malignancy of disease (Pronina et al., 2009). Hypermethylation of the promoter region, is a common event in cancers and studies have found that *SEMA3B* promoter hypermethylation is responsible for silencing its expression in breast and lung cancer (da Costa Prando et al., 2011, Pronina et al., 2016). It has previously been suggested that down-regulation of *SEMA3B* expression in cancer is due to methylation of the *SEMA3B* promoter. A previous study in breast cancer showed that MCF-7, T47D and MDA-MB-231 cell-lines exhibited complete methylation of tumour suppressor genes and that loss of gene expression correlated with hypermethylation of the CpG island promoter sequence of *RASSF1A.* These studies suggested that methylation of the *SEMA3B* gene, which is located upstream of *RASSF1* at 3p21.3 is an important mechanism of *SEMA3B* gene inactivation (Dammann et al., 2001, Dworkin et al., 2009, Pronina et al., 2009). Interestingly, da Costa Prando *et al.* showed that MCF-10A cells did not express *RASSF1A,* revealed by a lack of methylation in these cells (da Costa Prando et al., 2011). Moreover, in gastric cancer, it was observed that the methylation level was significantly higher in tumour tissue when compared to normal tissue ($P<0.05$) (Chen et al., 2014). In the same study, treatment of gastric cancer cells with 5-Aza-2'-deoxycytidine resulted in increased expression of *SEMA3B* mRNA level (Chen et al., 2014). In another study, in lung and renal cancer, similar results of SEMA3B methylation were found with methylation negatively correlated with downregulation of *SEMA3B* and therefore likely to be contributing to the suppression function of *SEMA3B* gene (Loginov et al., 2015). All these findings suggest a

relationship between methylation status and gene expression pattern in breast cancer. Therefore, the SEMA3B reduction seen in our cell-lines may be due to methylation.

The Western blotting data confirms the qPCR finding that SEMA3B is expressed in all cell-lines tested, and shows that the SEMA3B protein identified is in a completely cleaved form ~51 kDa in most of the cell-lines. These findings are not in agreement with the qPCR finding, with no decreased protein expression across the sequence. However, the data is consistent with a previous study showing SEMA3B cleavage in MDA-MB-231 cells and in some lung cancer H661 cells (Varshavsky et al., 2008) which may be responsible for disabling its function as a tumour inhibitor.

In addition to proteolytic cleavage, it is possible that Sema3B variants are generated by alternative splicing. Although alternative splicing of this gene has been reported to generate 15 splice variants with potential for eight of these to translate into proteins of different molecular sizes (Ensemble database) to my knowledge there are not studies in the literature reporting the existence of SEMA3B protein variants that might have multiple and tissue specific functions.

SEMA3B contains the conserved pro-protein convertase (PCC) recognition sequence site and therefore is cleaved by furin-like pro-protein convertases to generate fragments of SEMA3B that are considered to be inactive (Varshavsky et al., 2008). This was confirmed using a furin-like pro-protein convertase inhibitor on the invasive MDA-MB-231 cells, which resulted in the expression of the full-length 83 kDa SEMA3B protein suggesting that it is the furin-like-pro-protein convertases, which generates the inactive ~51 kDa SEMA3B product (Varshavsky et al., 2008). Interestingly full-length SEMA3B ~83 kDa was expressed only in normal epithelial MCF-10A cell suggesting that active SEMA3B may be down-regulated with increasing malignancy of the lesion. This may be a result of increasing pro-protein convertase activity with increasing lesion malignancy which will be investigated in chapter 5.

The Western blot technique was used to examine SEMA3B protein expression in our panel of cell-lines. Despite the advantages provided by this technique, including its ability to detect low levels of protein in a sample, and the sensitivity, and specificity, Western blotting has its limitations. It is a time-consuming and expensive technique and each step and conditions require optimisation. Moreover, the primary antibodies may show off-target effects due to interacting with other proteins (Ghosh et al., 2014).

With the exception of MDA-MB-231 cells, to our knowledge, this is the first study exploring the protein expression of SEMA3B in a panel of increasing malignancy of breast cell-lines of models that representing the progression of breast cancer.

Finally, to confirm the validity of our *in vitro* cell-line models, immunohistochemistry was performed to establish any expression of SEMA3B in normal, pre-malignant, pre-invasive and invasive breast cancer tissue. It was previously reported from our group that SEMA3B expression decreases when the malignancy of breast lesion increases (Staton et al., 2011). Our data was in agreement with this previous study and showed that the expression of SEMA3B was reduced with the increasing malignancy of the lesion, with only a small amount of expression in invasive tissues. However, in the present study, the immunohistochemical staining was performed on microarray tissue slides while the study of Staton *et al*. was performed on whole tissue sections, which may allow better assessment. Despite many advantages of using immunohistochemistry to visualise the antigen-antibody interaction, there are some limitations that could interfere with the outcomes including cross-reactivity, resolution of antigen localisation and the thickness of the section used. Moreover, the colour intensity of patterns depends on the antibody concentration, therefore, optimisation should be performed in order to minimise non-specific background and staining has to be well optimised (O'Hurley et al., 2014). The limitation of this specific antibody is that it will bind both to the cleaved and non-cleaved form of SEMA3B, and there is no specific antibody available to distinguish between the two. The cell-line data would suggest that in breast cancer, SEMA3B is likely to be present in the inactive cleaved form. Although IHC demonstrated a decrease in SEMA3B with increasing lesion malignancy in breast cancer, the sample size is too small to assess this statistically. The overall sample size (102 cases) was large, but the number of tissue subtypes in each group was small, especially for ductal hyperplasia and DCIS tissues. Further studies on a larger sample size would enhance these findings.

In conclusion, this chapter has characterised an *in vitro* model of breast cancer development and progression and established that SEMA3B expression is reduced with the development of cancer. Furthermore, it has shown that when SEMA3B is expressed in malignant and invasive tissues, it is likely to be cleaved. There is some suggestion that SEMA3B may act as a tumour suppressor in lung cancer (Tomizawa et al., 2001). So, therefore, the next chapter will establish the effect full-length

SEMA3B will have on the breast cells to see if it is indeed a tumour suppressor in breast cancer.

Chapter 4: The Effect of Full-length Recombinant SEMA3B (rSEMA3B) on Breast Epithelial and Tumour Cells.

4.1 Introduction

The data in chapter 3 demonstrated that *SEMA3B* mRNA expression was highest in normal breast epithelial cells compared to breast cancer cell-lines. Moreover, the data showed that full-length SEMA3B was only found in the normal epithelial cells, and pre-malignant, pre-invasive and invasive breast cancer cell only expressed cleaved SEMA3B. Previous study in endometrial cancer revealed loss of activity of the cleaved fragment of SEMA3B (Nguyen et al., 2011). The activity of SEMA3B was determined by investigating the effect of the full-length SEMA3B restoration in the cell proliferation and migration of HEC-1B and Ishikawa, which are endometrial cancer cell-lines and observed that cell proliferation was decreased in SEMA3B-transfected cells compared with mock transfected cells. In addition, when SEMA3B expression was restored in cancer cells, the number of migrated cells was significantly reduced suggesting that the cleavage by pro-protein convertases of tumour cells may abolish the function of SEMA3B in inhibition of tumorigenesis (Nguyen et al., 2011). Furthermore, the effect of SEMA3B restoration on invasive capabilities of ovarian cancer cells, showed a reduction in their invasive potential (Joseph et al., 2010).

In the same context, the cleaved fragment of SEMA3B was unable to inhibit angiogenic mechanisms in a variety of *in vitro* assays including tube formation and migration (Joseph et al., 2010). In order to test this further Varshavsky *et al*., (2008) generated a point mutation in the SEMA3B gene which resulted in a protein that was resistant to cleavage by pro-protein convertases. They reported that this mutated SEMA3B was able to inhibit endothelial cell proliferation and induce apoptosis efficiently compared with the native SEMA3B, which is cleaved (Varshavsky et al., 2008). The anti-angiogenic effects of SEMA3B are mediated by neuropilins, which originally suggested that SEMA3B may compete with vascular endothelial growth factor ($VEGF_{165}$) for binding to neuropilins, thereby inhibiting the angiogenic effect of $VEGF_{165}$, and controlling pathological angiogenesis (Castro-Rivera et al., 2004). However, SEMA3B acts as an anti-angiogenic factor of endothelial cells and stimulates programmed cell death in endothelial cells even in the absence of VEGF, suggesting that the anti-angiogenic effect of SEMA3B could be due to a direct

inhibitory effect of SEMA3B itself that is mediated by neuropilins without any competition with VEGF (Castro-Rivera et al., 2004). SEMA3B has been found to be inactive in lung cancer suggesting the active form might have an important role in preventing the tumour progression (Tomizawa et al., 2001) Furthermore, in ovarian cancer, transfection of the full length SEMA3B into ovarian cancer cells resulted in reduced anchorage-independent growth *in vitro* and decreased tumour formation *in vivo* (Tse et al., 2002). In breast cancer, treatment of MDA-MB-213 cells with conditioned medium from Cos7 cells which were transfected with the full-length SEMA3B resulted in a 50% reduction in MDA-MB-231 cell number suggesting a role for SEMA3B in tumour growth inhibition (Castro-Rivera et al., 2004). Our current study in chapter 3, showed that SEMA3B protein was increased in normal tissue, and tends to decrease with increasing disease malignancy. Moreover, wherever SEMA3B is expressed in pre-malignant and malignant breast tissue, it is likely to be cleaved and therefore inactive.

Data from the literature shows that cleaved SEMA3B is inactive but full-length SEMA3B will inhibit breast cancer cell proliferation and apoptosis in lung cancer as well as having an effect on angiogenesis (Castro-Rivera et al., 2004). Therefore, this chapter aimed to test the hypothesis that full-length SEMA3B inhibits breast cancer progression. This hypothesis will be tested using a recombinant full-length SEMA3B protein in the following aims:

1. Establish whether full-length SEMA3B when added to the cells, is cleaved by proteins produced by the cells

2. Establish the effect of full-length SEMA3B on HUVEC as positive control cells, as it has previously been shown that SEMA3B inhibits migration and angiogenesis of HUVEC cells and therefore could have a role in angiogenesis (Varshavsky et al., 2008).

3. Establish the effect of full-length SEMA3B on proliferation, migration and invasion of breast cells representing stages of breast cancer development, namely normal epithelial MCF-10A cells, pre-invasive DCIS.com and invasive MDA-MB-231 cells.

4.2 Methods

4.2.1 Western blot analysis

Western blotting was used to assess the integrity/stability of recombinant SEMA3B when exposed to breast cancer cells and normal breast epithelial cells and their conditioned media. Cells, cell lysates and conditioned medium were treated with different concentrations of rSEMA3B by two different protocols as described in section 2.10.10. Samples were quantified and separated on a 10% SDS-PAGE gel, and then blotted onto PVDF and probed with the antibody for SEMA3B. β-actin the housekeeping protein was used as a loading control as described in section 2.10. In some instances, β-actin appeared to be present in cell conditioned media samples when analysed by western blotting. This was most likely due to some contamination of conditioned media by cells that were not efficiently removed by centrifugation during the conditioned media collection process.

4.2.2 Cell counting assay

This assay was used to investigate the effect of rSEMA3B on the growth pattern of the cell-lines. The work conducted measured the viability and total cell count after 24, 48 and 72 hours of exposure. The cells were treated with different concentrations of rSEMA3B and were counted at the different time points as described in section 2.3.2. Untreated and untreated tumour and non-tumour cell-lines were seeded at $2x10^4$ in 12-well plates with three replicates of each condition and incubated over a 72 hours period, and the viable cells were counted, as described in section 2.3.1.

4.2.3 MTS assay

This assay was used to assess the effect of rSEMA3B on the metabolic activity of tumour and non-tumour breast cells. Cells were seeded at $5x10^3$ in 96-well plate and treated with different concentrations of rSEMA3B for 24, 48 and 72 hours and the optical densities were measured at the absorbance of 490nm as described in section 2.3.3 and 2.3.4.

4.2.4 Scratch (wound healing) assay

This assay was used to assess the effect of rSEMA3B on the ability of cells to migrate. Cells were seeded at $1x10^5$ in 24-well plate and the scratch was made before treating the cells with different concentrations of rSEMA3B for 24 and 36 hours, and the gap closure was measured as described in section 2.4.2 and 2.5.

4.2.5 Invasion assay

This assay was used to assess the effect of rSEMA3B on the invasion of the MDA-MB-231 cells. HUVEC cells were used as a positive control for this assay. A pre-coated Matrigel invasion chamber was used. Cells were seeded and treated with different concentrations of rSEMA3B for 72 hours for MDA-MB-231 and 24 hours for HUVEC cells, as described in section 2.7. Photomicrographs were taken using a microscope, and the invaded cells were counted as defined in section 2.6.5.

4.2.6 Statistical analysis

All data were analysed using GraphPad Prism 7 software, with all statistical analyses performed by comparing treated with untreated cells. The tests used were the one-way ANOVA test with Dunnetts multiple comparison test. Data expressed as mean ± SD from at least three independent experiments. A P value of <0.05 was taken to be significant.

4.3 Results

4.3.1 Effect of the cells and conditioned medium on the cleavage of recombinant SEMA3B

This experiment was carried out to evaluate whether adding the recombinant SEMA3B to the cells for 24 and/or 48 hours will have an effect on the full-length recombinant SEMA3B in the conditioned medium and cell lysates and to see whether it remains full-length and is therefore likely to have an effect on the cells. Western blot analysis was carried out, and SEMA3B protein expression of all treated/untreated cells and conditioned medium was analysed and compared to the untreated control**.** Three different cell-lines were chosen for representing an element of breast cancer progression included normal MCF-10A, pre-invasive DCIS.com and invasive MDA-MB-231 cells.

4.3.1.1 Effect of MCF-10A cells and their conditioned medium on the full-length recombinant SEMA3B

MCF-10A cells were treated with rSEMA3B and incubated for different times(24 and 48 hours) to investigate the effect of cells and conditioned medium on the rSEMA3B protein expression and to find out whether adding full-length of SEMA3B will be cleaved by proteins produced by the cells. Our result showed that the full-length of rSEMA3B (83 kDa) in both MCF-10A cells and conditioned medium was detected in more abundance and was not being cleaved after 24 and 48 hours. However, 51 kDa cleaved SEMA3B fragments were observed in both untreated cells and conditioned medium but not in treated lanes (figure 4.1). These data suggest that MCF-10A cells treated with full-length recombinant SEMA3B do not cleave the SEMA3B in the assay conditions and therefore, the effect of full-length SEMA3B can be investigated in these cells, using the recombinant protein.

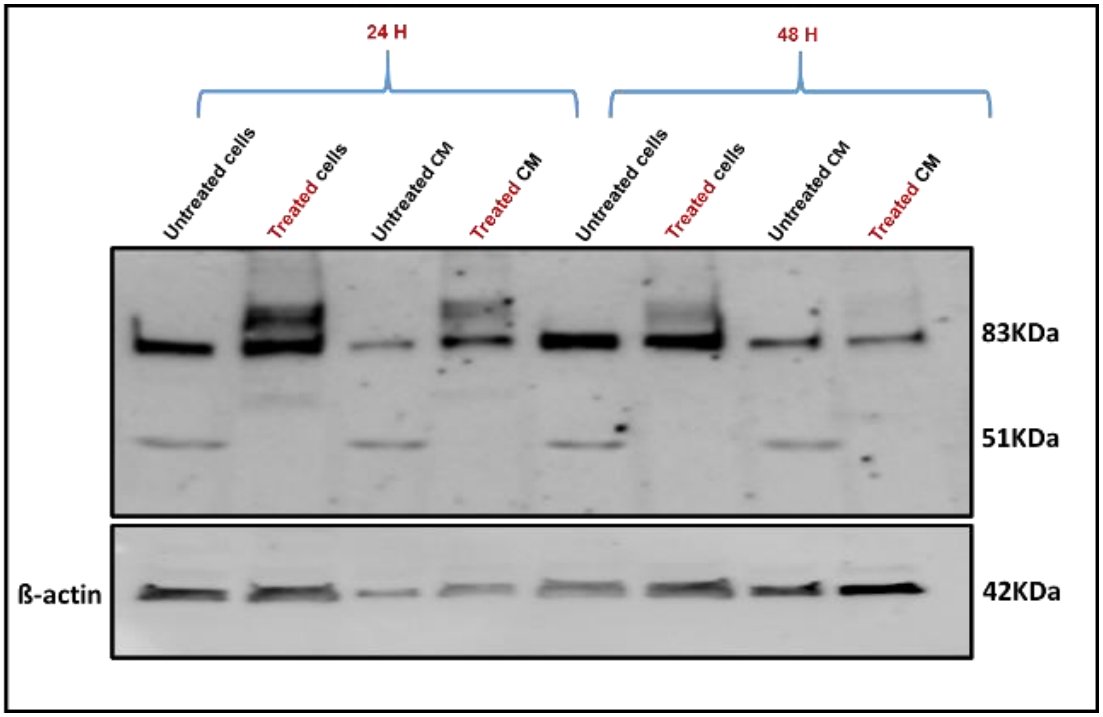

Figure 4.1: Effect of MCF-10A cells on the expression of rSEMA3B. Cells and conditioned medium were treated with recombinant SEMA3B protein (2 µg/ml) for 24 and 48 hours. Cell lysates were extracted, and conditioned medium (CM) was collected and the amount of the protein was quantified by BCA for both cell lysate and CM, and both were separated on a 10% SDS-PAGE gel, and then blotted onto PVDF and probed with the anti-SEMA3B antibody. To confirm that the amount of protein in each lane was equal, the membrane was stripped and re-probed with anti-β-actin housekeeping protein as a loading control. The sizes of molecular weight markers are indicated in kDa. Representative immunoblot shown of n=3.

4.3.1.2 Effect of DCIS.com cells and their conditioned medium on the full-length recombinant SEMA3B

DCIS.com cells were treated with rSEMA3B (2 µg/ml) for 24 and 48 hours. The cell lysates were then extracted, and conditioned medium was collected to analyse by Western blot. We found that after both 24 and 48 hours the recombinant SEMA3B was only partially cleaved yielding only a small band at 51 kDa in addition to the full-length band in both cell lysates and conditioned medium. However, there is far more of the recombinant SEMA3B present in the conditioned media, and this data suggests that the full-length SEMA3B is able to enter the cells where it is only partially cleaved. Therefore, the activity of full-length SEMA3B can be tested in these cells over a 48 hour time point (figure 4.2 and 4.3)

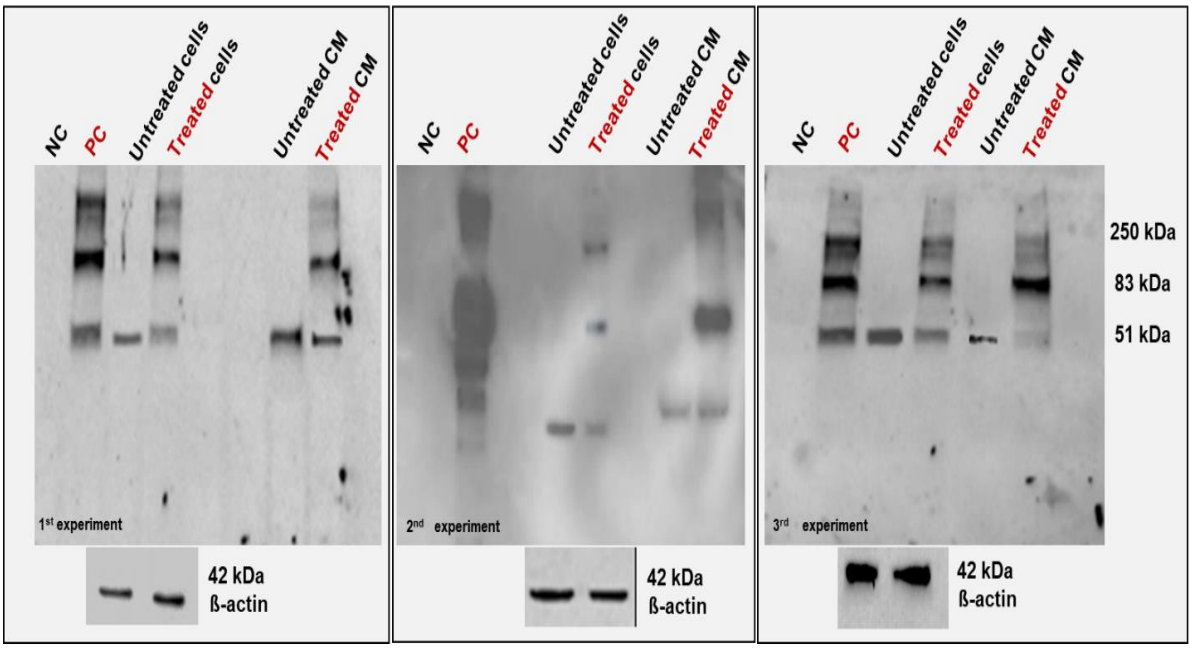

Figure 4.2: The effect of DCIS.com cells on recombinant SEMA3B after 24 hours treatment. DCIS.com cells were treated with rSEMA3B (2 µg/ml) for 24 hours and then cell lysates were extracted and conditioned medium was collected to be quantified and investigated by Western blot. 20 µg of protein of both cell lysate and conditioned medium was used and separated on a 10% SDS-PAGE gel, and then blotted onto PVDF and probed with the anti-SEMA3B antibody. To confirm that the amount of protein in each lane was equal, the membrane was stripped and re-probed with anti-β-actin housekeeping protein as a loading control. The sizes of molecular weight markers are indicated in kDa. NC= negative control (medium only), PC= positive control (rSEMA3B only) and CM= conditioned medium. Immunoblots from three independent experiments are shown.

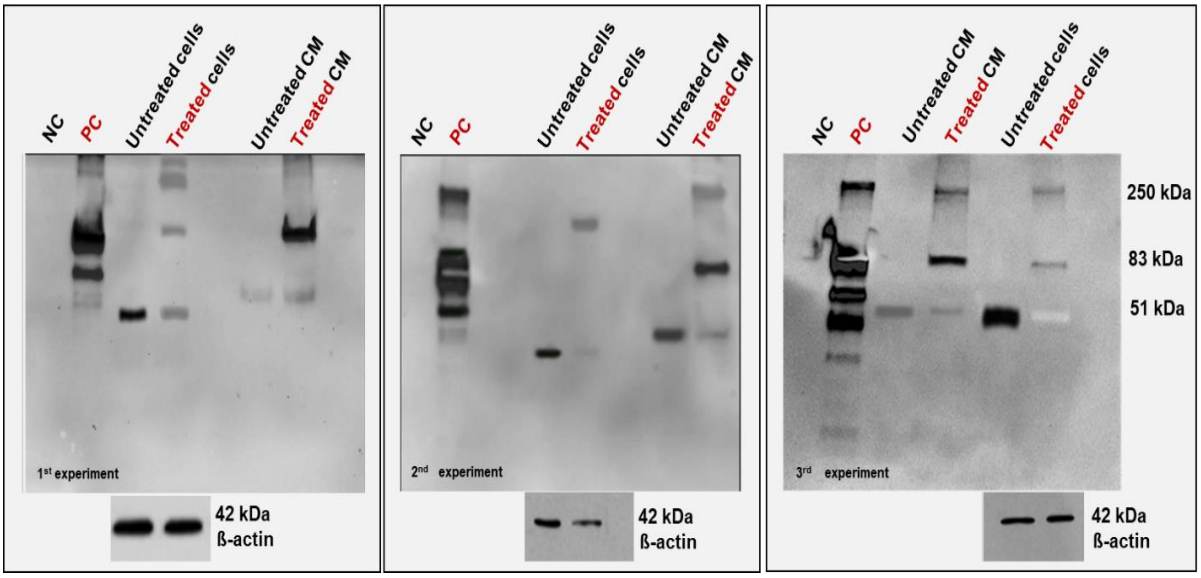

Figure 4.3: The effect of DCIS.com cells on recombinant SEMA3B after 48 hours treatment. DCIS.com cells were treated with rSEMA3B (2 µg/ml) for 48 hours and then cell lysates were extracted and conditioned medium was collected to be quantified and investigated by Western blot. 20 µg of protein was used and separated on a 10% SDS-PAGE gel, and then blotted onto PVDF and probed with the anti-SEMA3B antibody. To confirm that the amount of protein in each lane was equal, the membrane was stripped and re-probed with anti-β-actin housekeeping protein as a loading control. The sizes of molecular weight markers are indicated in kDa. NC= negative control (medium only), PC= positive control (rSEMA3B only) and CM= conditioned medium. Immunoblots from three independent experiments are shown.

4.3.1.3 Effect of MDA-MB-231 cells and their conditioned medium on the full-length recombinant SEMA3B

The cancer genome atlas (TCGA) database suggests that there is a significant downregulation of SEMA3B in triple negative breast cancer patients (Shahi *et al.*, 2017). Accordingly, since SEMA3B expression was seen at very low levels in basal subtypes, we thought it would be interesting to use the MDA-MB-231 cell-line as a model to test the effect of these cells on the full-length of recombinant SEMA3B protein.

MDA-MB-231 cells treated with recombinant SEMA3B for 24 and 48 hours, were investigated for the evidence of the full-length SEMA3B in the lysates and conditioned medium of the invasive MDA-MB-231. It shows the full-length SEMA3B was partially cleaved yielding faint bands in treated lanes at 51 kDa after 24 hours, in addition to the full-length bands detected in both cell lysates and conditioned medium at 83 kDa. However, similar bands of full-length SEMA3B (83 kDa) were detected after 48 hours in both cell lysates and conditioned medium, but were faint in treated cell lysates (figure 4.4 and 4.5).

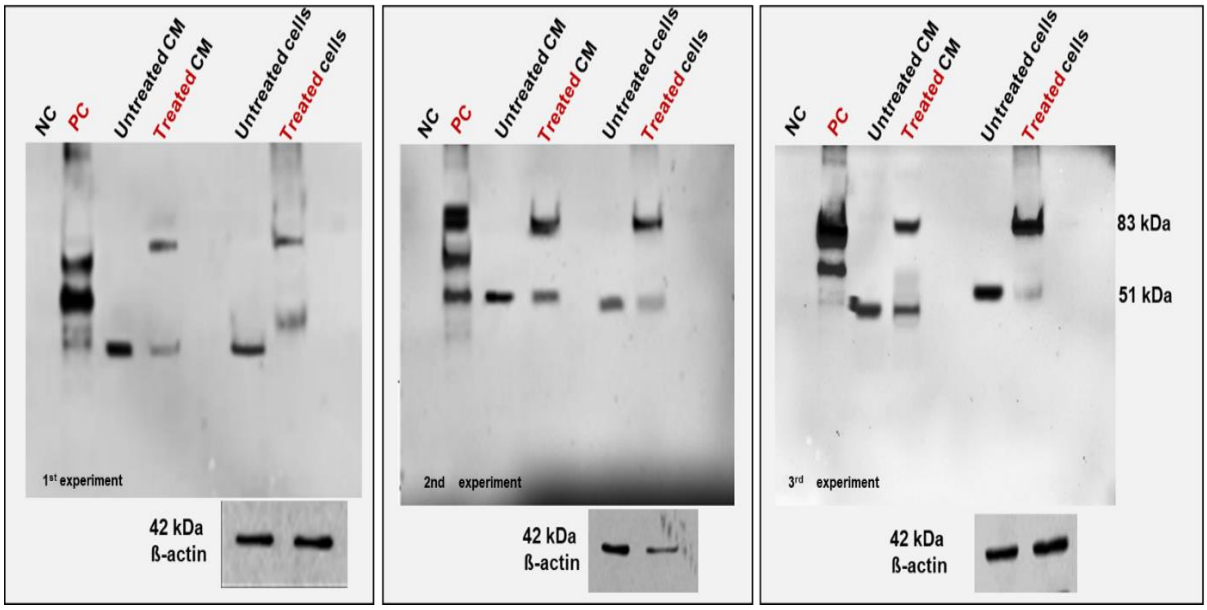

Figure 4.4: The effect of MDA-MB-231 cells on recombinant SEMA3B after 24 hours treatment. MDA-MB-231 cells were treated with rSEMA3B (2 µg/ml) for 24 hours, and then cell lysates were extracted, and conditioned medium was collected to be quantified and investigated by Western blot. 20 µg of protein of both lysate and conditioned medium was used and separated on a 10% SDS-PAGE gel, and then blotted onto PVDF and probed with the anti-SEMA3B antibody. To confirm that the amount of protein in each lane was equal, the membrane was stripped and re-probed with anti-β-actin housekeeping protein as a loading control. The sizes of molecular weight markers are indicated in kDa. NC= negative control (medium only), PC= positive control (rSEMA3B only) and CM= conditioned medium. Immunoblots from three independent experiments are shown.

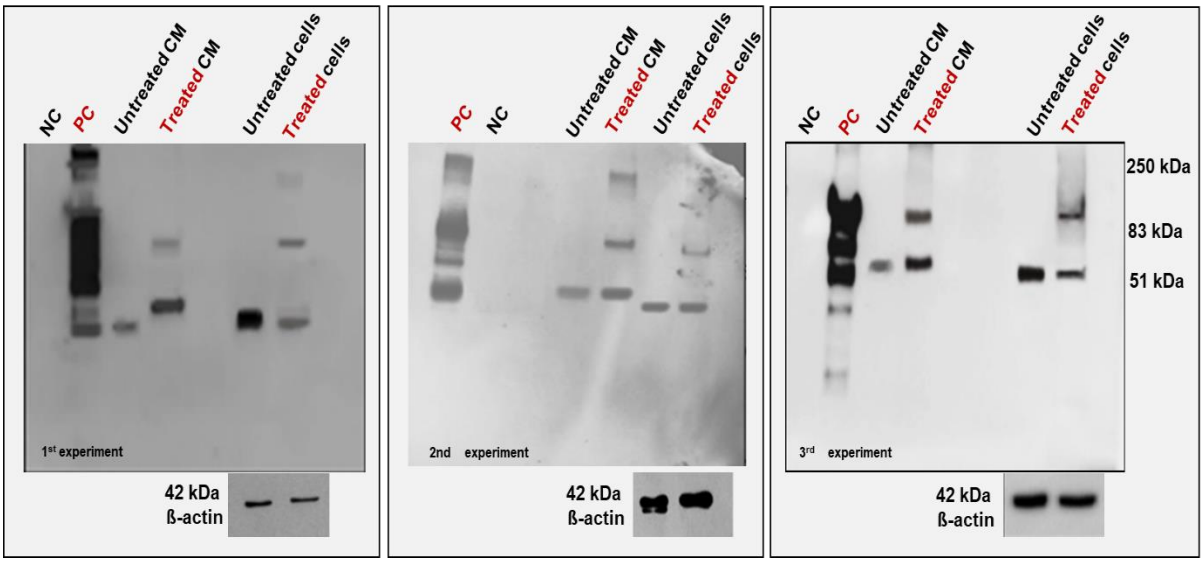

Figure 4.5: The effect of MDA-MB-231 cells on recombinant SEMA3B after 48 hours treatment. MDA-MB-231 cells were treated with rSEMA3B (2 µg/ml) for 48 hours and then cell lysates were extracted, and conditioned medium was collected to be quantified and investigated by Western blot. 20 µg of protein of both cell lysate and conditioned medium was used and separated on a 10% SDS-PAGE gel, and then blotted onto PVDF and probed with the anti-SEMA3B antibody. To confirm that the amount of protein in each lane was equal, the membrane was stripped and re-probed with anti-β-actin housekeeping protein as a loading control. The sizes of molecular weight markers are indicated in kDa. NC= negative control (medium only), PC= positive control (rSEMA3B only) and CM= conditioned medium. Immunoblots from three independent experiments are shown.

4.3.2 Effect of recombinant full-length SEMA3B on cell growth

To study the effect of recombinant SEMA3B protein on cell growth of cell-lines representing breast cancer progression, normal breast epithelial (MCF-10A), pre-invasive (DCIS.com) and invasive (MDA-MB-231) cells were treated with a range of recombinant SEMA3B concentrations and the cell number and cell death measured after 24, 48 and 72 hours. HUVECs were used as a positive control for the experiment as it is known that SEMA3B inhibits the growth of these cells (Castro-Rivera et al., 2004, Varshavsky et al., 2008).

As shown in figure 4.6, the effect of rSEMA3B on the cell growth of the normal epithelial cells MCF-10A showed no significant differences between the treated and untreated cells over 72 hours. In addition, the effect of rSEMA3B on the viability of MCF-10A cells has no effect either on killing or on inhibiting the cell growth (figure 4.6). However, in DCIS.com cells, 48 hours of treatment with SEMA3B significantly inhibited their cell growth ($P<0.01$; one way ANOVA) achieving significance at 0.5, 1 and 2 µg ($P=0.0168$, Dunnett's test). After 72 hours the growth was even more significantly inhibited ($P<0.0001$; One-way ANOVA). In contrast, there was no killing effect on cell viability (figure 4.7). Similarly, the effect of rSEMA3B on invasive MDA-MB-231 cells after 48 and 72 hours showed significantly reduced cell growth ($P<0.0001$; one way ANOVA) at a dose equal to 0.5, 1 and 2 µg ($P <0.0001$, Dunnett's test) compared with the untreated control. However, rSEMA3B inhibited cell growth but did not cause cell death (figure 4.8).

We observed similar behaviour in HUVEC cells. The effect of rSEMA3B after 48 and 72 hours, significantly decreased the cell growth of HUVEC cells ($P<0.0001$, one way ANOVA) at a dose equal to 1 and 2 µg ($P <0.0001$, Dunnett's test) compared to untreated control (figure 4.9), these data suggest that full-length SEMA3B is more likely to inhibit the cell growth by causing cell cycle arrest rather than apoptosis, suggesting its possible role in cytostatic rather than cytotoxic.

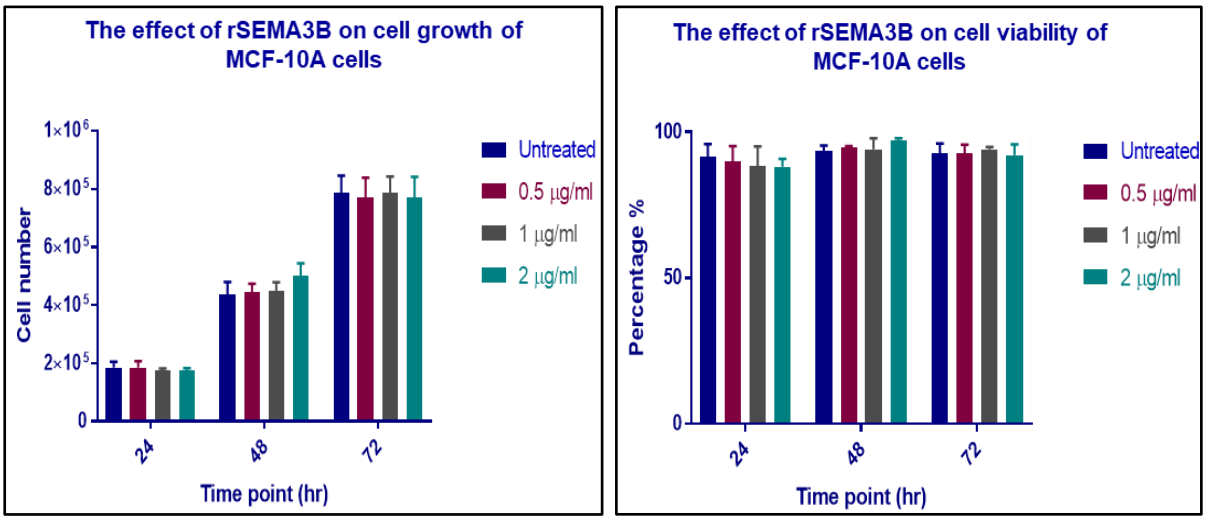

Figure 4.6: The effect of rSEMA3B on the cell growth and viability of normal epithelial MCF-10A cells. Cells were seeded at 2x10^4 in 12-well plates and incubated with the rSEMA3B treatment for 24, 48 and 72 hours. The cell growth was observed and measured by counting the cell number using a cell counting chamber (left). The percentage cell viability was measured (right). Data are presented as mean ± SD from three independent experiments and it was analysed statistically by one-way ANOVA to compare the treated cells with the untreated control cells.

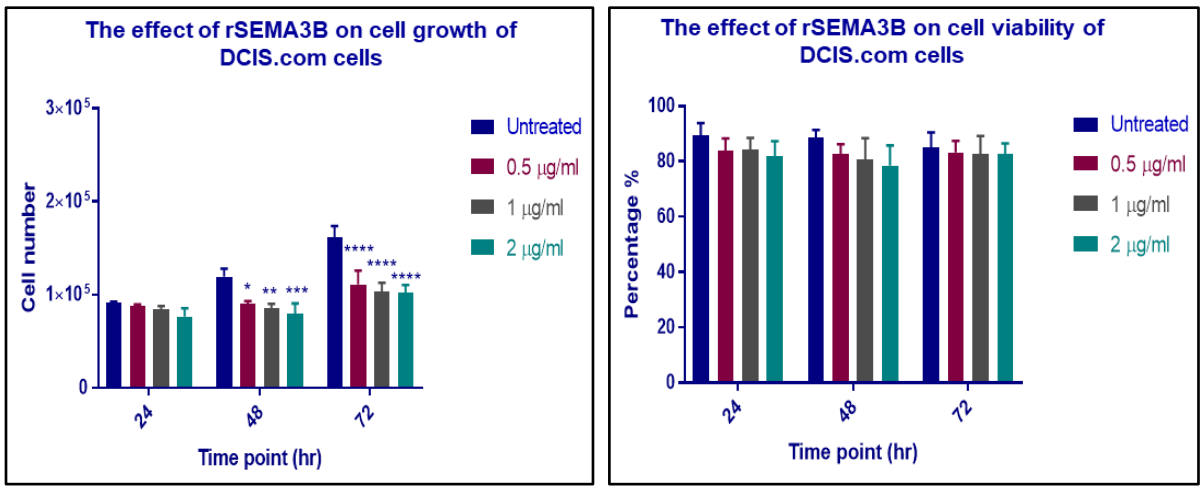

Figure 4.7: The effect of rSEMA3B on the cell growth and viability of pre-invasive DCIS.com. Cells were seeded at 2x10^4 in 12-well plates and incubated with different concentrations of rSEMA3B treatment (0, 0.5,1 and 2 µg) for 24, 48 and 72 hours. The cell growth was observed and measured by counting the cell number using a cell counting chamber (left). The percentage cell viability was measured (right). Data are presented as mean ± SD from three independent experiments, and it was analysed statistically by one-way ANOVA, Dunnett's multiple comparison test was used to compare the treated cells with the untreated control cells (left). * indicates P=0.0168, ** indicates P= 0.0025, *** indicates P=0.0003 and **** indicates P <0.0001.

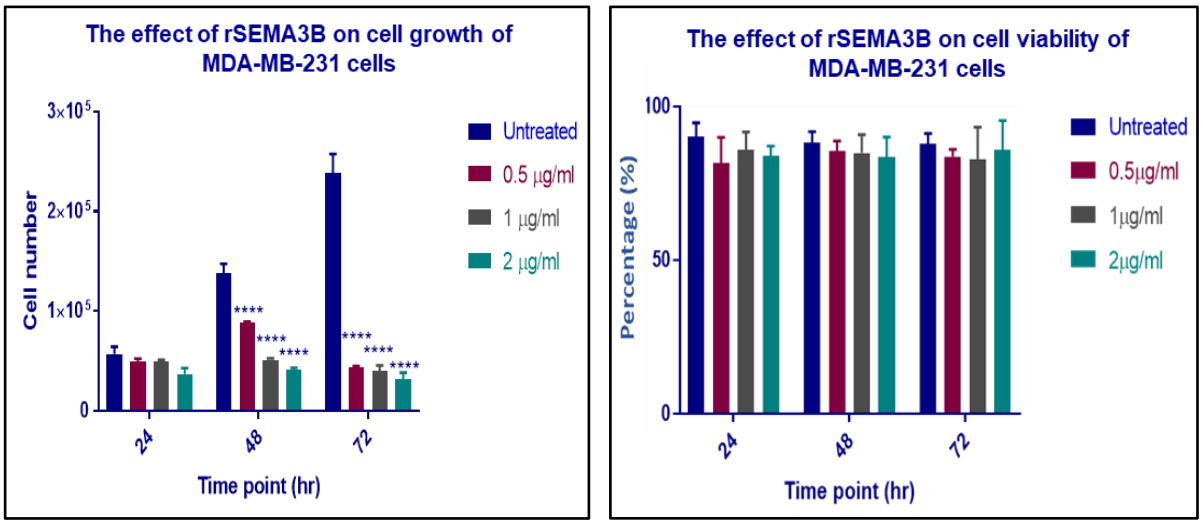

Figure 4.8: The effect of rSEMA3B on the cell growth and viability of invasive MDA-MB-231 cells. 2x10^4 cells were seeded at 12-well plate. The effect of rSEM3B was evaluated by treating the cells with different concentrations of rSEMA3B (0, 0.5, 1 and 2 µg). Cell growth was measured at three-time intervals (24, 48 and 72 hours) by counting the cell number using a cell counting chamber (left). The percentage of cell viability was measured (right). Data are presented as mean ± SD of three independent experiments. Data was analysed statistically by one-way ANOVA, Dunnett's multiple comparison test was used to compare the treated with the untreated control cells. **** indicates P <0.0001.

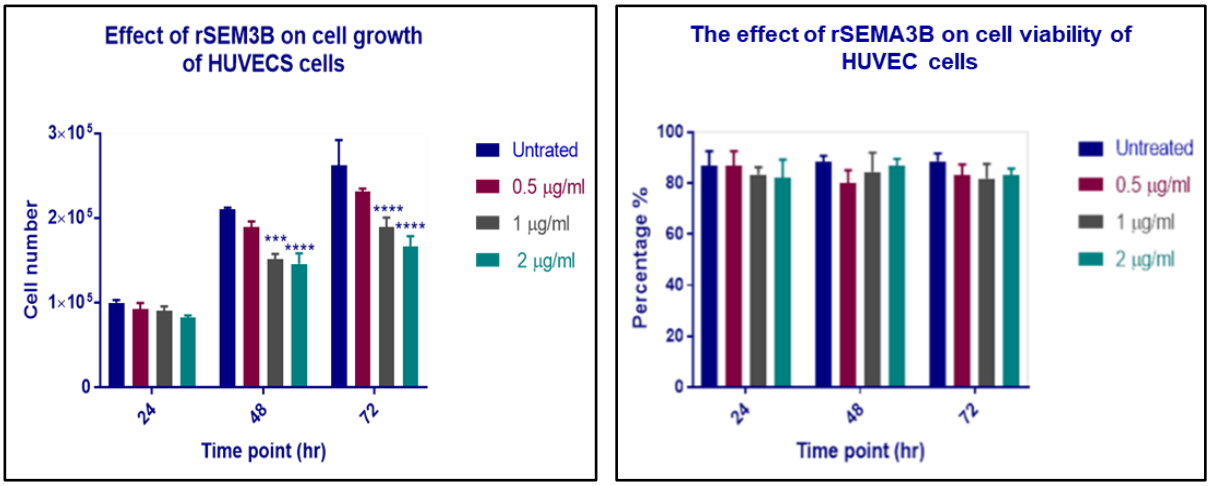

Figure 4.9: The effect of rSEMA3B on the cell growth and viability of HUVEC cells. 2x10^4 cells were seeded at 12-well plate. The effect of rSEM3B was evaluated by treating the cells with different concentrations of rSEMA3B (0, 0.5, 1 and 2 µg). Cell growth was measured at three-time intervals (24, 48 and 72 hours) by counting the cell number using a cell counting chamber (left). The percentage of cell viability was measured (right). Data presented the mean ± SD of three independent experiments. Data was analysed statistically by one-way ANOVA, Dunnett's multiple comparison test was used to compare the treated with the untreated control cells. *** indicates P=0.0001 and **** indicates P <0.0001.

4.3.3 Effect of recombinant SEMA3B on metabolic activity

The effect of rSEMA3B on cellular metabolic activity was evaluated using the MTS assay, which measures the activity of a mitochondrial dehydrogenase. Normal epithelial MCF-10A cells, pre-invasive DCIS.com and invasive MDA-MB-231 cells in addition to HUVEC cells were treated with different concentrations of rSEMA3B (0, 0.5, 1 and 2 µg) and compared with the control (untreated cells). The cellular response was measured at three-time intervals, namely 24, 48 and 72 hours, as described in section 2.3.4. The rSEMA3B showed no effect on the cellular metabolic activity of normal epithelial cells (figure 4.10), pre-invasive DCIS.com cells (figure 4.10), invasive MDA-MB-231 cells (figure 4.11) and HUVECs cells (figure 4.11) compared with the untreated control cells suggesting that rSEMA3B has no effect on metabolism of cells despite the effect seen on cell growth.

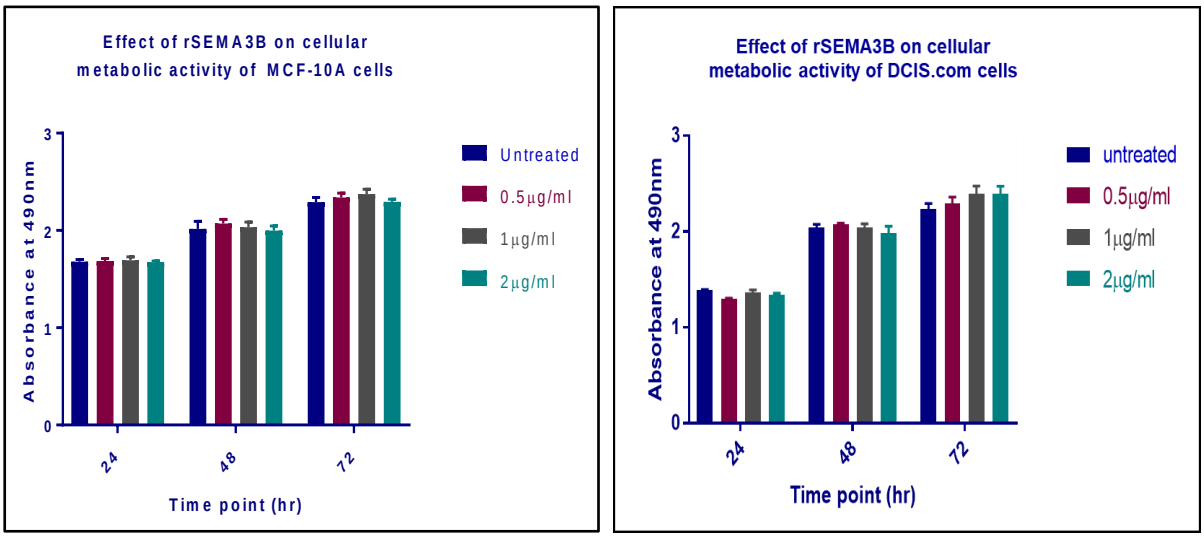

Figure 4.10: Effect of rSEMA3B on the cellular metabolic activity of normal epithelial MCF-10A and DCIS.com cells. MCF-10A cells (left) and DCIS.com cells (right) were seeded at $5x10^3$ in 96-well plate and incubated with different concentrations of rSEMA3B (0,0.5,1 and 2 µg) for 24, 48 and 72 hours. MTS reagent (20 µl) was added and incubated for three hours before the absorbance was measured by a spectrophotometer at 490 nm. Data are presented as mean ± SD from three independent experiments, and it was analysed statistically by one-way ANOVA.

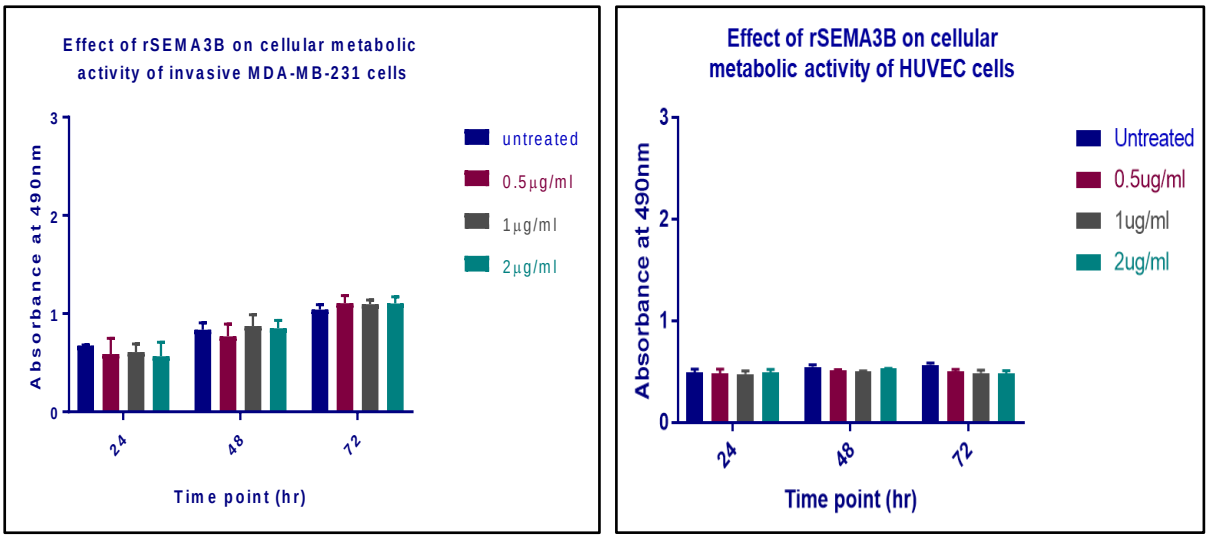

Figure 4.11: Effect of rSEMA3B on the cellular metabolic activity of MDA-MB-231 and HUVEC cells. MDA-MB-231 (left) HUVEC cells (right) were seeded at $5x10^3$ in 96-well plate and incubated with different concentrations of rSEMA3B (0,0.5,1 and 2 µg) for 24, 48 and 72 hours. MTS reagent (20µl) was added and incubated for three hours before the absorbance was measured by a spectrophotometer at 490nm. The data are presented as mean ± SD from three independent experiments. Data was analysed statistically by one-way ANOVA.

4.3.4 Effect of recombinant SEMA3B on cell migration

As recombinant SEMA3B had a significant effect on cell growth of DCIS.com, MDA-MB-231 and HUVECs, it was next interesting to study its effect on migration by testing the ability of the cells to migrate in the presence of rSEMA3B. However, MCF-10A and DCIS.com cells did not migrate as shown in chapter 3, and therefore, the effect of SEMA3B on the migration of these cells was not assessed. The effect of rSEMA3B was evaluated by treating the MDA-MB-231 cell-lines with different concentrations of rSEMA3B (0, 0.5, 1 and 2 µg) and measuring scratch closure over 24 and 36 hours as described in 2.5. HUVEC cells were used as a positive control in this assay as SEMA3B is known to inhibit angiogenic processes.

The result showed that MDA-MB-231 cells migrated to close the wound when untreated, and when they were treated with rSEMA3B, the migration was slowed. Indeed, rSEMA3B caused a significant, concentration-dependent inhibition in migration of MDA-MB-231 cells over 24 and 36 ($P<0.01$, one way ANOVA) achieving significance at 1 µg/ml ($P = 0.0436$, Dunnett's test) and 2 µg/ml ($P<0.0001$, Dunnett's test) compared with the untreated cells (figure 4.12).

Similarly HUVEC migration was significantly decreased in the presence of rSEMA3B after 24 hours ($P=0.05$, one-way ANOVA) at a dose equal to 0.5 µg/ml ($P=0.0355$, Dunnett's test), 1 µg/ml ($P =0.0010$, Dunnett's test) and 2 µg/ml ($P<0.0001$, Dunnett's test). Moreover, after 36 hours, the migration was more significantly inhibited ($P<0.0001$, one-way ANOVA), at 0.5, 1 and 2 µg/ml ($P<0.0001$, Dunnett's test) (figure 4.13). Thus, the presence or expression of full-length SEMA3B is likely to inhibit the migration of invasive breast cancer cells as well as endothelial cell.

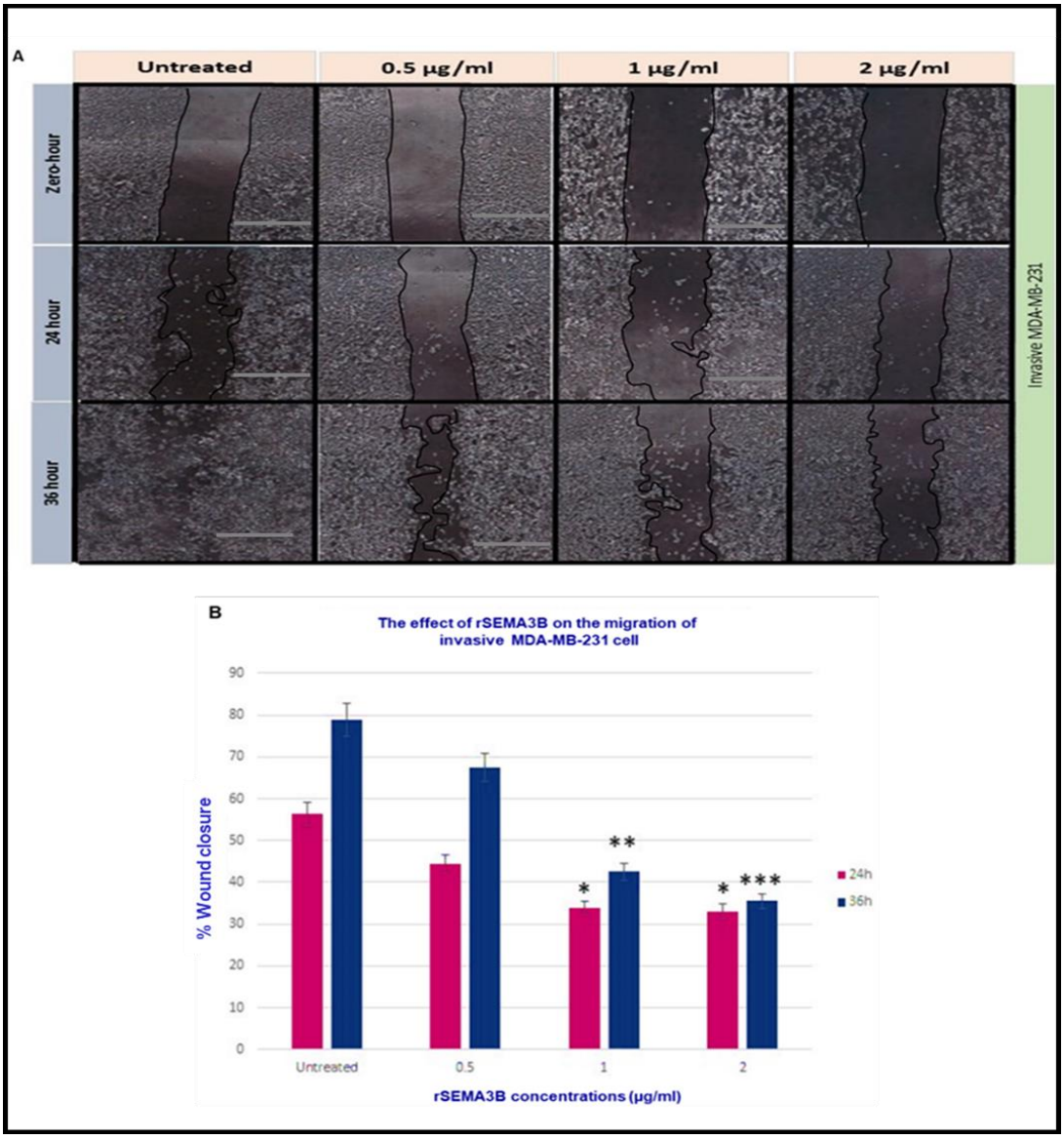

Figure 4.12: Effect of rSEMA3B on the migration of invasive MDA-MB-231 cells. A) The scratch assay was conducted in untreated/treated MDA-MB-231cells. Gap closure was measured at 0, 24 and 36 hours after cells were scratched using ImageJ software. Cell migration was calculated and expressed as the percentage of gap closure relative to the untreated control cells. Scale bar = 200 µm. **B)** Data is presented as the percentage of the gap closure for both time points 24 and 36 hours. These data are the mean ± SD of three independent experiments. Data was analysed statistically by two way ANOVA. Tukey's multiple comparisons test was used to compare the treated cells to untreated control. * represents P= 0.0436, ** represents P=0.0061 and *** represents P=0.0001.

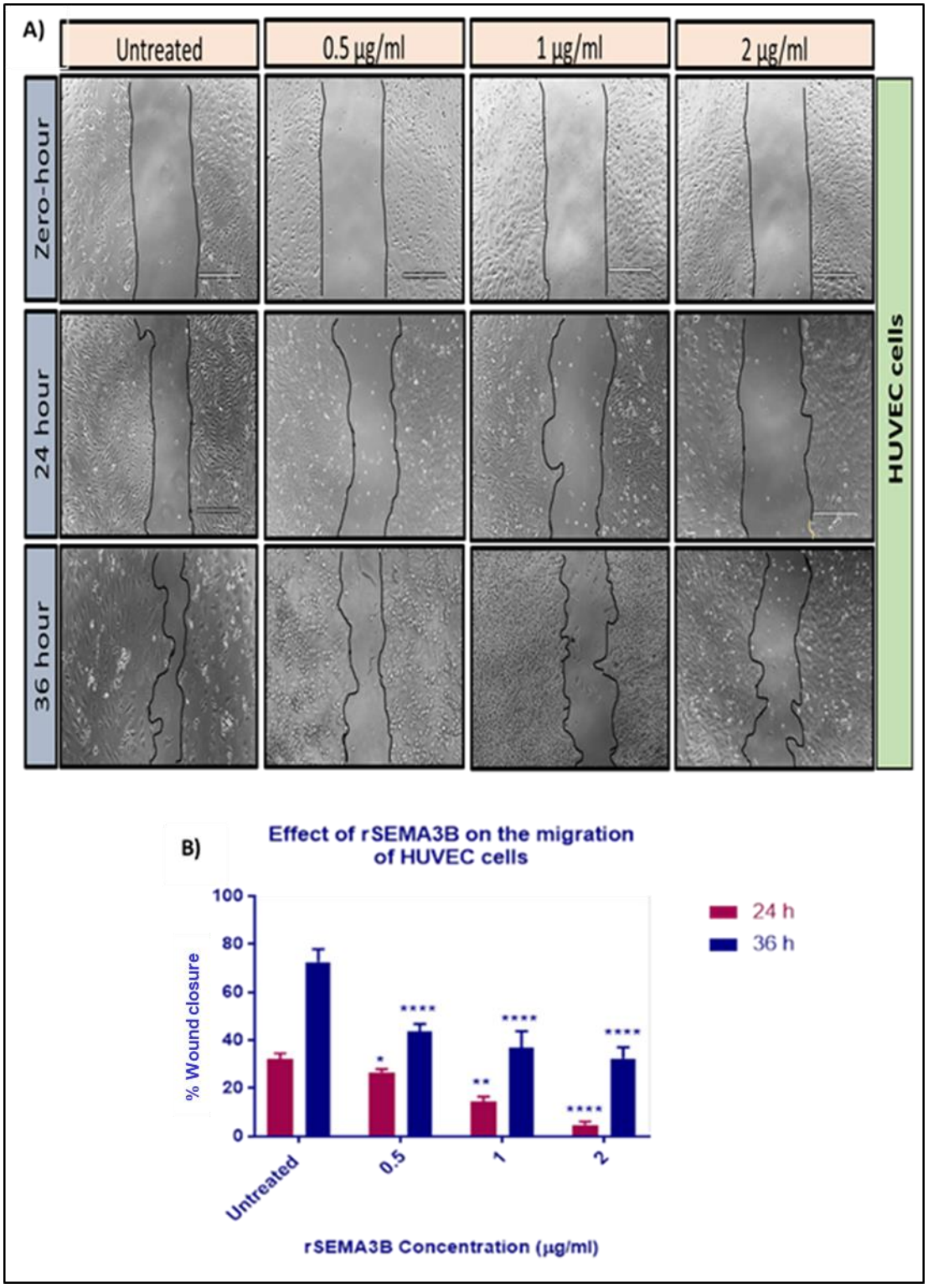

Figure 4.13: Effect of rSEMA3B on the migration of HUVEC cells. A) The scratch assay was conducted in untreated/treated HUVEC cells. Cell migration was measured at 24 and 36 hours after cells were scratched, and it was analysed using ImageJ software. Scale bar = 100 µm. **B)** Data present the percentage of the gap closure for both time points 24 and 36 hours. These data are the mean ± SD of three independent experiments. Data was analysed statistically by two-way ANOVA, Tukey's multiple comparisons test was used to compare the treated to the untreated control cells.*P= 0.0355, **P= 0.0010 and ****P<0.0001.

4.3.5 Effect of SEMA3B on the invasion of MDA-MB-231 and HUVEC cells

Invasion is a feature of malignant cells that potentially contributes to cancer progression, and therefore the effect of full-length recombinant SEMA3B was tested on the invasion of these cells. As the experiments in Chapter 3 demonstrated that MCF-10A and DCIS.com cells did not invade, the effect of rSEMA3B was only investigated in the invasive MDA-MB-231 and HUVEC cells. Cell invasion of MDA-MB-231 and HUVEC cells was measured at 72 and 24 hours, respectively, as described in 2.7.

The recombinant SEMA3B significantly inhibited invasion of the MDA-MB-231 cells after 72 hours in a dose-dependent manner ($P<0.0001$, one way ANOVA). Compared to the untreated cells, rSEMA3B at 0.5, 1 and 2 µg/ml suppressed invasion by ~50%, 84.83% and 89.6 % respectively ($P<0.0001$, Dunnett's test) (figure 4.14). Moreover, rSEMA3B treatment significantly decreased invasion in HUVEC cells after 24 hours ($P<0.0001$, one way ANOVA). Compared with the untreated cells, rSEMA3B at 1 µg/ml ($P= 0.0009$, Dunnett's test) and 2 µg/ml ($P<0.0001$, Dunnett's test) significantly reduced invasion by 55.6 % and 75.4 % respectively (figure 4.15). These data showed that rSEMA3B inhibits invasion and invasiveness of malignant cells and HUVEC cells.

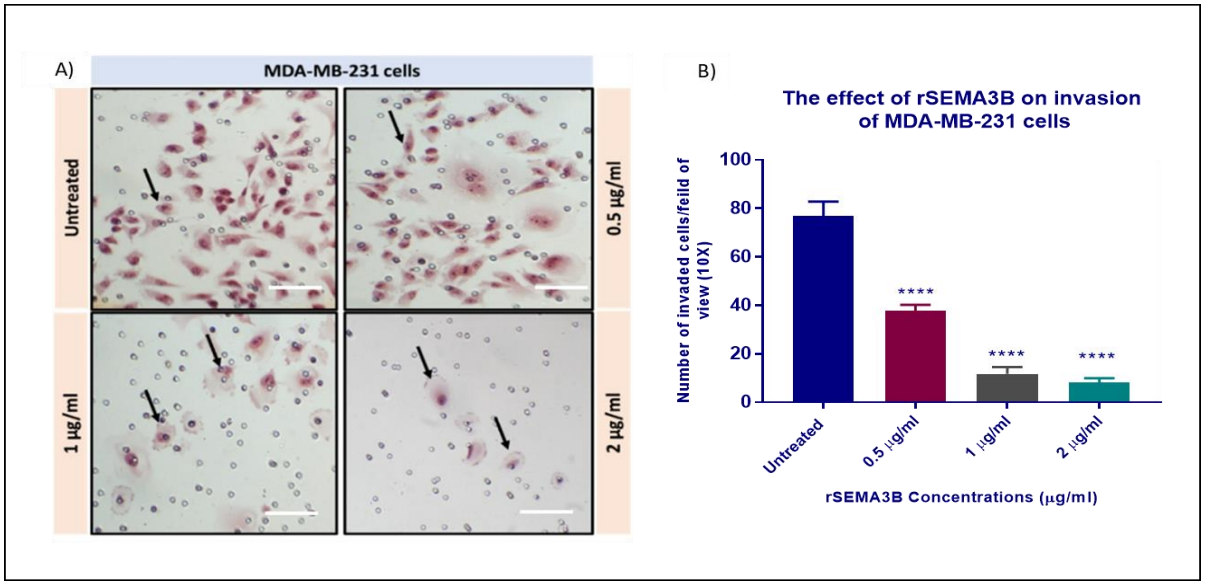

Figure 4.14: rSEMA3B inhibits MDA-MB-231 cell invasion. A) Photomicrographs of stained MDA-MB-231 cells that invaded through a transwell membrane in the presence of untreated control and different concentrations of rSEMA3B. Scale bar = 200 µm. **B)** The graph representing the number of invaded cells/ field of view (10x) that invaded through a porous transwell insert in the presence of different concentrations SEMA3B (0.5,1, 2 µg/ml) compared with untreated control. These data are the mean ± SD of three independent experiments. Data was analysed statistically by one-way ANOVA, Dunnett's multiple comparisons test. **** represents P<0.0001.

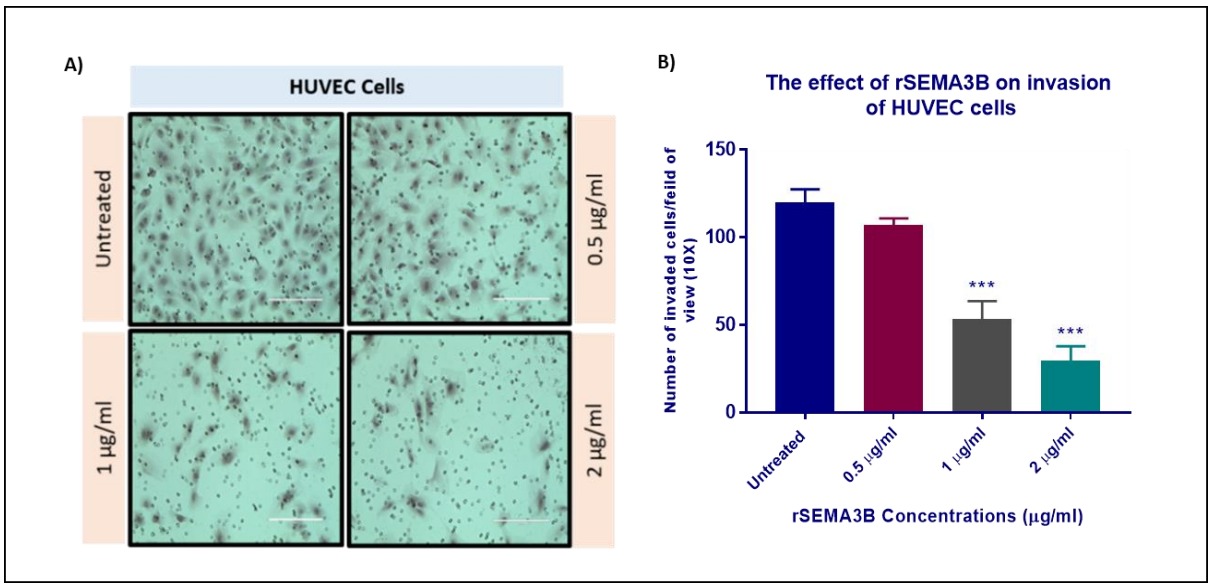

Figure 4.15: rSEMA3B inhibits HUVEC cell invasion. A) Photomicrographs of stained HUVEC cells that invaded through a transwell membrane in the presence of untreated control and different concentrations of SEMA3B (0, 0.5, 1 and 2 µg/ml). Scale bar = 100 µm. **B)** The graph representing the number of invaded cells/ field of view (10x) that invaded through a porous transwell insert in the presence of different concentrations rSEMA3B compared with untreated control. These data are the mean ± SD of three independent experiments. Data was analysed statistically by one-way ANOVA, Dunnett's multiple comparisons test was used to compare the treated to untreated control cells. *** represents P= 0.0051 and *** represents P=0.0009 respectively.

4.3.6 Effect of cell lysate and conditioned medium on the full-length recombinant SEMA3B

The data presented so far in this chapter suggest that full-length SEMA3B is active in breast cancer cells, but the Western blots suggest that breast cancer cells produce more cleaved SEMA3B than normal and pre-invasive cells. To assess whether the full-length SEMA3B can be cleaved by proteins produced by the cells, cell lysates and conditioned medium were generated from the cells and then incubated with rSEMA3B for 3 hours to establish whether any of the proteins present in the lysates and/or conditioned medium may be capable of cleaving SEMA3B. The same three chosen cell lines were used representing normal, pre-invasive and invasive cell-lines as described in 2.10.10.

4.3.6.1 Effect of MCF-10A cell lysate and conditioned medium on the full-length recombinant SEMA3B

Cell lysates and conditioned medium were generated from MCF-10A cells and were incubated with rSEMA3B as described in 2.10.10. Our results showed that the full-length rSEMA3B in both lysate and the conditioned medium had not been proteolytically cleaved to a 51 kDa fragment compared to the untreated lysate and conditioned medium (figure 4.16). An 83 kDa fragment corresponds to the active SEMA3B while the 51 kDa fragment is the product of the processing of 83 kDa by furin-like pro-protein convertases which corresponds to the inactive form of SEMA3B. This result demonstrates that cell lysate and conditioned medium from MCF-10A cells are incapable of cleaving rSEMA3B to produce a 51 kDa fragment, when compared to the generated fragments in untreated lanes. Unexpectedly, the endogenous 51 kDa protein could no longer be detected in lysates that were incubated with SEMA3B. It is not clear why this occurred and further tests would be needed to establish whether this was associated with further cleavage/degradation of the endogenous fragment or other reasons. This was specific for the MCF-10A cells and not the other cell lines. These data suggested that different processing takes place during intercellular maturation, resulting in the inactivation of SEMA3B and formation of several SEMA3B isoforms.

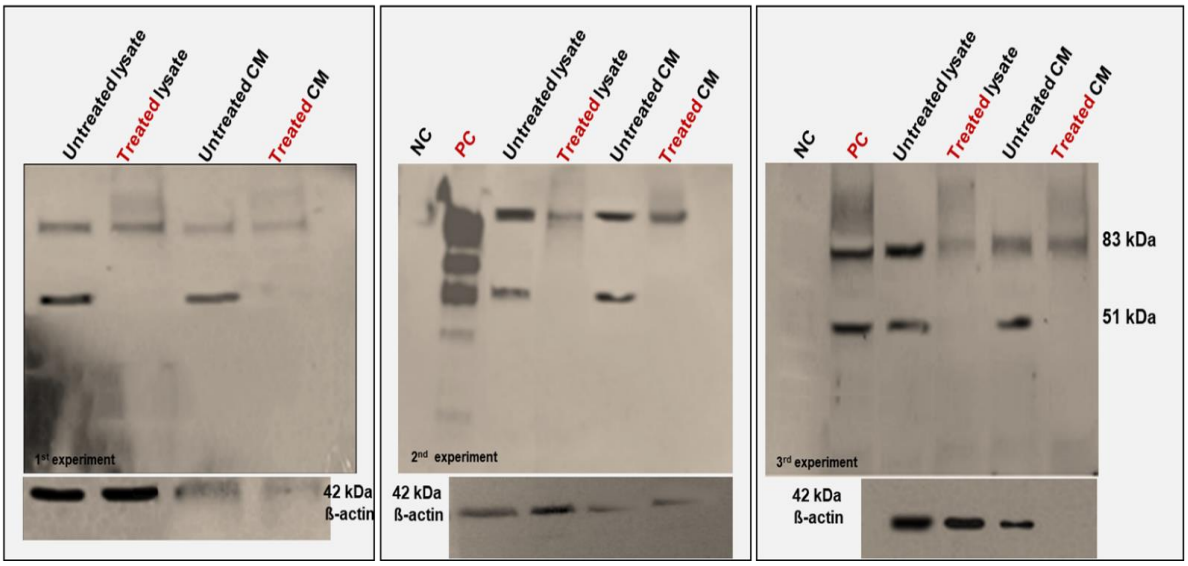

Figure 4.16: Effect of MCF-10A cell lysate and conditioned medium on the full-length recombinant SEMA3B. MCF-10A cell lysates and conditioned medium were generated from the cells to be treated with rSEMA3B (2µg/ml) for three hours, and then cell lysates were extracted, and conditioned medium was collected to be quantified and investigated by Western blot. 20 µg of protein of both cell lysate and conditioned medium was used and separated on a 10% SDS-PAGE gel, and then blotted onto PVDF and probed with the anti-SEMA3B antibody. To confirm that the amount of protein in each lane was equal, the membrane was stripped and re-probed with anti-β-actin housekeeping protein as a loading control. The sizes of molecular weight markers are indicated in kDa. An 83 kDa indicates the active form of SEMA3B and the 51 kDa inactive form of SEMA3B. NC= negative control (medium only), PC= positive control (rSEMA3B only) and CM= conditioned medium. Immunoblots from three independent experiments are shown. Presence of β-actin in conditioned media samples indicates some contamination of these sample with cells.

4.3.6.2 Effect of DCIS.com cell lysate and conditioned medium on the full-length recombinant SEMA3B

In the same manner as in MCF-10A, the pre-invasive DCIS.com cell lysates and conditioned medium were generated and treated with rSEMA3B for three hours as described in 2.10.10 to be investigated by Western blot. As shown in figure 4.17, the result showed that in treated lysate, two fragments were generated at 51 kDa and 83 kDa. The cell lysate was able to cleave the full-length of rSEMA3B partially suggesting that the cell lysate contains a factor that can cleave the full-length recombinant SEMA3B. In comparison, there is only a faint 51 kDa band in the treated conditioned medium in addition to a clear band detected as well at 83 kDa suggesting that there is less ability to cleave the protein in the conditioned medium.

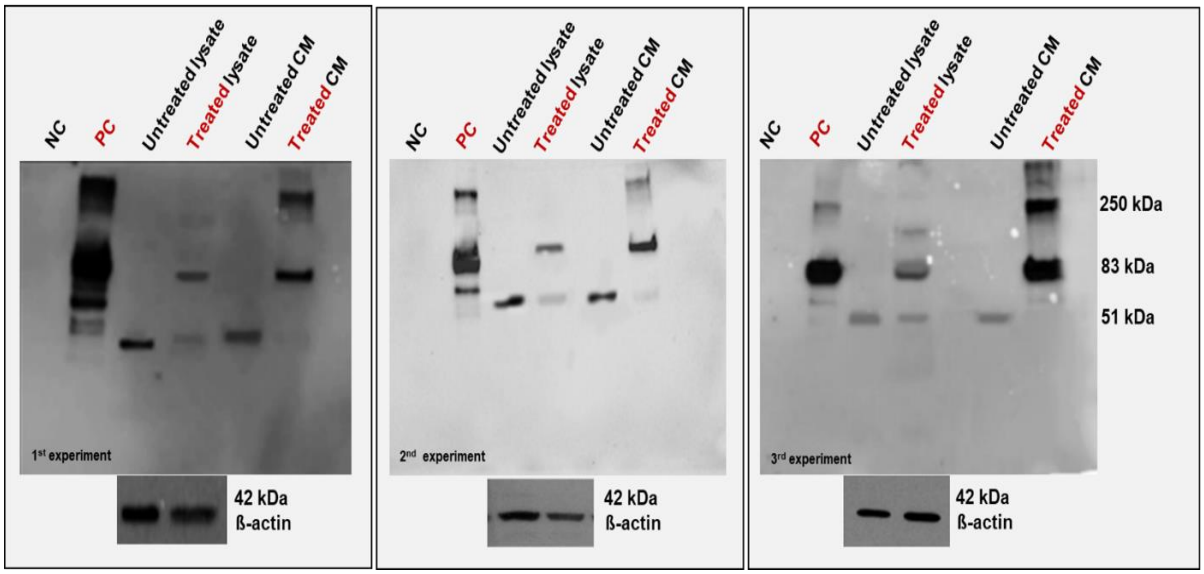

Figure 4.17: Effect of DCIS.com cell lysate and conditioned medium on the full-length recombinant SEMA3B. DCIS.com cell lysates and conditioned medium were generated from the cells to be treated with rSEMA3B (2 µg/ml) for three hours and then cell lysates were extracted and conditioned medium was collected to be quantified and investigated by Western blot. 20 µg of protein of both lysate and conditioned medium was used and separated on a 10% SDS-PAGE gel, and then blotted onto PVDF and probed with the anti-SEMA3B antibody. To confirm that the amount of protein in each lane was equal, the membrane was stripped and re-probed with anti-β-actin housekeeping protein as a loading control. The sizes of molecular weight markers are indicated in kDa. An 83 kDa indicates the active form of SEMA3B and the 51 kDa inactive form of SEMA3B. NC= negative control (medium only), PC= positive control (rSEMA3B only) and CM= conditioned medium. Immunoblots from three independent experiments are shown.

4.3.6.3 Effect of MDA-MB-231 cell lysate and conditioned medium on the full-length recombinant SEMA3B

MDA-MB-231 cell lysate and conditioned medium were generated from the cells and treated with rSEMA3B for three hours and investigated by Western blot as described in 2.10.10. Our result of treated MDA-MB-231 cell lysate and conditioned medium showed that the full-length of rSEMA3B in both lysate and conditioned medium has not been completely cleaved. However, the cleaved form at 51 kDa in the treated lysate was much stronger than in all other cells suggesting that the severity of cells could play a role in this. Moreover, there were faint bands at 250 kDa in the treated conditioned medium lane which were not detected in the treated lysate lane suggesting, that could be some factor produced by the cells to degrade the protein (figure 4.18).

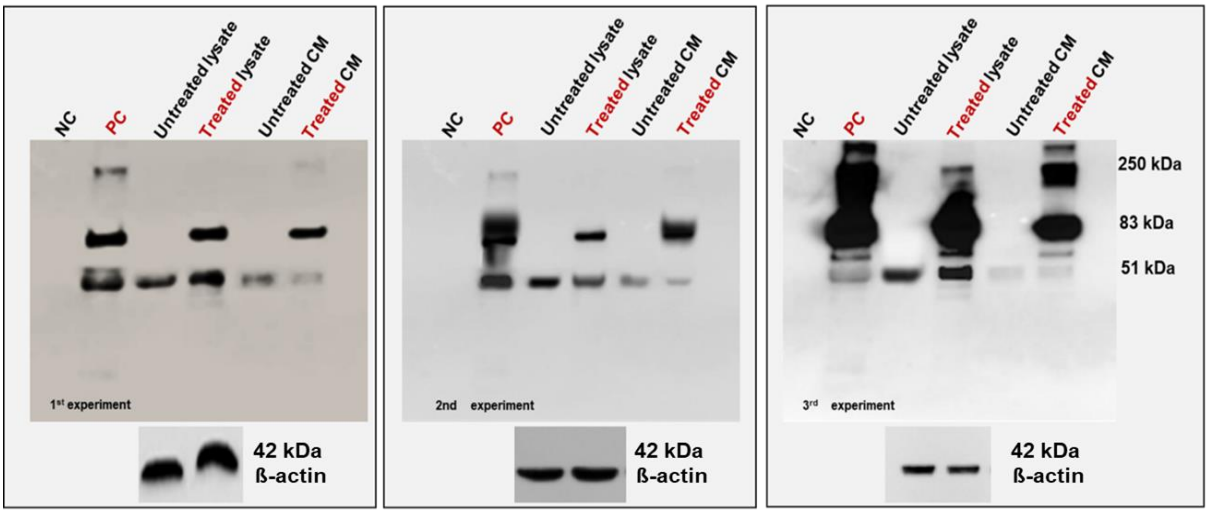

Figure 4.18: Effect of MDA-MB-231 cell lysate and conditioned medium on the full-length recombinant SEMA3B. MDA-MB-231 cell lysates and conditioned medium were generated from the cells to be treated with rSEMA3B (2 µg/ml) for three hours and then cell lysates were extracted and conditioned medium was collected to be quantified and investigated by Western blot. 20 µg of protein of both cell lysate and conditioned medium was used and separated on a 10% SDS-PAGE gel, and then blotted onto PVDF and probed with the anti-SEMA3B antibody. To confirm that the amount of protein in each lane was equal, the membrane was stripped and re-probed with anti-β-actin housekeeping protein as a loading control. The sizes of molecular weight markers are indicated in kDa. An 83 kDa indicates the active form of SEMA3B and the 51 kDa inactive form of SEMA3B. NC= negative control (medium only), PC= positive control (rSEMA3B only) and CM= conditioned medium. Immunoblots from three independent experiments are shown.

4.4 Discussion

The data in chapter 3 demonstrated that when SEMA3B is expressed by breast cancer cells, it is cleaved to a 51 kDa protein. Previous studies have suggested that although SEMA3B is a tumour suppressor, when it is cleaved it is less active suggesting proteolytic processing may be a reason for a less potent SEMA3B in cancer (Varshavsky et al., 2008). Therefore, this study aimed to investigate whether full-length SEMA3B acts as a tumour suppressor by inhibiting cell growth, metabolic activity, migration and invasion of normal breast epithelial cells, pre-invasive and invasive breast cancer cell-lines. As SEMA3B is known to inhibit angiogenesis the data with the breast cell-lines was compared to HUVEC, which are known to respond to recombinant SEMA3B (Varshavsky et al., 2008). To the best of our knowledge, the present study is the first report to document the effect of breast tumour and non-tumour cells on the stability of the exogenous recombinant SEMA3B and the impact of this protein on cell based functional assays. Recombinant SEMA3B protein full-length was tested at various concentrations including (0, 0.5, 1 and 2 µg). However, it was first important to establish whether exogenous recombinant SEMA3B would be cleaved by the breast cell-lines, particularly as their own SEMA3B is cleaved. We demonstrated that MCF-10A and DCIS.com cells do not cleave the recombinant SEMA3B by 48 hours suggesting that if it was added to an assay for less than 48 hours, then it would remain as full-length. As stated above, unexpectedly, in experiments where cells were incubated with rSEMA3B, the endogenous 51 kDa fragments could no longer be detected. It may be that the endogenous protein degraded during the duration of the incubation. The endogenous protein may be more difficult to fold correctly if exogenous protein was present at a high concentration. Additionally, high exogenous recombinant protein may interfere with the expression of the endogenous protein when added to live cells.

MDA-MB-231 cells showed partially cleavage of the full-length SEMA3B after 24 hours, but this increased over 48 hours in both cells and conditioned medium suggesting that the full-length of rSEMA3B in invasive cells may be cleaved by a protein produced inside the cells potentially contributing negatively with the anti-tumorigenic activities of SEMA3B. However, the full-length SEMA3B was partially cleaved in these cells suggesting that the fragment of the full-length SEMA3B can be active and its effect can be tested in functional assays. The abundance of cleaved bands of rSEMA3B in invasive cells showed a time-dependent increase.

These observations are supported by a previous study that demonstrated that the cleavage product of SEMA3B generated by furin-like pro-protein convertases, which are usually increased in the tumour, show lack of bioactivity and unable to perform its normal function or to support the antiangiogenic activity (Varshavsky et al., 2008).

Next, we examined the effect of the recombinant SEMA3B on cell growth of the chosen cells. Treatment with recombinant SEMA3B protein significantly reduced the growth of pre-invasive DCIS.com and invasive MDA-MB-231 cells when compared to the untreated control. However, in the normal epithelial MCF-10A cells, we observed no effect of rSEMA3B on the cell growth of these cells. In our growth assay, our data demonstrate similar findings to those previously reported with the same effect of SEMA3B on the growth inhibition of MDA-MB-231 breast cancer cell-line in response to full-length SEMA3B, as with a 50-60 % inhibition in cell growth by the transfected conditioned medium of SEMA3B (Castro-Rivera et al., 2004).

Moreover, our findings agree with the results of Shahi *et al*. who reported the effect of SEMA3B overexpression in MDA-MB-231 cells using a colony formation assay, as demonstrating inhibition of cellular proliferation and colony formation in cells expressing SEMA3B (Shahi et al., 2017). The findings using Western blot showed that rSEMA3B is partially cleaved in invasive cancer cells, but it is more likely to be still active. However, these findings indicate that the rSEMA3B contributed to decreasing tumour cell growth, suggesting that the anti-tumour effect of SEMA3B could be used as a new approach in the treatment of breast cancer.

In addition to the effect on cell growth, an effect on the metabolism of the cells and the viability of cells over a 72 hours period was measured. In contrast to the data on cell growth, recombinant SEMA3B had no significant effect on metabolism or viability in the breast cells, strongly suggesting that SEMA3B affects cell cycle progression. There is no previous literature published in breast cancer using the same assay. However, a previous study in oesophagal squamous cell carcinoma demonstrated that SEMA3B is able to arrest oesophagal cancer cell-lines at the G1/S checkpoint by inhibition of phosphatidylinositol 3-kinase/AKT signalling and upregulation of p53 and p21 expression, which may support our findings (Tang et al., 2016).

In contrast, our MTS assay results of breast tumour and non-tumour cells are contradictory to those reported by Tse *et al*, who showed that the metabolic activity of

ovarian cancer cells, identified using the XTT assay, was lower in SEMA3B transfected cells by 1.2-1.6 fold change, when compared to control cells (>2-fold higher) (Tse et al., 2002).

We then analysed the functional consequences of HUVEC treated with rSEMA3B. It is important to point out that the HUVEC cell-line was used as a positive control for the effect of SEMA3B as it has been shown that SEMA3B inhibits their cell migration and angiogenesis (Varshavsky et al., 2008). Expression of rSEMA3B significantly decreased the HUVEC cell growth when compared to untreated cells. In agreement with our result, the previous published study demonstrated that mutated SEMA3B (resistance to cleavage by PPCs) regulates HUVEC by decreasing their proliferation and cell viability (Varshavsky et al., 2008). However, the recombinant SEMA3B did not affect HUVEC cells viability in term of cellular metabolism, as we did not observe any differences between the treated and untreated cells in response to rSEMA3B.

Although class 3 semaphorin is normally found highly expressed in endothelial cells, it inhibited their proliferation and migration. During vascular development, endothelial cells produce autocrine chemorepulsive signals to the endogenous semaphorin, which localize at adjacent adhesive sites in spreading endothelial cells. These chemorepulsive signals result in disruption to the endogenous semaphorin function, leading to stimulation of integrin-mediated adhesion and migration to the extracellular matrices, to fix that disruption. However, the exogenous semaphorin protein antagonizes the integrin activation and consequently its function as a suppressor protein and therefore suppresses the HUVEC cell proliferation and migration. This is a possible explanation of how the SEMA3B inhibits the function of HUVEC cells (Serini et al., 2003).

Having established that recombinant SEMA3B could inhibit cell growth, it was essential to establish whether the full-length SEMA3B protein would also affect migration and invasion, both of which are important aspects of tumour development and metastasis. Initially, we investigated the effect of recombinant SEMA3B on cell migration using the scratch assay. The data presented here were generated in the presence of mitomycin C to ensure that only migration was quantified as described earlier in chapter 3. The invasive MDA-MB-231 cells in the presence of rSEMA3B were unable to fill the gap in the scratch assay, as rSEMA3B inhibited the migration of these cells. This observation is supported by a previous study which revealed that MDA-MB-

231 cells expressing SEMA3B failed to fill the gap when compared with the control (Shahi et al., 2017).

Moreover, our data demonstrate that SEMA3B can inhibit invasion of the invasive breast cancer cells MDA-MB-231 cells suggesting that SEMA3B may potentially inhibit breast cancer invasion. Our findings are in agreement with a previous report performed in ovarian cancer cells in which overexpression of SEMA3B significantly reduced cell invasion (Joseph et al., 2010).

Furthermore, our data showed that rSEMA3B inhibited the cell migration of HUVEC cells. This finding was in agreement with the previous study showing that the migration of HUVEC cells, was inhibited by the overexpression of SEMA3B as identified by transwell chamber inserts (Rolny et al., 2008). These results suggest that SEMA3B may perhaps be able to function as an inhibitor of angiogenesis, since SEMA3B signals through NP1 which is found expressed on endothelial cells as well and that SEMA3B inhibits the migration of endothelial cells and hence can function as an inhibitor of angiogenesis (Varshavsky et al., 2008). However, there is no previous literature to compare these results to.

These data suggest that full-length SEMA3B may be acting as a tumour suppressor agent by inhibiting breast cancer cell growth, migration and invasion. However, as data from chapter 3 demonstrated in the breast cancer cells, SEMA3B is expressed as a smaller cleaved protein. In order to establish whether a protein produced in the cells and/or released into the conditioned media is responsible for cleaving SEMA3B, experiments were performed that incubated recombinant SEMA3B with cell lysates or conditioned medium for three hours and then determined the presence or absence of full-length SEMA3B.

The data from this experiment showed that MCF-10A cell lysate and conditioned medium were unable to cleave the recombinant SEMA3B while the DCIS.com cell lysates achieved partial cleavage, However, in the treated conditioned medium from DCIS.com cells, the intensity of the band was much less at 51 kDa as it was faint compared to the full-length band. This result showed a very high level of 83 kDa SEMA3B detected in the conditioned medium compared with the treated lysate, which may suggest the activity of this fragment is much more in conditioned medium. A similar finding was observed in the MDA-MB-231 cell lysate with a slight increase in

band intensity detected in the treated conditioned medium and lysate at 51 kDa compared to DCIS.com cells suggesting that MDA-MB-231 may be able to cleave the full-length more than the pre-invasive cells. These data suggested a specific mechanism is likely to exist inside the cell that cleaves the full-length SEMA3B. This finding does not exclude the possibility that the furin-like pro-protein convertases might also have a role in this process. The limitation of these experiments was with using treated lysate, the protein has degraded after three hours, and it could be more effective if we have incubated for longer periods of time. Previous studies revealed that the cleavage at the recognition site of PPCs is usually responsible for inactivation of SEMA3B (Adams et al., 1997, Varshavsky et al., 2008). Thus, our data could suggest the cells themselves are producing proteins capable of cleaving SEMA3B, which may be able to inhibit the anti-tumorigenic activities of SEMA3B. It should be noted that in these experiments the positive control of rSEMA3B was mixed with fresh medium but it was not incubated for the duration of the experiment at 37^{o}C (3 hours) in identical conditions to those used for the test samples. It would be important to test the stability of rSEMA3B in normal serum-free medium under the conditions of the assay, to exclude the possibility that rSEMA3B was cleaved by autoproteolytic degradation. It should also be mentioned that protease inhibitors that were used when lysates were extracted for analysis of rSEMA3B cleavage (see sections 2.10.10 and 4.3.6). Protease inhibitors were used in order to prevent excessive proteolytic degradation when cells were lysed. Although the inhibition action of the protease inhibitors used is reversible, there is still the possibility that some PPCs were also inhibited and therefore their full effect on cleaving rSEMA3B may have been masked.

The findings presented in this chapter might suggest a potential role for SEMA3B in breast cancer cells that may be of prognostic and therapeutic value, however, additional investigations are required to understand what regulates this protein cleavage as breast disease progress. Therefore, to complement this work, further experiments should determine the relative importance of how the expression of pro-protein convertases can affect the expression of SEMA3B since previous literature has suggested that the pro-protein convertase family of proteins may actively cleave class 3 semaphorins. The next chapter will establish the expression of pro-protein convertases in the cell-line models and breast cancer tissues to identify whether there is a correlation between pro-protein convertases expression and SEMA3B cleavage.

Chapter 5: Expression of Furin-like Pro-protein Convertases in Breast Cancer Progression

5.1 Introduction

The data presented in the previous chapter demonstrated that full-length recombinant SEMA3B has a significant effect on decreasing the growth, migration and invasion of breast cancer cells (Chapter 4). Expression of SEMA3B however, was completely cleaved in breast cancer cell lines, compared to normal breast epithelial cells as shown by Western blot analysis (performed in Chapter 3). This cleavage is thought to inactivate the tumour suppressor function of SEMA3B (Varshavsky et al., 2008). It is known that SEMA3B contains a PPC consensus cleavage motif RXK/RR (Barr, 1991, Varshavsky et al., 2008) as shown in figure 5.1. Therefore, it is likely that in breast cancer increased expression of PPCs results in cleavage of SEMA3B near the carboxyl terminus resulting in the generation of 51 kDa isoforms seen on Western blots, and inactivating the tumour suppressor function of the protein.

PPCs, are a family of subtilisin/Kexin-type serine endoproteases, which are usually responsible for the conversion of immature precursors to mature protein (Seidah and Prat, 2012), rather than inactivating proteins. However, several studies have shown that PPCs can regulate semaphorins by proteolytic activity (Adams et al., 1997, Varshavsky et al., 2008, Casazza et al., 2012), and PPCs are usually found to inactivate class-3 semaphorins (Adams et al., 1997, Varshavsky et al., 2008). That said, the functional consequence of the proteolytic processing events appears variable within the semaphorin family. Some members of the family demonstrate functional loss as a result of PPC cleavage e.g. SEMA3B (Varshavsky et al., 2008), SEMA3F (Futamura et al., 2007) and SEMA3A (Adams et al., 1997), while other family members, such as SEMA3E gained a pro-metastatic phenotype from PPC cleavage (Christensen et al., 2005).This is in contrast to activity of the un-cleaved full-length of SEMA3E which has anti-angiogenic activity (Casazza et al., 2012).

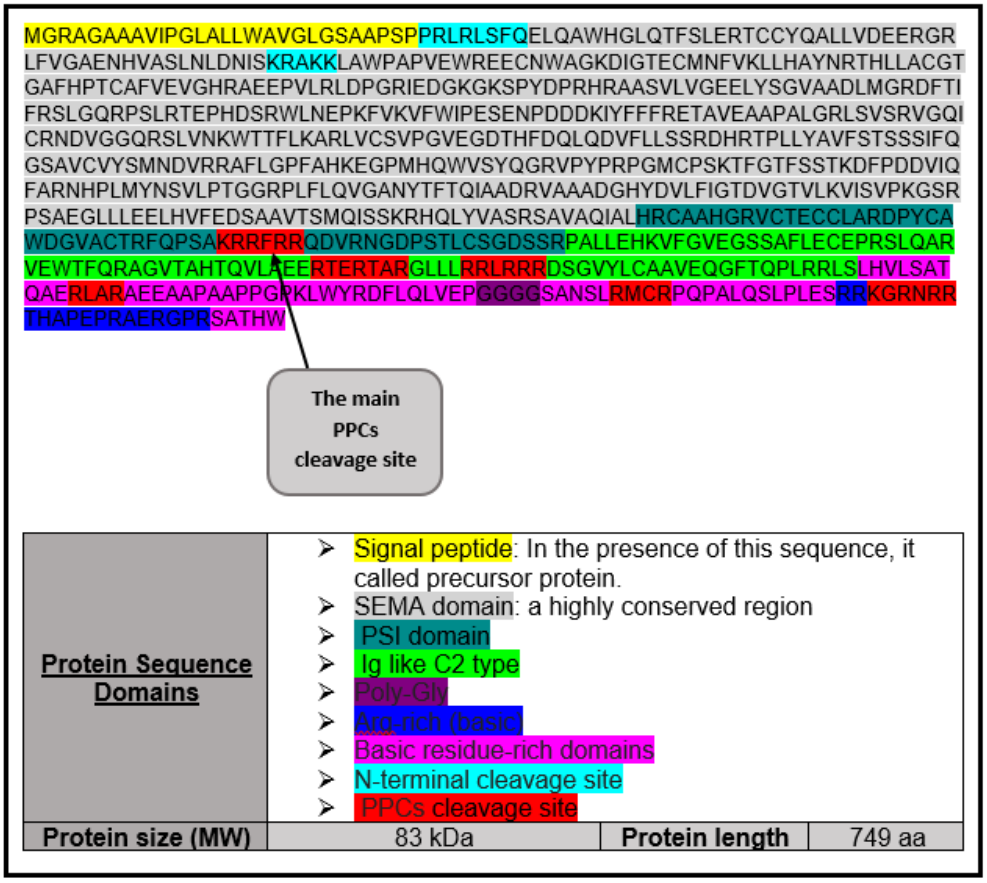

Figure 5.1: Sequence of SEMA3B showing the PCC cleavage sites. There is a cleavage site at N-terminal to make the protein active by removing the signal peptide and the pro-domain in turquoise. There are six potential PPC cleavage sites, which all highlighted in red present in C-terminal, and it is thought that cleavage at these sites could make the protein inactive or interfere with their activity. It is likely that the cleavage at SEMA3B sequence KRRFRR is the most common cleavage site for PCCs and this will generate a ~51 kDa NH2-terminal fragment and ~20 kDa at C-terminal, which is in agreement with observations in Chapter 3.
https://www.uniprot.org/uniprot/Q13214

Initially, SEMA3B is synthesized as an inactive precursor. The sequence of SEMA3B has a cleavage site at the N-terminal where the first cleavage takes place at position 24-25 to remove the signal peptide (1-24) in order to activate the protein. In addition, there are six possible cleavage sites for PPCs in the C-terminal, which generate differing length fragments that alter in their activity. For example cleavage at KRRFRR sequence able to generate a ~51 kDa NH2-terminal fragment and ~20 kDa at C-terminal while cleavage at KGRNRR found cross reactive with SEMA3A sequence where the furin processing sites found in SEMA3A (Parker et al., 2013).

It has been shown that SEMA3B cleavage to the p65 form inhibits the ability of SEMA3B to reduce the growth and metastasis of breast tumours. However, cleavage to the p83 form of SEMA3B is essential for SEMA3B to acquire an inhibitory phenotype in breast cancer (Varshavsky et al., 2008). PPCs have been shown to be involved in this cleavage process based on cleavage site mutation and furin-like pro-protein convertase inhibition studies (Adams et al., 1997, Varshavsky et al., 2008).

Previous studies have commonly claimed that furin is responsible for cleavage of SEMA3B and other class 3 semaphorins (Varshavsky et al., 2008, Toledano et al., 2019), but these experiments have used inhibitors which are not specific for furin, but actually inhibit the entire pro-protein convertase family, of which furin is just one member. Experiments which specifically inhibit furin show significant potential implications in treating some diseases such as human immunodeficiency virus (Hallenberger et al., 1992) and head and neck cancer (Bassi et al., 2001b) while the overexpression of furin enhances the acceleration of the disease status such as in ovarian cancer (Adams et al., 1997, Page et al., 2007). Indeed, the family of furin-like pro-protein convertases is now thought to be essential for the development of many diseases including cancer and pathogenic infections (Seidah and Prat, 2012) and overexpression of some members of the PPC family have been linked to carcinogenesis and contribute to invasiveness of cancer cells (Seidah and Prat, 2012). However, not all members of the PPC family have been implicated in cancers.

That said, due to upregulation of many of the furin-like pro-protein convertases in different cancers and metastases, they have been suggested as a potential therapeutic target to inhibit cancer progression (Seidah and Prat, 2012). However, previous attempts in mice to knock-out some members of the family such as furin, PCSK5 and PCSK8 resulted in embryonic lethality, which raises a potential concern of using inhibitors that knock out these molecules due to the possibility of unwanted toxic side-effects upon use in clinical settings (Essalmani et al., 2006, Creemers and Khatib, 2008).

In breast cancer, only a few members of the PPC family, including furin, PCSK6, PCSK7 and PCSK9 have previously been associated with breast cancer tumorigenicity, or investigated. Indeed, the role of the pro-protein convertase family and the possible involvement of these proteins in processing and/or degradation of SEMA3B is not clearly understood in breast cancer.

As SEMA3B is expressed in breast cancer, but in a fully cleaved form in both pre-invasive and invasive breast cancer and SEMA3B contains PPC cleavage sites we hypothesised that furin-like pro-protein convertases are expressed in breast cancer and cleave SEMA3B to produce inactive fragments. Therefore, qPCR, Western blotting and immunohistochemistry were performed on a panel of breast cell lines/tissues representing models of breast cancer progression to establish the expression of PPCs across the progression of breast cancer. Finally, attempts were made to inhibit PPC activity to establish whether it is a member of the PPC family that is responsible for SEMA3B cleavage in breast cancer.

Therefore, this chapter aimed to:

1. Establish the expression of PPCs in the cell line model of breast cancer progression (mRNA and protein) and relate this to both disease progression and SEMA3B cleavage.
2. Establish the expression of PPCs in breast tissue and relate this to disease progression.
3. Inhibit the activity of PPCs and to establish whether this will inhibit the cleavage of SEMA3B in breast cancer cells.

5.2 Methods

5.2.1 Quantitative PCR analysis

This technique was performed to investigate the mRNA expression of Furin and other pro-protein convertases in all cell lines using qPCR. RNA was extracted from the breast cell lines, then cDNA was synthesized to determine gene expression of all PPCs using SYBR® Green qPCR Master Mix relative to GAPDH housekeeping gene as described in 2.9. The validated PPCs qPCR primers ID and sequences are listed in table 2.1.4.

5.2.2 Western blot analysis

This analysis was used to assess the protein expression of all the PPCs in all cell lines. Total cell lysates were separated by 10% SDS-PAGE, and then transferred to a PVDF membrane using a semi-dry transfer machine and incubated with the relevant antibody. Chemiluminescence was used to detect any bands, with β-actin being used as a loading control as described in 2.10

5.2.3 Cytospin experiment

This method was used to confirm the Western blot and to assess the expression of proteins where antibodies did not work properly in Western Blots e.g. PCSK5 and PCSK8. Cells were trypsinised, cytospun onto slides and then immunocytochemistry used to confirm protein expression in the cells as described in 2.12.

5.2.4 Cell pellet experiment

Cell pellets were generated by trypsinising cells, spinning them into a pellet, and fixing them in 10% neutral buffered formalin (NBF) overnight at 4^{o}C. The fixative was removed, and cell pellets were covered gently by 300 µL molten agarose (2 g of agarose was added into distilled water and warmed up in a microwave until dissolved). The agar-cell pellet was left to solidify for a minute or so and then it was gently lifted from the bottom of the tube using a small spatula. The agarose was placed in labelled cassette and immersed in 70% ethanol ready for processing into wax and then sectioning (5 µm sections) by a skilled operator (Maggie Glover). All slides were processed by immunocytochemistry in the same manner as for immunohistochemistry with the slightly different protocol as described in 2.12.1.

5.2.5 Immunohistochemistry

This method was performed to investigate the PPC expressions in human microarray tissues representing a model of breast cancer development as detailed in table 2.10, along with relevant positive control tissues for each PPC. Each specimen was immunohistochemically stained for all PPCs members, then Semi-quantitative grading of staining from 0 (no stain) to 3 (strong stain) was carried out in both epithelial/tumour cells as described in 2.11 and 3.2.8.

5.2.6 Inhibition of proteolytic cleavage of furin-like pro-protein convertase

In order to determine the effect of inhibiting pro-protein convertase activity on the cleavage of SEMA3B, cells were treated with two different pan-inhibitors; namely, CMK and α-PDX as follows.

5.2.6.1 Decanoyl-RVKR-CMK inhibitor (CMK)

Decanoyl-RVKR-CMK is a potent and irreversible pan-inhibitor for furin-like pro-protein convertases (Couture et al., 2011). 1mg of CMK inhibitor was dissolved in 100 µl of DMSO and then used in the experiment at the relevant concentration dissolved in media. DCIS.com and MDA-MB-231 cells were cultured and seeded as previously described in 2.2.2. Then, they were incubated with and without 135 and 200 µmol/L CMK inhibitor for 24 hours. Cell lysates were then extracted, and conditioned medium was collected from the cells and was separated on a 10% SDS-PAGE gel, blotted onto PVDF, and probed with both anti-MT1-MMP (used as a positive control for this assay) and with an anti-SEMA3B antibody as described 2.10.

5.2.6.2 Alpha 1-PDX inhibitor (α-PDX)

Alpha1-PDX is a potent and selective inhibitor of furin and some PPCs, that contain a minimal furin consensus sequence, RXXR in its reactive loop which able α-PDX to block the activity of PPCs (Tsuji et al., 1999). According to the manufacturer, for a PPC inhibition assay, cells should be treated within the range of 8.0-20 µM. DCIS.com and MDA-MB-231 cells were cultured and seeded, as previously described in section 2.2.2. Then, they were incubated with and without 20 µM α-PDX inhibitor for 24 hours. Cell lysates were extracted, and conditioned medium was collected for Western blot as described in 2.10. Proteins were separated on a 10% SDS-PAGE gel, blotted onto

PVDF, and probed with both anti-MT1-MMP (used as a positive control for this assay) and with an anti-SEMA3B antibody as described in 2.10.

5.3 Results

As SEMA3B is cleaved in breast cancer cell lines and contains several PPC cleavage recognition sites, mRNA expression of all the PPC family members were first established in the cell lines representing different stages of disease progression. Then these mRNA data were compared with protein expression data in the cell lines, and then in tissue microarray slides, again containing different breast tissue stages (normal, atypical hyperplasia, DCIS and invasive tissues).

5.3.1 *Furin* mRNA expression in breast epithelial and cancer cell-lines

Furin is overexpressed in some cancers where it correlates with metastatic progression (Bassi et al., 2000) , and it is also thought to cleave SEMA3B (Varshavsky et al., 2008). Therefore, we determined the expression of furin mRNA by qPCR using the same cell lines as described 2.9 to establish whether expression of furin is associated with progression of breast disease.

As shown in figure 5.2, the non-malignant MCF-10A and pre-malignant MCF-10AT breast cell lines expressed significantly higher levels of furin mRNA compared to other cells. When the levels of furin mRNA were compared to the normal MCF-10A, DCIS.com ($P= 0.0010$, Dunnett's test), MCF-7 ($P<0.0001$, Dunnett's test), T47D ($P= 0.0005$, Dunnett's test) and MDA-MB-231 cells ($P<0.0001$, Dunnett's test) had a significantly lower expression of furin mRNA. That said, furin was more highly expressed in the metastatic bone homing MDA-MB-231-BM cells than the pre-invasive and invasive cell-lines.

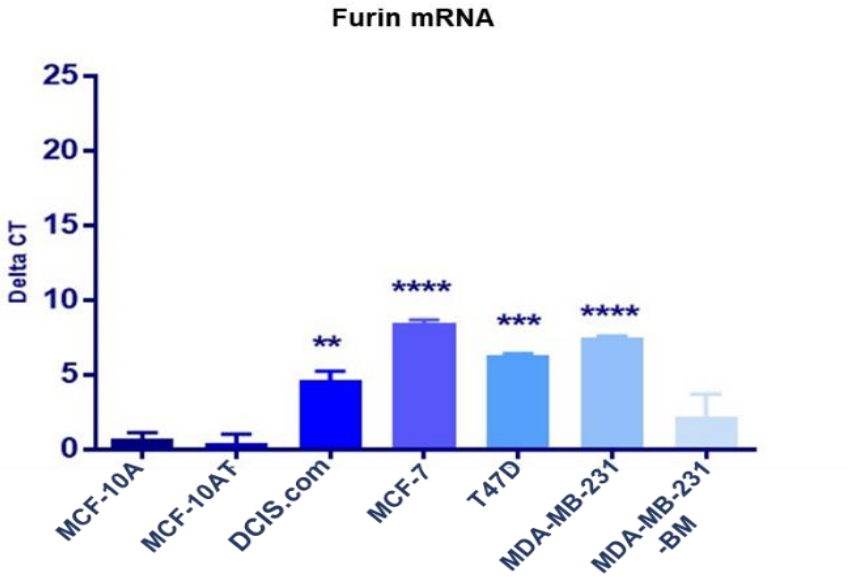

Figure 5.2: qPCR analysis of furin mRNA expression in breast normal/cancer cells lines. RNA was extracted from cells and cDNA was synthesised and was analysed by qPCR. GAPDH was used to confirm the integrity of RNA. Data are presented as a ratio to GAPDH. Delta Ct is presented on the Y-axis and was calculated by subtracting the mean of cell Ct from the mean of the reference gene. Data is presented as the mean +/- SD of three independent experiments. The lower the Ct level, the greater the amount of target nucleic acid in the sample. Data was analysed statistically by one-way ANOVA with post hoc Dunnett's multiple comparisons. P values were generated, and ** represent P<0.01, *** represent P<0.001 and **** represent P<0.0001 compared to the expression of furin in normal epithelial MCF-10A cells.

5.3.2 *PCSK1* mRNA in breast epithelial and cancer cell-lines

PCSK1 is known to be expressed primarily in neuronal and endocrine cells (Seidah et al., 1991). However, little is known about its role in breast cancer. The *PCSK1* mRNA expression was therefore investigated in all breast cell lines as described 2.9.

As shown in figure 5.3, the expression pattern of *PCSK1* mRNA was similar to that of *SEMA3B* with a significantly higher level of *PCSK1* expression detected in MCF-10A cells compared to all other cell lines, which had significantly lower levels of *PCSK1* expression compared to the normal MCF-10A cells (P<0.0001, one-way ANOVA, Dunnett's test).

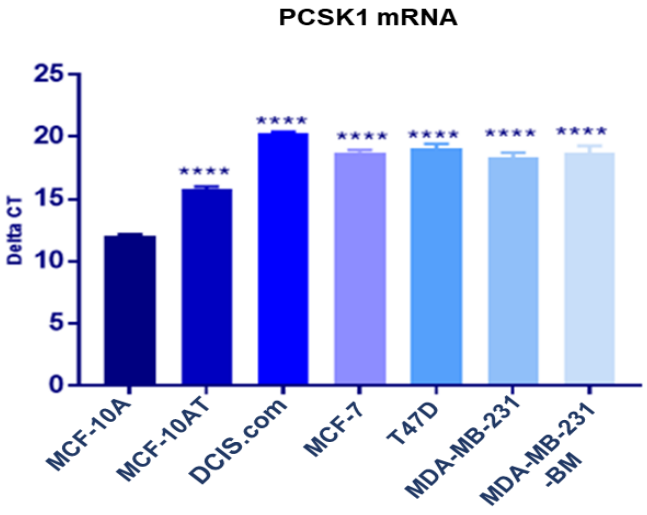

Figure 5.3: qPCR analysis of PCSK1 mRNA expression in expression in breast normal/cancer cells lines: RNA was extracted from cells and cDNA was synthesised and was analysed by qPCR. GAPDH was used to confirm the integrity of RNA. Data are presented as a ratio to GAPDH. The Y-axis represented the Delta Ct, was calculated by subtracting the mean of cell Ct from the mean of the reference gene. Data is presented as the mean +/- SD of three independent experiments. The lower the Ct level, the greater the amount of target nucleic acid in the sample. Data was analysed statistically by one-way ANOVA with post hoc Dunnett's multiple comparisons. P values were generated, and ** represent P<0.01, *** represent P<0.001 and **** represent P<0.0001 compared to the expression of PCSK1 in normal epithelial MCF-10A cells.

5.3.3 *PCSK2* mRNA in breast epithelial and cancer cell-lines

A previous study revealed that PCSK2 is not important for normal embryonic development, but it helps to control the maturation of several regulatory precursor proteins (Scamuffa et al., 2006). However, mutations in *PCSK2* have been linked with multiple defects and disease such as hypoglycemia and a deficiency in circulating glucagon (Scamuffa et al., 2006), but its role in cancer has not been clearly identified yet. Therefore, it was interesting to study this member of the PPC family across the breast cell lines. As shown in figure 5.4, the expression of *PCSK2* was fairly low in the non-malignant MCF-10A and pre-invasive DCIS.com cells and compared to the normal MCF-10A, the gene expression of *PCSK2* was significantly increased in MCF-10AT (P=0.0026, Dunnett's test), MCF-7 (P=0.0462, Dunnett's test), T47D (P=0.0026, Dunnett's test) cells. Moreover, the highest expression of PCSK2 was detected in metastatic bone homing MDA-MB-231-BM cells (P<0.0001, Dunnett's test) suggesting that generally *PCSK2* is increased in breast cancer cells compared to non-cancerous cells, with the exception of MCF-10AT cells.

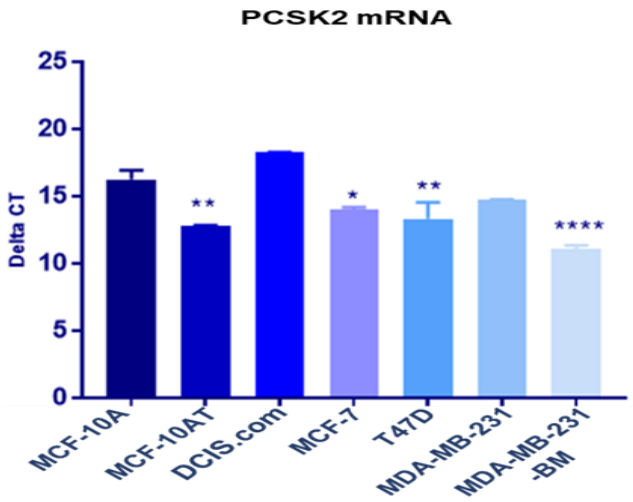

Figure 5.4: qPCR analysis of PCSK2 mRNA expression in expression in breast normal/cancer cells lines. RNA was extracted from cells and cDNA was synthesised, and that was analysed by qRT-PCR. GAPDH was used to confirm the integrity of RNA and data are presented as a ratio to GAPDH. The Y-axis represented the Delta Ct, was calculated by subtracting the mean of cell Ct from the mean of the reference gene. Data is presented as the mean +/- SD of three independent experiments. The lower the Ct level, the greater the amount of target nucleic acid. The data was analysed statistically by one-way ANOVA with post hoc Dunnett's multiple comparisons. P values were generated and * represent P=0.0462, ** represent P=0.0026 and **** represents P<0.0001 compared to the expression of PCSK2 in normal epithelial MCF-10A cells.

5.3.4 *PCSK4* mRNA in breast epithelial and cancer cell-lines

PCSK4 has been shown to be expressed highly in reproductive tissues including testes, ovaries, and placenta, and the absence of PCSK4 is associated with male and female infertility in mice (Gyamera-Acheampong and Mbikay, 2009). However, there is no previous study that has looked at its expression in breast cancer. Therefore, it was interesting to study the expression of *PCSK4* in the panel of breast cell lines as described in 2.9. As shown in figure 5.5, the majority of the cell lines tested showed similar, fairly low levels of *PCSK4* expression, except for T47D cells which had a significantly higher expression compared to the normal MCF-10A cells (P=0.0069, Dunnett's test).

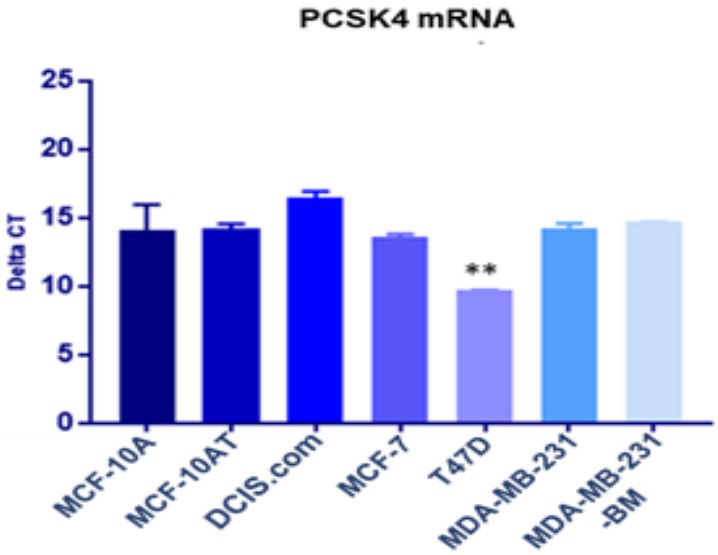

Figure 5.5: qPCR analysis of *PCSK4* mRNA expression in expression in breast normal/cancer cells lines: RNA was extracted from cells and cDNA was synthesised, and that was analysed by qRT-PCR. GAPDH was used to confirm the integrity of RNA and data are presented as a ratio to GAPDH. The Y-axis represented the Delta Ct, was calculated by subtracting the mean of cell Ct from the mean of the reference gene. Data is presented as the mean +/- SD of three independent experiments. The lower the Ct level, the greater the amount of target nucleic acid. The data was analysed statistically by one-way ANOVA with post hoc Dunnett's multiple comparisons. P values were generated, and ** represent P=0.0069 compared to the expression of PCSK4 in normal epithelial MCF-10A cells.

5.3.5 *PCSK5* mRNA in breast epithelial and cancer cell-lines

PCSK5 has a widespread tissue distribution, but the highest density of PCSK5 is found in adrenal cortex and intestine small intestine (Essalmani et al., 2006). However, studies linking PCSK5 to cancer are limited (Sun et al., 2009) and indeed, one previous study failed to detect expression of *PCSK5* mRNA in breast cancer cells (Cheng et al., 1997). However, that study did not include all the cell lines in the panel used in this thesis, and therefore qPCR was performed on these cells as described 2.9. As shown in figure 5.6, there was low expression of *PCSK5* mRNA detected in all the cell lines with MCF-7 cells showing the highest expression across all the investigated cell lines and was significantly higher than the normal breast epithelial cell line, MCF-10A (P=0.01, Dunnett's test). In contrast the lowest expression of PCSK5 was in T47D and MDA-MB-231 cells where expression was significantly lower than MCF-10A cells (P=0.0002 and P=0.0002 respectively, Dunnett's test).

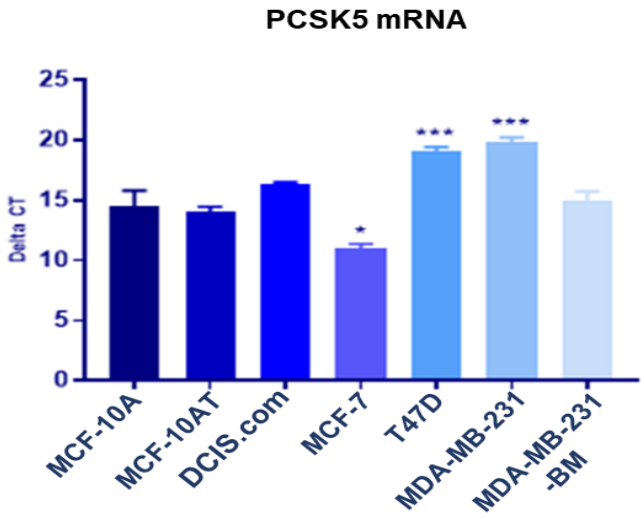

Figure 5.6: qPCR analysis of *PCSK5* mRNA expression in expression in breast normal/cancer cells lines: RNA was extracted from cells and cDNA was synthesised, and that was analysed by qRT-PCR. GAPDH was used to confirm the integrity of RNA and data are presented as a ratio to GAPDH. The Y-axis represented the Delta Ct, was calculated by subtracting the mean of cell Ct from the mean of the reference gene. Data is presented as the mean +/- SD of three independent experiments. The lower the Ct level, the greater the amount of target nucleic acid. The data was analysed statistically by one-way ANOVA with post hoc Dunnett's multiple comparisons. P values were generated and * represents P=0.01 and *** represents P= 0.0002 compared to the expression of PCSK5 in normal epithelial MCF-10A cells.

5.3.6 *PCSK6* mRNA in breast epithelial and cancer cell-lines

PCSK6 is located on the same chromosome as furin, chromosome 15, so it is possible that it may have similar regulation, expression and function to furin. Indeed, a previous study has demonstrated that PCSK6 is linked with breast cancer progression (Wang et al., 2015). Therefore, qPCR was performed on the representative cell lines of breast disease progression as described in 2.9. However, as shown in figure 5.7, although *PCSK6* mRNA expression was detected in all cell lines, there was no significant difference see between them when compared to the normal MCF-10A cells.

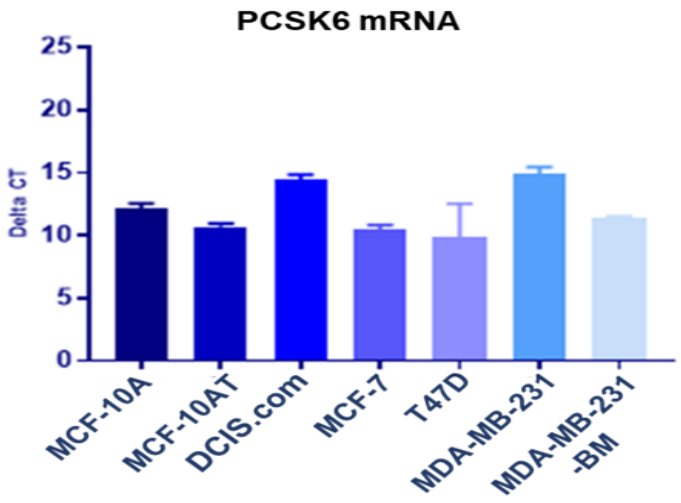

Figure 5.7: qPCR analysis of *PCSK6* mRNA expression in expression in breast normal/cancer cells lines: RNA was extracted from cells and cDNA was synthesised, and that was analysed by qRT-PCR. GAPDH was used to confirm the integrity of RNA and data are presented as a ratio to GAPDH. The Y-axis represented the Delta Ct, was calculated by subtracting the mean of cell Ct from the mean of the reference gene. Data is presented as the mean +/- SD of three independent experiments. The data was analysed statistically by one-way ANOVA. The lower the Ct level, the greater the amount of target nucleic acid.

5.3.7 *PCSK7* mRNA in breast epithelial and cancer cell-lines

There is some evidence in the literature to suggest that PCSK7 may have a role in breast cancer as overexpression of PCSK7 was identified in aggressive breast cancers (Cheng et al., 1997). Therefore, since we believed that one of the PPC family is responsible for the cleavage of SEMA3B, the gene expression of *PCSK7* was investigated in all cell lines used as described in 2.9. As shown in figure 5.8, *PCSK7* was detected in all the cell lines with T47D and DCIS.com expressing the most. When compared to the normal MCF-10A cells this increase in expression was significant (T47D cells; P<0.0001, Dunnett's test and DCIS.com P<0.0001, Dunnett's test). In contrast, the expression of *PCSK7* in all other cell lines was significantly reduced compared to the MCF-10A cells; MCF-10AT (P=0.0011, Dunnett's test), MCF-7 (P<0.0001, Dunnett's test), MDA-MB-231 (P<0.0001, Dunnett's test) and MDA-MB-231-BM (P=0.0005, Dunnett's test).

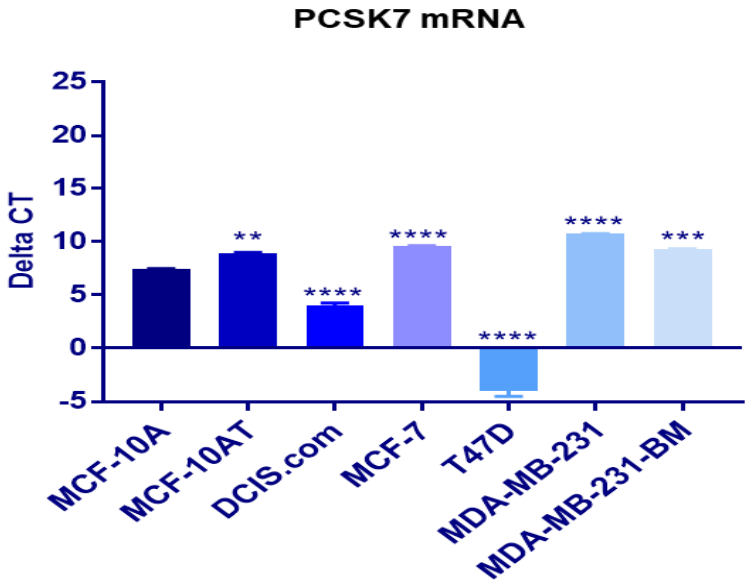

Figure 5.8: qPCR analysis of *PCSK7* mRNA expression in expression in breast normal/cancer cells lines: RNA was extracted from cells and cDNA was synthesised, and that was analysed by qRT-PCR. GAPDH was used to confirm the integrity of RNA and data are presented as a ratio to GAPDH. The Y-axis represented the Delta Ct, was calculated by subtracting the mean of cell Ct from the mean of the reference gene. The lower the Ct level, the greater the amount of target nucleic acid. Data is presented as the mean +/- SD of three independent experiments. The data was analysed statistically by one-way ANOVA with post hoc Dunnett's multiple comparisons. P values were generated and ** represents P=0.0011, *** represents P= 0.0005 and **** represents P<0.0001 compared to the expression of PCSK7 in normal epithelial MCF-10A cells.

5.3.8 *PCSK8* mRNA in breast epithelial and cancer cell-lines

Previous studies have shown that expression of *PCSK8* mRNA was decreased in lung cancer tissue compared to normal lung tissue (Demidyuk et al., 2013), however, nothing is known about its role or expression in breast cancer. Therefore, *PCSK8* mRNA was investigated by qPCR as described in 2.9 in all our breast cell lines. As shown in figure 5.9, *PCSK8* mRNA was detected in all cell lines with T47D showing the highest level of expression (P<0.0001, Dunnett's test compared to the normal MCF-10A cells). MCF-10A, DCIS.com and MDA-MB-231-BM cells had similar levels of expression with significantly lower expression seen in MCF-10AT (P=0.01, Dunnett's test), MCF-7 (P=0.01, Dunnett's test) and MDA-MB-231 (P=0.02, Dunnett's test) when compared to MCF-10A cells.

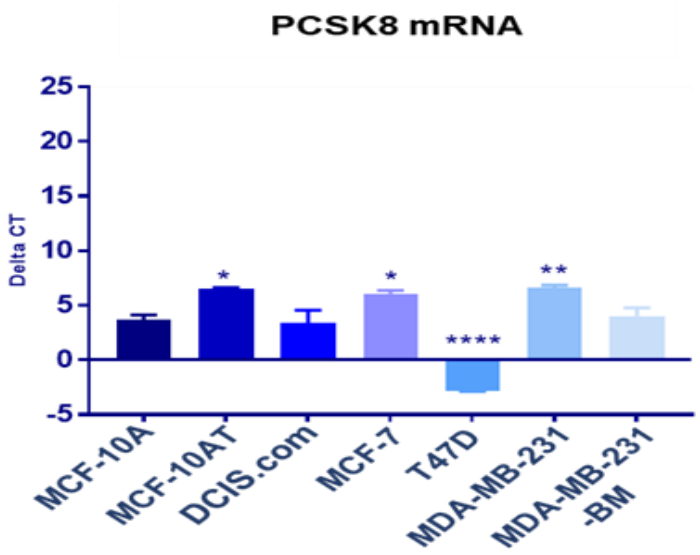

Figure 5.9: qPCR analysis of *PCSK8* mRNA expression in expression in breast normal/cancer cells lines: RNA was extracted from cells and cDNA was synthesised, and that was analysed by qRT-PCR. GAPDH was used to confirm the integrity of RNA and data are presented as a ratio to GAPDH. The Y-axis represented the Delta Ct, was calculated by subtracting the mean of cell Ct from the mean of the reference gene. The lower the Ct level, the greater the amount of target nucleic acid. Data is presented as the mean +/- SD of three independent experiments. The data was analysed statistically by one-way ANOVA with post hoc Dunnett's multiple comparisons. P values were generated and * represents P=0.01, ** represents P=0.02 and **** represents P<0.0001 compared to the expression of PCSK8 in normal epithelial MCF-10A cells.

5.3.9 *PCSK9* mRNA in breast epithelial and cancer cell-lines

PCSK9 has been shown to be a vital regulator of lipid metabolism and associated with cholesterol homeostasis (Levy et al., 2013), with high expression of PCSK9 leading to increase the level of cholesterol. A previous study found a strong association between the increased level of cholesterol due to PCSK9 and the risk of breast cancer (Nelson et al., 2014), suggesting a possible role of PCSK9 in breast cancer progression. In order to assess the *PCSK9* mRNA expression in our breast cancerous and non-cancerous cells, qPCR was performed as described in 2.9. As shown in figure 5.10, *PCSK9* was expressed in all cell lines, with maximal expression in MCF-10A and MDA-MB-231 cells, and only a slight (non-significant) reduction in MCF-10AT cells. *PCSK9* expression was significantly reduced in all malignant cells except MDA-MB-231 cells when compared to MCF-10A cells; DCIS.com (P<0.0001, Dunnett's test), MCF-7 (P<0.0001, Dunnett's test), T47D (P<0.0001, Dunnett's test) and MDA-MB-231-BM (P= 0.0002, Dunnett's test).

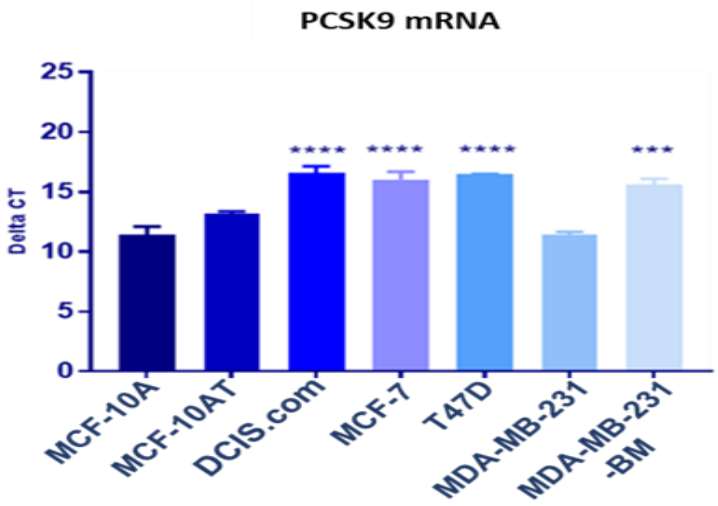

Figure 5.10: qPCR analysis of *PCSK9* mRNA expression in expression in breast normal/cancer cells lines: RNA was extracted from cells and cDNA was synthesised, and that was analysed by qRT-PCR. GAPDH was used to confirm the integrity of RNA and data are presented as a ratio to GAPDH. The Y-axis represented the Delta Ct, was calculated by subtracting the mean of cell Ct from the mean of the reference gene. The lower the Ct level, the greater the amount of target nucleic acid. Data is presented as the mean +/- SD of three independent experiments. The data was analysed statistically by one-way ANOVA with post hoc Dunnett's multiple comparisons. P values were generated and *** represents P= 0.0002, and **** represents P<0.0001 compared to the expression of PCSK9 in normal epithelial MCF-10A cells.

5.3.10 Furin protein expression in normal breast and cancer cell-lines and conditioned medium

Having established that furin mRNA was present in the breast cell lines, it was important to establish whether this was translated to protein, as it would be protein that would be responsible for SEMA3B cleavage. Presence of furin protein was determined by western blotting on the same breast cancer cell extracts as described in 2.10, with HepG2 cells used as a positive control as furin has previously been identified in these cells (Mori et al., 1999).

Furin protein expression, determined in cell lysates using antibodies directed against the C-terminal of furin of human origin (figure 5.11) was seen in all cell lines in two main forms, the full-length at ~97 kDa which is known to be inactive and the mature form at ~70 kDa (active form) (Rehemtulla et al., 1992). The full-length form, was found to be most highly expressed in the normal, pre-malignant and pre-invasive cell lines compared to the invasive cells. In contrast, the expression of the mature form (~70 kDa), gradually increased with increasing malignancy of disease and was significantly higher in most of the invasive breast cancer cell lines, including T47D ($P=0.0468$, Dunnett's test), MDA-MB-231 ($P=0.0324$, Dunnett's test) and MDA-MB-231-BM ($P=0.0233$, Dunnett's test) compared to MCF-10A cells. However, in MCF-7 cells, the expression of furin was similar to that in non-cancerous cells with no significant differences.

In conditioned medium, the full-length furin (~97 kDa) was not seen in any cell line conditioned medium. However, the expression of furin at 70 kDa was found to be the most expressed in the conditioned medium of MDA-MB-231 cells with faint expression detected in other cells except for MCF-10A and MDA-MB-231-BM (figure 5.12). These findings suggest that furin may be responsible for the cleavage of SEMA3B protein; however, the expression pattern of furin does not mirror that of the *furin* mRNA expression.

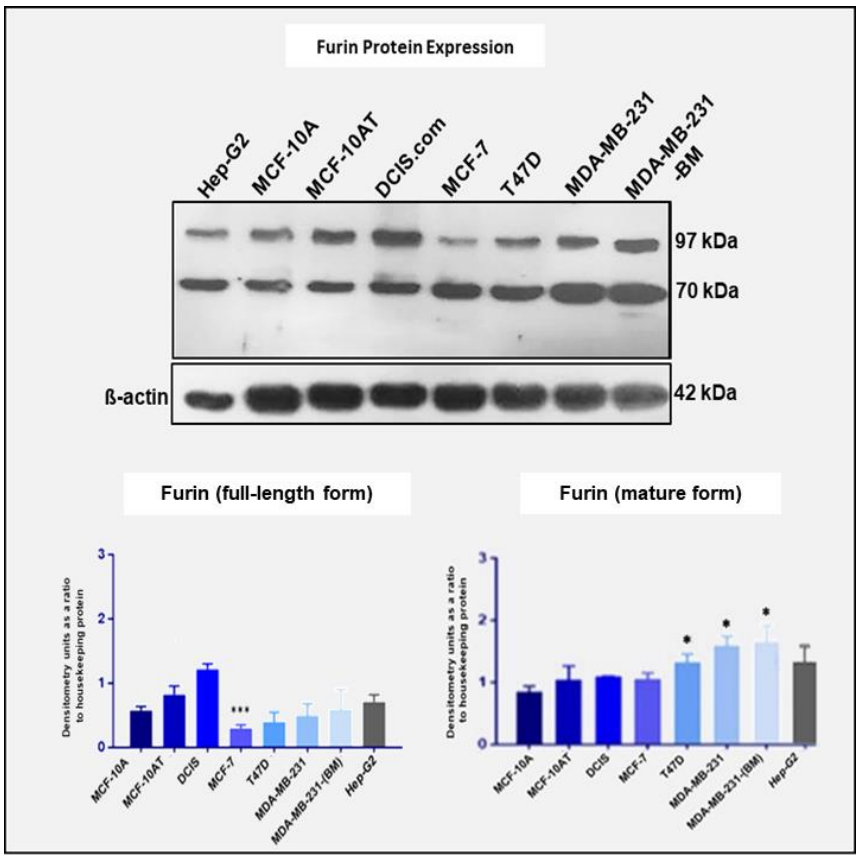

Figure 5.11: Furin protein expression in normal breast and cancer cell-lines as determined by Western blot. Cell lysates were separated on a 10% SDS-PAGE gel, and then blotted onto PVDF and probed with the anti-furin antibody. Hep-G2 was used as a positive control for furin expression. To confirm that the amount of protein in each lane was equal, the membrane was stripped and re-probed with anti-β-actin housekeeping protein as a loading control. Densitometry analysis was performed for all cells using ImageJ software to assess relative band densities. Data is represented as the mean+/- SD of three independent experiments. Data was analysed statistically by one-way ANOVA with post hoc Dunnett's multiple comparisons. P values were generated, and * represent $P<0.01$ and *** represent $P= 0.0002$ compared to the expression of furin in normal epithelial MCF-10A cells. The sizes of molecular weight markers are indicated in kDa. Representative immunoblot shown of n=3.

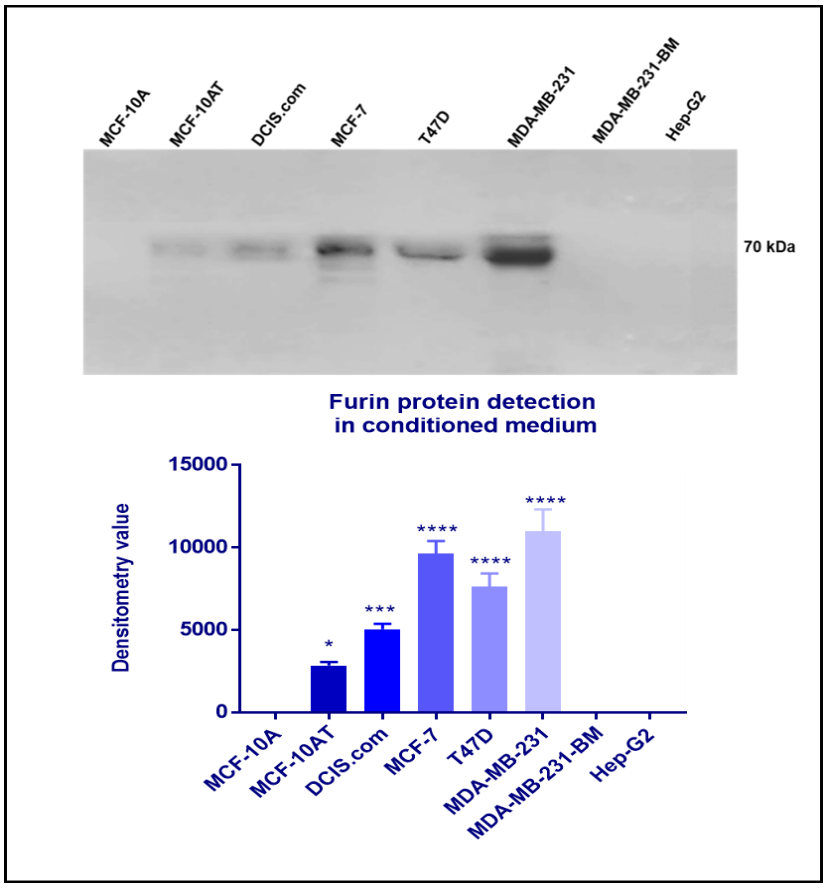

Figure 5.12: Furin protein detection in conditioned medium of normal breast and cancer cell-lines as determined by Western blot. Cells were seeded and starved for 24 hours and conditioned medium was generated to be collected and separated on a 10% SDS-PAGE gel, and then blotted onto PVDF and probed with the anti-furin antibody. Hep-G2 lysate was used as a positive control for furin expression. Densitometry analysis was performed for all cells using ImageJ software to assess band densities and presented as densitometry value. Data are the mean ± SD of three independent experiments. Data was analysed statistically by ordinary one-way ANOVA followed by a post hoc Dunnett's test (* represent P= 0.0282, *** represent P= 0.0002 and **** represent P<0.0001 in comparison to normal MCF-10A cells). Representative immunoblot shown of n=3.

5.3.11 PCSK1 protein expression in normal breast and cancer cell-lines and conditioned medium

To evaluate whether the PCSK1 gene expression observations were translated to the protein level, Western blot was performed in all the cell line lysates and conditioned medium, with cell lysates extracted and conditioned medium was collected and investigated as described in 2.10. HepG2 cells were again used as positive controls as they have previously been shown to express this protein (ProteinAtlas).

As shown in figure 5.13, in cell lysates, the antibody used detected two different isoforms of PCSK1, one at 84 kDa, which is active form, and one at 66 kDa which is also active and thought to be the most catalytically active form of PCSK1, although this isoform is thought to be less stable than the 84 kDa form (Blanco et al., 2015). The protein expression of the largest isoform did not correlate with the gene expression, as the lowest expression of PCSK1 protein was detected in MCF-10A at 84 kDa. However, compared to the normal MCF-10A cells, in all other cells, there was a strong expression of PCSK1 and that was significantly higher in MCF-10AT ($P<0.0001$, Dunnett's test), DCIS.com ($P=0.0002$, Dunnett's test), MCF-7 ($P<0.0001$, Dunnett's test), T47D ($P=0.0002$, Dunnett's test), MDA-MB-231 ($P<0.0001$, Dunnett's test) and MDA-MB-231-BM ($P<0.0001$, Dunnett's test) than in MCF-10A cells. This pattern matches somewhat with the cleavage of SEMA3B suggesting that this protein has the potential to be involved in SEMA3B cleavage. Interestingly, the expression of PCSK1 at 66 kDa, the most active form of the protein, was only detected in MCF-10A and MCF-10AT cells, suggesting that this is less likely to be responsible for SEMA3B cleavage. In conditioned medium, the PCSK1 protein was detected only as the 84 kDa form which was the highest in MCF-10A while the 66 kDa was not secreted in any cells, in contrast to cell lysates which could suggest the degradation of this form due to its instability (figure 5.14).

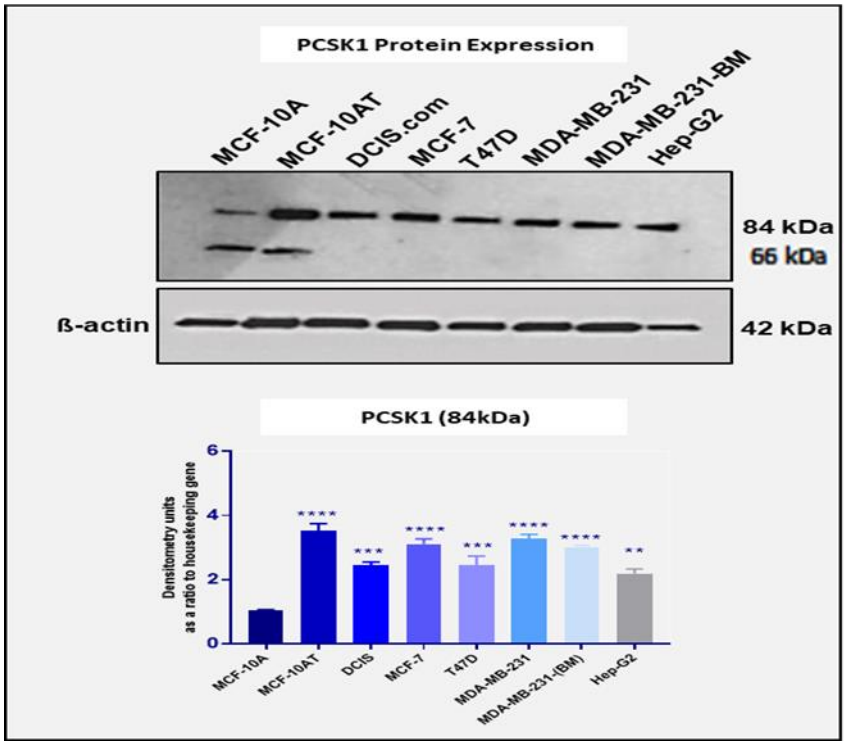

Figure 5.13: PCSK1 protein expression in normal breast and cancer cell-lines as determined by Western blot. Cell lysates were separated on a 10% SDS-PAGE gel, and then blotted onto PVDF and probed with the anti-PCSK1 antibody. Hep-G2 was used as a positive control for PCSK1 expression. To confirm that the amount of protein in each lane was equal, the membrane was stripped and re-probed with anti-β-actin housekeeping protein as a loading control. Densitometry analysis was performed for all cells using ImageJ software to assess relative band densities. Data is represented as the mean+/- SD of three independent experiments. Data was analysed statistically by one-way ANOVA with post hoc Dunnett's multiple comparisons. The P values were generated and ** represent P=0013, *** represent P=0.0002 and **** represents P<0.0001 compared to MCF-10A. The sizes of molecular weight markers are indicated in kDa. Representative immunoblot shown of n=3.

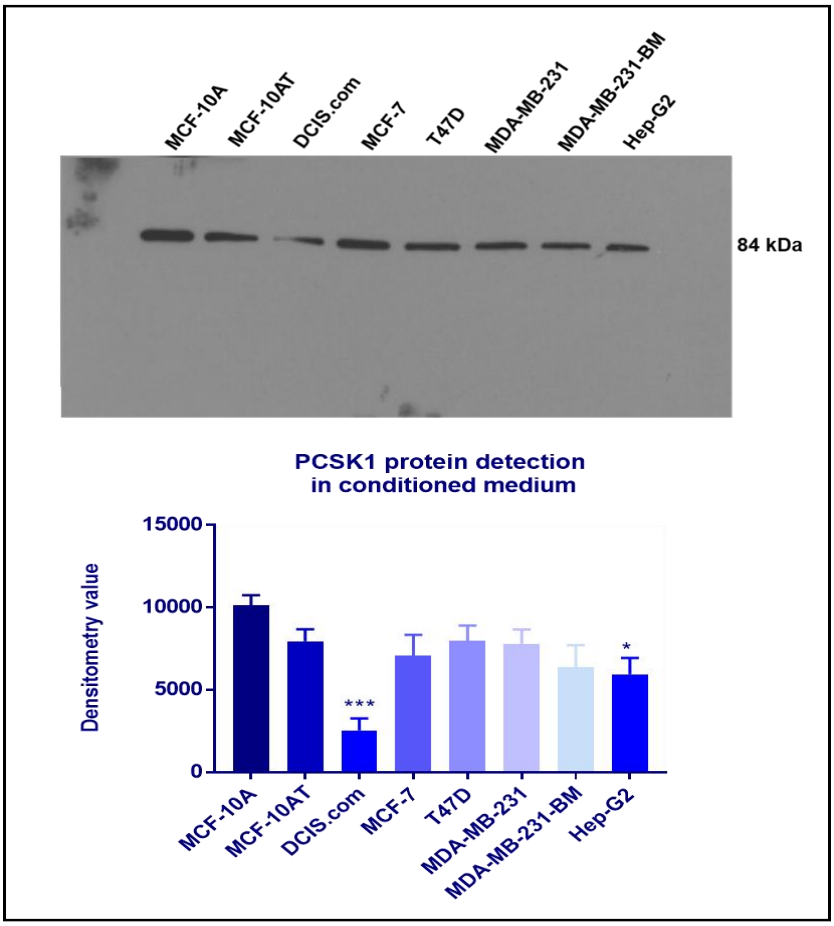

Figure 5.14: PCSK1 protein detection in conditioned medium of normal breast and cancer cell-lines as determined by Western blot. Cells were seeded and starved for 24 hours and conditioned medium was generated to be collected and separated on a 10% SDS-PAGE gel, and then blotted onto PVDF and probed with the anti-PCSK1 antibody. Hep-G2 lysate was used as a positive control for PCSK1 expression. Densitometry analysis was performed for all cells using ImageJ software to assess band densities and presented as densitometry value. Data are the mean ± SD of three independent experiments. Data was analysed statistically by ordinary one-way ANOVA followed by a post hoc Dunnett's test (* represent P= 0.0368 and *** represent P= 0.0003 in comparison to normal MCF-10A cells). Representative immunoblot shown of n=3.

5.3.12 PCSK2 protein expression in normal breast and cancer cell-lines and conditioned medium

Again, Western blot analysis was performed on all cell line lysates and conditioned medium to establish whether mRNA expression translated into protein expression. HepG2 was used as a positive control as it has previously been shown to express PCSK2 (R & D system).

All cell lines expressed PCSK2 protein at 71 kDa which is the inactive form of this protein (Tzimas et al., 2005). T47D cells showed a significant low expression of PCSK2 compared to MCF-10A ($P<0.0001$, Dunnett's test) (Figure 5.15). Interestingly additional bands were observed in MCF-7, T47D and Hep-G2 at a higher molecular weight, 100 kDa, which is likely to be the pro-form of PCSK2. A faint band was detected at 68 kDa only in MCF-7 and previous studies have suggested that this is the active form (Mbikay et al., 1997, Tzimas et al., 2005). If this is the only active form of the protein, this expression pattern does not match that of SEMA3B cleavage and it is unlikely that this protein is responsible for that cleavage.

In conditioned medium, the PCSK2 protein was detected only as the 71 kDa form but these bands appeared very faint in MCF-7, T47D, MDA-MB-231 and MDA-MB-231-BM and almost not secreted by the other cell lines (figure 5.16).

.

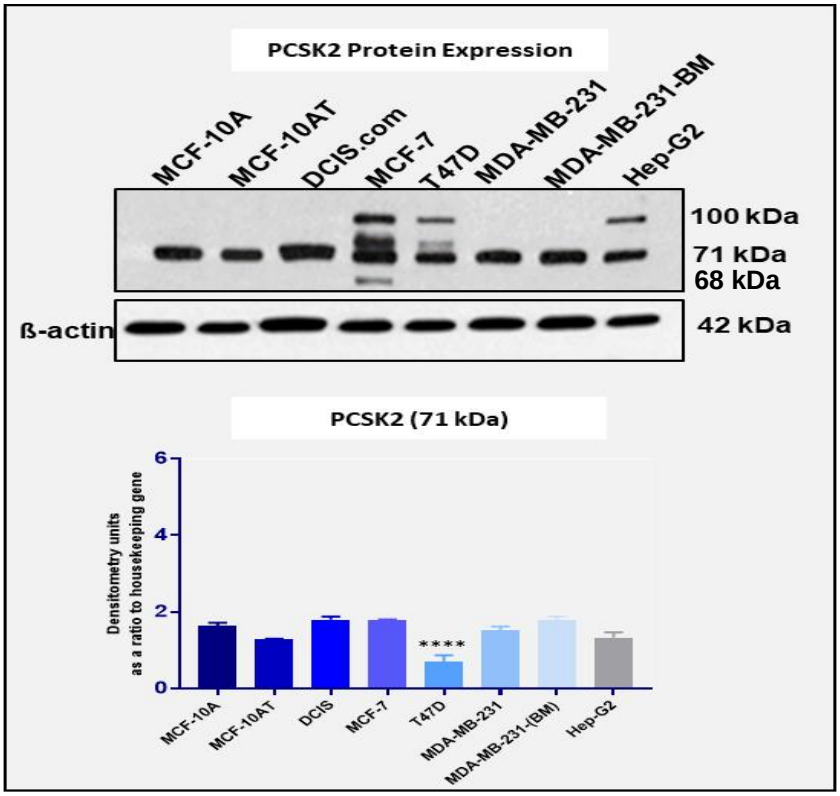

Figure 5.15: PCSK2 protein expression in normal breast and cancer cell-lines as determined by Western blot. Cell lysates were separated on a 10% SDS-PAGE gel, and then blotted onto PVDF and probed with the anti-PCSK2 antibody. Hep-G2 was used as a positive control for PCSK2 expression. To confirm that the amount of protein in each lane was equal, the membrane was stripped and re-probed with anti-β-actin housekeeping protein as a loading control. Densitometry analysis was performed for all cells using ImageJ software to assess relative band densities. Data is represented as the mean+/- SD of three independent experiments. Data was analysed statistically by one-way ANOVA with post hoc Dunnett's multiple comparisons. The P-value was generated and **** represent P<0.0001 compared to MCF-10A. The sizes of molecular weight markers are indicated in kDa. Representative immunoblot shown of n=3.

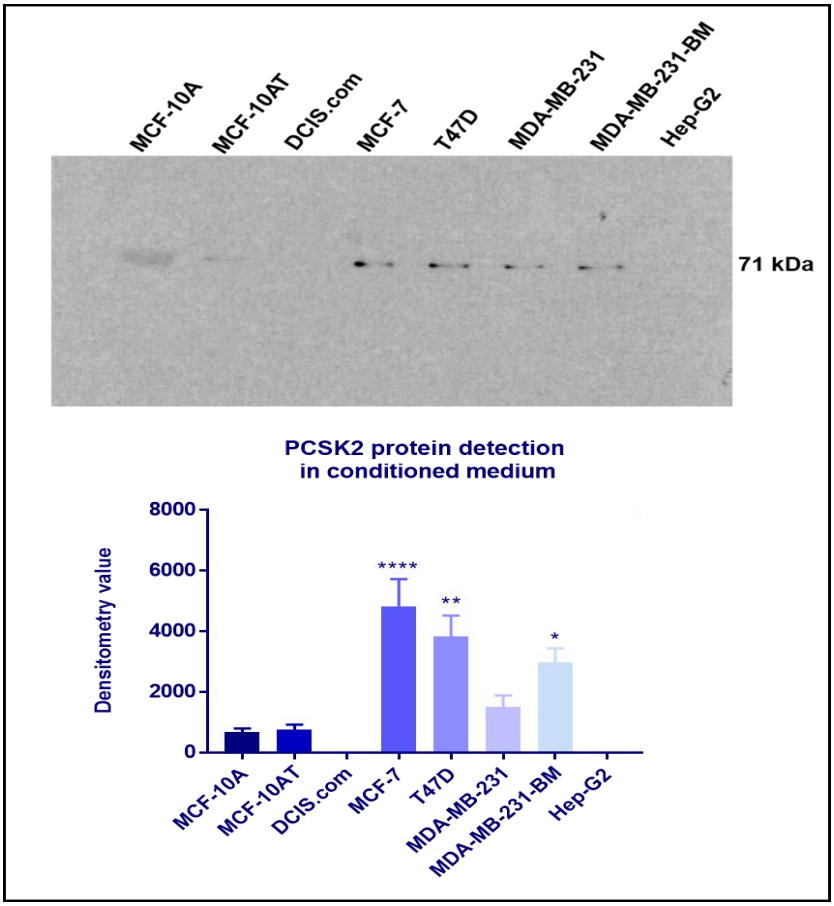

Figure 5.16: PCSK2 protein detection in conditioned medium of normal breast and cancer cell-lines as determined by Western blot. Cells were seeded and starved for 24 hours and conditioned medium was generated to be collected and separated on a 10% SDS-PAGE gel, and then blotted onto PVDF and probed with the anti-PCSK2 antibody. Hep-G2 lysate was used as a positive control for PCSK2 expression. Densitometry analysis was performed for all cells using ImageJ software to assess band densities and presented as densitometry value. Data are the mean ± SD of three independent experiments. Data was analysed statistically by ordinary one-way ANOVA followed by a post hoc Dunnett's test (* represent P= 0.0150, ** represent P=0.0010 and **** represent P<0.0001 in comparison to normal MCF-10A cells). Representative immunoblot shown of n=3.

5.3.13 PCSK4 protein expression in normal breast and cancer cell-lines and conditioned medium

This experiment was carried out to detect PCSK4 protein expression and was determined by Western blotting on the same breast cancer cell extracts and conditioned medium as described in 2.10. Ovarian cell lysates were used as a positive control for PCSK4 as its expression has previously been identified in these cells (Gyamera-Acheampong and Mbikay, 2009).

PCSK4 has two isoforms, which are found at 82 kDa and 26 kDa (Basak et al., 2008) and as shown in figure 5.17, in cell lysates, only the 26 kDa isoform was detected in these experiments. MCF-10A, MCF-10AT, MCF-7 and T47D cells expressed similar levels of PCSK4 26 kDa protein to the positive control, with DCIS ($P=0.0004$, Dunnett's test) and MDA-MB-231 cells ($P=0.0324$, Dunnett's) expressing significantly less protein than the MCF-10A cells. MDA-MB-231-BM cells did not express the PCSK4 protein in any experiment as shown by an absence of band.

In conditioned medium, the PCSK4 was faintly secreted only by DCIS.com at 26 kDa with no secretion detected in other cells (figure 5.18). To our knowledge, this is the first study that has identified the expression of PCSK4 in a different spectrum of breast normal and cancer cell lines.

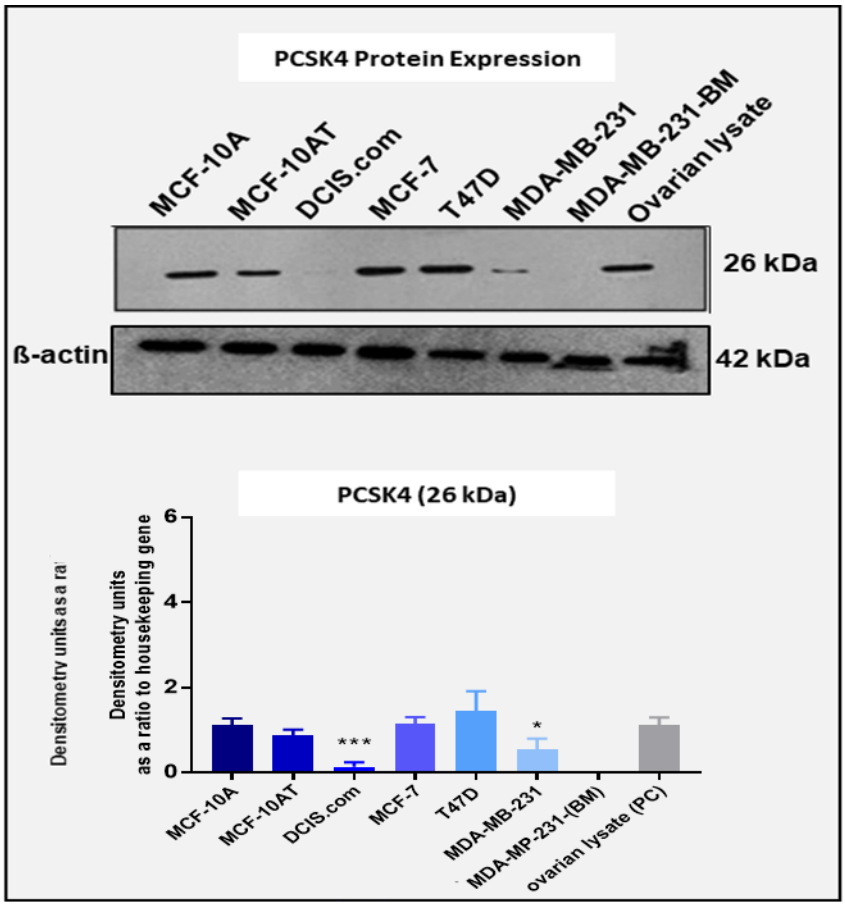

Figure 5.17: PCSK4 protein expression in normal breast and cancer cell-lines as determined by Western blot. Cell lysates were separated on a 10% SDS-PAGE gel, and then blotted onto PVDF and probed with the anti-PCSK4 antibody. Ovarian lysate was used as a positive control for PCSK4 expression. To confirm that the amount of protein in each lane was equal, the membrane was stripped and re-probed with anti-β-actin housekeeping protein as a loading control. Densitometry analysis was performed for all cells using ImageJ software to assess relative band densities. Data is represented as the mean+/- SD of three independent experiments. Data was analysed statistically by one-way ANOVA with post hoc Dunnett's multiple comparisons. The P-value was generated and* represent P=0.0324 and **** represent P=0.0001 compared to MCF-10A. The sizes of molecular weight markers are indicated in kDa. Representative immunoblot shown of n=3.

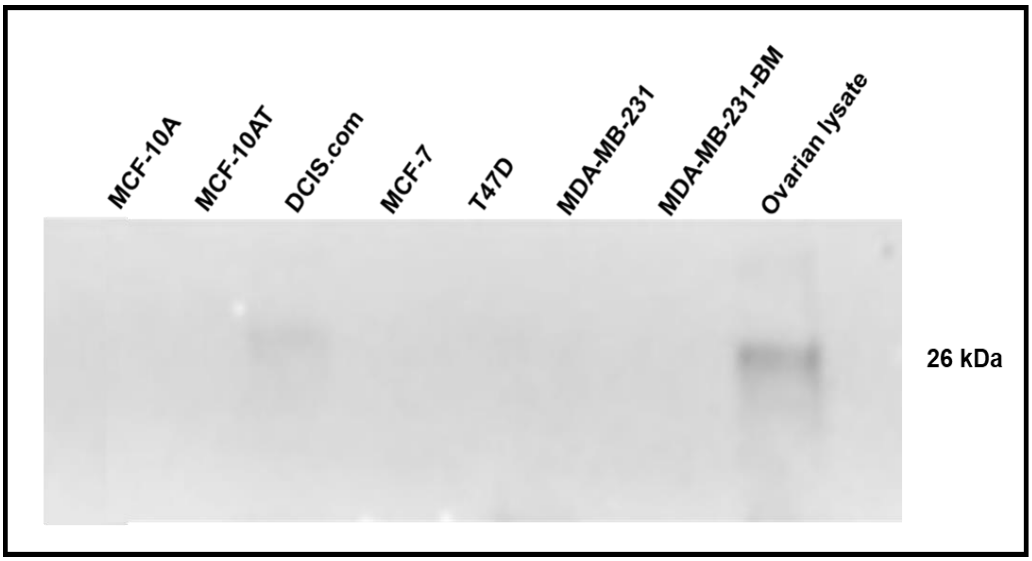

Figure 5.18: PCSK4 protein detection in conditioned medium of normal breast and cancer cell-lines as determined by Western blot. Cells were seeded and starved for 24 hours and conditioned medium was generated to be collected and separated on a 10% SDS-PAGE gel, and then blotted onto PVDF and probed with the anti-PCSK4 antibody. Ovarian lysate was used as a positive control for PCSK4 expression. The sizes of molecular weight markers are indicated in kDa. Representative immunoblot shown of n=3.

5.3.14 PCSK5 protein expression in normal breast and cancer cell-lines and conditioned medium

Western blot was carried out to assess the expression of PCSK5 as we did with other PPC family members, however; it was not possible to detect the protein expression by Western blot for this protein, despite changing protocol and antibodies. Therefore, the protein expression in cells was assessed by cytospin technique to establish whether or not PCSK5 protein is expressed in breast cells. The data from these experiments are shown later (5.25).

5.3.15 PCSK6 protein expression in normal breast and cancer cell-lines and secretion in conditioned medium

Previous studies have shown that PCSK6 is associated with the progression of breast cancer and we demonstrated mRNA expression in all the breast cell lines detected. Therefore, the protein expression of PCSK6 was assessed by Western blot as described in 2.10. HepG2 cell lysates were used as a positive control for PCSK6 as its expression has previously been identified in these cells (Couture et al., 2015). As shown in figure 5.19, in cell lysates, little or no protein was detected in most of the cell lines, with protein expression detected in MCF-10A, MCF-10AT, DCIS.com and MDA-MB-231-BM cells. This is in contrast to the gene expression data where PCSK6 mRNA was identified in all these cells. T47D cells had the highest expression of PCSK6 protein, with very low expression detected in MCF-7 and MDA-MB-231 cells.

In conditioned medium, no protein was secreted in the conditioned medium of MCF-10A, MCF-10AT and DCIS.com. However, T47D had the most secretion of PCSK6 while in MDA-MB-231 and MCF-7 only faint bands were detected (figure 5.20). These data do not mirror the cleavage of SEMA3B suggesting that this protein is less likely to be involved.

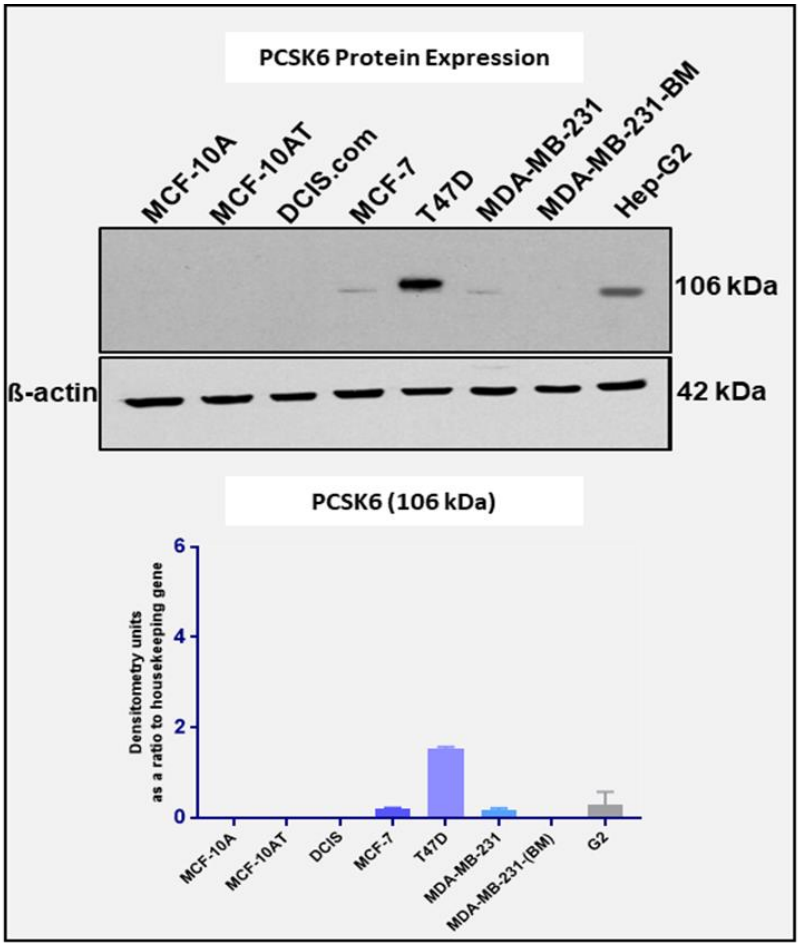

Figure 5.19: PCSK6 protein expression in normal breast and cancer cell-lines as determined by Western blot. Cell lysates were separated on a 10% SDS-PAGE gel, and then blotted onto PVDF and probed with the anti-PCSK6 antibody. HepG2 lysate was used as a positive control for PCSK6 expression. To confirm that the amount of protein in each lane was equal, the membrane was stripped and re-probed with anti-β-actin housekeeping protein as a loading control. Densitometry analysis was performed for all cells using ImageJ software to assess relative band densities. Data is represented as the mean+/- SD of three independent experiments. Data was analysed statistically by one-way ANOVA. The sizes of molecular weight markers are indicated in kDa. Representative immunoblot shown of n=3.

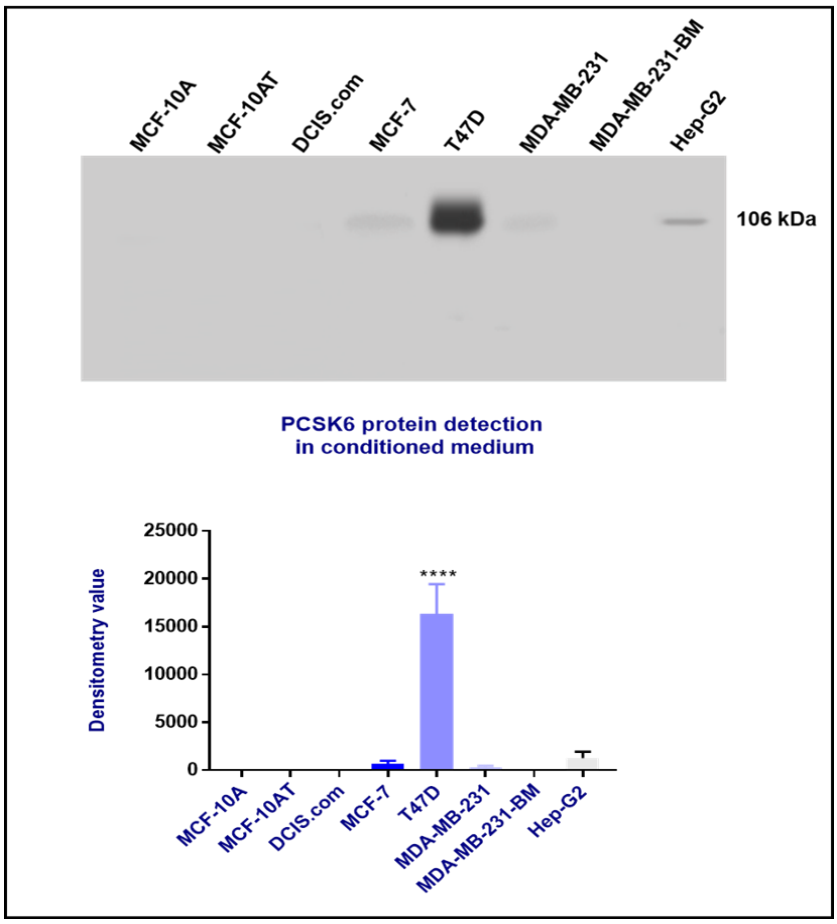

Figure 5.20: PCSK6 protein detection in conditioned medium of normal breast and cancer cell-lines as determined by Western blot. Cells were seeded and starved for 24 hours and conditioned medium was generated to be collected and separated on a 10% SDS-PAGE gel, and then blotted onto PVDF and probed with the anti-PCSK6 antibody. Hep-G2 lysate was used as a positive control for PCSK6 expression. Densitometry analysis was performed for all cells using ImageJ software to assess band densities and presented as densitometry value. Data are the mean ± SD of three independent experiments. Data was analysed statistically by ordinary one-way ANOVA followed by a post hoc Dunnett's test (**** represent $P<0.0001$ in comparison to normal MCF-10A cells). Representative immunoblot shown of n=3.

5.3.16 PCSK7 protein expression in normal breast cancer cell-lines and conditioned medium

To evaluate the protein expression of PCSK7 in the cell lines, Western blot was carried out as described in 2.10. HepG2 cell lysates were used as a positive control for PCSK7 as its expression has previously been identified in these cells (Mori et al., 1999).

As shown in figure 5.21, in cell lysates, two different molecular weight bands were detected in each lane. The higher molecular weight at 86 kDa represents the pro-form of PCSK7 (inactive), while the lower molecular weight 64 kDa represents the processed form of PCSK7 (active). The expression of the pro-form of PCSK7, 86 kDa, was largely unchanged across the sequence with no significant differences, with the exception of no expression being detected in T47D and only a very faint band detected in MDA-MB-231-BM. At the lower molecular weight 64 kDa, similar level of expression was observed in MCF-10A and MCF-10AT with a significantly increased expression of PCSK7 detected in DCIS.com ($P=0.0043$, Dunnett's test), MCF-7 ($P=0.0014$, Dunnett's test) and MDA-MB-231 ($P=0.0279$, Dunnett's test) compared to MCF-10A cells. However, there was no protein expression of PCSK7 detected in T47D and MDA-MB-231-BM cell lines at 64kDa. This lack of protein expression in T47D cells is in complete contrast to the mRNA data where T47D cells demonstrated the highest expression.

In conditioned medium experiment, we observed clear similarities between the malignant and non-malignant cells at 64 kDa with slightly high intensity of bands seen in MDA-MB-231. However, no secretion of PCSK7 was detected in T47D in conditioned medium (figure 5.22).

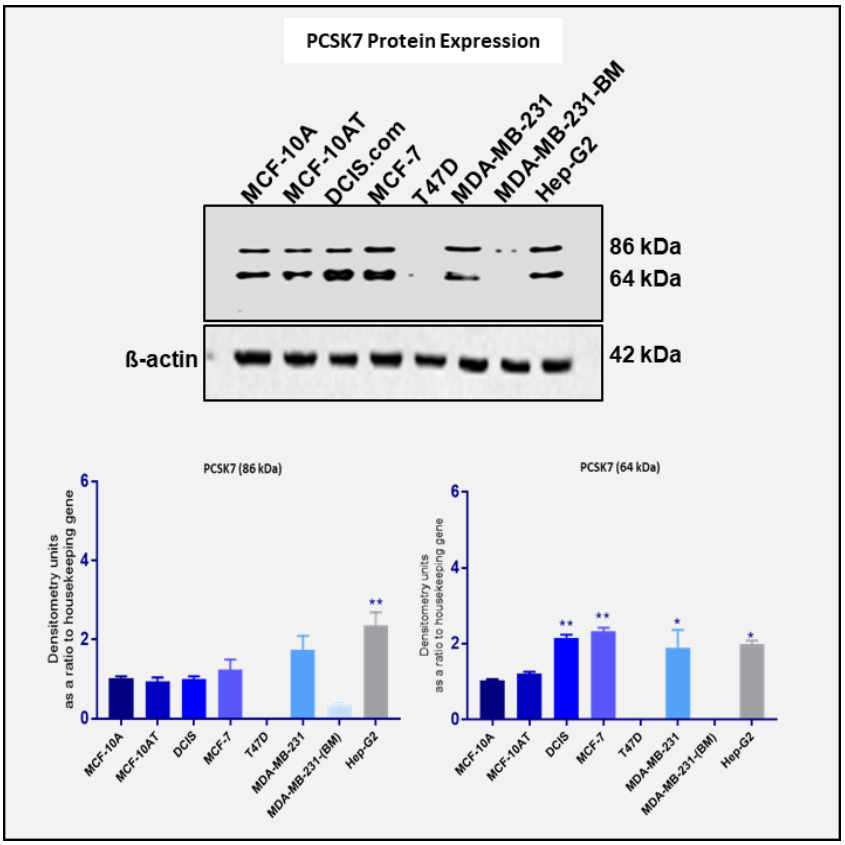

Figure 5.21: PCSK7 protein expression in normal breast and cancer cell-lines as determined by Western blot. Cell lysates were separated on a 10% SDS-PAGE gel, and then blotted onto PVDF and probed with the anti-PCSK7 antibody. HepG2 lysate was used as a positive control for PCSK7 expression. To confirm that the amount of protein in each lane was equal, the membrane was stripped and re-probed with anti-β-actin housekeeping protein as a loading control. Densitometry analysis was performed for all cells using ImageJ software to assess relative band densities. Data is represented as the mean+/- SD of three independent experiments. Data was analysed statistically by one-way ANOVA. The P-value was generated and * represents P=0.0279 and** represent P=0.0043 & P=0.0014 compared to MCF-10A cells. Representative immunoblot shown of n=3.

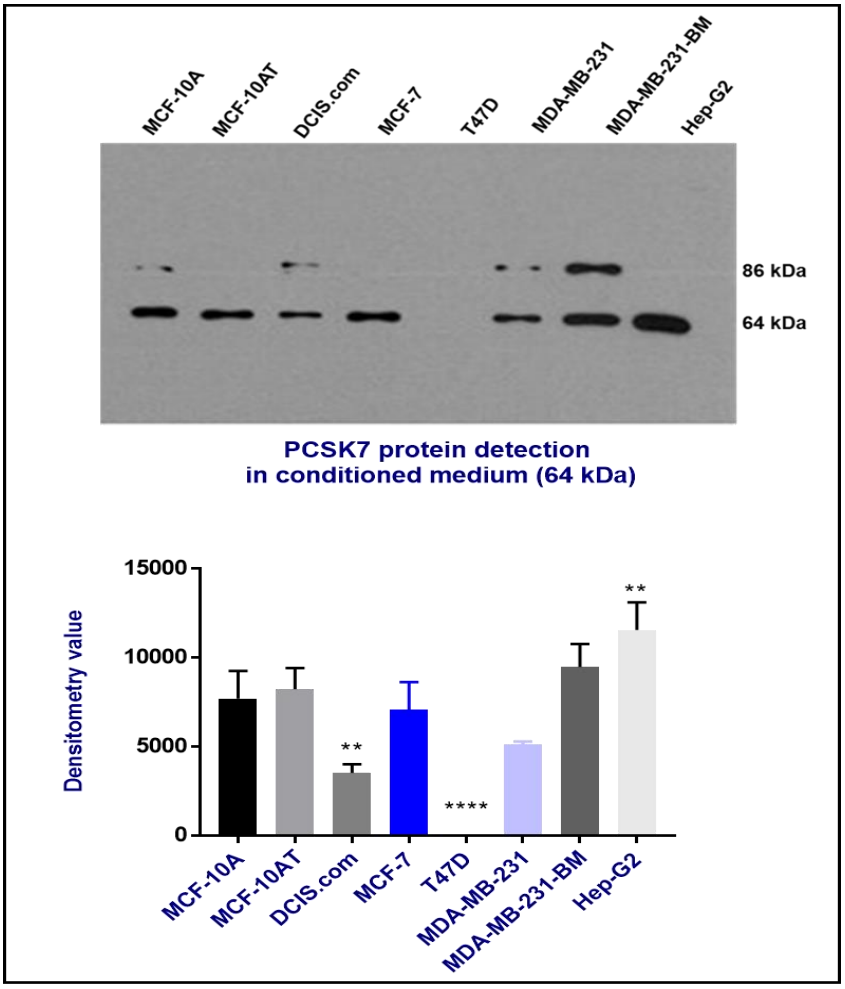

Figure 5.22: PCSK7 protein detection in conditioned medium of normal breast and cancer cell-lines as determined by Western blot. Cells were seeded and starved for 24 hours and conditioned medium was generated to be collected and separated on a 10% SDS-PAGE gel, and then blotted onto PVDF and probed with the anti-PCSK7 antibody. Hep-G2 lysate was used as a positive control for PCSK7 expression. Densitometry analysis was performed for all cells using ImageJ software to assess band densities and presented as densitometry value. Data are the mean ± SD of three independent experiments. Data was analysed statistically by ordinary one-way ANOVA followed by a post hoc Dunnett's test (** represent P=0.0081 and **** represent P<0.0001 in comparison to normal MCF-10A cells). Representative immunoblot shown of n=3.

5.3.17 PCSK8 protein expression in normal breast and cancer cell-lines

Again, Western blot of PCSK8 was carried out on all cell lines, but as with PCSK5, it was not possible to detect the protein in Western blots using the only antibodies available. This suggests that it is in part due to the quality of the antibodies. Therefore, the PCSK8 protein expression in cells was assessed by cytospin and by cell pelleting and subsequent staining, the results of which are described later in this chapter.

5.3.18 PCSK9 protein expression in normal breast and cancer cell-lines and conditioned medium

Finally, PCSK9 protein expression was investigated in all the cell lines and conditioned medium by Western blot as described in 2.10. HepG2 cell lysates were used as a positive control for PCSK9 as its expression has previously been identified in these cells (Dubuc et al., 2004). As shown in figure 5.23, there was a single band at 62 kDa (active form) (Glerup et al., 2017) seen in all breast cell lines with a slight increase in expression seen with increasing malignancy of the cell line achieving significance in comparison to MCF-10A cells, in T47D ($P=0.0028$, Dunnett's test), MDA-MB-231 ($P=0.0471$, Dunnett's test) and MDA-MB-231-BM cells ($P=0.0028$, Dunnett's test). However, the protein level of PCSK9 did not reflect the gene expression levels as the gene expression was highest in MCF-10A, MCF-10AT and MDA-MB-231 cells.

In conditioned medium results revealed that PCSK9 existed in the conditioned medium of MCF-7, T47D, MDA-MB-231 and MDA-MB-231-BM. Moreover, there were faint bands detected in both MCF-10AT and DCIS.com. However, the expression of PCSK9 in the conditioned medium was lower than that in the cell lysate, possibly because of the processing before secretion (figure 5.24). The PCSK9 in conditioned medium of MCF-10A was not detected. These results could suggest the possible role of PCSK9 in SEMA3B cleavage.

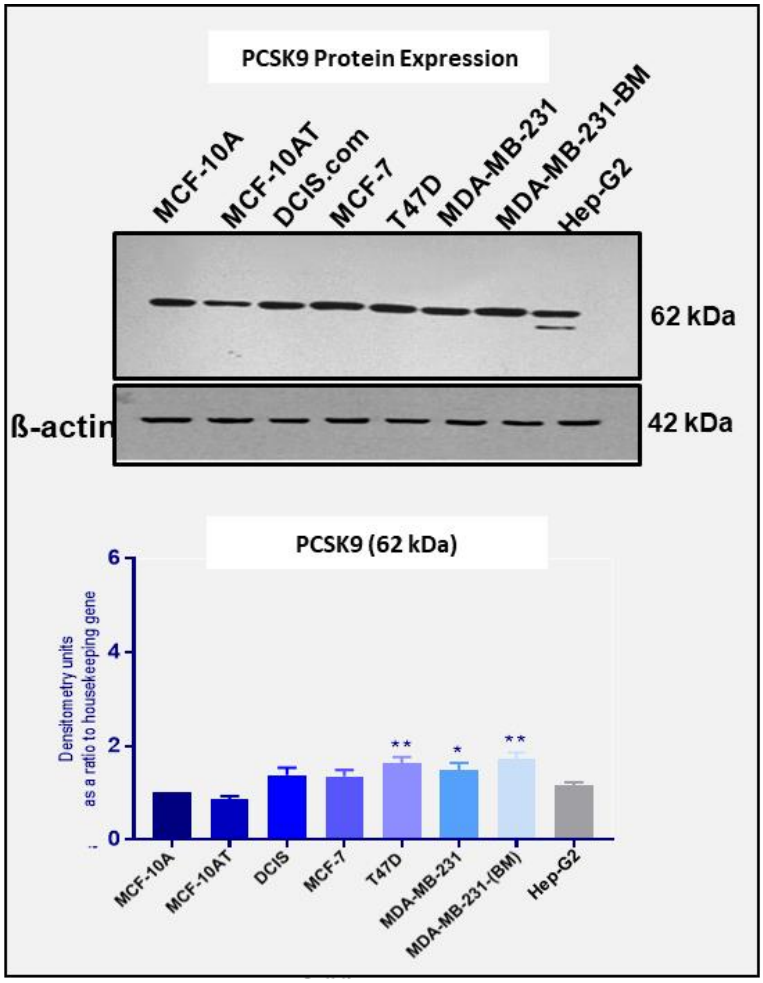

Figure 5.23: PCSK9 protein expression in normal breast and cancer cell-lines as determined by Western blot. Cell lysates were separated on a 10% SDS-PAGE gel, and then blotted onto PVDF and probed with the anti-PCSK9 antibody. HepG2 lysate was used as a positive control for PCSK9 expression. To confirm that the amount of protein in each lane was equal, the membrane was stripped and re-probed with anti-β-actin housekeeping protein as a loading control. Densitometry analysis was performed for all cells using ImageJ software to assess relative band densities. Data is represented as the mean+/- SD of three independent experiments. Data was analysed statistically by one-way ANOVA followed by Dunnett's test. The P-value was generated and * represents P=0.0471 and ** represent P=0.0028 compared to MCF-10A cells. The sizes of molecular weight markers are indicated in kDa. Representative immunoblot shown of n=3.

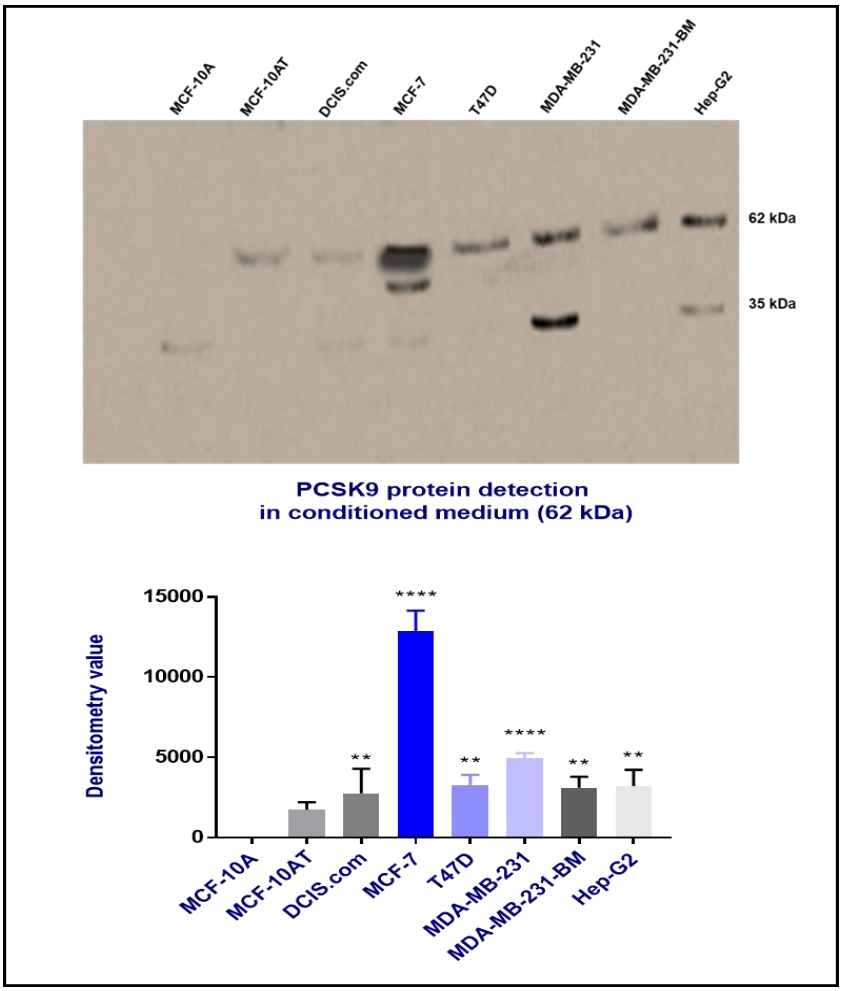

Figure 5.24: PCSK9 protein detection in conditioned medium of normal breast epithelial and cancer cell-lines as determined by Western blot. Cells were seeded and starved for 24 hours and conditioned medium was generated to be collected and separated on a 10% SDS-PAGE gel, and then blotted onto PVDF and probed with the anti-PCSK9 antibody. Hep-G2 lysate was used as a positive control for PCSK9 expression. Densitometry analysis was performed for all cells using ImageJ software to assess band densities and presented as densitometry value. Data are the mean ± SD of three independent experiments. Data was analysed statistically by ordinary one-way ANOVA followed by a post hoc Dunnett's test (** represent P=0.0021 and **** represent P<0.0001 in comparison to normal MCF-10A cells). The sizes of molecular weight markers are indicated in kDa. Representative immunoblot shown of n=3.

5.3.19 Measurement of protein expression of all PPCs in cell-lines using cytospin technique

As it was not possible to detect some of the pro-protein convertases by Western blotting, the cytospin technique was performed to study protein expression by concentrating the cells into a small area and doing immunocytochemistry as described in 2.12. Heamatoxylin was used to stain the nucleus and analysis was performed by assessing intensity of brown stain in the cells.

As shown in 5.25 and 5.26, brown stain indicating the presence of PPCs were seen in nearly all cell lines for nearly all proteins. However, again, in agreement with the Western blots, it was not possible to detect PCSK8 in any cell line under any condition using this technique. MCF-10A showed weak expression of PCSK1, PCSK2, PCSK4, PCSK5, PCSK7 and moderate expression of furin, PCSK6 and PCSK9. The pre-malignant MCF-10AT showed moderate expression of PCSK1, PCSK2, furin, and PCSK4, and there was a strong expression of PCSK5, PCSK6, PCSK7, and PCSK9 in these cells. The pre-invasive DCIS.com cells showed only a moderate expression of PCSK1 while all other PPCs were strongly expressed in these cells. In invasive cells, MCF-7 had moderate expression of PCSK1, furin, PCSK4, PCSK6, PCSK7 and a strong expression of PCSK2, PCSK5 and PCSK9. T47D cells had moderate expression of all PPCs except for PCSK9, which was strongly expressed. MDA-MB-231 cells showed a strong expression of all PPCs in these cells with no obvious differences between them. MDA-MB-231-BM cells showed similar expression of PPCs to those found in MDA-MB-231 cells, with the exception of a lower level of PCSK4. Taken together these data suggest that PCSK1, PCSK2, PCSK4, PCSK5 and PCSK7 show the pattern of low expression in MCF-10A and higher expression in all other cell lines that match with reduced SEMA3B cleavage in MCF-10A cells and full cleavage in all other cell-lines.

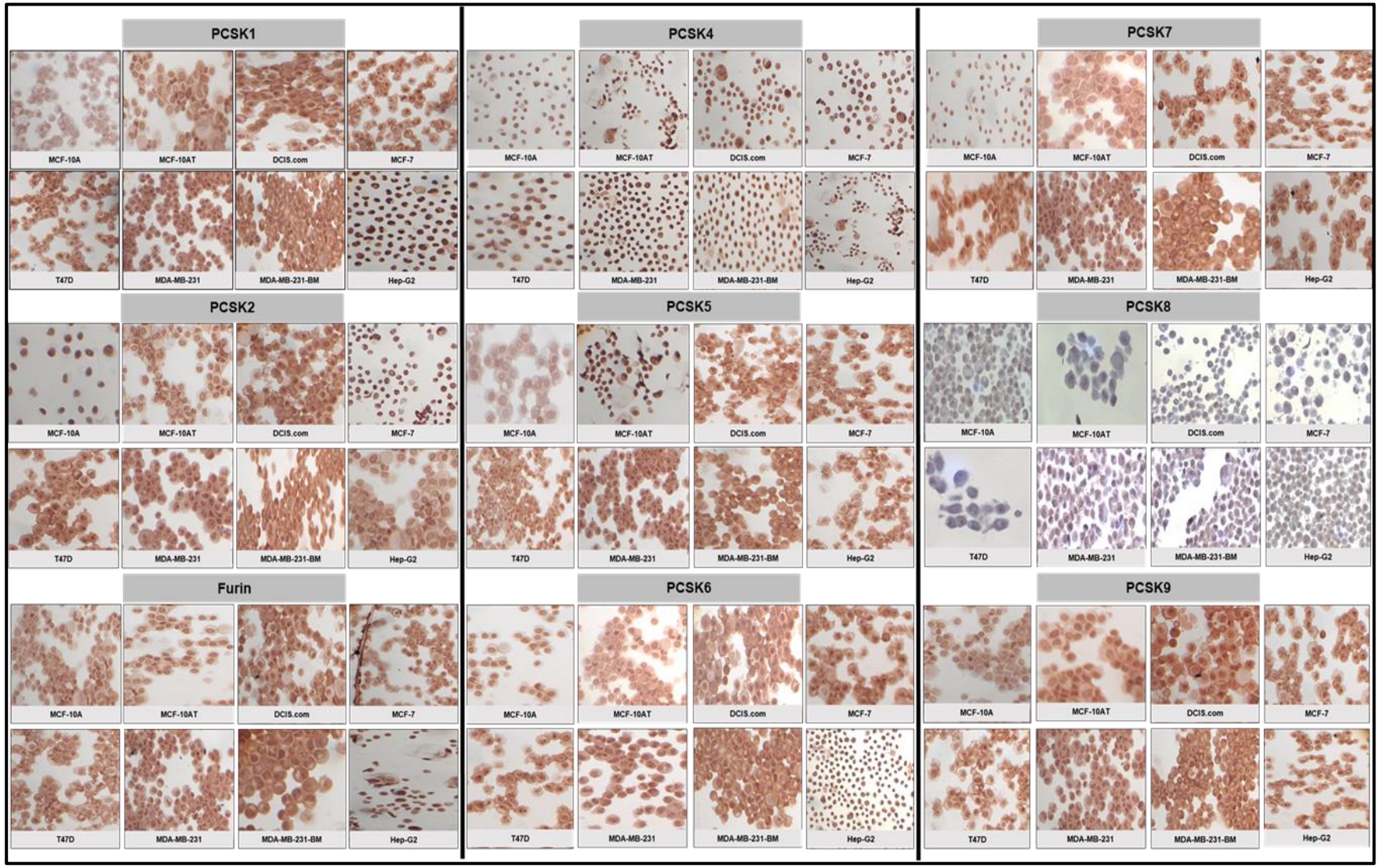

Figure 5.25: Expression of PPC family as determined by cytospin and immunocytochemistry. Representative images of cytospin preparations stained using immunocytochemistry with anti-furin, anti-PCSK1, anti-PCSK2, anti-PCSK4, anti-PCSK5, anti-PCSK6, anti-PCSK7, anti-PCSK8 and anti-PCSK9 antibodies counterstained with Gill's haematoxylin. Scale bar =500 px**.**

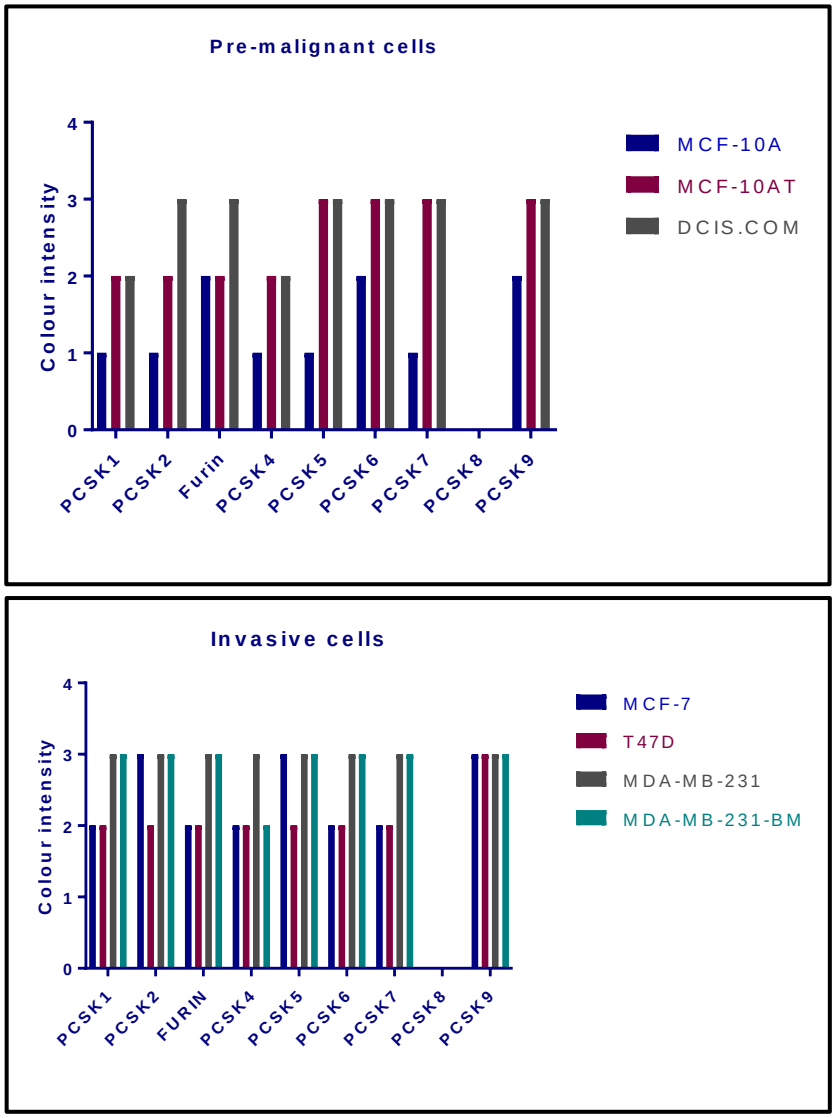

Figure 5.26: Representative cytospin analysis of PPCs in all cell-lines. The images were scored for the intensity of stain and represented graphically**.**

5.3.20 Protein expression using cell pellet in cell-lines

PCSK8 was not detected in either Western blots or using the cytospin technique. As the antibody data sheet stated that it could be used for immunohistochemistry, the protein expression of PCSK8 in the cell lines was investigated by a different technique called cell pelleting as described in 5.2.4. The cell pellets were fixed and processed to wax and immunohistochemistry was used to determine PCSK8 expression. As shown in figure 5.27, strong expression of PCSK8 was seen in all cell lines suggesting that this protein is expressed in breast tumour and non-tumour cells in similar levels. All the cells showed good contrast and the dye stained almost all cells cytoplasm and membrane with the slightly different colour intensity found in MCF-10A cells. This data suggests the presence of PCSK8 protein in all cells used.

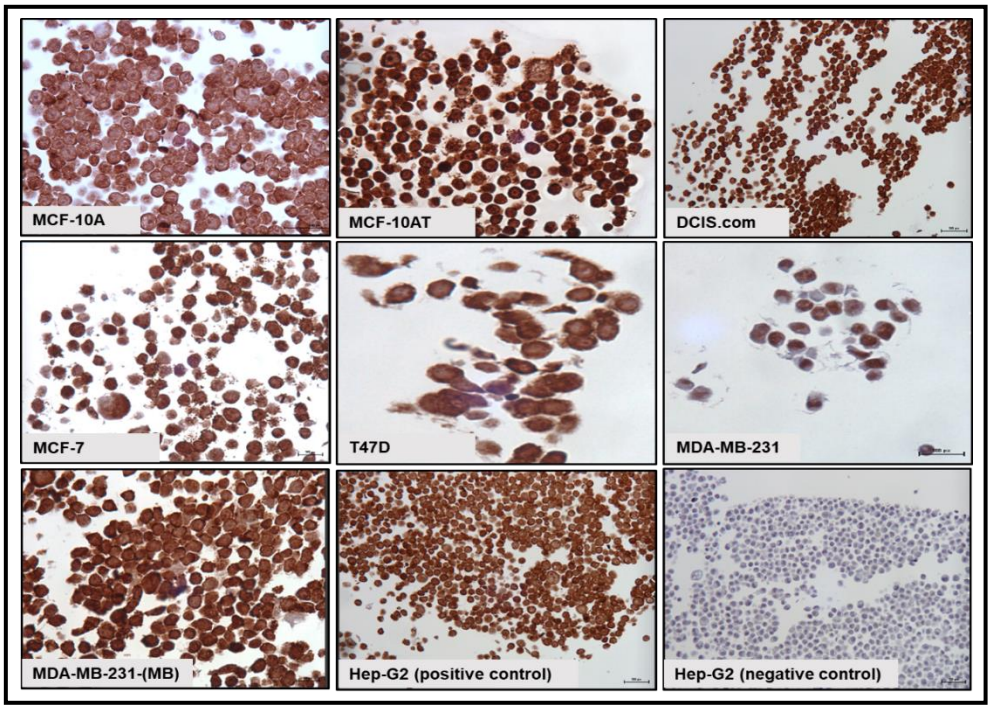

Figure 5.27: Representative images of breast normal and cancer cells processed by cell pellet technique. Cells were trypsinized, and the cell pellet collected and solidified by adding the molten agarose to be placed into a cassette for processing. The cells were probed by the PCSK8 antibody (1:50), and counterstained with haematoxylin. The scale bar = 500px

5.3.21 Assessment of pro-protein convertases protein expression in human breast tissue

In order to investigate whether the pro-protein convertases are expressed in human breast tissues of similar morphology to the cell lines, and whether the pattern of expression seen in cell lines matches those seen in human tissues of breast disease, immunohistochemical staining was performed on tissues representing different breast cancer stages as described 2.11. Each tissue microarray slide was stained for different pro-protein convertases and scored to assess the intensity of staining as described in 2.11.2. The data were analysed by correlation with SEMA3B and with disease progression.

Furin expression has not been previously investigated at a protein level in breast cancer. As shown in figure 5.28, a moderate to strong cytoplasmic expression of furin was seen in 63% of normal tissues, 56% of atypical ductal hyperplasia (ADH) and 50% of ductal carcinoma *in situ* (DCIS), and this expression was decreased with increasing severity to invasive cancer tissue where 33% of the samples had moderate to high expression. Stats data obtained from the staining intensity analysis using spearman's non-parametric correlation showed that there was a weak positive correlation between SEMA3B and furin expression (Spearman's rho= 0.290, P= 0.015) and significant inverse relationship with disease progression (Spearman's rho= -0.292, P= 0.01).

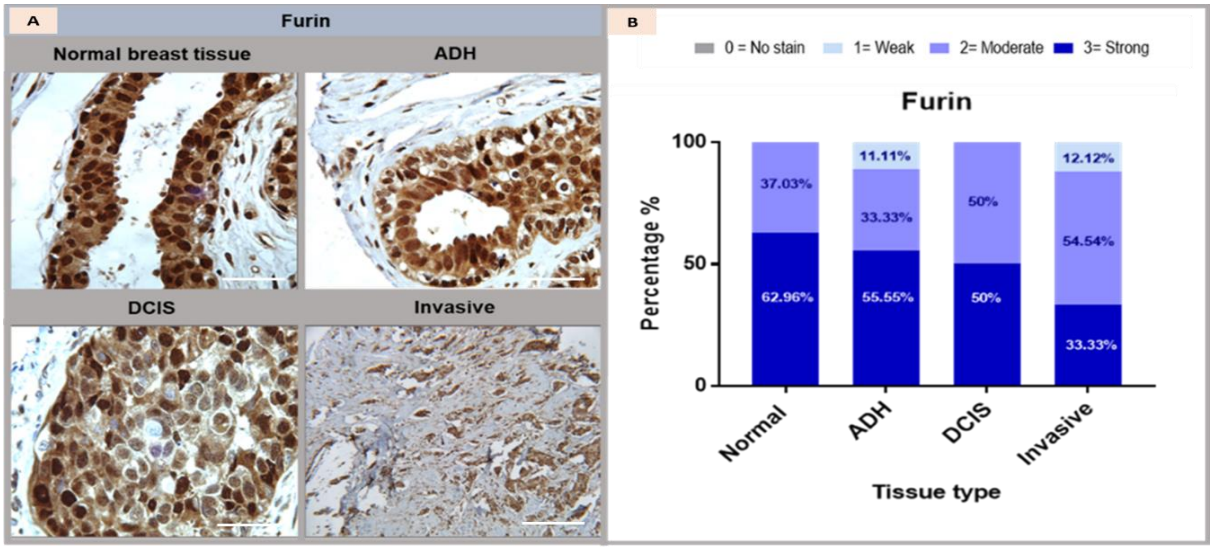

Figure 5.28: Expression of furin in breast tissue lesions. A) Representative photographs of furin staining by immunohistochemistry in normal breast ducts (normal), atypical ductal hyperplasia (ADH), DCIS and invasive cancer tissues (invasive). All images were taken using a x20 objective lens and the scale bar = 100 µm. **B)** Each sample was scored for intensity of stain and presented graphically as the percentage of cases with each expression intensity.

Cytoplasmic expression of **PCSK1** seen in 64% of normal tissues, and increasing to 89% in ADH and 100% in DCIS tissues. In invasive tissue, the strongest expression was decreased to 54.54% (figure 5.29) Like in furin, there was a positive correlation between SEMA3B and PCSK1 expression (Spearman's rho = 0.348, P=0.003), but no significant correlation between PCSK1 and disease progression (increasing malignancy).

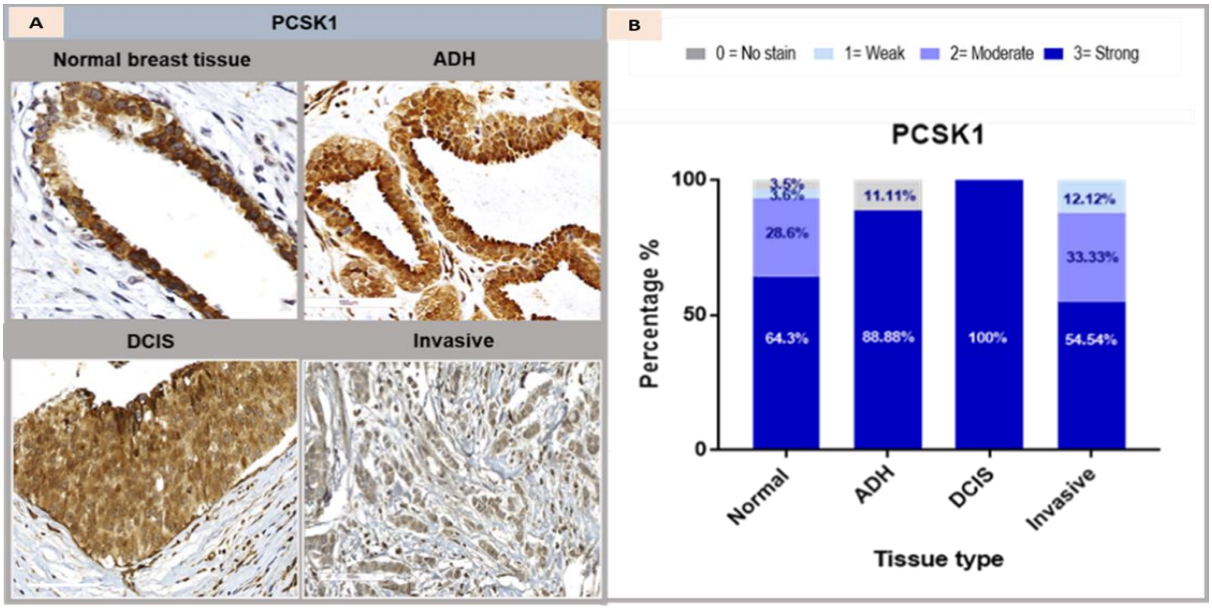

Figure 5.29: Expression of PCSK1 in breast tissue lesions. A) Representative photographs of PCSK1 staining by immunohistochemistry in normal breast ducts (normal), atypical ductal hyperplasia (ADH), DCIS and invasive cancer tissues (invasive). All images were taken using a x20 objective lens and the scale bar = 100 µm. **B)** Each sample was scored for intensity of stain and presented graphically as the percentage of cases with each expression intensity.

High levels of **PCSK2** expression were seen in pre-malignant and pre-invasive tissues with strong cytoplasmic staining in 71 % of the normal breast ducts, and increasing slightly to 78% in ADH and 87% in DICS. In contrast, the expression of PCSK2 decreased in invasive cancer sections so that only 42 % had strong staining. There was no significant relationship between PCSK2 and SEMA3B or with increasing lesion malignancy (figure 5.30). However, this is in agreement with the Western blotting findings but not with the gene expression result.

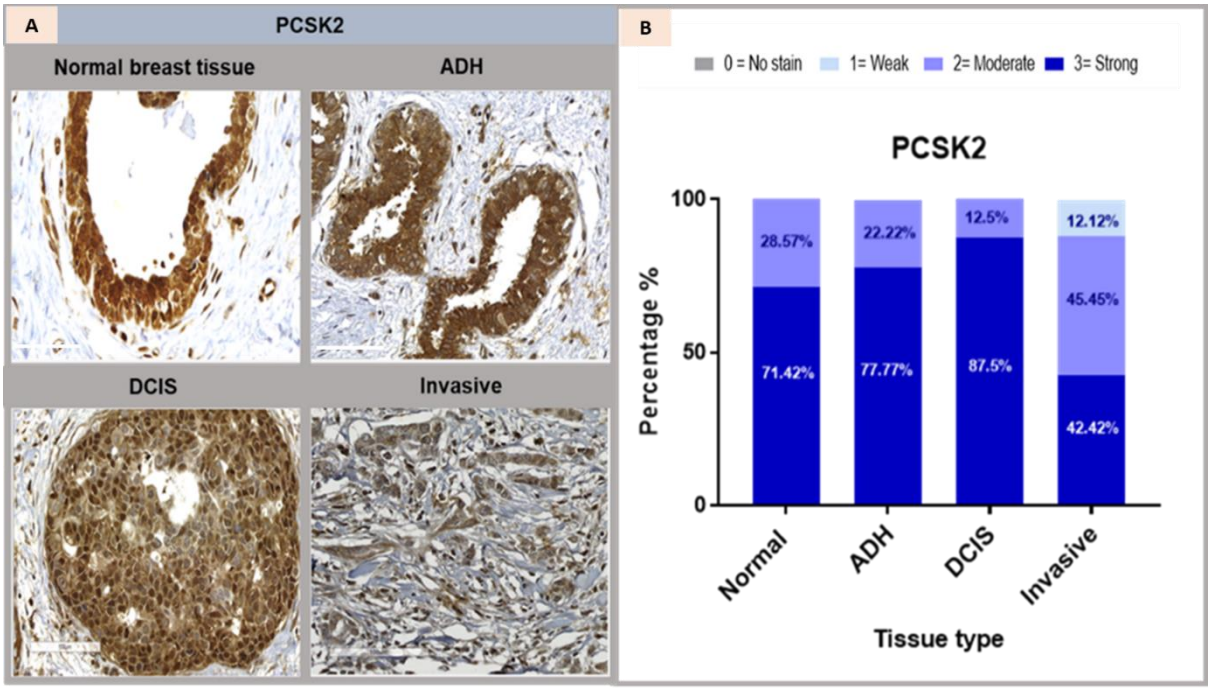

Figure 5.30: Expression of PCSK2 in breast tissue lesions. A) Representative photographs of PCSK2 staining by immunohistochemistry in normal breast ducts (normal), atypical ductal hyperplasia (ADH), DCIS and invasive cancer tissues (invasive). All images were taken using a x20 objective lens and the scale bar = 100 µm. **B)** Each sample was scored for intensity of stain and presented graphically as the percentage of cases with each expression intensity.

Strong cytoplasmic expressions of **PCSK4** was detected in 100% of normal tissues, 90% of ADH and 65.5% of DCIS, decreasing to 30% of invasive breast cancer tissues. Moreover, there was a positive correlation between SEMA3B and PCSK4 expression (Spearman's rho = 0.460, P=0.01), and a strong inverse correlation between PCSK4 and the class/lesion malignancy (Spearman's rho = -.657**, P=0.01) (figure 5.31).

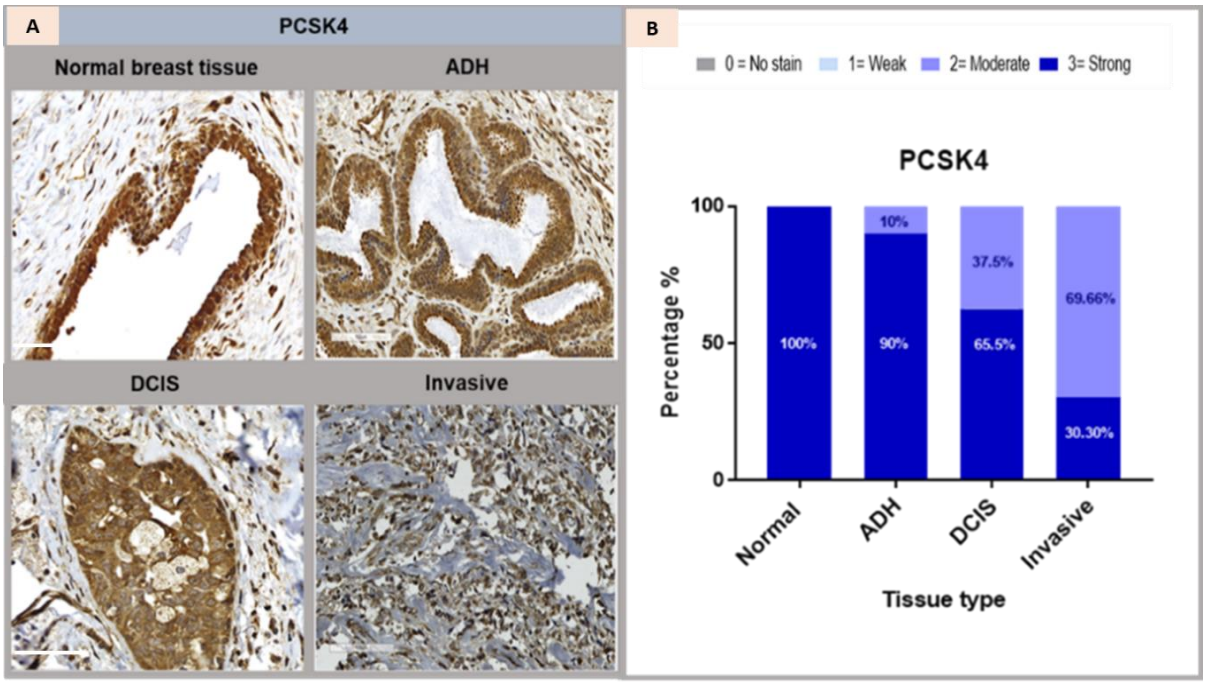

Figure 5.31: Expression of PCSK4 in breast tissue lesions. A) Representative photographs of PCSK4 staining by immunohistochemistry in normal breast ducts (normal), atypical ductal hyperplasia (ADH), DCIS and invasive cancer tissues (invasive). All images were taken using a x20 objective lens and the scale bar = 100 µm. **B)** Each sample was scored for intensity of stain and presented graphically as the percentage of cases with each expression intensity.

High levels of **PCSK5** expression were seen with intense cytoplasmic staining in 100% of the ducts of a normal breast, ADH and DCIS. In contrast, invasive carcinoma tissues had reduced expression of PCSK5 with 82% showing strong staining compared with the normal tissue. There was a weakly inversely correlation of PCSK5 with the class/lesion intensity (Spearman's rho = -.304**; P=0.008) (figure 5.32).

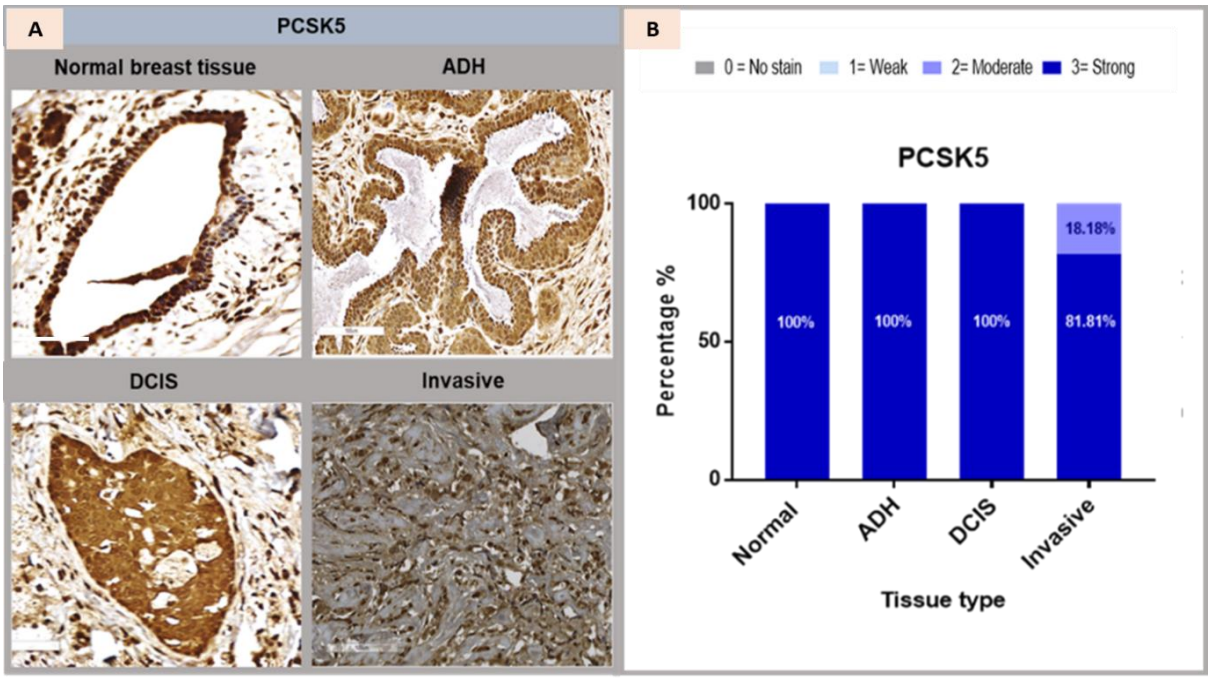

Figure 5.32: Expression of PCSK5 in breast tissue lesions. A) Representative photographs of PCSK5 staining by immunohistochemistry in normal breast ducts (normal), atypical ductal hyperplasia (ADH), DCIS and invasive cancer tissues (invasive). All images were taken using a x20 objective lens and the scale bar = 100 µm. **B)** Each sample was scored for intensity of stain and presented graphically as the percentage of cases with each expression intensity.

Strong cytoplasmic expression of **PCSK6** was detected in 73.91% of normal ductal tissues. This expression was decreased to 28.57% in ADH and 25% in DCIS. The expression of PCSK6 in invasive tissue was increased to 45.45% compared to ADH and DCIS; however, this was still lower than in normal tissues. It should be noted that the small sample size of both ADH and DCIS may account for some of these differences. There was no correlation between PCSK6 expression and SEMA3B or lesion class/malignancy (figure 5.33).

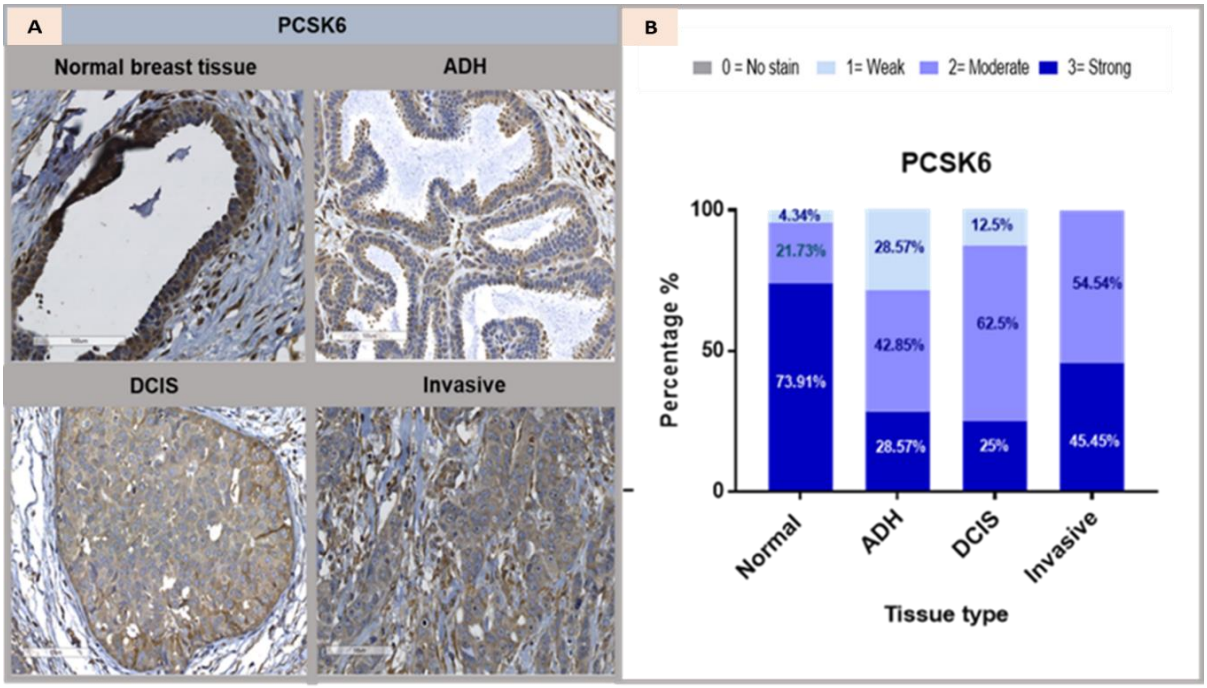

Figure 5.33: Expression of PCSK6 in breast tissue lesions. A) Representative photographs of PCSK6 staining by immunohistochemistry in normal breast ducts (normal), atypical ductal hyperplasia (ADH), DCIS and invasive cancer tissues (invasive). All images were taken using a x20 objective lens and the scale bar = 100 µm. **B)** Each sample was scored for intensity of stain and presented graphically as the percentage of cases with each expression intensity.

There was a strong expression of **PCSK7** in the cytoplasm of epithelial cells in of 54% normal breast ducts and this expression increased slightly to 67% in ADH, and 75% in DCIS, but was reduced down to 33% in invasive cancers (figure 5.34). This resulted in a positive correlation between PCSK7 and SEMA3B expression (Spearman's rho= 0.499, P=0.01), although there was no correlation seen with class/increasing lesion malignancy.

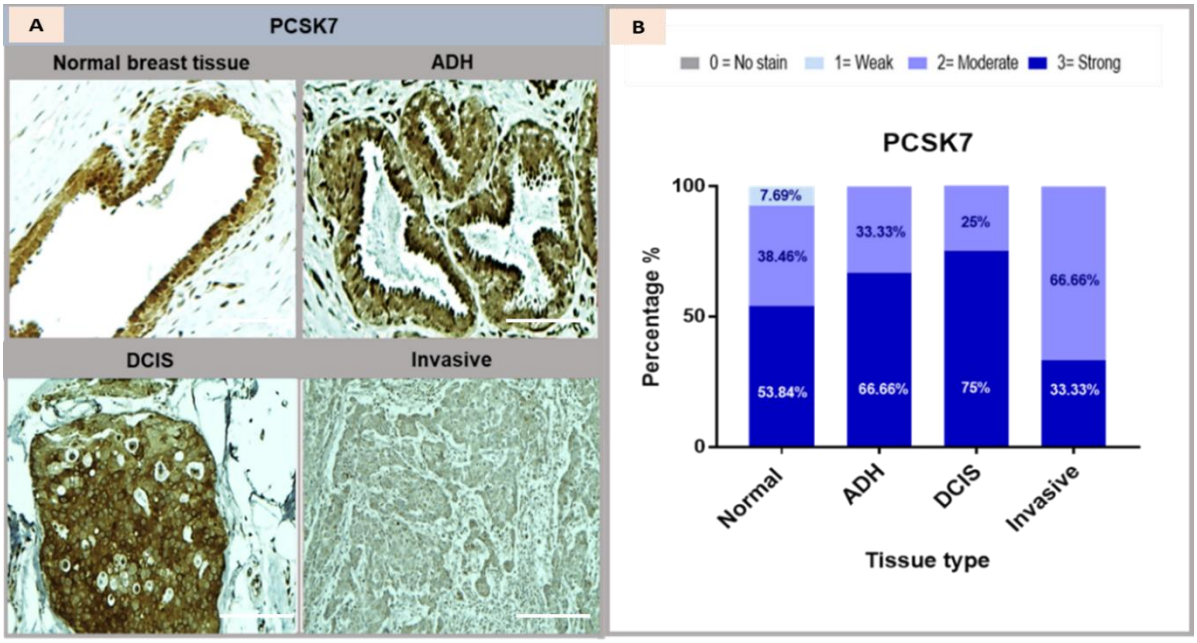

Figure 5.34: Expression of PCSK7 in breast tissue lesions. Representative photographs of PCSK7 staining by immunohistochemistry in normal breast ducts (normal), atypical ductal hyperplasia (ADH), DCIS and invasive cancer tissues (invasive). All images were taken using a x20 objective lens and the scale bar = 100 µm. Each sample was scored for intensity of stain and presented graphically as the percentage of cases with each expression intensity.

In contrast to the other PPCs, **PCSK8** expression was much weaker in normal breast tissue with only 4% of lesions expressing strong levels of PCSK8 in the epithelial cells. PCSK8 expression increased in ADH, with 10% of the lesions strongly expressing and 80% moderately expressing PCSK8, and further increased in DCIS with 12.5% of the lesions strongly expressing and 87.5% moderately expressing PCSK8. The expression was further increased in invasive tissue with 51.51% showing strong expression (figure 5.35).

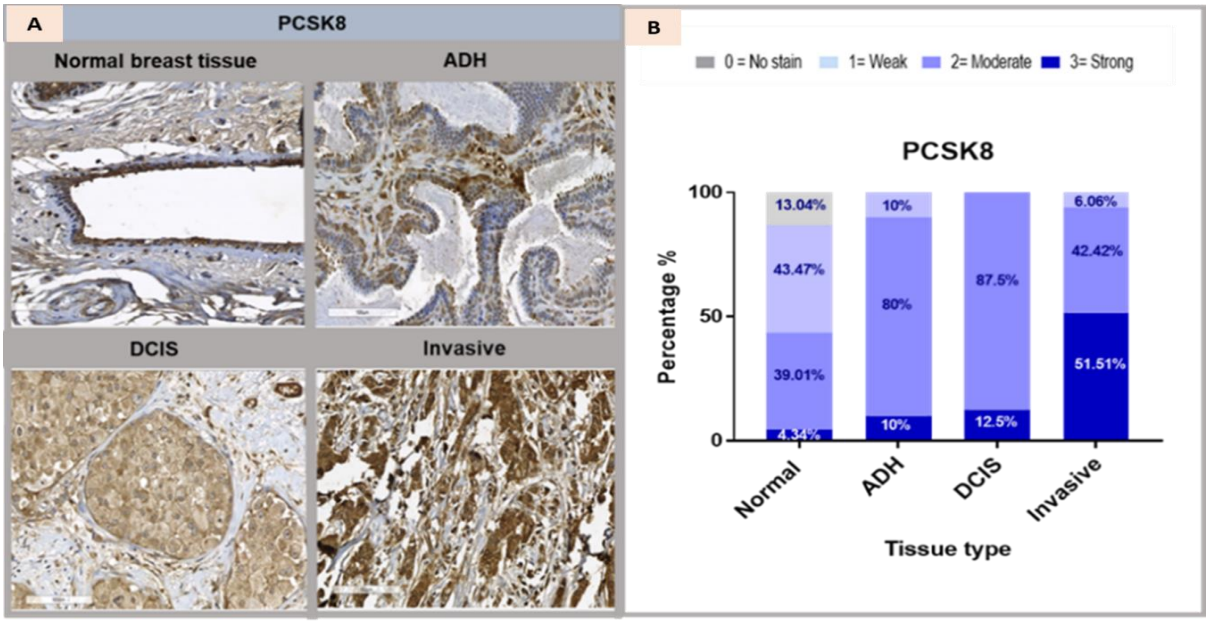

Figure 5.35: Expression of PCSK8 in breast tissue lesions. A) Representative photographs of PCSK8 staining by immunohistochemistry in normal breast ducts (normal), atypical ductal hyperplasia (ADH), DCIS and invasive cancer tissues (invasive). All images were taken using a x20 objective lens and the scale bar = 100 µm. **B)** Each sample was scored for intensity of stain and presented graphically as the percentage of cases with each expression intensity

Strong expression of **PCSK9** was identified within the cytoplasm of 100% of the normal ductal epithelium, and decreased with increasing lesion malignancy to 66.66% of ADH, 26% of DCIS and 12.12% of invasive tissues. PCSK9 was therefore positively correlated with SEMA3B expression (Spearman's rho= 0.415, P=0.01), and strongly inversely correlated with the class/increasing lesion malignancy (Spearman's rho = -0.765, P=0.01) (figure 5.36).

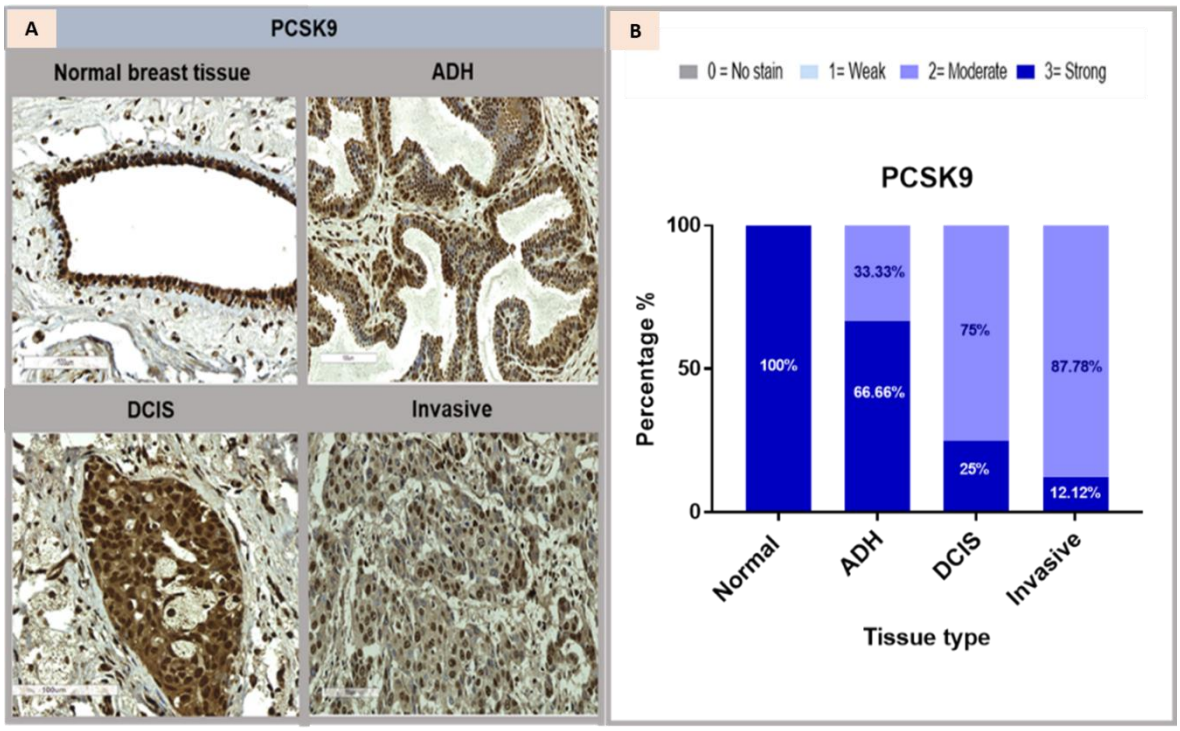

Figure 5.36: Expression of PCSK9 in breast tissue lesions. A) Representative photographs of PCSK9 staining by immunohistochemistry in normal breast ducts (normal), atypical ductal hyperplasia (ADH), DCIS and invasive cancer tissues (invasive). All images were taken using a x20 objective lens and the scale bar = 100 µm. **B)** Each sample was scored for intensity of stain and presented graphically as the percentage of cases with each expression intensity.

5.3.22 Inhibition of PPCs activity in DCIS.com and MDA-MB-231 breast cancer cells

Having shown that SEMA3B expression correlates with a number of PPCs in breast cancer tissues, and that the pattern of expression of some of the PPCs is high in cell-lines where SEMA3B is cleaved and low in the MCF-10A cells where full-length SEMA3B is present, it was necessary to investigate whether this SEMA3B cleavage was indeed caused by PPCs. In order to do this, pan-PPC inhibitors were used to treat DCIS and MDA-MB-231 cells and see if SEMA3B cleavage was inhibited using Western blot analysis for the presence of full-length and cleaved SEMA3B. MT1-MMP was used as a positive control for the inhibitors as it is known that MT1-MMP is processed by PPC cleavage to a shorter, active form, and that pan-inhibitors of PPCs prevent this (Cepeda et al., 2016).

- **Using decanoyl-RVKR-CMK inhibitor**

Initially different concentrations of the pan-PPC decanoyl-RVKR-CMK inhibitor (0,135, 200 µM/L) were used to treat DCIS and MDA-MB-231 cells for 24 hours. As shown in figure 5.37, the activity of the inhibitor was confirmed as it prevented cleavage of MT1-MMP in the MDA-MB-231 cells. However, the cleavage of SEMA3B was not inhibited in either DCIS.com or MDA-MB-231 breast cancer cells either in cell lysates or in conditioned medium, as confirmed by lack of an ~83 kDa band. Due to the toxicity effect of this inhibitor on cells (Varshavsky et al., 2008), it was not possible to use a dose higher than 200 µM/L and so an alternative inhibitor was used.

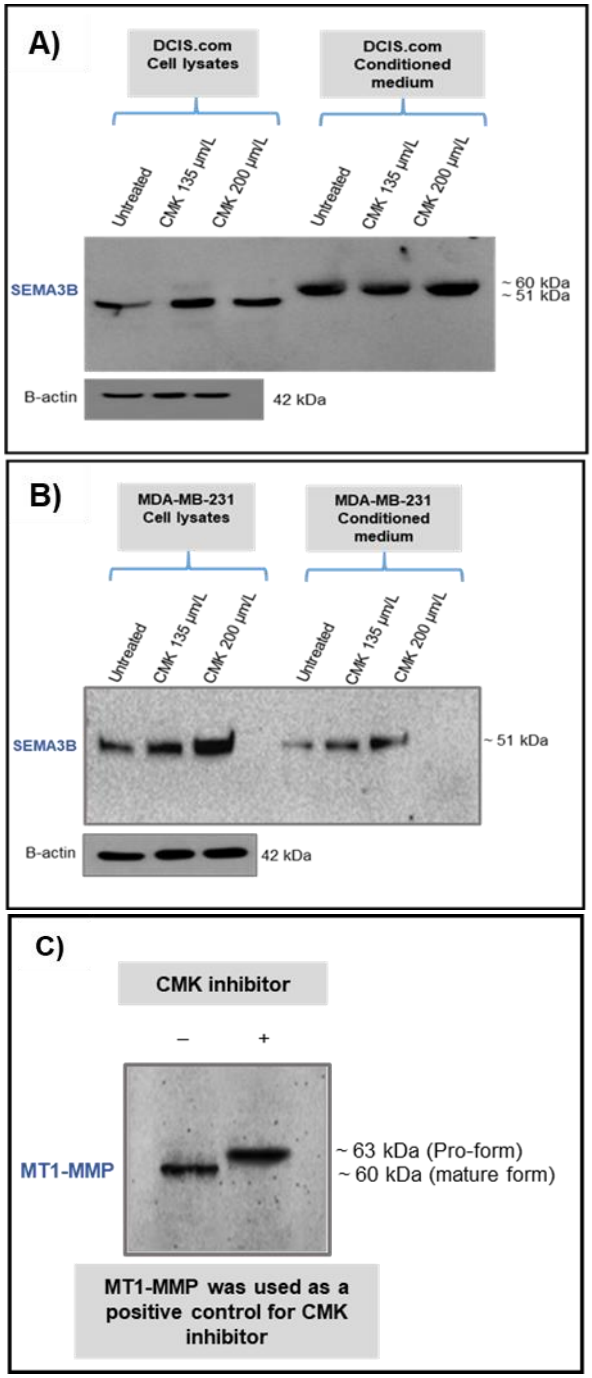

Figure 5.37: Inhibition of PPCs activity using decanoyl-RVKR-CMK inhibitor. Representative immunoblots of treated and untreated **(A)** DCIS.com and **(B)** MDA-MB-231 cells with PPCs inhibitor. Both DCIS.com and MDA-MB-231 cells were incubated with (+) and without (-) 135, 200 µmol/L decanoyl-RVKR-CMK inhibitor for 24 hours. Cell lysates were extracted, and conditioned medium was collected from the cells and was separated on a 10% SDS-PAGE gel, blotted onto PVDF, and probed with an anti-SEMA3B antibody. **(C)** MT1-MMP was used as a positive control. To confirm that the amount of protein in each lane was equal, the membrane was stripped and re-probed with anti-β-actin housekeeping protein as a loading control. The sizes of molecular weight markers are indicated in kDa. For A, B and C, representative immunoblots shown of n=3.

- **Using α1-antitrypsin Portland (α1-PDX) inhibitor**

Although α1-PDX was originally considered a selective and potent furin inhibitor *in vitro*, it has been found that α1-PDX inhibits some of the other pro-protein convertases (Benjannet et al., 1997). This suggests that this inhibitor may be useful in determining whether furin and/or other PPCs are involved in SEMA3B cleavage. The cells were therefore treated with α1-PDX, and investigated by Western blot, as described in 2.10. The DCIS.com and MDA-MB-231 cells were treated with α1-PDX (20 μM) for 24 hours and then cell lysates and conditioned media were collected as described in 5.2.6.2. MT1-MMP was again used as a positive control (Coppola et al., 2008).

As shown in figure 5.38, the α1-PDX was shown to be active by the presence of the full-length pro-form of MT1-MMP in the treated MDA-MB-231 cells. When probing the media and lysates for SEMA3B, in all untreated cell lysates and conditioned media there is only a 51 kDa band seen, consistent with the data described in chapter 3. However, treatment with α1-PDX resulted in the appearance of different molecular weight bands in both cell lysates and conditioned media including higher molecular weight at 65 kDa (cleaved form) and at 83 kDa (full-length form) suggesting that the cleavage of SEMA3B was partially inhibited by the α1-PDX, leading to the generation of a mixture of full-length SEMA3B and cleaved SEMA3B.

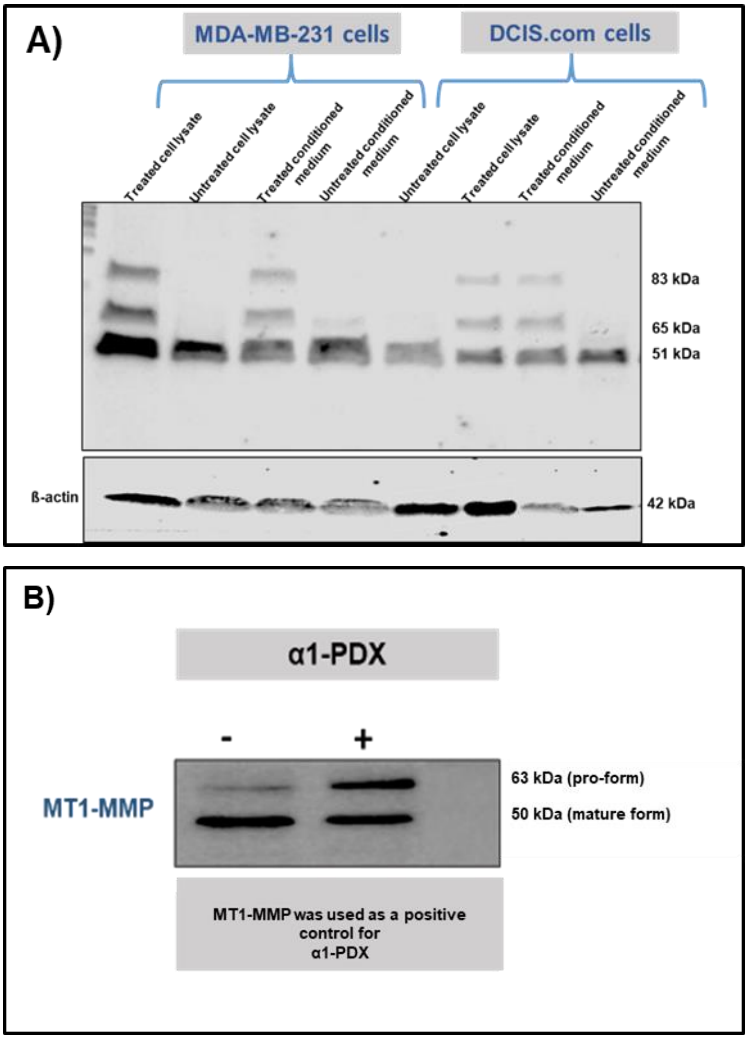

Figure 5.38: Inhibition of PPCs activity in DCIS.com and MDA-MB-231 breast cancer cells using α1-PDX. A) Representative immunoblots of treated and untreated DCIS.com and MDA-MB-231 cell lysates and conditioned media with α1-PDX inhibitor. Both DCIS.com and MDA-MB-231 cells were incubated with (+) and without (-) 20 µM α1-PDX inhibitor for 24 hours. Cell lysates were extracted, and conditioned medium was collected from the cells and was separated on a 10% SDS-PAGE gel, blotted onto PVDF, and probed with an anti-SEMA3B antibody. MT1-MMP was used as a positive control. **B)** The activity of the α1-PDX inhibitor was confirmed using MDA-MB-231 cells and detecting MT1-MMP expression. To confirm that the amount of protein in each lane was equal, the membrane was stripped and re-probed with anti-β-actin housekeeping protein as a loading control. The sizes of molecular weight markers are indicated in kDa. For A and B, representative immunoblots shown of n=3.

5.4 Discussion

Previous studies have suggested that cleavage of SEMA3B is due to furin, but these studies were flawed in that they used a pan-PPC inhibitor (Varshavsky et al., 2008) and are thus unable to exclude the possibility that other proteins may be involved. The aim of this chapter was therefore to establish which, if any, of the pro-protein convertases are expressed in breast cell-lines and tissues, and could therefore be responsible for cleaving SEMA3B. The IHC data in this chapter show that a number of the PPCs, including furin, PCSK1, PCSK4, PCSK5, PCSK7 and PCSK9, had protein expression that correlated with SEMA3B expression in the tissue samples. The expression of some of these PPCs was low where full-length SEMA3B was found in the cell-lines, i.e. in MCF-10A cells, but higher in the other cell-lines where SEMA3B was cleaved, based on cytospin (PCSK1, PCSK4, PCSK5, PCSK7 and PCSK9) and Western blot (furin, PCSK1 and PCSK7) analyses. As a result, two PPC inhibitors were used to see whether they could inhibit SEMA3B cleavage in breast cancer cell-lines. Treatment with one of the inhibitors, α1-PDX, did result in the production of full-length SEMA3B, suggesting that at least some of the PPCs are responsible for SEMA3B cleavage in breast cancer.

Since the expression of many of the PPCs has not previously been described, or has only been studied in a very limited way, each will be discussed here in turn.

Gene and protein expression analysis of pro-protein convertases within breast tumour and non-tumour cells and tissues

The gene expression of each of the PPCs was first examined in breast cell-lines in order to explore whether there is a differential expression between non-malignant and malignant cells and whether there is a potential correlation with SEMA3B cleavage. We found in chapter three that the highest amounts of SEMA3B mRNA were found in normal MCF-10A cells compared to other cell-lines (figure 3.6). In this current chapter, we screened seven malignant and non-malignant breast cell-lines, MCF-10A, MCF-10AT, DCIS.com, MCF-7, T47D, MDA-MB-231 and MDA-MB-231-BM, for the expression of the nine members of the human convertases gene and protein family. We found that all cell-lines expressed all candidate PPC genes as follows (table 5.1).

5.4.1 Furin expression in breast cancer progression

Previous studies have suggested that furin is widely distributed across several human tissues, but that it expresses at a low level in normal tissues (Paleyanda et al., 1997). Our findings, however, showed that *furin* mRNA expression was higher in normal cells than in invasive breast cancer cells. This observation is consistent with that found in respect to SEMA3B in chapter 1. Furthermore, the furin gene expression in the MCF-7, T47D and MDA-MB-231 breast cancer cell lines is similar to that reported in a study by Cheng *et al*. (1997). In contrast to our finding, however, Cheng *et al*.'s study showed that there was no detectable expression of furin in normal breast tissue while we showed high levels of *furin* mRNA expression in normal breast cells. The differences between these findings may be due to the use of normal breast tissues whilst we used normal breast MCF-10A cells in our experiment. Another study examining furin expression in lung cancer also reported results that contrast with ours, with Northern blot analysis showing higher expression of *furin* mRNA in non-small-cell lung carcinoma compared to relatively low expression in normal lung tissues (Schalken et al., 1987). Our results concerning furin, however, are similar to those in Mbikay *et al*.'s (1997) study showing *furin* mRNA expression to be three times higher in non-malignant tissues than in small-cell lung carcinomas.

Despite the assumption that protein expression should reflect the gene expression level, such a correlation does not always exist in the same cell lines (Yu et al., 2007). Our data, for example, shows that the protein level of furin did not reflect that observed in the gene. At a protein level, the processed and active form of furin was expressed at significantly higher levels in invasive cells than in MCF-10A cells, while the gene expression was at the lowest level in invasive cells. These findings are in agreement with a previous study that suggested that an extracellular form of furin (the shedded form) could be involved in the processing of some precursor proteins, although this study was not able to establish whether these proteins process to their functional form as a result of the membrane-anchored form of furin or its shed entity (Denault et al., 2002). In our data, the higher molecular weight of the protein that was highly expressed in the pre-malignant cells (97 kDa) suggest that it could represent the pro-form. If so, it would suggest that the post-translational cleavage occurs within the cell and that the smaller (70 kDa) form, which lacks the transmembrane domain, represents the shed furin which is the active form that may be responsible for SEMA3B cleavage.

Furin undergoes two autocatalytic cleavages to be fully active. When activated, it cycles between the trans-Golgi network, the cell surface and endosomes (Jaaks and Bernasconi, 2017). It is enriched in the trans-Golgi network, where it works to cleave other proteins and many substrates. Studies indicate, however, that the cleavage of the substrate by furin might take place intracellularly, or it could be cleaved and released by the fusion of endocytic furin-containing compartments, which contain substrate (Band et al., 2001). Although some studies have shown that furin-mediated cleavage is associated with promoting substrate functions e,g metalloproteinases, others suggest that cleavage by furin could have a negative effect on substrate functions (Lee et al., 2001, Jaaks and Bernasconi, 2017).

Furin has been known to mediate cleavage at the paired basic amino acid recognition site (Adams et al., 1997). The sequence alignment of SEMA3B contains recognition sites for the endoprotease furin (K/RXRR) which is conserved in its sequence. Indeed, there are three different sites in the SEMA3B sequence that contain the furin-like pro-protein cleavage site, namely KRRFRR (positions 549–554), RRLRRR (positions 632–637) and KGRNRR (positions 726–731) on the C-terminal (figure 5.1) where cleavage of PPCs usually taken place (UniProt). Despite the fact that SEMA3B has multiple furin protease recognition motifs, each of which might lead to the release of the C-terminal of this protein, there is no previous study explaining the exact cleavage site of furin-like pro-protein convertases within the SEMA3B sequence. That said, when cleavage occurs after position 555, which previous studies have assumed is the most common cleavage site, the resulting 60 kDa fragment has been found to be inactive (Varshavsky et al., 2008). Cleavage at position 555 could impair the binding of SEMA3B to its receptors, as it has been suggested that the C-terminal is involved in neuropilin binding (Adams et al., 1997), which can suggest the loss of SEMA3B activity in some biological settings.

In our data, we found that the active (70 kDa) protein form of furin was higher in invasive cells than in normal cells, which may explain why any SEMA3B present in these cells was completely cleaved, whereas the 97 kDa form that was highly expressed in normal cells is not thought to cause cleavage. In agreement with this finding, a previous study on SEMA3F showed that furin deficient cells produce the unprocessed form of SEMA3F while the processed form was only found in cells that overexpressed furin (Parker et al., 2010). Furthermore, in agreement with our

observations, furin protein expression has been identified to be upregulated in several cancers, including non-small-cell lung carcinomas, where it has been shown to correlate with the invasive potential of non-small-cell lung carcinoma cell lines (Bassi et al., 2017). Bassi *et al*. (2001) investigated the protein expression level of furin in head and neck squamous cell carcinoma cell lines and found that the highest level of furin was found in the most invasive head and neck squamous carcinoma cell lines, which is also in agreement with our data. (Bassi et al., 2001b).

Little is known about the expression of the pro-protein convertases and their localisation in human breast cancer tissues; therefore, the expression of PPCs in the normal and malignant breast tissue was investigated in this study using immunohistochemistry. The localisation of the staining in respect to most PPCs was mostly cytoplasmic but, with some proteins, plasma membrane staining was noted. The result obtained from the microarray tissue slides showed that there was moderate to strong cytoplasmic staining of most of the PPCs whose expression decreased with increased disease malignancy. In the present study, the strong staining of furin reduced by 29.63% from normal tissue to invasive tissue, but this was non-significant. In contrast, a previous study in lung cancer revealed that the most invasive tissue of squamous lung cell carcinoma showed elevated furin expression (Lopez de Cicco et al., 2002). To our knowledge, this is the first study exploring the expression of furin protein in breast cancer tissue.

5.4.2 PCSK1 expression in breast cancer progression

PCSK1, like other pro-protein convertases, is important for homeostasis and is involved in the control of a number of physiological processes in health and disease (Demidyuk et al., 2013). In particular PCSK1 has been linked to cancers with neuroendocrine features, although its role is not restricted to those tissues (Mbikay et al., 1997). Duhamel *et al*. (2015) found that PCSK1 is expressed in macrophages and lymphocytes, and that there is a link between inhibition of PCSK1 expression and the activation of macrophages that promote the cytotoxic immune response and therefore inhibit cancer cell viability (Duhamel et al., 2015).

Little is known, however, about PCSK1's role in normal breast cells or in breast cancer. Our observations showed that *PCSK1* mRNA expression was lower in invasive cells compared to normal ones. This result contrasts with Cheng *et al*. (1997), who demonstrated a higher expression of PCSK1 in MCF-7, T47D and MDA-MB-231

breast cancer cells than in normal breast tissues. Zhang *et al.* (2013) also reported that the *PCSK1* gene expression was higher in breast tumour tissues than in normal breast tissue. Similarly, the Northern blot analysis in Creemers *et al*. (1992) found *PCSK1* mRNA expression to be abundant in lung cancer cells but undetectable in normal lung cells.

Importantly, however, our study shows that the protein expression of PCSK1 is not correlated with its gene level, since our observations of higher expression of *PCSK1* mRNA in normal cells compared to invasive cells are reversed at the protein level: more, PCSK1 protein (with a molecular weight of 84 kDa) was detected in invasive cells than in normal cells which was detected at (66 kDa). A previous study found that 87 kDa PCSK1 has lower enzymatic activity than the 66 kDa form, which is less stable but more active, and also that these forms (87 and 66 kDa) are accumulated in dense-core secretory granules prior to secretion (Hoshino et al., 2011). Interestingly, we observed the 66 kDa form only in the MCF-10A and MCF-10AT cell lines, suggesting the activity of PCSK1 in non-malignant cells. This would then correlate with the gene expression results. Furthermore, on the PCSK1 protein sequence, we found that there is cross-reactivity with PCSK2 at RRGDL, position 517-521, and this could explain why PCSK1 requires an additional action of PCSK2 to accomplish the proteolytic cleavage of some substrates (Stijnen et al., 2016).

Although there have been only a few studies on PCSK1 in breast cancer, a study on human breast adenocarcinoma has shown upregulation of proPCSK1 in tumour tissues by Western blot, which is in agreement with our findings (Zhang et al., 2013). Zhang *et al*.'s study did not mention the difference between the two fragments of PCSK1, however. We suggest that the 84 kDa fragment that we detected in the invasive cells may not be as active as the 66 kDa one detected in normal cells.

The immunohistochemistry data, however, seems to suggest that there is a reduction in the expression of PCSK1 in invasive breast cancer tissue, suggesting that PCSK1 may be have less beneficial effects in breast cancer progression. On the other hand, the positive correlation between the PCSK1 and SEMA3B expressions suggests that if this PCSK1 is active, when SEMA3B is present, it might have a role in SEMA3B cleavage.

5.4.3 PCSK2 expression in breast cancer progression

In contrast to furin and PCSK1, a high level of *PCSK2* mRNA expression was detected in invasive T47D and MDA-MB-231-BM cells (figure 5.4). This finding contradicts the previous study of Cheng *et al*. (1997), who reported a lack of *PCSK2* mRNA gene expression in human breast cancer by qPCR, and also Zhang *et al*. (2013), who observed a higher gene expression of *PCSK2* in normal breast tissues compared to breast adenocarcinoma tissues ($P<0.05$). In agreement with our data, however, a previous study using Northern blot analysis showed *PCSK2* mRNA to be more abundant in small cell lung carcinomas compared to the non-malignant tissues (Zhang et al., 2013).

In the current study, expression of PCSK2 was similar for both gene and protein, with both being higher in invasive cells than normal cells. In agreement with our findings but in lung cancer, Mbikay *et al*. (1997) observed higher expression of PCSK2 in lung cancer cells at 68 kDa than in normal cells, and concluded that the 68 kDa fragment represents the most active form of this protein. Interestingly, we observed this band at 68 kDa only in MCF-7 cells. This finding could suggest that PCSK2 is more likely to be involved in the progression of breast cancer.

Our immunohistochemistry data, however, did not match the Western blot data since the expression of PCSK2 decreased with increasing malignancy. A previous study of Zhang *et al*. 2013, revealed higher expression of PCSK2 in normal breast tissue than in tumour breast tissue, which was in agreement with our observation.

5.4.4. PCSK4 expression in breast cancer progression

In respect to PCSK4, this study was the first to explore *PCSK4* mRNA expression in breast cancer, observing higher expression in invasive cells. As with PCSK2, the protein expression of PCSK4 was correlated with its gene level since we found high expression of PCSK4 in invasive cells with the highest expression detected in T47D cells with the 26 kDa isoform. According to the (UniProt) website, there are two isoforms for PCSK4 (82 and 26 kDa). The 82 kDa form is predicted to be the pro-form of PCSK4. In most of the cell lines we tested, however, we detected the 26 kDa form of PCSK4, except for the DCIS.com and MDA-MB-231-BM cell lines.

Although the identity and the activity of the 26 kDa fragment is not fully understood, since there is no previous data to compare this data to, it is predicted to be the active

form of PCSK4 on the basis that this fragment has an active site at its C-terminal, suggesting that it forms part of the activation process of PPCs. The immunohistochemistry staining showed a positive correlation between the protein expression of PCSK4 and SEMA3B in breast tissues, suggesting that PCSK4 may be involved in SEMA3B cleavage, but there is no previous literature with which to compare these results directly.

5.4.5 PCSK5 expression in breast cancer progression

Two differentially spliced isoforms of PCSK5 have been identified, including a short 915 aa soluble PCSK5 A (Lusson et al., 1993) and a long membrane-bound 1877 aa PCSK5 B (Nakagawa et al., 1993). The function of PCSK5 in breast tissues and breast cancer has not previously been addressed, however. Our results showed high levels of *PCSK5* mRNA expression in invasive MCF-7 cells (figure 5.6). In contrast, the only previous study to have investigated the expression of PCSK5 in breast cancer, reported an absence of *PCSK5* gene expression in human breast cancer (Cheng et al., 1997). In agreement with our present data but in lung cancer, Bassi *et al*. (2005) observed a correlation between the level of PCSK5 expression and the aggressiveness of both lung cancer and head and neck derived squamous cell carcinoma cell lines, characterised by a high expression of PCSK5. We were not able to detect the protein expression of PCSK5 due to the limitations of the antibody. Faced with this failure of the Western blot analysis, however, we used cytospin to assess the expression of PCSK5 in cells. The cytospin data matched the gene expression since a strong expression of PCSK5 was detected in invasive cells. The data may potentially be improved by repeating the experiment using different antibodies, but time constraints prevented this. The immunohistochemistry staining showed a weak inverse correlation between the protein expression of PCSK5 and the class and lesion intensity in breast tissues, but there is no previous literature to compare these results directly. Nonetheless, it appears that the gene and protein expression of PCSK5 followed the same pattern, i.e. lower in normal cells and tissues. These data suggest that PCSK5 may correlate with the SEMA3B cleavage since low expression of PCSK5 was apparent when the full-length of SEMA3B is present in MCF-10A.

5.4.6 PCSK6 expression in breast cancer progression

As both furin and PCSK6 are located on the same chromosome (Nour et al., 2005), it has been suggested that they might share a similar function and that they may be responsible for the cleavage of SEMA3B. In our data, *PCSK6* mRNA expression was detected in all cell lines with no significant differences. This is in contrast to a previous study which showed a higher expression of PCSK6 in human breast cancer compared to normal breast tissue (Cheng et al., 1997). Using normal breast tissue rather than cell-lines could explain the differences between our findings. In another study, Wang *et al.* (2015) confirmed the importance of PCSK6 in breast cancer progression since they reported that silencing the *PCSK6* gene in MDA-MB-231 cells led to a significant decrease in the invasiveness of breast cancer (Wang et al., 2015).

Through Western blot, PCSK6 expression was detected in invasive cells, with the highest expression found in T47D cells, although this data did not match with the *PCSK6* gene expression. The impact of PCSK6 expression in breast cancer is not yet clearly understood, however, to our knowledge, there has been no previous work that we can compare with ours that has used Western blot analysis to determine on the expression of PCSK6 in breast cancer. Nevertheless, a study looking at spindle cell carcinoma in mice described a significant upregulation of PCSK6 protein in these cells, suggesting its involvement in the malignancy of tumour cells, and this is consistent with our findings (Hubbard et al., 1997). In contrast with this, Bassi et al. (2001b) investigated PCSK6 expression in human head and neck cancer cell lines, including those with high invasive abilities (SCC71, A253 and Detroit 562, as well as Fadu, which is characterised as the most aggressive cell line). Bassi et al.'s study showed only faint PCSK6 expression in most of these cells, with no expression at all detected in the most aggressive Fadu cells. Interestingly, there is a debate in the literature about the role of PCSK6 expression in carcinogenesis. Some observations revealed that overexpression of PCSK6 enhances the cell invasiveness, e.g. in skin, lung and prostate cancer, while others showed reduced PCSK6 expression with increasing malignancy in some cancers such as ovarian cancer (Mahloogi et al., 2002, Fu et al., 2003). Our IHC data demonstrated a clear pattern of decreasing PCSK6 expression with increasing malignancy by 27.45%. No previous studies have used IHC staining, however, and thus there is nothing to compare our results to, although a study conducted on non-small cell lung cancer demonstrated that the expression of PCSK6

in these tissues was significantly higher than in normal lung tissues, and that this expression increased with increasing disease malignancy (Lin et al., 2015) which was inconsistent with our data.

5.4.7 PCSK7 expression in breast cancer progression

The RT-PCR results revealed that *PCSK7* mRNA level expression was high in DCIS.com and T47D cells and fluctuated in the other cells compared with the normal MCF-10A cells. Our result is partly consistent with the previous report by Cheng *et al*. (1997), since this also showed *PCSK7* mRNA expression to be high in T47D breast cancer cells. Whereas our study showed *PCSK7* mRNA to be lower in MCF-7 and MDA-MB-231 cell lines than in normal cells, however, the Cheng *et al*. (1997) study reported high expression in these cell lines. Comparatively little is known about the expression of PCSK7 in breast cancer progression, although PCSK7 expression is decreased in ovarian cancer cells compared to normal ones (Page et al., 2007).

To investigate whether the differential expression of *PCSK7* mRNA was maintained at the protein level, cell lines were screened by Western blotting. Generally, we observed two different protein fragments in each lane, but for some, like T47D and MDA-MB-231-BM, no PCSK7 protein expression was detected. The intensity of the upper band at 86 kDa was slightly less than that of the lower one at 64 kDa. The lack of protein expression in T47D was particularly striking since *PCSK7* gene expression was high in this cell line. However, PCSK7 protein expression was detected at 64 kDa in both MCF-7 and MDA-MB-231 cells suggesting that the more invasive cells may express more PCSK7 than less invasive ones.

Although the *PCSK7* mRNA expression was higher in breast cancer cells (Cheng et al., 1997), until now, there have been no reports regarding the protein expression of PCSK7 in breast cancer. A study characterising the properties of the protein sequence of PCSK7, however, has shown that this protein can cleave substrates at paired basic residues, which can provide evidence for how PCSK7 functions as a member of PPCs. The sequence of the 89 kDa protein also corresponds to the zymogen cleavage site of PCSK7 (Munzer et al., 1997). Since PCSK7 is expressed at only a low level in MCF-10A, in which we have confirmed the presence of the full-length of SEMA3B, this might suggest a role of PCSK7 in SEMA3B cleavage. The result obtained from the microarray tissue slides, however, revealed a moderate to strong cytoplasmic

expression of PCSK7 (63.84%) which downregulated with increasing lesion malignancy of breast cancer. There was a positive correlation between SEMA3B expression and the expression of PCSK7 in the breast cancer tissues.

5.4.8 PCSK8 expression in breast cancer progression

Our present study seems to be the first attempt to assess the expression of PCSK8 in breast cancer. The qPCR data showed that *PCSK8* expression was highest in T47D cells and decreased in normal cells. The PCSK8 protein is synthesised as a 148 kDa form, which is a pro-form (zymogen) that is processed to the membrane, and a 106 kDa form, which is a processed form of PCSK8 that transforms into a 98 kDa active form of the protein (Seidah et al., 1999). For reasons we were not able to ascertain, however, attempts to detect the protein by both Western blot and cytospin assay failed for all cell lines. As a result, we sought to study protein expression using a different assay, known as cell pellet followed by immunohistochemistry.

The cell pellet assay showed a strong expression of PCSK8 in all cell lines with no significant differences observed between the normal and the invasive cells. The immunohistochemistry data of PCSK8 was the only protein among the nine PPCs that was found to increase with increasing malignancy. Interestingly, while our data showed a positive correlation between PCSK8 and lesion malignancy, it also showed an inverse correlation between SEMA3B and PCSK8, with SEMA3B down-regulated in the developing tumours.

5.4.9 PCSK9 expression in breast cancer progression

Our evaluation of *PCSK9* mRNA levels in malignant and non-malignant breast cells showed higher expression in both normal MCF-10A and invasive MDA-MB-231 cells compared with other cells. There are no other studies of PCSK9 in breast cancer with which to compare our results to, although it is known that PCSK9 regulates low-density lipoprotein (LDL) cholesterol homeostasis and that loss of function in the PCSK9 gene is associated with hypocholesterolaemia while increased function is associated with hypercholesterolaemia (Abifadel et al., 2003). PCSK9 controls the LDL level by binding to its receptor (LDLR) cell surface for degradation (Sun et al., 2012). This is interesting since elevation of the cholesterol level is strongly linked with an increased risk of breast cancer (Hu et al., 2012), which could suggest an indirect effect of PCSK9 in breast cancer progression. There is no direct study in the literature investigating the

expression of PCSK9 in breast cancer. However, a previous study has looked at PCSK9 in human hepatocellular carcinoma, observing that *PCSK9* mRNA expression is lower in human hepatocellular carcinoma compared to normal control tissue (P=0.02), while serum levels of PCSK9 were significantly higher among patients with hepatocellular carcinoma (Bhat et al., 2015). The study of Bhat et al., might suggest different mechanisms taking place between the expression of *PCSK9* mRNA and the protein processing. In our findings, the protein level of PCSK9 was correlated with the gene expression in MDA-MB-231, whereas the protein expression was lower in normal cells than in invasive ones. This agrees with the previous work that suggests a link between PCSK9 and breast cancer through its promotion of LDL-cholesterol, as discussed above (Hu et al., 2012, Laisupasin et al., 2013). To our knowledge, however, no work has been done on the direct effect of PCSK9 in breast cancer. The IHC result exhibited a different pattern of PCSK9 expression which did not match the Western blot data. There was a strong cytoplasmic expression of PCSK9 (100%) in normal tissues but expression reduced with increasing lesion malignancy in breast cancer.

It is not easy to explain why there are these dissimilarities between our findings and other studies. In respect to the qPCR results, however, it is most likely due to variances in the experimental platforms used: qPCR, RT-PCR and Northern blot analysis. In addition, differences in the extraction methods for PCR may have played a role in the discrepancies (Mahittikorn et al., 2005). One other possible reason that could interfere with the qPCR result is the use of an inappropriate internal control gene. Using stable reference genes is important for accurate quantification of mRNA levels. To minimise this issue, in this study, GAPDH was used as a normalising gene and to confirm the integrity of RNA. It has been found that GAPDH and ACTB (β-actin) were the most stable reference genes in basal breast cancer MDA-MB-231 cells and in ER+ breast cancer MCF-7 and T47D cell lines (Liu et al., 2015). Similarly, Morse *et al*. (2005) found that GAPDH is the least variable gene in the MCF-10A cell line. For these reasons, GAPDH was chosen for its stability expression in all cell lines used. Moreover, variations in results could be attributed to the use of different laboratories and the high passage number of cell lines. Cells are known to exhibit phenotypic drift with increasing passage number so in order to minimise these alterations, low passage numbers were used in this project.

This study showed a different pattern of PPC genes expressions in different breast cancer cell lines, suggesting that breast cancer cells are likely to react differently with different members of the PPC family. Our immunostaining data did not correlate with the protein expression of the cell lines obtained from Western blot analysis. Unlike the cell lines expression data, most of the PPCs expressions in tissue decreased with increased disease malignancy; however, it is unclear whether these proteins are active or not in these tissues as there are currently no antibodies that will distinguish between the active and inactive forms of the proteins. Moreover, detection of the target proteins depends on the antibodies that are used, since choosing a good and specific antibody is crucial for both Western blotting and immunohistochemistry (Liu et al., 2016). For some PPCs, we used the same antibodies for both applications and they were selected on the basis of their performance in Western blot analyses. This decision was based on a previous study that identified that antibodies that detect a single band consistent with the mass of the protein of interest are more likely to be specific in IHC analyses (Uhlen et al., 2016). However, that said, some of our antibodies detected more than one band, however, which may in part explain the lack of correlation between some of the Western blot and IHC findings. In addition, the differences in how samples are treated in different applications can interfere with the ability of the antibody to bind to its target. Sample preparation and sample size are also likely to make a difference.

Interestingly, our data shows an inverse correlation between SEMA3B and the disease progression; in other words, as a lesion malignancy increases SEMA3B expression decreased, a finding that is in line with the previous study of (Staton et al., 2011). On the other hand, furin, PCSK1, PCSK2, PCSK4, PCSK7 and PCSK9 were all positively correlated with the expression of SEMA3B to varying degrees, which suggests that if these PPCs are all active when SEMA3B is present it is likely to be cleaved. To conclude, our data have established that there is a different expression of PPCs in a breast disease state with the majority reducing with increasing lesion malignancy.

Table 5.1: A comparison of the mRNA expression and protein expression of the PPCs in the cell lines used.

	Target	Cell lines						
		MCF-10A	MCF-10AT	DCIS.com	MCF-7	T47D	MDA-MB-231	MDA-MB-231-BM
mRNA expression	PCSK1							
Protein expression								
mRNA expression	PCSK2							
Protein expression								
mRNA expression	Furin							
Protein expression								
mRNA expression	PCSK4							
Protein expression								
mRNA expression	PCSK5							
Protein expression								
mRNA expression	PCSK6							
Protein expression								
mRNA expression	PCSK7							
Protein expression								
mRNA expression	PCSK8							
Protein expression								
mRNA expression	PCSK9							
Protein expression								

	Low expression
	High expression
	Similar expression
	No expression
	It was not possible to detect by WB

5.4.10 Inhibition study of PPCs

The gene and protein expression data presented here indicate that at least some of the PPCs have expression patterns that suggest that they are present in the correct places to cleave SEMA3B; i.e. they correlate with SEMA3B in tissues and are low in normal breast cells and high in breast cancer cell lines. Based on this, it was then necessary to determine whether inhibition of these proteins would restore the full-length of SEMA3B. Two different inhibitors were used in this assay, the pan-PPC decanoyl-RVKR-CMK and alpha1-PDX inhibitor.

CMK is a potent PPC inhibitor and is able to act intracellularly, where it reduces cleavage of some of the PPCs substrates (Bassi et al., 2003). Although the study presented in this chapter using the CMK inhibitor did result in inhibition of MT1-MMP processing to the active shorter form, it did not result in re-expression of full-length SEMA3B. This result is in apparent conflict with those of others who have shown that CMK does inhibit furin-like pro-protein convertases to produce full-length SEMA3B (Varshavsky et al., 2008). This discrepancy can be explained by differences in the method conditions, however, since Varshavsky and colleagues used MDA-MB-231 cells that had been transfected to express recombinant SEMA3B, rather than the untransformed cells and native SEMA3B expression used in this study.

Interestingly, the CMK inhibitor blocks the activity of PPCs by blocking the catabolic pocket activity at RVKR sites (Tian and Jianhua, 2010). Since these are only found in the protein alignments of PCSK4, PCSK6 and PCSK8, however, CMK may not be as effective at inhibiting the other PPC proteins. That said, the 3D structure of this catabolic pocket in these three PPCs is similar to that found in furin, where the site is [K/R]-X-V-X-K-R, and this may suggest that this inhibitor will also inhibit furin (Tian and Jianhua, 2010). Since MT1-MMP cleavage was inhibited by CMK in our study, and this protein is known to be cleaved by furin (Bassi et al., 2003), this would suggest that the CMK inhibitor can inhibit furin, and that furin, PCSK4, PCSK6 and PCSK8 are not involved in SEMA3B cleavage.

A second inhibitor, α1-PDX, which is highly selective for furin and some other of the PPCs such as PCSK5 and PCSK6 (Tsuji et al., 1999, Hada et al., 2012), was then used to inhibit PPC activity in DCIS and MDA-MB-231 cell lines. Treatment of cells with α1-PDX (20 µM) resulted in inhibition of activation of MT1-MMP, as demonstrated by the appearance of the full-length pro-form on the Western blot. This was as

expected since α1-PDX effectively blocks processing of precursor proteins at RXK/RR sites, which are found in MT1-MMP, and is in agreement with a study that showed that α1-PDX inhibits furin in head and neck squamous cell carcinoma, as well as inhibiting activation of MT1-MMP (Bassi et al., 2001a). Importantly for the current study, α1-PDX treatment resulted in the appearance of higher molecular weight SEMA3B proteins (at 51 kDa and at 83 kDa), and we also observed a decrease in the cleaved form of SEMA3B compared to untreated cells. These data would suggest that at least one of the PPCs inhibited by α1-PDX is involved in cleavage of SEMA3B. On the other hand, full inhibition of SEMA3B cleavage was not achieved, suggesting either that the experimental conditions were not ideal for full inhibition of the PPCs, or that other proteins are involved in SEMA3B cleavage.

In conclusion, this chapter has shown for the first time that the majority of the PPC family are expressed in human breast cancer, both in cell lines and in tissues. In many cases, the expression in tissues shows an inverse relationship with increasing lesion malignancy, suggesting that these proteins may be switched off as breast cancer progresses. Furthermore, the data suggest that furin, PCSK1, PCSK4, PCSK5, PCSK7 and PCSK9 have the right expression pattern to be candidates for SEMA3B cleavage. The data from the inhibitors, however, would suggest that furin and PCSK4 are not involved in SEMA3B cleavage, since CMK, which is known to inhibit these proteins, did not inhibit SEMA3B cleavage. Treatment with α1-PDX did not fully restore all SEMA3B to full-length and therefore further work is required to establish which PPC is involved in cleaving SEMA3B and whether other proteinases are also involved.

Chapter 6: General Discussion

6.1 Summary of main outcomes and general discussion

Class 3 Semaphorins are a family of secreted proteins that are important for the development of different physiological systems and maintenance of many tissues. Class 3 semaphorins are known for their roles in nervous system development, where they have been identified as axonal growth cone guidance molecules (Yazdani and Terman, 2006). Recently, they have been shown to play an inhibitory role in tumour progression and angiogenesis (especially SEMA3B and SEMA3F). Several studies have explored the inhibitory effects of SEMA3B on tumour progression and angiogenesis as potential therapeutic agents for cancers such as lung cancer (Castro-Rivera et al., 2004) and ovarian cancer (Joseph et al., 2010). However, the contribution of SEMA3B to breast cancer progression remains relatively unclear in comparison to other vertebrate semaphorins.

Recent findings suggest that loss or mutations in SEMA3B may contribute to the development of breast cancer. Indeed SEMA3B is one of the known frequent allelic losses (up to 40%) in the LUCA region (3p21.3) in breast cancer, emphasizing its potential role in tumour development (Senchenko et al., 2004). In addition to allelic loss, methylation appears to be a mechanism of SEMA3B gene inactivation, and a previous study in breast cancer has shown that increased methylation in invasive breast cancer results in silencing of SEMA3B gene and therefore a loss of SEMA3B protein (Burbee et al., 2001, da Costa Prando et al., 2011).

Although the majority of previous studies focused on methylation and allelic loss of SEMA3B (Burbee et al., 2001, Tse et al., 2002, Pronina et al., 2009, da Costa Prando et al., 2011), as playing a role in the tumorigenesis process, other studies suggested that post-translational processing including proteolysis were linked with some of the functional effects of SEMA3B. Proteolytic cleavage by furin-like pro-protein convertases of semaphorins is essential for activity of some semaphorins, but additional cleavage can result in inactivation, depending on where the cleavage occurs and on which semaphorin is cleaved. Cleavage of SEMA3B by furin-like pro-protein convertases resulted in the secretion of two fragments whose sizes corresponded to those expected from cleavage at the conserved dibasic consensus sites (Varshavsky

et al., 2008). These 61 kDa and 20 kDa fragments are believed to be inactive forms of SEMA3B (Varshavsky et al., 2008). Varshavsky and colleagues used a pan inhibitor of the pro-protein convertase family to demonstrate that this family could cleave SEMA3B in breast cancer cells that were transformed to overexpress the protein (Varshavsky et al., 2008), but their work did not make it clear which of the PPCs was responsible. Indeed, very little was known regarding the expression of the PPC family of enzymes in the development of breast cancer. Therefore, this thesis aimed to test the hypothesis that pro-protein convertase cleavage of SEMA3B results in inactivation of SEMA3B in invasive breast cancer.

The work performed in chapter 3 of this thesis demonstrated that the gene expression of SEMA3B in the majority of breast cancer cells was decreased compared to normal MCF-10A cells (figure 3.6). These results are in agreement with a previous study identifying a decrease in SEMA3B mRNA in invasive breast cancer (Pronina et al., 2009), and would suggest that this may be due to allelic deletion or promoter hypermethylation, in agreement with previous studies (Tse et al., 2002, Castro-Rivera et al., 2004, da Costa Prando et al., 2011). In addition, the IHC data in the tumour microarrays also suggested that protein expression was reduced with increasing breast cancer lesion malignancy (figure 3.9) which was in agreement with previous literature that found decreases in SEMA3B expression with increasing lesion malignancy of breast cancer (Staton et al., 2011). Again, this down-regulation of SEMA3B expression could be due to a combination of allelic deletion and promoter hypermethylation. It is important to note however, that the antibodies used for IHC cannot distinguish between full-length and cleaved SEMA3B, so it was unclear whether the SEMA3B present in the tissues was full-length or cleaved. Indeed, at present there are no commercially available antibodies that can answer this question.

In order to start investigating this, Western blotting in the cell-lines was performed, and showed that the full-length SEMA3B protein was seen only in normal MCF-10A cells while in all other cell-lines any SEMA3B present, was completely cleaved (figure 3.7). This finding therefore suggested that where SEMA3B is present in breast cancer it is likely to be cleaved, and previous studies have shown that the cleaved 61 kDa SEMA3B protein is inactive (Varshavsky et al., 2008). As SEMA3B is thought to act as a tumour suppressor (Castro-Rivera et al., 2004), this would suggest that cleavage of SEMA3B would mean that it can no longer inhibit tumour growth/progression.

However, there are very few studies that have investigated the effect of full-length SEMA3B in breast cancer (Castro-Rivera et al., 2004).

One study suggested that transfecting breast cancer cells with full-length SEMA3B would enable studying the full-length protein in breast cancer cells (Castro-Rivera et al., 2004). This study showed that full-length SEMA3B did inhibit 50 % of the cell growth of breast cancer MDA-MB-231 cell-line. An alternative attempt to study the effect of full-length SEMA3B inhibited the activity of pro-protein convertases thereby restoring full-length SEMA3B and this study showed that SEMA3B had inhibition effect on tumour formation in MDA-MB-435 melanoma cells (Varshavsky et al., 2008).

As the above studies suggested that full-length SEMA3B acts as a tumour suppressor, but the evidence for this in breast cancer is limited we chose to investigate this in a different way. In chapter 4, we examined the activity of full-length recombinant SEMA3B on the proliferation, metabolic activity, migration and invasion of breast cancer cells. Our approach was to investigate the role of SEMA3B in breast cancer by demonstrating the effect of the full-length SEMA3B on the cell growth and metabolic activity of breast cancer progression. In this study, the tumour suppressor activity of the rSEMA3B has been profiled across a panel of cells, representing normal MCF-10A cells, pre-invasive DCIS.com and invasive MDA-MB-231 cells, using different functional assays. In the cell-counting assay, rSEMA3B was found to inhibit the cell growth of DCIS.com and MDA-MB-231 cells in a dose-dependent manner (figure 4.7 and 4.8). This finding suggests that full-length SEMA3B is efficient as a tumour suppressor on its own with respect to its ability to inhibit the proliferation of the pre-invasive and invasive cells, and can exert direct effects on these cells but had no effect on their cell viability and metabolic activity. Therefore, the data in this thesis demonstrate that full-length SEMA3B can produce an anti-proliferative effect *in vitro* indicating that SEMA3B can act directly on target cells. These findings were in agreement with a previous study that showed that SEMA3B overexpression had an inhibition effect on cellular proliferation of breast cancer MDA-MB-231 cell-line (Shahi et al., 2017). The anti-proliferative effect of SEMA3B may be due to the ability of SEMA3B to down-regulate the Akt pathway, which modulates the function of several substrates included in the regulation of cell survival and cellular growth (Castro-Rivera et al., 2008).

In the same context, we showed that full-length SEMA3B was able to decrease the migration of MDA-MB-231 cells compared to control cells (figure 4.12). However, there is no previous literature with which to compare these results directly.

The initial stage of cancer metastasis involves phenotypical and genotypical alterations indicating the acquisition of metastatic potential. SEMA3B was shown to inhibit invasion in ovarian cancer (Joseph et al., 2010). In this current study, the invasion ability of breast cancer MDA-MB-231 cells was significantly inhibited by the full-length SEMA3B in comparison to control cells (figure 4.14), suggesting the effectiveness of exogenous SEMA3B expression in reducing the invasive potential of breast cancer cells through Matrigel. In light of the previous study of the regulation and function of SEMA3B in ovarian cancer that showed inhibition of MMP-9 and MMP-2 activity by SEMA3B, this may be one mechanism by which SEMA3B may potentially diminish metastatic development, including migration and cell invasion (Joseph et al., 2010). However, further work is needed to confirm these findings and to establish whether this is the only mechanism by which SEMA3B is working to inhibit invasion. So far, our results suggest that SEMA3B can function as a potent tumour suppressor of breast cancer invasion.

As class 3 semaphorins are known to inhibit angiogenesis, to ensure that the recombinant protein was active in our experimental systems, we used the same concentrations of SEMA3B on human umbilical vein endothelial cells. In all cases SEMA3B inhibited proliferation (figure 4.9), migration (figure 4.13) and invasion (figure 4.15) demonstrating its activity as an anti-angiogenic protein in agreement with previous studies which showed similar anti-angiogenic activity *in vitro* (Rolny et al., 2008, Varshavsky et al., 2008). Our finding is also supported by the fact that SEMA3B can regulate angiogenesis and metastasis by competing with VEGF family members for neuropilin binding (Castro-Rivera et al., 2004), suggesting that SEMA3B-mediated suppression of tumour growth was associated with an anti-angiogenic phenotype.

In order to ensure that the recombinant full-length SEMA3B protein remained full-length for the duration of the assays and therefore that the activity seen was due to this and not a cleaved protein, we incubated the breast cell-lines with the recombinant SEMA3B. Interestingly, we found that MCF-10A and DCIS.com did not induce cleavage of full-length SEMA3B protein over 48 hours suggesting that the recombinant protein would retain activity within that time period (figure 4.1, 4.2 and 4.3). However,

the invasive MDA-MB-231 cells demonstrated partial cleavage of the full-length SEMA3B over 48 hours as cleavage of SEMA3B was observed in both cells and conditioned medium suggesting that the full-length of SEMA3B may be affected in these cells in a time-dependent manner.

In a similar manner, we incubated the breast cell lysates with the recombinant SEMA3B protein for three hours. We found that both MCF-10A cell lysate and conditioned medium were unable to cleave the full-length SEMA3B. However, the full-length SEMA3B showed a partial cleavage in the invasive MDA-MB-231 cell lysate and to a lesser extent in DCIS.com lysate. This data suggests that there are proteins produced inside the cells that may be responsible for this cleavage (figure 4.4 and 4.5). This data was in agreement with a previous study of Varshavsky *et al*.,2008, who suggested that SEMA3B cleavage in MDA-MB-231 cells is most likely to be due to the activity of furin. However, their study had used pan-PPC inhibitors, and therefore other members of the PPCs family could have a role cleaving SEMA3B and may contribute to enhancing the malignant phenotype.

Therefore, in chapter 5, we examined the presence of all the PPCs in the breast cell-lines, surprisingly, the gene expression of furin (figure 5.2), PCSK1 (figure 5.3), and PCSK9 (figure 5.10), were the highest in normal MCF-10A with a gradual decrease in gene expression seen with increasing the malignant and invasive potential of the cell-lines. However, the gene expression pattern of most PPCs was lowest in MCF-10A cells compared to the other cells suggesting the possibility that some of the PPCs have increased expression with increasing malignancy of breast cancer, and it may be those PPCs that could be responsible for SEMA3B cleavage. Very few studies have investigated PPC gene expression, and some of these findings were in contrast with a previous study of Cheng *et al*., 1997 who observed that the expression of PCSK1 and furin were upregulated in breast cancer cells compared to the normal breast tissues (Cheng et al., 1997). It should be noted that the study of Cheng *et al*., used normal human breast tissues in their experiment instead of using normal epithelial MCF-10A cell-lines that we used in this current study, which may account for some of the differences seen.

However, the protein levels did not fully match up with the mRNA expression and in the cell-lines, the expression of furin, PCSK1, PCSK2, PCSK6, PCSK7 and PCSK9 were lower in normal breast cells compared to the invasive cells. This suggests that

there may be enhanced translation of the mRNA resulting in increased protein concentrations in invasive breast cancer cells. In addition, post transcriptional modifications that occur after mRNA is translated into protein could influence protein stability and a protein's half-life. This can result in differences in protein levels independent of transcript levels and that may explain the reasons for the discrepancy between the levels of mRNA and protein in some cell lines (Liu et al., 2016). Similarly, these data suggest that one or more of these PPCs may be involved in SEMA3B cleavage, as there were low levels of them detected in MCF-10A where full-length SEMA3B is found.

However, it may not be as simple as that as, for example, despite the detection of high levels of 84 kDa PCSK1 in invasive cells, a previous study suggested that this protein may not be as active as the 66 kDa PCSK1 detected in normal cells (Hoshino et al., 2011). Therefore, if the 66 kDa PCSK1 is more active, and this was detected in both MCF-10A and MCF-10AT, this may well exclude the possibility of PCSK1 being responsible for SEMA3B cleavage. Although several studies have demonstrated a possible role of furin in cleavage of SEMA3B in lung and ovarian cancers, its role on SEMA3B in breast cancer is not yet understood. Furthermore, to our knowledge, there are no previous studies which have investigated the protein expression of PCSK2, PCSK6, PCSK7 and PCSK9 using Western blot in breast cancer and therefore it is not known if they have a role in SEMA3B cleavage.

The question remains as to where and when SEMA3B produced by the cells is cleaved. The cleaved SEMA3B product is found in the cell lysates and is also released into the medium, which could possibly suggest that SEMA3B is cleaved inside the cells, maybe in the Golgi where the PPCs are known to be active. This is important when we consider the expression pattern of PPCs in cell lysates compared to the PPCs released into the media. Indeed, in the conditioned media only the active forms of the PPCs were detected compared to the cell lysates where different PPCs bands were identified with some representing inactive and some active enzymes. However, the differences between amounts of the PPCs found in the conditioned media was not as pronounced as in the lysates, and generally less protein was found. In some ways this is unsurprising as measuring the protein expression in the culture medium is known to be challenging as the presence of serum residues in cell culture due to improper washing of cells may yield different protein concentrations (Chevallet et al.,

2007). In order to minimize this, cells were incubated in serum-free media for 24 hours to avoid any cross-reactivity between the FBS and the antibodies of interest and then their conditioned medium was collected for investigation.

As so few previous studies have investigated the expression of PPCs in breast cancer, we then identified the expression of these enzymes in breast tissue using IHC. Interestingly, generally all PPCs except PCSK8 are expressed in normal epithelium, but for the most part their expression decreases with increasing malignancy of the lesion, suggesting that as breast cancer progresses they are no longer active. However, protein expression of PPCs in cell-lines were not similar to that detected in tissues as in cell-lines, furin, PCSK1, PCSK2, PCSK6, PCSK7 and PCSK9 detected at the lowest level in normal cells compared to invasive cells while in tissues, all PPCs appeared expressed at the highest level in normal tissue compared to invasive tissue. These differences could be because the antibodies used are not specific for the active isoforms of PPCs, and therefore any PPC present will be detected whether it is active or not.

Interestingly there was a positive correlation between SEMA3B expression and the expression of furin, PCSK1, PCSK2, PCSK4, PCSK7 and PCSK9, in the breast cancer tissues. This suggests that these proteins are active when SEMA3B is present, and therefore may potentially cleave the SEMA3B thereby abolishing the ability of SEMA3B to act as tumour suppressor as breast cancer progresses. Cleavage of SEMA3B to its inactive form by furin-like PPCs has been demonstrated in cell-lines but whether SEMA3B inactivation by furin or other PPCs family members is responsible for invasiveness of cancer cells or cancer development is currently not well-explained. Thus, we next attempted to show whether or not inhibition of PPCs activity will restore the full-length of SEMA3B in the breast cancer cells.

The majority of PPCs inhibitors work by targeting the catalytic site of the enzyme, but these inhibitors are not specific for single PPCs (Fugere et al., 2002). CMK, is a highly potent inhibitor of PPCs, although not specific for one individual protein, and has previously been used to suggest a role for PPCs in SEMA3B cleavage (Varshavsky et al., 2008). However, in this thesis even when high concentrations of CMK (200 μM) were used, no effect was seen on SEMA3B, with full cleavage still happening in DCIS and MDA-MB-231 cells. This could possibly suggest that the PPCs have no role in SEMA3B cleavage, but this is unlikely as one previous study demonstrated that CMK

at the same concentration was effective in reducing the cleavage of SEMA3B (Varshavsky et al. 2008). Interestingly despite suggestions that CMK is a pan-PPC inhibitor there are some studies which suggest that although CMK can inhibit PCSK6 in skin squamous cell carcinoma cell-lines resulting in reduced tumour development (Bassi et al., 2010), and can inhibit furin activity, it had no effect on the activity of PCSK7 (Bessonnard et al., 2015). Furthermore, there is a suggestion that CMK inhibitor has poor cell permeability (Basak, 2005), and it is known that the PPCs mostly act in the Golgi. Taken together these data suggest that CMK may not be the best inhibitor to confirm an effect of PPCs on SEMA3B cleavage so an alternative inhibitor was used.

Although previous studies identified α1-PDX as a selective inhibitor for furin (Anderson et al., 1993) more recently evidence has appeared that α1-PDX inhibits other PPCs family members including PCSK1, PCSK5 and PCSK6 (Vollenweider et al., 1996, Benjannet et al., 1997). Importantly, we have shown that α1-PDX has effectively resulted in inhibition of activation of PPCs as demonstrated by the appearance of the full-length SEMA3B form on the Western blot (figure 5.35). These data therefore confirm that SEMA3B is cleaved by at least one or more of the PPC family members, although exactly which PPC remains to be seen.

6.2 Limitations of the study

One of the main limitations of this study is conducting work with cultured cell-lines, as this has obvious disadvantages, including contamination with mycoplasma, genotypic and phenotypic drift, which can alter the behaviour of the cells, and these develop during their continual culture (Geraghty et al., 2014). Therefore, the majority of cell-lines used were bought fresh from the ATCC to avoid any contamination that may raise of using old cryopreserved cells in-house, regular mycoplasma testing was carried out in order to ensure that cells are mycoplasma free, and low passage numbers were used throughout this thesis work. In addition it would have been advantageous to undertake fingerprint analysis for all cell-lines; however, this was not performed due to time and money constraints. It is also important to note, that cell-lines used by different laboratories may show a difference in their biological properties, even with having a similar karyotype, due to differences in the culturing conditions before storage. Indeed, some groups will grow the breast cancer cell-lines in DMEM whereas we used RPMI and this may alter their behaviour slightly. It should also be noted that

direct comparison between the different cell-lines used in this study was difficult as although we managed to grow most of the cell-lines in the same media with the same supplements this was not possible for MCF10A cells. The MCF-10A required different media including large amount of supplements, including cholera toxin, EGF, hydrocortisone and insulin. Without these, this cell-line would not grow, but this difference in media supplements may result in some of the differences seen between the cell-lines. For future work it would be advantageous to use the same media for all the cell lines tested to ensure results seen were a result of the cell-line and not the supplements. The limitations of the different proliferation assays have already been discussed in chapter 3, but other *in vitro* phenotypic assays also had limitations. For example, in the scratch (wound healing) assay, creating identical scratches was difficult to re-produce among experiments resulting in different size scratches. The other limitation of this assay is that scratching of the monolayer can lead to damage of the extracellular matrix components, and cells resulting in the release of factors that may change the cell migration activity. In order to get round these difficulties the transwell migration or Boyden chamber assays could have been used, but money constraints prevented this.

As mentioned throughout the thesis there were some difficulties relating to some of the antibodies, with not all of them working in both Western blotting and IHC. Furthermore, the antibodies tended to be designed to pick up all cleavage products of the protein and not to distinguish between active and inactive forms. This is a common restriction of antibody based data where it is difficult to design antibodies to pick up only specific protein cleavage products.

For investigating the different proteins in breast tissue using IHC, tissue microarray slides were used, where a core was taken from each different breast tissue and then included into the same block and were subjected to the same conditions including temperature, solutions concentrations and the same period of incubations which are providing more consistent results. This is useful for consistency of staining, however the cores from each tissue were small (5mm) so only a small sample is taken from each patient sample, so some interesting observations may be missed using this method. It would have been good, had ethical approval been in place, to use whole sections of key tissues to get a bigger picture of what was happening. The advantage

of the microarray is that there was a large overall sample size, but a limitation was that the number of specimens in each group was relatively small.

Another limitation to this study is that we relied on using PPCs inhibitors including CMK and α1-PDX, and although the CMK inhibitor was effective in a previous study (Varshavsky et al., 2008), it showed no effect on our cells. However, one limitation of the CMK inhibitor is that is a pan-inhibitor which is a non-selective inhibitor of all individual PPCs. In addition, it has been reported to exhibit some cytotoxic effects and poor stability (Remacle et al., 2010), which prevented us from using more than 200 µmol/L to avoiding potential downsides of toxicity.

6.3 Future perspectives

The data shown in this thesis suggests that full-length SEMA3B inhibits breast cancer cell activity *in vitro* and that SEMA3B is cleaved in breast cancer cell-lines compared to normal breast epithelial cells. Although previous studies have suggested that the cleaved SEMA3B is inactive, it would be interesting to generate recombinant cleaved SEMA3B and treat the cells with it to confirm this supposition. In addition, one of the next key steps would be to design antibodies that distinguish between full-length and cleaved SEMA3B to truly establish whether the SEMA3B expressed in human tissue samples is cleaved with progression to breast cancer.

As our data suggest that PPCs are present where SEMA3B is expressed, with expression correlating, and the data from the α1-PDX study suggests that at least some of the PPCs may be involved in SEMA3B cleavage, the next step would be to identify which PPCs are involved. This could be done by using siRNA for specific PPCs to investigate which member is involved in SEMA3B cleavage. RNA interference by siRNA is a process in which double-stranded RNA complexes can target specific genes for silencing through transfection to allow genes in cultured cells to be silenced (Leung and Whittaker, 2005) and therefore suppress the relevant PPCs expression with varying degrees of efficacy which will allow to confirm the endogenous processing of SEMA3B and identify the convertase(s) involved in this processes. This is important since SEMA3B is a tumour suppressor so methods to generate full-length SEMA3B may be an effective anti-tumour agent. Hence, SEMA3B expression can be measured in PPCs knockdown cells by qRT-PCR and Western blotting and compared these cells to scrambled siRNA treated cells in order to assess their activity in phenotypic assays.

As α1-PDX resulted in the expression of full-length SEMA3B, it would be good to then investigate whether α1-PDX had an effect on tumour cell biology and could therefore be used as a potential therapy. This could be done by treating the cells *in vitro* and then analysing their proliferation, migration and invasion in comparison to untreated or vehicle treated control. Should α1-PDX treatment *in vitro* have an inhibitory effect on breast cancer cells, the studies could progress *in vivo* to establish whether α1-PDX will inhibit breast cancer growth and/or progression depending on the model used. The *in vivo* studies will also give an idea of the safety of the α1-PDX when used as a treatment in a whole body situation.

The other aspect of SEMA3B biology, which has not been investigated in this thesis, is that SEMA3B signals through a complex involving plexins and NP-1 and NP-2. This signalling complex is responsible for the downstream activity of SEMA3B in breast and endothelial cells, and therefore it would be advantageous to study plexin and NP-1 and NP-2 expression in a panel of breast diseases cells, and compare them to normal and benign tumours, and correlate them with SEMA3B expression. This would give a more complete picture of SEMA3B potential in the development of breast cancer.

6.4 Final conclusion

In conclusion, the data in this thesis have shown that wherever SEMA3B is expressed in pre-malignant and malignant breast tissue, it is likely to be cleaved and therefore inactive. The full-length SEMA3B has an anti-proliferative effect on cell growth of pre-invasive and invasive breast cancer cells and has a cytostatic effect on the proliferation of these cells, causing cell cycle arrest, but not apoptosis. In addition, full-length SEMA3B has proved successful in decreasing cancer cell migration and invasion in breast cancer. Our results further suggest that PPCs may contribute to tumour progression through the inactivation of the tumour suppressor activity of SEMA3B. Our results point to a potential beneficial effect of α1-PDX by inhibiting PPCs activity, resulting in re-emergence of full-length SEMA3B in breast cancer cells and therefore α1-PDX may potentially help in reducing tumour progression.

References

Abifadel, M., Varret, M., Rabes, J. P., Allard, D., Ouguerram, K., Devillers, M., Cruaud, C., Benjannet, S., Wickham, L., Erlich, D., Derre, A., Villeger, L., Farnier, M., Beucler, I., Bruckert, E., Chambaz, J., Chanu, B., Lecerf, J. M., Luc, G., Moulin, P., Weissenbach, J., Prat, A., Krempf, M., Junien, C., Seidah, N. G. and Boileau, C. (2003) 'Mutations in PCSK9 cause autosomal dominant hypercholesterolemia', *Nat Genet,* 34(2), pp. 154-6.

Adams, R. H., Lohrum, M., Klostermann, A., Betz, H. and Puschel, A. W. (1997) 'The chemorepulsive activity of secreted semaphorins is regulated by furin-dependent proteolytic processing', *Embo j,* 16(20), pp. 6077-86.

Ahmad, N., Ammar, A., Storr, S. J., Green, A. R., Rakha, E., Ellis, I. O. and Martin, S. G. (2018) 'IL-6 and IL-10 are associated with good prognosis in early stage invasive breast cancer patients', *Cancer immunology, immunotherapy : CII,* 67(4), pp. 537-549.

Aka, J. A. and Lin, S. X. (2012) 'Comparison of functional proteomic analyses of human breast cancer cell lines T47D and MCF7', *PLoS One,* 7(2), pp. e31532.

Akagi, M., Kawaguchi, M., Liu, W., McCarty, M. F., Takeda, A., Fan, F., Stoeltzing, O., Parikh, A. A., Jung, Y. D., Bucana, C. D., Mansfield, P. F., Hicklin, D. J. and Ellis, L. M. (2003) 'Induction of neuropilin-1 and vascular endothelial growth factor by epidermal growth factor in human gastric cancer cells', *Br J Cancer,* 88(5), pp. 796-802.

Allison, K. H. (2012) 'Molecular pathology of breast cancer: what a pathologist needs to know', *Am J Clin Pathol,* 138(6), pp. 770-80.

Anderson, E. D., Thomas, L., Hayflick, J. S. and Thomas, G. (1993) 'Inhibition of HIV-1 gp160-dependent membrane fusion by a furin-directed alpha 1-antitrypsin variant', *J Biol Chem,* 268(33), pp. 24887-91.

Anini, Y., Mayne, J., Gagnon, J., Sherbafi, J., Chen, A., Kaefer, N., Chretien, M. and Mbikay, M. (2010) 'Genetic deficiency for proprotein convertase subtilisin/kexin type 2 in mice is associated with decreased adiposity and protection from dietary fat-induced body weight gain', *Int J Obes (Lond),* 34(11), pp. 1599-607.

Appleton, B. A., Wu, P., Maloney, J., Yin, J., Liang, W. C., Stawicki, S., Mortara, K., Bowman, K. K., Elliott, J. M. and Desmarais, W. (2007) 'Structural studies of neuropilin/antibody complexes provide insights into semaphorin and VEGF binding', *The EMBO journal,* 26(23), pp. 4902-4912.

Arpino, G., Bardou, V. J., Clark, G. M. and Elledge, R. M. (2004) 'Infiltrating lobular carcinoma of the breast: tumor characteristics and clinical outcome', *Breast Cancer Res,* 6(3), pp. R149-56.

Arpino, G., Laucirica, R. and Elledge, R. M. (2005) 'Premalignant and in situ breast disease: biology and clinical implications', *Ann Intern Med,* 143(6), pp. 446-57.

Artenstein, A. W. and Opal, S. M. (2011) 'Proprotein convertases in health and disease', *N Engl J Med,* 365(26), pp. 2507-18.

Artigiani, S., Barberis, D., Fazzari, P., Longati, P., Angelini, P., van de Loo, J. W., Comoglio, P. M. and Tamagnone, L. (2003) 'Functional regulation of semaphorin receptors by proprotein convertases', *J Biol Chem,* 278(12), pp. 10094-101.

Avelar-Freitas, B. A., Almeida, V. G., Pinto, M. C., Mourao, F. A., Massensini, A. R., Martins-Filho, O. A., Rocha-Vieira, E. and Brito-Melo, G. E. (2014) 'Trypan blue exclusion assay by flow cytometry', *Braz J Med Biol Res,* 47(4), pp. 307-15.

Balmana, J., Diez, O., Rubio, I. T. and Cardoso, F. (2011) 'BRCA in breast cancer: ESMO Clinical Practice Guidelines', *Ann Oncol,* 22 Suppl 6, pp. vi31-4.

Band, A. M., Maatta, J., Kaariainen, L. and Kuismanen, E. (2001) 'Inhibition of the membrane fusion machinery prevents exit from the TGN and proteolytic processing by furin', *FEBS Lett,* 505(1), pp. 118-24.

Barr, P. J. (1991) 'Mammalian subtilisins: the long-sought dibasic processing endoproteases', *Cell,* 66(1), pp. 1-3.

Basak, A. (2005) 'Inhibitors of proprotein convertases', *Journal of Molecular Medicine,* 83(11), pp. 844-855.

Basak, A., Shervani, N. J., Mbikay, M. and Kolajova, M. (2008) 'Recombinant proprotein convertase 4 (PC4) from Leishmania tarentolae expression system: purification, biochemical study and inhibitor design', *Protein Expr Purif,* 60(2), pp. 117-26.

Basak, A., Touré, B. B., Lazure, C., Mbikay, M., Chrétien, M. and Seidah, N. G. (1999) 'Enzymic characterization in vitro of recombinant proprotein convertase PC4', *The Biochemical journal,* 343 Pt 1(Pt 1), pp. 29-37.

Bassi, D. E., Fu, J., Lopez de Cicco, R. and Klein-Szanto, A. J. (2005) 'Proprotein convertases: "master switches" in the regulation of tumor growth and progression', *Mol Carcinog,* 44(3), pp. 151-61.

Bassi, D. E., Lopez De Cicco, R., Mahloogi, H., Zucker, S., Thomas, G. and Klein-Szanto, A. J. (2001a) 'Furin inhibition results in absent or decreased invasiveness and tumorigenicity of human cancer cells', *Proc Natl Acad Sci U S A,* 98(18), pp. 10326-31.

Bassi, D. E., Mahloogi, H., Al-Saleem, L., Lopez De Cicco, R., Ridge, J. A. and Klein-Szanto, A. J. (2001b) 'Elevated furin expression in aggressive human head and neck tumors and tumor cell lines', *Mol Carcinog,* 31(4), pp. 224-32.

Bassi, D. E., Mahloogi, H. and Klein-Szanto, A. J. (2000) 'The proprotein convertases furin and PACE4 play a significant role in tumor progression', *Mol Carcinog,* 28(2), pp. 63-9.

Bassi, D. E., Mahloogi, H., Lopez De Cicco, R. and Klein-Szanto, A. (2003) 'Increased furin activity enhances the malignant phenotype of human head and neck cancer cells', *Am J Pathol,* 162(2), pp. 439-47.

Bassi, D. E., Zhang, J., Cenna, J., Litwin, S., Cukierman, E. and Klein-Szanto, A. J. P. (2010) 'Proprotein convertase inhibition results in decreased skin cell proliferation, tumorigenesis, and metastasis', *Neoplasia (New York, N.Y.),* 12(7), pp. 516-526.

Bassi, D. E., Zhang, J., Renner, C. and Klein-Szanto, A. J. (2017) 'Targeting proprotein convertases in furin-rich lung cancer cells results in decreased in vitro and in vivo growth', *Mol Carcinog,* 56(3), pp. 1182-1188.

Bender, R. J. and Mac Gabhann, F. (2013) 'Expression of VEGF and semaphorin genes define subgroups of triple negative breast cancer', *PLoS One,* 8(5), pp. e61788.

Benjannet, S., Rhainds, D., Essalmani, R., Mayne, J., Wickham, L., Jin, W., Asselin, M. C., Hamelin, J., Varret, M., Allard, D., Trillard, M., Abifadel, M., Tebon, A., Attie, A. D., Rader, D. J., Boileau, C., Brissette, L., Chretien, M., Prat, A. and Seidah, N. G. (2004) 'NARC-1/PCSK9 and its natural mutants: zymogen cleavage and effects on the low density lipoprotein (LDL) receptor and LDL cholesterol', *J Biol Chem,* 279(47), pp. 48865-75.

Benjannet, S., Savaria, D., Laslop, A., Munzer, J. S., Chrétien, M., Marcinkiewicz, M. and Seidah, N. G. (1997) 'α1-Antitrypsin Portland Inhibits Processing of Precursors Mediated by Proprotein Convertases Primarily within the Constitutive Secretory Pathway', *Journal of Biological Chemistry,* 272(42), pp. 26210-26218.

Benoy, I. H., Salgado, R., Van Dam, P., Geboers, K., Van Marck, E., Scharpe, S., Vermeulen, P. B. and Dirix, L. Y. (2004) 'Increased serum interleukin-8 in patients with early and metastatic breast cancer correlates with early dissemination and survival', *Clin Cancer Res,* 10(21), pp. 7157-62.

Bessette, D. C., Tilch, E., Seidens, T., Quinn, M. C., Wiegmans, A. P., Shi, W., Cocciardi, S., McCart-Reed, A., Saunus, J. M., Simpson, P. T., Grimmond, S. M., Lakhani, S. R., Khanna, K. K., Waddell, N., Al-Ejeh, F. and Chenevix-Trench, G. (2015) 'Using the MCF10A/MCF10CA1a Breast Cancer Progression Cell Line Model to Investigate the Effect of Active, Mutant Forms of EGFR in Breast Cancer Development and Treatment Using Gefitinib', *PLoS One,* 10(5), pp. e0125232.

Bessonnard, S., Mesnard, D. and Constam, D. B. (2015) 'PC7 and the related proteases Furin and Pace4 regulate E-cadherin function during blastocyst formation', *J Cell Biol,* 210(7), pp. 1185-97.

Bhat, M., Skill, N., Marcus, V., Deschenes, M., Tan, X., Bouteaud, J., Negi, S., Awan, Z., Aikin, R., Kwan, J., Amre, R., Tabaries, S., Hassanain, M., Seidah, N. G., Maluccio, M., Siegel, P. and Metrakos,

P. (2015) 'Decreased PCSK9 expression in human hepatocellular carcinoma', *BMC Gastroenterol,* 15, pp. 176.

Bhattacharjee, H. K., Bansal, V. K., Nepal, B., Srivastava, S., Dinda, A. K. and Misra, M. C. (2016) 'Is Interleukin 10 (IL10) Expression in Breast Cancer a Marker of Poor Prognosis?', *Indian journal of surgical oncology,* 7(3), pp. 320-325.

Bielenberg, D. R., Pettaway, C. A., Takashima, S. and Klagsbrun, M. (2006) 'Neuropilins in neoplasms: expression, regulation, and function', *Exp Cell Res,* 312(5), pp. 584-93.

Blanco, E. H., Ramos-Molina, B. and Lindberg, I. (2015) 'Revisiting PC1/3 Mutants: Dominant-Negative Effect of Endoplasmic Reticulum-Retained Mutants', *Endocrinology,* 156(10), pp. 3625-3637.

Bombonati, A. and Sgroi, D. C. (2011) 'The molecular pathology of breast cancer progression', *J Pathol,* 223(2), pp. 307-17.

Brodaczewska, K. K., Szczylik, C., Fiedorowicz, M., Porta, C. and Czarnecka, A. M. (2016) 'Choosing the right cell line for renal cell cancer research', *Mol Cancer,* 15(1), pp. 83.

Burbee, D. G., Forgacs, E., Zochbauer-Muller, S., Shivakumar, L., Fong, K., Gao, B., Randle, D., Kondo, M., Virmani, A., Bader, S., Sekido, Y., Latif, F., Milchgrub, S., Toyooka, S., Gazdar, A. F., Lerman, M. I., Zabarovsky, E., White, M. and Minna, J. D. (2001) 'Epigenetic inactivation of RASSF1A in lung and breast cancers and malignant phenotype suppression', *J Natl Cancer Inst,* 93(9), pp. 691-9.

Butti, R., Kumar, T. V., Nimma, R. and Kundu, G. C. (2018) 'Impact of semaphorin expression on prognostic characteristics in breast cancer', *Breast cancer (Dove Medical Press),* 10, pp. 79-88.

Capparuccia, L. and Tamagnone, L. (2009) 'Semaphorin signaling in cancer cells and in cells of the tumor microenvironment–two sides of a coin', *Journal of cell science,* 122(11), pp. 1723-1736.

Carraro, Dirce M., Elias, Eliana V. and Andrade, Victor P. (2014) 'Ductal carcinoma in situ of the breast: morphological and molecular features implicated in progression', *Bioscience Reports,* 34(1), pp. e00090.

Carrer, A., Zacchigna, S., Balani, A., Pistan, V., Adami, A., Porcelli, F., Scaramucci, M., Roseano, M., Turoldo, A., Prati, M. C., Dell'Omodarme, M., de Manzini, N. and Giacca, M. (2008) 'Expression profiling of angiogenic genes for the characterisation of colorectal carcinoma', *Eur J Cancer,* 44(12), pp. 1761-9.

Casazza, A., Kigel, B., Maione, F., Capparuccia, L., Kessler, O., Giraudo, E., Mazzone, M., Neufeld, G. and Tamagnone, L. (2012) 'Tumour growth inhibition and anti-metastatic activity of a mutated furin-resistant Semaphorin 3E isoform', *EMBO Mol Med,* 4(3), pp. 234-50.

Castro-Rivera, E. (2005) *The Role of Semaphorin 3B (SEMA3B) in the Pathogenesis of Breast Cancer*: TEXAS UNIV AT DALLAS SOUTHWESTERN MEDICAL CENTER.

Castro-Rivera, E., Ran, S., Brekken, R. A. and Minna, J. D. (2008) 'Semaphorin 3B inhibits the phosphatidylinositol 3-kinase/Akt pathway through neuropilin-1 in lung and breast cancer cells', *Cancer Res,* 68(20), pp. 8295-303.

Castro-Rivera, E., Ran, S., Thorpe, P. and Minna, J. D. (2004) 'Semaphorin 3B (SEMA3B) induces apoptosis in lung and breast cancer, whereas VEGF165 antagonizes this effect', *Proc Natl Acad Sci U S A,* 101(31), pp. 11432-7.

Cepeda, M. A., Pelling, J. J., Evered, C. L., Williams, K. C., Freedman, Z., Stan, I., Willson, J. A., Leong, H. S. and Damjanovski, S. (2016) 'Less is more: low expression of MT1-MMP is optimal to promote migration and tumourigenesis of breast cancer cells', *Mol Cancer,* 15(1), pp. 65.

Chavey, C., Bibeau, F., Gourgou-Bourgade, S., Burlinchon, S., Boissière, F., Laune, D., Roques, S. and Lazennec, G. (2007) 'Oestrogen receptor negative breast cancers exhibit high cytokine content', *Breast cancer research : BCR,* 9(1), pp. R15-R15.

Chen, R., Zhuge, X., Huang, Z., Lu, D., Ye, X., Chen, C., Yu, J. and Lu, G. (2014) 'Analysis of SEMA3B methylation and expression patterns in gastric cancer tissue and cell lines', *Oncol Rep,* 31(3), pp. 1211-8.

Cheng, M., Watson, P. H., Paterson, J. A., Seidah, N., Chretien, M. and Shiu, R. P. (1997) 'Pro-protein convertase gene expression in human breast cancer', *Int J Cancer,* 71(6), pp. 966-71.

Chevallet, M., Diemer, H., Van Dorssealer, A., Villiers, C. and Rabilloud, T. (2007) 'Toward a better analysis of secreted proteins: the example of the myeloid cells secretome', *Proteomics,* 7(11), pp. 1757-70.

Christensen, C., Ambartsumian, N., Gilestro, G., Thomsen, B., Comoglio, P., Tamagnone, L., Guldberg, P. and Lukanidin, E. (2005) 'Proteolytic processing converts the repelling signal Sema3E into an inducer of invasive growth and lung metastasis', *Cancer Res,* 65(14), pp. 6167-77.

Coppola, J. M., Bhojani, M. S., Ross, B. D. and Rehemtulla, A. (2008) 'A small-molecule furin inhibitor inhibits cancer cell motility and invasiveness', *Neoplasia (New York, N.Y.),* 10(4), pp. 363-370.

Couture, F., D'Anjou, F. and Day, R. (2011) 'On the cutting edge of proprotein convertase pharmacology: from molecular concepts to clinical applications', *Biomolecular concepts,* 2(5), pp. 421-438.

Couture, F., D'Anjou, F., Desjardins, R., Boudreau, F. and Day, R. (2012) 'Role of proprotein convertases in prostate cancer progression', *Neoplasia (New York, N.Y.),* 14(11), pp. 1032-1042.

Couture, F., Ly, K., Levesque, C., Kwiatkowska, A., Ait-Mohand, S., Desjardins, R., Guerin, B. and Day, R. (2015) 'Multi-Leu PACE4 Inhibitor Retention within Cells Is PACE4 Dependent and a Prerequisite for Antiproliferative Activity', *Biomed Res Int,* 2015, pp. 824014.

Couture, F., Sabbagh, R., Kwiatkowska, A., Desjardins, R., Guay, S. P., Bouchard, L. and Day, R. (2017) 'PACE4 Undergoes an Oncogenic Alternative Splicing Switch in Cancer', *Cancer Res,* 77(24), pp. 6863-6879.

Cowell, C. F., Weigelt, B., Sakr, R. A., Ng, C. K. Y., Hicks, J., King, T. A. and Reis-Filho, J. S. (2013) 'Progression from ductal carcinoma in situ to invasive breast cancer: Revisited', *Molecular Oncology,* 7(5), pp. 859-869.

Creemers, J. W., Choquet, H., Stijnen, P., Vatin, V., Pigeyre, M., Beckers, S., Meulemans, S., Than, M. E., Yengo, L., Tauber, M., Balkau, B., Elliott, P., Jarvelin, M. R., Van Hul, W., Van Gaal, L., Horber, F., Pattou, F., Froguel, P. and Meyre, D. (2012) 'Heterozygous mutations causing partial prohormone convertase 1 deficiency contribute to human obesity', *Diabetes,* 61(2), pp. 383-90.

Creemers, J. W. and Khatib, A. M. (2008) 'Knock-out mouse models of proprotein convertases: unique functions or redundancy?', *Front Biosci,* 13, pp. 4960-71.

Creemers, J. W., Roebroek, A. J. and Van de Ven, W. J. (1992) 'Expression in human lung tumor cells of the proprotein processing enzyme PC1/PC3. Cloning and primary sequence of a 5 kb cDNA', *FEBS Lett,* 300(1), pp. 82-8.

CRUK (2015) *Breast cancer incidence statistics*. United Kingdom: Cancer Research UK. Available at: http://www.cancerresearchuk.org/health-professional/cancer-statistics/statistics-by-cancer-type/breast-cancer/incidence-invasive#ref-0 (Accessed: December 2015 2015).

D'Anjou, F., Routhier, S., Perreault, J.-P., Latil, A., Bonnel, D., Fournier, I., Salzet, M. and Day, R. (2011) 'Molecular Validation of PACE4 as a Target in Prostate Cancer', *Translational oncology,* 4(3), pp. 157-172.

da Costa Prando, E., Cavalli, L. R. and Rainho, C. A. (2011) 'Evidence of epigenetic regulation of the tumor suppressor gene cluster flanking RASSF1 in breast cancer cell lines', *Epigenetics,* 6(12), pp. 1413-24.

Dammann, R., Yang, G. and Pfeifer, G. P. (2001) 'Hypermethylation of the cpG island of Ras association domain family 1A (RASSF1A), a putative tumor suppressor gene from the 3p21.3 locus, occurs in a large percentage of human breast cancers', *Cancer Res,* 61(7), pp. 3105-9.

Dawson, P. J., Wolman, S. R., Tait, L., Heppner, G. H. and Miller, F. R. (1996) 'MCF10AT: a model for the evolution of cancer from proliferative breast disease', *Am J Pathol,* 148(1), pp. 313-9.

DeBerardinis, R. J. (2008) 'Is cancer a disease of abnormal cellular metabolism? New angles on an old idea', *Genet Med,* 10(11), pp. 767-77.

DeBerardinis, R. J. and Chandel, N. S. (2016) 'Fundamentals of cancer metabolism', *Science advances,* 2(5), pp. e1600200-e1600200.

Declercq, J., Brouwers, B., Pruniau, V. P., Stijnen, P., Tuand, K., Meulemans, S., Prat, A., Seidah, N. G., Khatib, A. M. and Creemers, J. W. (2015) 'Liver-Specific Inactivation of the Proprotein Convertase FURIN Leads to Increased Hepatocellular Carcinoma Growth', *Biomed Res Int,* 2015, pp. 148651.

Demidyuk, I. V., Shubin, A. V., Gasanov, E. V., Kurinov, A. M., Demkin, V. V., Vinogradova, T. V., Zinovyeva, M. V., Sass, A. V., Zborovskaya, I. B. and Kostrov, S. V. (2013) 'Alterations in gene expression of proprotein convertases in human lung cancer have a limited number of scenarios', *PLoS One,* 8(2), pp. e55752.

Denault, J., Bissonnette, L., Longpre, J., Charest, G., Lavigne, P. and Leduc, R. (2002) 'Ectodomain shedding of furin: kinetics and role of the cysteine-rich region', *FEBS Lett,* 527(1-3), pp. 309-14.

Dias, K., Dvorkin-Gheva, A., Hallett, R. M., Wu, Y., Hassell, J., Pond, G. R., Levine, M., Whelan, T. and Bane, A. L. (2017) 'Claudin-Low Breast Cancer; Clinical & Pathological Characteristics', *PloS one,* 12(1), pp. e0168669-e0168669.

Dikeakos, J. D., Mercure, C., Lacombe, M. J., Seidah, N. G. and Reudelhuber, T. L. (2007) 'PC1/3, PC2 and PC5/6A are targeted to dense core secretory granules by a common mechanism', *Febs j,* 274(16), pp. 4094-102.

Dubuc, G., Chamberland, A., Wassef, H., Davignon, J., Seidah, N. G., Bernier, L. and Prat, A. (2004) 'Statins upregulate PCSK9, the gene encoding the proprotein convertase neural apoptosis-regulated convertase-1 implicated in familial hypercholesterolemia', *Arterioscler Thromb Vasc Biol,* 24(8), pp. 1454-9.

Duhamel, M., Rodet, F., Delhem, N., Vanden Abeele, F., Kobeissy, F., Nataf, S., Pays, L., Desjardins, R., Gagnon, H., Wisztorski, M., Fournier, I., Day, R. and Salzet, M. (2015) 'Molecular Consequences of Proprotein Convertase 1/3 (PC1/3) Inhibition in Macrophages for Application to Cancer Immunotherapy: A Proteomic Study', *Mol Cell Proteomics,* 14(11), pp. 2857-77.

Dunigan, D. D., Waters, S. B. and Owen, T. C. (1995) 'Aqueous soluble tetrazolium/formazan MTS as an indicator of NADH- and NADPH-dependent dehydrogenase activity', *Biotechniques,* 19(4), pp. 640-9.

Dupont, W. D. and Page, D. L. (1985) 'Risk factors for breast cancer in women with proliferative breast disease', *N Engl J Med,* 312(3), pp. 146-51.

Dupont, W. D., Parl, F. F., Hartmann, W. H., Brinton, L. A., Winfield, A. C., Worrell, J. A., Schuyler, P. A. and Plummer, W. D. (1993) 'Breast cancer risk associated with proliferative breast disease and atypical hyperplasia', *Cancer,* 71(4), pp. 1258-65.

Dworkin, A. M., Huang, T. H. M. and Toland, A. E. (2009) 'Epigenetic alterations in the breast: Implications for breast cancer detection, prognosis and treatment', *Seminars in cancer biology,* 19(3), pp. 165-171.

Eastwood, S. L., Law, A. J., Everall, I. P. and Harrison, P. J. (2003) 'The axonal chemorepellant semaphorin 3A is increased in the cerebellum in schizophrenia and may contribute to its synaptic pathology', *Mol Psychiatry,* 8(2), pp. 148-55.

Ellis, L. M. (2006) 'The role of neuropilins in cancer', *Mol Cancer Ther,* 5(5), pp. 1099-107.

Engels, C. C., Fontein, D. B., Kuppen, P. J., de Kruijf, E. M., Smit, V. T., Nortier, J. W., Liefers, G. J., van de Velde, C. J. and Bastiaannet, E. (2014) 'Immunological subtypes in breast cancer are prognostic for invasive ductal but not for invasive lobular breast carcinoma', *Br J Cancer,* 111(3), pp. 532-8.

Eroles, P., Bosch, A., Perez-Fidalgo, J. A. and Lluch, A. (2012) 'Molecular biology in breast cancer: intrinsic subtypes and signaling pathways', *Cancer Treat Rev,* 38(6), pp. 698-707.

Esquivel-Velazquez, M., Ostoa-Saloma, P., Palacios-Arreola, M. I., Nava-Castro, K. E., Castro, J. I. and Morales-Montor, J. (2015) 'The role of cytokines in breast cancer development and progression', *J Interferon Cytokine Res,* 35(1), pp. 1-16.

Essalmani, R., Hamelin, J., Marcinkiewicz, J., Chamberland, A., Mbikay, M., Chretien, M., Seidah, N. G. and Prat, A. (2006) 'Deletion of the gene encoding proprotein convertase 5/6 causes early embryonic lethality in the mouse', *Mol Cell Biol,* 26(1), pp. 354-61.

Eubank, T. D., Roberts, R., Galloway, M., Wang, Y., Cohn, D. E. and Marsh, C. B. (2004) 'GM-CSF induces expression of soluble VEGF receptor-1 from human monocytes and inhibits angiogenesis in mice', *Immunity,* 21(6), pp. 831-42.

Fowble, B., Hanlon, A. L., Patchefsky, A., Freedman, G., Hoffman, J. P., Sigurdson, E. R. and Goldstein, L. J. (1998) 'The presence of proliferative breast disease with atypia does not significantly influence outcome in early-stage invasive breast cancer treated with conservative surgery and radiation', *Int J Radiat Oncol Biol Phys,* 42(1), pp. 105-15.

Friedenreich, C., Bryant, H., Alexander, F., Hugh, J., Danyluk, J. and Page, D. (2000) 'Risk factors for benign proliferative breast disease', *Int J Epidemiol,* 29(4), pp. 637-44.

Fu, Y., Campbell, E. J., Shepherd, T. G. and Nachtigal, M. W. (2003) 'Epigenetic regulation of proprotein convertase PACE4 gene expression in human ovarian cancer cells', *Mol Cancer Res,* 1(8), pp. 569-76.

Fugere, M., Limperis, P. C., Beaulieu-Audy, V., Gagnon, F., Lavigne, P., Klarskov, K., Leduc, R. and Day, R. (2002) 'Inhibitory potency and specificity of subtilase-like pro-protein convertase (SPC) prodomains', *J Biol Chem,* 277(10), pp. 7648-56.

Futamura, M., Kamino, H., Miyamoto, Y., Kitamura, N., Nakamura, Y., Ohnishi, S., Masuda, Y. and Arakawa, H. (2007) 'Possible role of semaphorin 3F, a candidate tumor suppressor gene at 3p21.3, in p53-regulated tumor angiogenesis suppression', *Cancer Res,* 67(4), pp. 1451-60.

Garcia-Tunon, I., Ricote, M., Ruiz, A. A., Fraile, B., Paniagua, R. and Royuela, M. (2007) 'Influence of IFN-gamma and its receptors in human breast cancer', *BMC Cancer,* 7, pp. 158.

Gaur, P., Bielenberg, D. R., Samuel, S., Bose, D., Zhou, Y., Gray, M. J., Dallas, N. A., Fan, F., Xia, L. and Lu, J. (2009) 'Role of class 3 semaphorins and their receptors in tumor growth and angiogenesis', *Clinical Cancer Research,* 15(22), pp. 6763-6770.

Gensberg, K., Jan, S. and Matthews, G. M. (1998) 'Subtilisin-related serine proteases in the mammalian constitutive secretory pathway', *Semin Cell Dev Biol,* 9(1), pp. 11-7.

Geraghty, R. J., Capes-Davis, A., Davis, J. M., Downward, J., Freshney, R. I., Knezevic, I., Lovell-Badge, R., Masters, J. R., Meredith, J., Stacey, G. N., Thraves, P. and Vias, M. (2014) 'Guidelines for the use of cell lines in biomedical research', *Br J Cancer,* 111(6), pp. 1021-46.

Geretti, E., Shimizu, A. and Klagsbrun, M. (2008) 'Neuropilin structure governs VEGF and semaphorin binding and regulates angiogenesis', *Angiogenesis,* 11(1), pp. 31-9.

Ghosh, R., Gilda, J. E. and Gomes, A. V. (2014) 'The necessity of and strategies for improving confidence in the accuracy of western blots', *Expert review of proteomics,* 11(5), pp. 549-560.

Glerup, S., Schulz, R., Laufs, U. and Schlüter, K.-D. (2017) 'Physiological and therapeutic regulation of PCSK9 activity in cardiovascular disease', *Basic Research in Cardiology,* 112(3), pp. 32.

Gluzman-Poltorak, Z., Cohen, T., Herzog, Y. and Neufeld, G. (2000) 'Neuropilin-2 is a receptor for the vascular endothelial growth factor (VEGF) forms VEGF-145 and VEGF-165 [corrected]', *The Journal of biological chemistry,* 275(24), pp. 18040-18045.

Gooch, J. L., Herrera, R. E. and Yee, D. (2000) 'The role of p21 in interferon gamma-mediated growth inhibition of human breast cancer cells', *Cell growth & differentiation: the molecular biology journal of the American Association for Cancer Research,* 11(6), pp. 335-342.

Grote, H. J., Schmiemann, V., Geddert, H., Rohr, U. P., Kappes, R., Gabbert, H. E. and Böcking, A. (2005) 'Aberrant promoter methylation of p16INK4a, RARB2 and SEMA3B in bronchial aspirates from patients with suspected lung cancer', *International Journal of Cancer,* 116(5), pp. 720-725.

Gu, C., Yoshida, Y., Livet, J., Reimert, D. V., Mann, F., Merte, J., Henderson, C. E., Jessell, T. M., Kolodkin, A. L. and Ginty, D. D. (2005) 'Semaphorin 3E and plexin-D1 control vascular pattern independently of neuropilins', *Science,* 307(5707), pp. 265-8.

Guillemot, J., Canuel, M., Essalmani, R., Prat, A. and Seidah, N. G. (2013) 'Implication of the proprotein convertases in iron homeostasis: proprotein convertase 7 sheds human transferrin receptor 1 and furin activates hepcidin', *Hepatology,* 57(6), pp. 2514-24.

Gupta, G. P. and Massague, J. (2006) 'Cancer metastasis: building a framework', *Cell,* 127(4), pp. 679-95.

Guray, M. and Sahin, A. A. (2006) 'Benign breast diseases: classification, diagnosis, and management', *Oncologist,* 11(5), pp. 435-49.

Guttmann-Raviv, N., Shraga-Heled, N., Varshavsky, A., Guimaraes-Sternberg, C., Kessler, O. and Neufeld, G. (2007) 'Semaphorin-3A and semaphorin-3F work together to repel endothelial cells and to inhibit their survival by induction of apoptosis', *J Biol Chem,* 282(36), pp. 26294-305.

Gyamera-Acheampong, C. and Mbikay, M. (2009) 'Proprotein convertase subtilisin/kexin type 4 in mammalian fertility: a review', *Hum Reprod Update,* 15(2), pp. 237-47.

Hada, K., Isshiki, K., Matsuda, S., Yuasa, K. and Tsuji, A. (2012) 'Engineering of α1-antitrypsin variants with improved specificity for the proprotein convertase furin using site-directed random mutagenesis', *Protein Engineering, Design and Selection,* 26(2), pp. 123-131.

Hallenberger, S., Bosch, V., Angliker, H., Shaw, E., Klenk, H. D. and Garten, W. (1992) 'Inhibition of furin-mediated cleavage activation of HIV-1 glycoprotein gp160', *Nature,* 360(6402), pp. 358-61.

Hamidullah, Changkija, B. and Konwar, R. (2012) 'Role of interleukin-10 in breast cancer', *Breast Cancer Res Treat,* 133(1), pp. 11-21.

Harvat, B. L. and Jetten, A. (1996) 'Gamma-interferon induces an irreversible growth arrest in mid-G1 in mammary epithelial cells which correlates with a block in hyperphosphorylation of retinoblastoma', *Cell growth & differentiation: the molecular biology journal of the American Association for Cancer Research,* 7(3), pp. 289-300.

Herzog, Y., Kalcheim, C., Kahane, N., Reshef, R. and Neufeld, G. (2001) 'Differential expression of neuropilin-1 and neuropilin-2 in arteries and veins', *Mech Dev,* 109(1), pp. 115-9.

Hesson, L., Bièche, I., Krex, D., Criniere, E., Hoang-Xuan, K., Maher, E. R. and Latif, F. (2004) 'Frequent epigenetic inactivation of RASSF1A and BLU genes located within the critical 3p21. 3 region in gliomas', *Oncogene,* 23(13), pp. 2408-2419.

Hirohashi, S. (1998) 'Inactivation of the E-cadherin-mediated cell adhesion system in human cancers', *Am J Pathol,* 153(2), pp. 333-9.

Holliday, D. L. and Speirs, V. (2011) 'Choosing the right cell line for breast cancer research', *Breast Cancer Res,* 13(4), pp. 215.

Hoshino, A., Kowalska, D., Jean, F., Lazure, C. and Lindberg, I. (2011) 'Modulation of PC1/3 activity by self-interaction and substrate binding', *Endocrinology,* 152(4), pp. 1402-11.

Hota, P. K. and Buck, M. (2012) 'Plexin structures are coming: opportunities for multilevel investigations of semaphorin guidance receptors, their cell signaling mechanisms, and functions', *Cellular and Molecular Life Sciences,* 69(22), pp. 3765-3805.

Hu, J., La Vecchia, C., de Groh, M., Negri, E., Morrison, H. and Mery, L. (2012) 'Dietary cholesterol intake and cancer', *Ann Oncol,* 23(2), pp. 491-500.

Hu, M., Yao, J., Carroll, D. K., Weremowicz, S., Chen, H., Carrasco, D., Richardson, A., Violette, S., Nikolskaya, T., Nikolsky, Y., Bauerlein, E. L., Hahn, W. C., Gelman, R. S., Allred, C., Bissell, M. J., Schnitt, S. and Polyak, K. (2008) 'Regulation of in situ to invasive breast carcinoma transition', *Cancer Cell,* 13(5), pp. 394-406.

Huang, S., Ullrich, S. E. and Bar-Eli, M. (1999) 'Regulation of tumor growth and metastasis by interleukin-10: the melanoma experience', *J Interferon Cytokine Res,* 19(7), pp. 697-703.

Hubbard, F. C., Goodrow, T. L., Liu, S. C., Brilliant, M. H., Basset, P., Mains, R. E. and Klein-Szanto, A. J. (1997) 'Expression of PACE4 in chemically induced carcinomas is associated with spindle cell tumor conversion and increased invasive ability', *Cancer Res,* 57(23), pp. 5226-31.

Hulkower, K. I. and Herber, R. L. (2011) 'Cell migration and invasion assays as tools for drug discovery', *Pharmaceutics,* 3(1), pp. 107-124.

Hunter, K. W., Crawford, N. P. S. and Alsarraj, J. (2008) 'Mechanisms of metastasis', *Breast cancer research : BCR,* 10 Suppl 1(Suppl 1), pp. S2-S2.

Ingvarsson, S., Eiriksdóttir, G., Bergþórsson, J. Þ., Sigurðsson, H., Guðmundsson, J., Skírnisdóttir, S., Egilsson, V. and Barkardóttir, R. B. (2015) 'Mapping of chromosome 3 alterations in human breast cancer using microsatellite PCR markers: Correlation with clinical variables'.

Ito, M., Ito, G., Kondo, M., Uchiyama, M., Fukui, T., Mori, S., Yoshioka, H., Ueda, Y., Shimokata, K. and Sekido, Y. (2005) 'Frequent inactivation of RASSF1A, BLU, and SEMA3B on 3p21.3 by promoter hypermethylation and allele loss in non-small cell lung cancer', *Cancer Lett,* 225(1), pp. 131-9.

Jaaks, P. and Bernasconi, M. (2017) 'The proprotein convertase furin in tumour progression', *Int J Cancer,* 141(4), pp. 654-663.

Jesinger, R. A. (2014) 'Breast anatomy for the interventionalist', *Tech Vasc Interv Radiol,* 17(1), pp. 3-9.

Ji, L., Nishizaki, M., Gao, B., Burbee, D., Kondo, M., Kamibayashi, C., Xu, K., Yen, N., Atkinson, E. N. and Fang, B. (2002) 'Expression of several genes in the human chromosome 3p21. 3 homozygous deletion region by an adenovirus vector results in tumor suppressor activities in vitro and in vivo', *Cancer research,* 62(9), pp. 2715-2720.

Jin, X. and Mu, P. (2015) 'Targeting Breast Cancer Metastasis', *Breast cancer : basic and clinical research,* 9(Suppl 1), pp. 23-34.

Johno, H., Takahashi, S. and Kitamura, M. (2010) 'Influences of acidic conditions on formazan assay: a cautionary note', *Appl Biochem Biotechnol,* 162(6), pp. 1529-35.

Johnstone, C. N., Chand, A., Putoczki, T. L. and Ernst, M. (2015) 'Emerging roles for IL-11 signaling in cancer development and progression: Focus on breast cancer', *Cytokine Growth Factor Rev,* 26(5), pp. 489-98.

Joseph, D., Ho, S. M. and Syed, V. (2010) 'Hormonal regulation and distinct functions of semaphorin-3B and semaphorin-3F in ovarian cancer', *Mol Cancer Ther,* 9(2), pp. 499-509.

Julien, F., Bechara, A., Fiore, R., Nawabi, H., Zhou, H., Hoyo-Becerra, C., Bozon, M., Rougon, G., Grumet, M. and Püschel, A. W. (2005) 'Dual functional activity of semaphorin 3B is required for positioning the anterior commissure', *Neuron,* 48(1), pp. 63-75.

Jung, S., Wang, M., Anderson, K., Baglietto, L., Bergkvist, L., Bernstein, L., van den Brandt, P. A., Brinton, L., Buring, J. E., Eliassen, A. H., Falk, R., Gapstur, S. M., Giles, G. G., Goodman, G., Hoffman-Bolton, J., Horn-Ross, P. L., Inoue, M., Kolonel, L. N., Krogh, V., Lof, M., Maas, P., Miller, A. B., Neuhouser, M. L., Park, Y., Robien, K., Rohan, T. E., Scarmo, S., Schouten, L. J., Sieri, S., Stevens, V. L., Tsugane, S., Visvanathan, K., Wilkens, L. R., Wolk, A., Weiderpass, E., Willett, W. C., Zeleniuch-Jacquotte, A., Zhang, S. M., Zhang, X., Ziegler, R. G. and Smith-Warner, S. A. (2016) 'Alcohol consumption and breast cancer risk by estrogen receptor status: in a pooled analysis of 20 studies', *International journal of epidemiology,* 45(3), pp. 916-928.

Justus, C. R., Leffler, N., Ruiz-Echevarria, M. and Yang, L. V. (2014) 'In vitro cell migration and invasion assays', *J Vis Exp,* (88).

Khatib, A. M., Siegfried, G., Prat, A., Luis, J., Chretien, M., Metrakos, P. and Seidah, N. G. (2001) 'Inhibition of proprotein convertases is associated with loss of growth and tumorigenicity of HT-29 human colon carcinoma cells: importance of insulin-like growth factor-1 (IGF-1) receptor processing in IGF-1-mediated functions', *J Biol Chem,* 276(33), pp. 30686-93.

Kim, H. S., Jung, M., Choi, S. K., Moon, W. K. and Kim, S. J. (2016) 'Different Biological Action of Oleic Acid in ALDHhigh and ALDHlow Subpopulations Separated from Ductal Carcinoma In Situ of Breast Cancer', *PLoS One,* 11(9), pp. e0160835.

Klein-Szanto, A. J. and Bassi, D. E. (2017) 'Proprotein convertase inhibition: Paralyzing the cell's master switches', *Biochem Pharmacol,* 140, pp. 8-15.

Konoshita, T., Gasc, J. M., Villard, E., Takeda, R., Seidah, N. G., Corvol, P. and Pinet, F. (1994) 'Expression of PC2 and PC1/PC3 in human pheochromocytomas', *Mol Cell Endocrinol,* 99(2), pp. 307-14.

Koukoulis, G. K., Virtanen, I., Korhonen, M., Laitinen, L., Quaranta, V. and Gould, V. E. (1991) 'Immunohistochemical localization of integrins in the normal, hyperplastic, and neoplastic breast. Correlations with their functions as receptors and cell adhesion molecules', *Am J Pathol,* 139(4), pp. 787-99.

Kozlowski, L., Zakrzewska, I., Tokajuk, P. and Wojtukiewicz, M. Z. (2003) 'Concentration of interleukin-6 (IL-6), interleukin-8 (IL-8) and interleukin-10 (IL-10) in blood serum of breast cancer patients', *Rocz Akad Med Bialymst,* 48, pp. 82-4.

Kroemer, G. and Pouyssegur, J. (2008) 'Tumor Cell Metabolism: Cancer's Achilles' Heel', *Cancer Cell,* 13(6), pp. 472-482.

Kruger, R. P., Aurandt, J. and Guan, K.-L. (2005) 'Semaphorins command cells to move', *Nature Reviews Molecular Cell Biology,* 6(10), pp. 789-800.

Kuroki, T., Trapasso, F., Yendamuri, S., Matsuyama, A., Alder, H., Williams, N. N., Kaiser, L. R. and Croce, C. M. (2003) 'Allelic loss on chromosome 3p21.3 and promoter hypermethylation of semaphorin 3B in non-small cell lung cancer', *Cancer Res,* 63(12), pp. 3352-5.

Laisupasin, P., Thompat, W., Sukarayodhin, S., Sornprom, A. and Sudjaroen, Y. (2013) 'Comparison of Serum Lipid Profiles between Normal Controls and Breast Cancer Patients', *J Lab Physicians,* 5(1), pp. 38-41.

Lakhani, S. R., Collins, N., Stratton, M. R. and Sloane, J. P. (1995) 'Atypical ductal hyperplasia of the breast: clonal proliferation with loss of heterozygosity on chromosomes 16q and 17p', *J Clin Pathol,* 48(7), pp. 611-5.

Lapierre, M., Siegfried, G., Scamuffa, N., Bontemps, Y., Calvo, F., Seidah, N. G. and Khatib, A. M. (2007) 'Opposing function of the proprotein convertases furin and PACE4 on breast cancer cells' malignant phenotypes: role of tissue inhibitors of metalloproteinase-1', *Cancer Res,* 67(19), pp. 9030-4.

Leak, T. S., Keene, K. L., Langefeld, C. D., Gallagher, C. J., Mychaleckyj, J. C., Freedman, B. I., Bowden, D. W., Rich, S. S. and Sale, M. M. (2007) 'Association of the proprotein convertase subtilisin/kexin-type 2 (PCSK2) gene with type 2 diabetes in an African American population', *Molecular Genetics and Metabolism,* 92(1), pp. 145-150.

Lee, R., Kermani, P., Teng, K. K. and Hempstead, B. L. (2001) 'Regulation of cell survival by secreted proneurotrophins', *Science,* 294(5548), pp. 1945-8.

Leonard, G. D. and Swain, S. M. (2004) 'Ductal carcinoma in situ, complexities and challenges', *J Natl Cancer Inst,* 96(12), pp. 906-20.

Lerman, M. I. and Minna, J. D. (2000) 'The 630-kb lung cancer homozygous deletion region on human chromosome 3p21. 3: identification and evaluation of the resident candidate tumor suppressor genes', *Cancer research,* 60(21), pp. 6116-6133.

Leung, R. K. and Whittaker, P. A. (2005) 'RNA interference: from gene silencing to gene-specific therapeutics', *Pharmacol Ther,* 107(2), pp. 222-39.

Levy, E., Ouadda, A. B. D., Spahis, S., Sane, A. T., Garofalo, C., Grenier, É., Emonnot, L., Yara, S., Couture, P., Beaulieu, J.-F., Ménard, D., Seidah, N. G. and Elchebly, M. (2013) 'PCSK9 plays a significant role in cholesterol homeostasis and lipid transport in intestinal epithelial cells', *Atherosclerosis,* 227(2), pp. 297-306.

Liang, C. C., Park, A. Y. and Guan, J. L. (2007) 'In vitro scratch assay: a convenient and inexpensive method for analysis of cell migration in vitro', *Nat Protoc,* 2(2), pp. 329-33.

Lim, L. Y., Vidnovic, N., Ellisen, L. W. and Leong, C. O. (2009) 'Mutant p53 mediates survival of breast cancer cells', *Br J Cancer,* 101(9), pp. 1606-12.

Lin, Y. E., Wu, Q. N., Lin, X. D., Li, G. Q. and Zhang, Y. J. (2015) 'Expression of paired basic amino acid-cleaving enzyme 4 (PACE4) correlated with prognosis in non-small cell lung cancer (NSCLC) patients', *J Thorac Dis,* 7(5), pp. 850-60.

Liu, L. L., Zhao, H., Ma, T. F., Ge, F., Chen, C. S. and Zhang, Y. P. (2015) 'Identification of valid reference genes for the normalization of RT-qPCR expression studies in human breast cancer cell lines treated with and without transient transfection', *PLoS One,* 10(1), pp. e0117058.

Liu, X., Wang, Y., Yang, W., Guan, Z., Yu, W. and Liao, D. J. (2016) 'Protein multiplicity can lead to misconduct in western blotting and misinterpretation of immunohistochemical staining results, creating much conflicting data', *Prog Histochem Cytochem,* 51(3-4), pp. 51-58.

Loginov, V., Khodyrev, D., Pronina, I., Malyukova, A., Kazubskaya, T., Ermilova, V., Gar'kavtseva, R., Zabarovskii, E. and Braga, E. (2009) 'Two CpG islands in the SEMA3B gene: Methylation in clear cell renal cell carcinoma', *Molecular biology,* 43(6), pp. 1014-1018.

Loginov, V. I., Dmitriev, A. A., Senchenko, V. N., Pronina, I. V., Khodyrev, D. S., Kudryavtseva, A. V., Krasnov, G. S., Gerashchenko, G. V., Chashchina, L. I., Kazubskaya, T. P., Kondratieva, T. T., Lerman, M. I., Angeloni, D., Braga, E. A. and Kashuba, V. I. (2015) 'Tumor Suppressor Function of the SEMA3B Gene in Human Lung and Renal Cancers', *PLoS One,* 10(5), pp. e0123369.

Lopez-Otin, C. and Bond, J. S. (2008) 'Proteases: multifunctional enzymes in life and disease', *J Biol Chem,* 283(45), pp. 30433-7.

Lopez de Cicco, R., Bassi, D. E., Page, R. and Klein-Szanto, A. J. (2002) 'Furin expression in squamous cell carcinomas of the oral cavity and other sites evaluated by tissue microarray technology', *Acta Odontol Latinoam,* 15(1-2), pp. 29-37.

Luchino, J., Hocine, M., Amoureux, M. C., Gibert, B., Bernet, A., Royet, A., Treilleux, I., Lecine, P., Borg, J. P., Mehlen, P., Chauvet, S. and Mann, F. (2013) 'Semaphorin 3E suppresses tumor cell death triggered by the plexin D1 dependence receptor in metastatic breast cancers', *Cancer Cell,* 24(5), pp. 673-85.

Lusson, J., Vieau, D., Hamelin, J., Day, R., Chretien, M. and Seidah, N. G. (1993) 'cDNA structure of the mouse and rat subtilisin/kexin-like PC5: a candidate proprotein convertase expressed in endocrine and nonendocrine cells', *Proc Natl Acad Sci U S A,* 90(14), pp. 6691-5.

Mahittikorn, A., Wickert, H. and Sukthana, Y. (2005) 'Comparison of five DNA extraction methods and optimization of a b1 gene nested PCR (nPCR) for detection of Toxoplasma gondii tissue cyst in mouse brain', *Southeast Asian J Trop Med Public Health,* 36(6), pp. 1377-82.

Mahloogi, H., Bassi, D. E. and Klein-Szanto, A. J. (2002) 'Malignant conversion of non-tumorigenic murine skin keratinocytes overexpressing PACE4', *Carcinogenesis,* 23(4), pp. 565-72.

Mahmood, T. and Yang, P. C. (2012) 'Western blot: technique, theory, and trouble shooting', *N Am J Med Sci,* 4(9), pp. 429-34.

Mains, R. E., Berard, C. A., Denault, J. B., Zhou, A., Johnson, R. C. and Leduc, R. (1997) 'PACE4: a subtilisin-like endoprotease with unique properties', *Biochem J,* 321 (Pt 3), pp. 587-93.

Makinen, T., Olofsson, B., Karpanen, T., Hellman, U., Soker, S., Klagsbrun, M., Eriksson, U. and Alitalo, K. (1999) 'Differential binding of vascular endothelial growth factor B splice and proteolytic isoforms to neuropilin-1', *J Biol Chem,* 274(30), pp. 21217-22.

Malfait, A.-M., Seymour, A. B., Gao, F., Tortorella, M. D., Le Graverand-Gastineau, M.-P. H., Wood, L. S., Doherty, M., Doherty, S., Zhang, W., Arden, N. K., Vaughn, F. L., Leaverton, P. E., Spector, T. D., Hart, D. J., Maciewicz, R. A., Muir, K. R., Das, R., Sorge, R. E., Sotocinal, S. G., Schorscher-Petcu, A., Valdes, A. M. and Mogil, J. S. (2012) 'A role for PACE4 in osteoarthritis pain: evidence from human genetic association and null mutant phenotype', *Annals of the rheumatic diseases,* 71(6), pp. 1042-1048.

Maquoi, E., Noel, A., Frankenne, F., Angliker, H., Murphy, G. and Foidart, J. M. (1998) 'Inhibition of matrix metalloproteinase 2 maturation and HT1080 invasiveness by a synthetic furin inhibitor', *FEBS Lett,* 424(3), pp. 262-6.

Martín-Satué, M. and Blanco, J. (1999) 'Identification of semaphorin E gene expression in metastatic human lung adenocarcinoma cells by mRNA differential display', *Journal of surgical oncology,* 72(1), pp. 18-23.

Mbikay, M., Sirois, F., Yao, J., Seidah, N. G. and Chrétien, M. (1997) 'Comparative analysis of expression of the proprotein convertases furin, PACE4, PC1 and PC2 in human lung tumours', *British journal of cancer,* 75(10), pp. 1509-1514.

Mercapide, J., Lopez De Cicco, R., Bassi, D. E., Castresana, J. S., Thomas, G. and Klein-Szanto, A. J. P. (2002) 'Inhibition of furin-mediated processing results in suppression of astrocytoma cell growth and invasiveness', *Clin Cancer Res,* 8(6), pp. 1740-6.

Migdal, M., Huppertz, B., Tessler, S., Comforti, A., Shibuya, M., Reich, R., Baumann, H. and Neufeld, G. (1998) 'Neuropilin-1 is a placenta growth factor-2 receptor', *Journal of Biological Chemistry,* 273(35), pp. 22272-22278.

Miller, F. R., Santner, S. J., Tait, L. and Dawson, P. J. (2000) 'MCF10DCIS.com xenograft model of human comedo ductal carcinoma in situ', *J Natl Cancer Inst,* 92(14), pp. 1185-6.

Mitsui, N., Inatome, R., Takahashi, S., Goshima, Y., Yamamura, H. and Yanagi, S. (2002) 'Involvement of Fes/Fps tyrosine kinase in semaphorin3A signaling', *EMBO J,* 21(13), pp. 3274-85.

Mojic, M., Takeda, K. and Hayakawa, Y. (2017) 'The Dark Side of IFN-gamma: Its Role in Promoting Cancer Immunoevasion', *Int J Mol Sci,* 19(1).

Mori, K., Imamaki, A., Nagata, K., Yonetomi, Y., Kiyokage-Yoshimoto, R., Martin, T. J., Gillespie, M. T., Nagahama, M., Tsuji, A. and Matsuda, Y. (1999) 'Subtilisin-like proprotein convertases, PACE4 and PC8, as well as furin, are endogenous proalbumin convertases in HepG2 cells', *J Biochem,* 125(3), pp. 627-33.

Munzer, J. S., Basak, A., Zhong, M., Mamarbachi, A., Hamelin, J., Savaria, D., Lazure, C., Hendy, G. N., Benjannet, S., Chretien, M. and Seidah, N. G. (1997) 'In vitro characterization of the novel proprotein convertase PC7', *J Biol Chem,* 272(32), pp. 19672-81.

Nagahama, M., Taniguchi, T., Hashimoto, E., Imamaki, A., Mori, K., Tsuji, A. and Matsuda, Y. (1998) 'Biosynthetic processing and quaternary interactions of proprotein convertase SPC4 (PACE4)', *FEBS Lett,* 434(1-2), pp. 155-9.

Nair, P. N., McArdle, L., Cornell, J., Cohn, S. L. and Stallings, R. L. (2007) 'High-resolution analysis of 3p deletion in neuroblastoma and differential methylation of the SEMA3B tumor suppressor gene', *Cancer Genet Cytogenet,* 174(2), pp. 100-10.

Nakagawa, T., Murakami, K. and Nakayama, K. (1993) 'Identification of an isoform with an extremely large Cys-rich region of PC6, a Kex2-like processing endoprotease', *FEBS Lett,* 327(2), pp. 165-71.

Nakamura, F. and Goshima, Y. (2002) 'Structural and functional relation of neuropilins', *Adv Exp Med Biol,* 515, pp. 55-69.

Nasarre, P., Gemmill, R. M. and Drabkin, H. A. (2014) 'The emerging role of class-3 semaphorins and their neuropilin receptors in oncology', *OncoTargets and therapy,* 7, pp. 1663.

Nasarre, P., Kusy, S., Constantin, B., Castellani, V., Drabkin, H. A., Bagnard, D. and Roche, J. (2005) 'Semaphorin SEMA3F has a repulsing activity on breast cancer cells and inhibits E-cadherin-mediated cell adhesion', *Neoplasia,* 7(2), pp. 180-9.

Nawabi, H., Briancon-Marjollet, A., Clark, C., Sanyas, I., Takamatsu, H., Okuno, T., Kumanogoh, A., Bozon, M., Takeshima, K., Yoshida, Y., Moret, F., Abouzid, K. and Castellani, V. (2010) 'A midline switch of receptor processing regulates commissural axon guidance in vertebrates', *Genes Dev,* 24(4), pp. 396-410.

Nelson, E. R., Chang, C.-y. and McDonnell, D. P. (2014) 'Cholesterol and breast cancer pathophysiology', *Trends in endocrinology and metabolism: TEM,* 25(12), pp. 649-655.

Neufeld, G., Shraga-Heled, N., Lange, T., Guttmann-Raviv, N., Herzog, Y. and Kessler, O. (2005) 'Semaphorins in cancer', *Front Biosci,* 10, pp. 751-60.

Neve, R. M., Chin, K., Fridlyand, J., Yeh, J., Baehner, F. L., Fevr, T., Clark, L., Bayani, N., Coppe, J. P., Tong, F., Speed, T., Spellman, P. T., DeVries, S., Lapuk, A., Wang, N. J., Kuo, W. L., Stilwell, J. L., Pinkel, D., Albertson, D. G., Waldman, F. M., McCormick, F., Dickson, R. B., Johnson, M. D., Lippman, M., Ethier, S., Gazdar, A. and Gray, J. W. (2006) 'A collection of breast cancer cell lines for the study of functionally distinct cancer subtypes', *Cancer Cell,* 10(6), pp. 515-27.

Nguyen, H., Ivanova, V. S., Kavandi, L., Rodriguez, G. C., Maxwell, G. L. and Syed, V. (2011) 'Progesterone and 1,25-dihydroxyvitamin D(3) inhibit endometrial cancer cell growth by upregulating semaphorin 3B and semaphorin 3F', *Mol Cancer Res,* 9(11), pp. 1479-92.

Nicolini, A., Carpi, A. and Rossi, G. (2006) 'Cytokines in breast cancer', *Cytokine Growth Factor Rev,* 17(5), pp. 325-37.

Niwa, Y., Akamatsu, H., Niwa, H., Sumi, H., Ozaki, Y. and Abe, A. (2001) 'Correlation of tissue and plasma RANTES levels with disease course in patients with breast or cervical cancer', *Clinical cancer research,* 7(2), pp. 285-289.

Nour, N., Mayer, G., Mort, J. S., Salvas, A., Mbikay, M., Morrison, C. J., Overall, C. M. and Seidah, N. G. (2005) 'The cysteine-rich domain of the secreted proprotein convertases PC5A and PACE4 functions as a cell surface anchor and interacts with tissue inhibitors of metalloproteinases', *Molecular biology of the cell,* 16(11), pp. 5215-5226.

Nutter, F., Holen, I., Brown, H. K., Cross, S. S., Evans, C. A., Walker, M., Coleman, R. E., Westbrook, J. A., Selby, P. J., Brown, J. E. and Ottewell, P. D. (2014) 'Different molecular profiles are associated with breast cancer cell homing compared with colonisation of bone: evidence using a novel bone-seeking cell line', *Endocr Relat Cancer,* 21(2), pp. 327-41.

O'Hurley, G., Sjostedt, E., Rahman, A., Li, B., Kampf, C., Ponten, F., Gallagher, W. M. and Lindskog, C. (2014) 'Garbage in, garbage out: a critical evaluation of strategies used for validation of immunohistochemical biomarkers', *Mol Oncol,* 8(4), pp. 783-98.

Ochi, K., Mori, T., Toyama, Y., Nakamura, Y. and Arakawa, H. (2002) 'Identification of semaphorin3B as a direct target of p53', *Neoplasia,* 4(1), pp. 82-87.

Osborne, C. K., Hobbs, K. and Trent, J. M. (1987) 'Biological differences among MCF-7 human breast cancer cell lines from different laboratories', *Breast Cancer Research and Treatment,* 9(2), pp. 111-121.

Page, D. L. and Dupont, W. D. (1990) 'Anatomic markers of human premalignancy and risk of breast cancer', *Cancer,* 66(6 Suppl), pp. 1326-35.

Page, M. J. and Di Cera, E. (2008) 'Serine peptidases: classification, structure and function', *Cell Mol Life Sci,* 65(7-8), pp. 1220-36.

Page, R. E., Klein-Szanto, A. J., Litwin, S., Nicolas, E., Al-Jumaily, R., Alexander, P., Godwin, A. K., Ross, E. A., Schilder, R. J. and Bassi, D. E. (2007) 'Increased expression of the pro-protein convertase furin predicts decreased survival in ovarian cancer', *Cell Oncol,* 29(4), pp. 289-99.

Paleyanda, R. K., Drews, R., Lee, T. K. and Lubon, H. (1997) 'Secretion of human furin into mouse milk', *J Biol Chem,* 272(24), pp. 15270-4.

Pan, Q., Chanthery, Y., Liang, W.-C., Stawicki, S., Mak, J., Rathore, N., Tong, R. K., Kowalski, J., Yee, S. F. and Pacheco, G. (2007) 'Blocking neuropilin-1 function has an additive effect with anti-VEGF to inhibit tumor growth', *Cancer cell,* 11(1), pp. 53-67.

Panet, F., Couture, F., Kwiatkowska, A., Desjardins, R., Guerin, B. and Day, R. (2017) 'PACE4 is an important driver of ZR-75-1 estrogen receptor-positive breast cancer proliferation and tumor progression', *Eur J Cell Biol,* 96(5), pp. 469-475.

Park, K. S., Dubon, M. J. and Gumbiner, B. M. (2015) 'N-cadherin mediates the migration of MCF-10A cells undergoing bone morphogenetic protein 4-mediated epithelial mesenchymal transition', *Tumour Biol,* 36(5), pp. 3549-56.

Parker, M. W., Hellman, L. M., Xu, P., Fried, M. G. and Vander Kooi, C. W. (2010) 'Furin processing of semaphorin 3F determines its anti-angiogenic activity by regulating direct binding and competition for neuropilin', *Biochemistry,* 49(19), pp. 4068-75.

Parker, M. W., Linkugel, A. D. and Vander Kooi, C. W. (2013) 'Effect of C-terminal sequence on competitive semaphorin binding to neuropilin-1', *Journal of molecular biology,* 425(22), pp. 4405-4414.

Pecina-Slaus, N. (2003) 'Tumor suppressor gene E-cadherin and its role in normal and malignant cells', *Cancer Cell Int,* 3(1), pp. 17.

Pinder, S. E. and Ellis, I. O. (2003) 'The diagnosis and management of pre-invasive breast disease: Ductal carcinoma in situ (DCIS) and atypical ductal hyperplasia (ADH) – current definitions and classification', *Breast Cancer Research,* 5(5), pp. 254.

Plaimauer, B., Mohr, G., Wernhart, W., Himmelspach, M., Dorner, F. and Schlokat, U. (2001) ''Shed' furin: mapping of the cleavage determinants and identification of its C-terminus', *Biochem J,* 354(Pt 3), pp. 689-95.

Podvin, S., Wojnicz, A. and Hook, V. (2018) 'Human brain gene expression profiles of the cathepsin V and cathepsin L cysteine proteases, with the PC1/3 and PC2 serine proteases, involved in neuropeptide production', *Heliyon,* 4(7), pp. e00673.

Polgar, L. (2005) 'The catalytic triad of serine peptidases', *Cell Mol Life Sci,* 62(19-20), pp. 2161-72.

Prahst, C., Heroult, M., Lanahan, A. A., Uziel, N., Kessler, O., Shraga-Heled, N., Simons, M., Neufeld, G. and Augustin, H. G. (2008) 'Neuropilin-1-VEGFR-2 complexing requires the PDZ-binding domain of neuropilin-1', *J Biol Chem,* 283(37), pp. 25110-4.

Prat, A., Parker, J. S., Karginova, O., Fan, C., Livasy, C., Herschkowitz, J. I., He, X. and Perou, C. M. (2010) 'Phenotypic and molecular characterization of the claudin-low intrinsic subtype of breast cancer', *Breast Cancer Research,* 12(5), pp. R68.

Pronina, I. V., Loginov, V. I., Burdennyy, A. M., Fridman, M. V., Kazubskaya, T. P., Dmitriev, A. A. and Braga, E. A. (2016) 'Expression and DNA methylation alterations of seven cancer-associated 3p genes and their predicted regulator miRNAs (miR-129-2, miR-9-1) in breast and ovarian cancers', *Gene,* 576(1 Pt 3), pp. 483-91.

Pronina, I. V., Loginov, V. I., Prasolov, V. S., Klimov, E. A., Khodyrev, D. S., Kazubskaia, T. P., Gar'kavtseva, R. F., Sulimova, G. E. and Braga, E. A. (2009) '[Alteration of SEMA3B gene expression levels in epithelial tumors]', *Mol Biol (Mosk),* 43(3), pp. 439-45.

ProteinAtlas, H. Available at: https://www.proteinatlas.org/ 2019).

Qu, Y., Han, B., Yu, Y., Yao, W., Bose, S., Karlan, B. Y., Giuliano, A. E. and Cui, X. (2015) 'Evaluation of MCF10A as a Reliable Model for Normal Human Mammary Epithelial Cells', *PLoS One,* 10(7), pp. e0131285.

Rakha, E. A., El-Sayed, M. E., Green, A. R., Lee, A. H., Robertson, J. F. and Ellis, I. O. (2007) 'Prognostic markers in triple-negative breast cancer', *Cancer,* 109(1), pp. 25-32.

Rehemtulla, A., Dorner, A. J. and Kaufman, R. J. (1992) 'Regulation of PACE propeptide-processing activity: requirement for a post-endoplasmic reticulum compartment and autoproteolytic activation', *Proc Natl Acad Sci U S A,* 89(17), pp. 8235-9.

Rehman, M. and Tamagnone, L. 'Semaphorins in cancer: biological mechanisms and therapeutic approaches'. *Seminars in cell & developmental biology*: Elsevier, 179-189.

Remacle, A. G., Gawlik, K., Golubkov, V. S., Cadwell, G. W., Liddington, R. C., Cieplak, P., Millis, S. Z., Desjardins, R., Routhier, S., Yuan, X. W., Neugebauer, W. A., Day, R. and Strongin, A. Y. (2010) 'Selective and potent furin inhibitors protect cells from anthrax without significant toxicity', *The international journal of biochemistry & cell biology,* 42(6), pp. 987-995.

Ren, L., Wang, X., Dong, Z., Liu, J. and Zhang, S. (2013) 'Bone metastasis from breast cancer involves elevated IL-11 expression and the gp130/STAT3 pathway', *Med Oncol,* 30(3), pp. 634.

Risinger, A. L., Dybdal-Hargreaves, N. F. and Mooberry, S. L. (2015) 'Breast Cancer Cell Lines Exhibit Differential Sensitivities to Microtubule-targeting Drugs Independent of Doubling Time', *Anticancer Res,* 35(11), pp. 5845-50.

Rivenbark, A. G., O'Connor, S. M. and Coleman, W. B. (2013) 'Molecular and cellular heterogeneity in breast cancer: challenges for personalized medicine', *Am J Pathol,* 183(4), pp. 1113-1124.

Rizzolio, S. and Tamagnone, L. (2011) 'Multifaceted role of neuropilins in cancer', *Curr Med Chem,* 18(23), pp. 3563-75.

Rohm, B., Ottemeyer, A., Lohrum, M. and Puschel, A. W. (2000) 'Plexin/neuropilin complexes mediate repulsion by the axonal guidance signal semaphorin 3A', *Mech Dev,* 93(1-2), pp. 95-104.

Rolny, C., Capparuccia, L., Casazza, A., Mazzone, M., Vallario, A., Cignetti, A., Medico, E., Carmeliet, P., Comoglio, P. M. and Tamagnone, L. (2008) 'The tumor suppressor semaphorin 3B triggers a prometastatic program mediated by interleukin 8 and the tumor microenvironment', *J Exp Med,* 205(5), pp. 1155-71.

Roskies, A. L. (1998) 'Dissecting semaphorin signaling', *Neuron,* 21(5), pp. 935-6.

Roth, V. (2006) *Doubling Time Computing, Available from: http://www.doubling-time.com/compute.php* [Website].

Rousselet, E., Benjannet, S., Hamelin, J., Canuel, M. and Seidah, N. G. (2011) 'The proprotein convertase PC7: unique zymogen activation and trafficking pathways', *J Biol Chem,* 286(4), pp. 2728-38.

Rovere, C., Barbero, P., Maoret, J. J., Laburthe, M. and Kitabgi, P. (1998) 'Pro-neurotensin/neuromedin N expression and processing in human colon cancer cell lines', *Biochem Biophys Res Commun,* 246(1), pp. 155-9.

Sabag, A. D., Smolkin, T., Mumblat, Y., Ueffing, M., Kessler, O., Gloeckner, C. J. and Neufeld, G. (2014) 'The role of the plexin-A2 receptor in Sema3A and Sema3B signal transduction', *J Cell Sci,* 127(Pt 24), pp. 5240-52.

Sabat, R., Grutz, G., Warszawska, K., Kirsch, S., Witte, E., Wolk, K. and Geginat, J. (2010) 'Biology of interleukin-10', *Cytokine Growth Factor Rev,* 21(5), pp. 331-44.

Saito, Y., Oinuma, I., Fujimoto, S. and Negishi, M. (2009) 'Plexin-B1 is a GTPase activating protein for M-Ras, remodelling dendrite morphology', *EMBO reports,* 10(6), pp. 614-621.

Sasaki, J., Geletzke, A., Kass, R. B., Klimberg, V. S., Copeland, E. M. and Bland, K. I. (2018) '5 - Etiology and Management of Benign Breast Disease', in Bland, K.I., Copeland, E.M., Klimberg, V.S. & Gradishar, W.J. (eds.) *The Breast (Fifth Edition)*: Elsevier, pp. 79-92.e5.

Scamuffa, N., Calvo, F., Chretien, M., Seidah, N. G. and Khatib, A. M. (2006) 'Proprotein convertases: lessons from knockouts', *Faseb j,* 20(12), pp. 1954-63.

Schalken, J. A., Roebroek, A. J., Oomen, P. P., Wagenaar, S. S., Debruyne, F. M., Bloemers, H. P. and Van de Ven, W. J. (1987) 'fur gene expression as a discriminating marker for small cell and nonsmall cell lung carcinomas', *J Clin Invest,* 80(6), pp. 1545-9.

Schnitt, S. J. (2003) 'Benign breast disease and breast cancer risk: morphology and beyond', *Am J Surg Pathol,* 27(6), pp. 836-41.

Schulz, R. and Schlüter, K.-D. (2017) 'PCSK9 targets important for lipid metabolism', *Clinical research in cardiology supplements,* 12(Suppl 1), pp. 2-11.

Scully, O. J., Bay, B. H., Yip, G. and Yu, Y. (2012) 'Breast cancer metastasis', *Cancer Genomics Proteomics,* 9(5), pp. 311-20.

Segarra, M., Ohnuki, H., Maric, D., Salvucci, O., Hou, X., Kumar, A., Li, X. and Tosato, G. (2012) 'Semaphorin 6A regulates angiogenesis by modulating VEGF signaling', *Blood,* 120(19), pp. 4104-15.

Seidah, N. G. (2017) 'The PCSK9 revolution and the potential of PCSK9-based therapies to reduce LDL-cholesterol', *Global cardiology science & practice,* 2017(1).

Seidah, N. G., Awan, Z., Chretien, M. and Mbikay, M. (2014) 'PCSK9: a key modulator of cardiovascular health', *Circ Res,* 114(6), pp. 1022-36.

Seidah, N. G., Benjannet, S., Wickham, L., Marcinkiewicz, J., Jasmin, S. B., Stifani, S., Basak, A., Prat, A. and Chretien, M. (2003) 'The secretory proprotein convertase neural apoptosis-regulated convertase 1 (NARC-1): liver regeneration and neuronal differentiation', *Proc Natl Acad Sci U S A,* 100(3), pp. 928-33.

Seidah, N. G. and Chrétien, M. (1999) 'Proprotein and prohormone convertases: a family of subtilases generating diverse bioactive polypeptides1Published on the World Wide Web on 17 August 1999.1', *Brain Research,* 848(1), pp. 45-62.

Seidah, N. G., Day, R., Marcinkiewicz, M. and Chretien, M. (1998) 'Precursor convertases: an evolutionary ancient, cell-specific, combinatorial mechanism yielding diverse bioactive peptides and proteins', *Annals of the New York Academy of Sciences,* 839(1), pp. 9-24.

Seidah, N. G., Marcinkiewicz, M., Benjannet, S., Gaspar, L., Beaubien, G., Mattei, M. G., Lazure, C., Mbikay, M. and Chretien, M. (1991) 'Cloning and primary sequence of a mouse candidate prohormone convertase PC1 homologous to PC2, Furin, and Kex2: distinct chromosomal localization and messenger RNA distribution in brain and pituitary compared to PC2', *Mol Endocrinol,* 5(1), pp. 111-22.

Seidah, N. G., Mayer, G., Zaid, A., Rousselet, E., Nassoury, N., Poirier, S., Essalmani, R. and Prat, A. (2008) 'The activation and physiological functions of the proprotein convertases', *Int J Biochem Cell Biol,* 40(6-7), pp. 1111-25.

Seidah, N. G., Mowla, S. J., Hamelin, J., Mamarbachi, A. M., Benjannet, S., Toure, B. B., Basak, A., Munzer, J. S., Marcinkiewicz, J., Zhong, M., Barale, J. C., Lazure, C., Murphy, R. A., Chretien, M. and Marcinkiewicz, M. (1999) 'Mammalian subtilisin/kexin isozyme SKI-1: A widely expressed proprotein convertase with a unique cleavage specificity and cellular localization', *Proc Natl Acad Sci U S A,* 96(4), pp. 1321-6.

Seidah, N. G. and Prat, A. (2012) 'The biology and therapeutic targeting of the proprotein convertases', *Nat Rev Drug Discov,* 11(5), pp. 367-83.

Seidah, N. G., Sadr, M. S., Chretien, M. and Mbikay, M. (2013) 'The multifaceted proprotein convertases: their unique, redundant, complementary, and opposite functions', *J Biol Chem,* 288(30), pp. 21473-81.

Sekido, Y., Bader, S., Latif, F., Chen, J. Y., Duh, F. M., Wei, M. H., Albanesi, J. P., Lee, C. C., Lerman, M. I. and Minna, J. D. (1996) 'Human semaphorins A(V) and IV reside in the 3p21.3 small cell lung cancer deletion region and demonstrate distinct expression patterns', *Proc Natl Acad Sci U S A,* 93(9), pp. 4120-5.

Senchenko, V. N., Liu, J., Loginov, W., Bazov, I., Angeloni, D., Seryogin, Y., Ermilova, V., Kazubskaya, T., Garkavtseva, R., Zabarovska, V. I., Kashuba, V. I., Kisselev, L. L., Minna, J. D., Lerman, M. I., Klein, G., Braga, E. A. and Zabarovsky, E. R. (2004) 'Discovery of frequent homozygous deletions in chromosome 3p21.3 LUCA and AP20 regions in renal, lung and breast carcinomas', *Oncogene,* 23(34), pp. 5719-28.

Serini, G., Valdembri, D., Zanivan, S., Morterra, G., Burkhardt, C., Caccavari, F., Zammataro, L., Primo, L., Tamagnone, L., Logan, M., Tessier-Lavigne, M., Taniguchi, M., Puschel, A. W. and Bussolino, F. (2003) 'Class 3 semaphorins control vascular morphogenesis by inhibiting integrin function', *Nature,* 424(6947), pp. 391-7.

Seyfried, T. N. and Huysentruyt, L. C. (2013) 'On the origin of cancer metastasis', *Critical reviews in oncogenesis,* 18(1-2), pp. 43-73.

Shahi, P., Wang, C. Y., Chou, J., Hagerling, C., Gonzalez Velozo, H., Ruderisch, A., Yu, Y., Lai, M. D. and Werb, Z. (2017) 'GATA3 targets semaphorin 3B in mammary epithelial cells to suppress breast cancer progression and metastasis', *Oncogene,* 36(40), pp. 5567-5575.

Shim, S.-O., Cafferty, W. B., Schmidt, E. C., Kim, B. G., Fujisawa, H. and Strittmatter, S. M. (2012) 'PlexinA2 limits recovery from corticospinal axotomy by mediating oligodendrocyte-derived Sema6A growth inhibition', *Molecular and Cellular Neuroscience,* 50(2), pp. 193-200.

Siegfried, G., Basak, A., Cromlish, J. A., Benjannet, S., Marcinkiewicz, J., Chretien, M., Seidah, N. G. and Khatib, A. M. (2003) 'The secretory proprotein convertases furin, PC5, and PC7 activate VEGF-C to induce tumorigenesis', *J Clin Invest,* 111(11), pp. 1723-32.

Simpson, J. F. (2009) 'Update on atypical epithelial hyperplasia and ductal carcinoma in situ', *Pathology,* 41(1), pp. 36-9.

Singh, H., Heng, S., Nicholls, P. K., Li, Y., Tai, L. T., Jobling, T., Salamonsen, L. A. and Nie, G. (2012) 'Proprotein convertases in post-menopausal endometrial cancer: distinctive regulation and non-invasive diagnosis', *Biochem Biophys Res Commun,* 419(4), pp. 809-14.

Singhai, R., Patil, V. W., Jaiswal, S. R., Patil, S. D., Tayade, M. B. and Patil, A. V. (2011) 'E-Cadherin as a diagnostic biomarker in breast cancer', *N Am J Med Sci,* 3(5), pp. 227-33.

Smith, C. J. and Osborn, A. M. (2009) 'Advantages and limitations of quantitative PCR (Q-PCR)-based approaches in microbial ecology', *FEMS Microbiol Ecol,* 67(1), pp. 6-20.

Soule, H. D., Maloney, T. M., Wolman, S. R., Peterson, W. D., Jr., Brenz, R., McGrath, C. M., Russo, J., Pauley, R. J., Jones, R. F. and Brooks, S. C. (1990) 'Isolation and characterization of a spontaneously immortalized human breast epithelial cell line, MCF-10', *Cancer Res,* 50(18), pp. 6075-86.

Staton, C. A. (2011) 'Class 3 semaphorins and their receptors in physiological and pathological angiogenesis', *Biochemical Society Transactions,* 39(6), pp. 1565.

Staton, C. A., Reed, M. W. R. and Brown, N. J. (2009) 'A critical analysis of current in vitro and in vivo angiogenesis assays', *International journal of experimental pathology,* 90(3), pp. 195-221.

Staton, C. A., Shaw, L. A., Valluru, M., Hoh, L., Koay, I., Cross, S. S., Reed, M. W. and Brown, N. J. (2011) 'Expression of class 3 semaphorins and their receptors in human breast neoplasia', *Histopathology,* 59(2), pp. 274-82.

Stijnen, P., Ramos-Molina, B., O'Rahilly, S. and Creemers, J. W. (2016) 'PCSK1 Mutations and Human Endocrinopathies: From Obesity to Gastrointestinal Disorders', *Endocr Rev,* 37(4), pp. 347-71.

Sun, X., Essalmani, R., Day, R., Khatib, A. M., Seidah, N. G. and Prat, A. (2012) 'Proprotein convertase subtilisin/kexin type 9 deficiency reduces melanoma metastasis in liver', *Neoplasia,* 14(12), pp. 1122-31.

Sun, X., Essalmani, R., Seidah, N. G. and Prat, A. (2009) 'The proprotein convertase PC5/6 is protective against intestinal tumorigenesis: in vivo mouse model', *Mol Cancer,* 8, pp. 73.

Sun, Y.-S., Zhao, Z., Yang, Z.-N., Xu, F., Lu, H.-J., Zhu, Z.-Y., Shi, W., Jiang, J., Yao, P.-P. and Zhu, H.-P. (2017) 'Risk Factors and Preventions of Breast Cancer', *International journal of biological sciences,* 13(11), pp. 1387-1397.

Suzuki, K., Okuno, T., Yamamoto, M., Pasterkamp, R. J., Takegahara, N., Takamatsu, H., Kitao, T., Takagi, J., Rennert, P. D., Kolodkin, A. L., Kumanogoh, A. and Kikutani, H. (2007) 'Semaphorin 7A initiates T-cell-mediated inflammatory responses through alpha1beta1 integrin', *Nature,* 446(7136), pp. 680-4.

Takahashi, T., Fournier, A., Nakamura, F., Wang, L. H., Murakami, Y., Kalb, R. G., Fujisawa, H. and Strittmatter, S. M. (1999) 'Plexin-neuropilin-1 complexes form functional semaphorin-3A receptors', *Cell,* 99(1), pp. 59-69.

Tamagnone, L., Artigiani, S., Chen, H., He, Z., Ming, G.-l., Song, H.-j., Chedotal, A., Winberg, M. L., Goodman, C. S. and Poo, M.-m. (1999) 'Plexins are a large family of receptors for transmembrane, secreted, and GPI-anchored semaphorins in vertebrates', *Cell,* 99(1), pp. 71-80.

Tang, H., Wu, Y., Liu, M., Qin, Y., Wang, H., Wang, L., Li, S., Zhu, H., He, Z., Luo, J., Wang, H., Wang, Q. and Luo, S. (2016) 'SEMA3B improves the survival of patients with esophageal squamous cell carcinoma by upregulating p53 and p21', *Oncol Rep,* 36(2), pp. 900-8.

Tani, Y., Tateno, T., Izumiyama, H., Doi, M., Yoshimoto, T. and Hirata, Y. (2008) 'Defective expression of prohormone convertase 4 and enhanced expression of insulin-like growth factor II by pleural solitary fibrous tumor causing hypoglycemia', *Endocr J,* 55(5), pp. 905-11.

Tazaki, E., Shishido-Hara, Y., Mizutani, N., Nomura, S., Isaka, H., Ito, H., Imi, K., Imoto, S. and Kamma, H. (2013) 'Histopathological and clonal study of combined lobular and ductal carcinoma of the breast', *Pathol Int,* 63(6), pp. 297-304.

Tellier, E., Nègre-Salvayre, A., Bocquet, B., Itohara, S., Hannun, Y. A., Salvayre, R. and Augé, N. (2007) 'Role for furin in tumor necrosis factor alpha-induced activation of the matrix metalloproteinase/sphingolipid mitogenic pathway', *Mol Cell Biol,* 27(8), pp. 2997-3007.

Thomas, R. L., Crawford, N. M., Grafer, C. M. and Halvorson, L. M. (2013) 'Pituitary adenylate cyclase-activating polypeptide (PACAP) in the hypothalamic-pituitary-gonadal axis: a review of the literature', *Reprod Sci,* 20(8), pp. 857-71.

Tian, S. and Jianhua, W. (2010) 'Comparative study of the binding pockets of mammalian proprotein convertases and its implications for the design of specific small molecule inhibitors', *International journal of biological sciences,* 6(1), pp. 89-95.

Todorovic-Rakovic, N. and Milovanovic, J. (2013) 'Interleukin-8 in breast cancer progression', *J Interferon Cytokine Res,* 33(10), pp. 563-70.

Toledano, S., Nir-Zvi, I., Engelman, R., Kessler, O. and Neufeld, G. (2019) 'Class-3 Semaphorins and Their Receptors: Potent Multifunctional Modulators of Tumor Progression', *International journal of molecular sciences,* 20(3), pp. 556.

Tomizawa, Y., Sekido, Y., Kondo, M., Gao, B., Yokota, J., Roche, J., Drabkin, H., Lerman, M. I., Gazdar, A. F. and Minna, J. D. (2001) 'Inhibition of lung cancer cell growth and induction of apoptosis after reexpression of 3p21.3 candidate tumor suppressor gene SEMA3B', *Proc Natl Acad Sci U S A,* 98(24), pp. 13954-9.

Tse, C., Xiang, R. H., Bracht, T. and Naylor, S. L. (2002) 'Human Semaphorin 3B (SEMA3B) located at chromosome 3p21.3 suppresses tumor formation in an adenocarcinoma cell line', *Cancer Res,* 62(2), pp. 542-6.

Tseng, C. H., Murray, K. D., Jou, M. F., Hsu, S. M., Cheng, H. J. and Huang, P. H. (2011) 'Sema3E/plexin-D1 mediated epithelial-to-mesenchymal transition in ovarian endometrioid cancer', *PLoS One,* 6(4), pp. e19396.

Tsuji, A., Hashimoto, E., Ikoma, T., Taniguchi, T., Mori, R., Nagahama, M. and Matsuda, Y. (1999) 'Inactivation of Proprotein Convertase, PACE4, by α1-Antitrypsin Portland (α1-PDX), a Blocker of Proteolytic Activation of Bone Morphogenetic Protein during Embryogenesis: Evidence That PACE4 Is Able to Form an SDS-Stable Acyl Intermediate with α1-PDX1', *The Journal of Biochemistry,* 126(3), pp. 591-603.

Tzimas, G. N., Chevet, E., Jenna, S., Nguyen, D. T., Khatib, A. M., Marcus, V., Zhang, Y., Chretien, M., Seidah, N. and Metrakos, P. (2005) 'Abnormal expression and processing of the proprotein convertases PC1 and PC2 in human colorectal liver metastases', *BMC Cancer,* 5, pp. 149.

Uhlen, M., Bandrowski, A., Carr, S., Edwards, A., Ellenberg, J., Lundberg, E., Rimm, D. L., Rodriguez, H., Hiltke, T., Snyder, M. and Yamamoto, T. (2016) 'A proposal for validation of antibodies', *Nat Methods,* 13(10), pp. 823-7.

UniProt. Available at: https://www.uniprot.org/uniprot/Q6UW60 2019).

Varshavsky, A., Kessler, O., Abramovitch, S., Kigel, B., Zaffryar, S., Akiri, G. and Neufeld, G. (2008) 'Semaphorin-3B is an angiogenesis inhibitor that is inactivated by furin-like pro-protein convertases', *Cancer Res,* 68(17), pp. 6922-31.

Venetsanakos, E., Beckman, I., Bradley, J. and Skinner, J. M. (1997) 'High incidence of interleukin 10 mRNA but not interleukin 2 mRNA detected in human breast tumours', *British journal of cancer,* 75(12), pp. 1826-1830.

Verweij, J. and Pinedo, H. M. (1990) 'Mitomycin C: mechanism of action, usefulness and limitations', *Anticancer Drugs,* 1(1), pp. 5-13.

Vollenweider, F., Benjannet, S., Decroly, E., Savaria, D., Lazure, C., Thomas, G., Chretien, M. and Seidah, N. G. (1996) 'Comparative cellular processing of the human immunodeficiency virus (HIV-1) envelope glycoprotein gp160 by the mammalian subtilisin/kexin-like convertases', *Biochem J,* 314 (Pt 2), pp. 521-32.

Wang, F., Wang, L. and Pan, J. (2015) 'PACE4 regulates proliferation, migration and invasion in human breast cancer MDA-MB-231 cells', *Mol Med Rep,* 11(1), pp. 698-704.

Wang, K., Ling, T., Wu, H. and Zhang, J. (2013) 'Screening of candidate tumor-suppressor genes in 3p21.3 and investigation of the methylation of gene promoters in oral squamous cell carcinoma', *Oncol Rep,* 29(3), pp. 1175-82.

Wang, L., Zeng, H., Wang, P., Soker, S. and Mukhopadhyay, D. (2003) 'Neuropilin-1-mediated vascular permeability factor/vascular endothelial growth factor-dependent endothelial cell migration', *J Biol Chem,* 278(49), pp. 48848-60.

Waugh, D. J. and Wilson, C. (2008) 'The interleukin-8 pathway in cancer', *Clin Cancer Res,* 14(21), pp. 6735-41.

Weiss, N., Stegemann, A., Elsayed, M. A. T., Schallreuter, K. U., Luger, T. A., Loser, K., Metze, D., Weishaupt, C. and Bohm, M. (2014) 'Inhibition of the prohormone convertase subtilisin-kexin isoenzyme-1 induces apoptosis in human melanoma cells', *J Invest Dermatol,* 134(1), pp. 168-175.

Wellings, S. R. and Jensen, H. M. (1973) 'On the origin and progression of ductal carcinoma in the human breast', *J Natl Cancer Inst,* 50(5), pp. 1111-8.

Whitaker, G. B., Limberg, B. J. and Rosenbaum, J. S. (2001) 'Vascular endothelial growth factor receptor-2 and neuropilin-1 form a receptor complex that is responsible for the differential signaling potency of VEGF165 and VEGF121', *Journal of Biological Chemistry,* 276(27), pp. 25520-25531.

WHO (2019) *World health organization*. Available at: http://gco.iarc.fr/today/home 2019).

Wicinski, M., Zak, J., Malinowski, B., Popek, G. and Grzesk, G. (2017) 'PCSK9 signaling pathways and their potential importance in clinical practice', *EPMA J,* 8(4), pp. 391-402.

Winberg, M. L., Noordermeer, J. N., Tamagnone, L., Comoglio, P. M., Spriggs, M. K., Tessier-Lavigne, M. and Goodman, C. S. (1998) 'Plexin A is a neuronal semaphorin receptor that controls axon guidance', *Cell,* 95(7), pp. 903-916.

Worzfeld, T. and Offermanns, S. (2014) 'Semaphorins and plexins as therapeutic targets', *Nature Reviews Drug Discovery,* 13, pp. 603.

Xiang, R.-H., Hensel, C. H., Garcia, D. K., Carlson, H. C., Kok, K., Daly, M. C., Kerbacher, K., van den Berg, A., Veldhuis, P. and Buys, C. H. (1996) 'Isolation of the human semaphorin III/F gene (SEMA3F) at chromosome 3p21, a region deleted in lung cancer', *Genomics,* 32(1), pp. 39-48.

Xiong, G., Wang, C., Evers, B. M., Zhou, B. P. and Xu, R. (2012) 'RORalpha suppresses breast tumor invasion by inducing SEMA3F expression', *Cancer Res,* 72(7), pp. 1728-39.

Xu, S., Hoglund, M., Hakansson, L. and Venge, P. (2000) 'Granulocyte colony-stimulating factor (G-CSF) induces the production of cytokines in vivo', *Br J Haematol,* 108(4), pp. 848-53.

Xu, Z., Hurchla, M. A., Deng, H., Uluckan, O., Bu, F., Berdy, A., Eagleton, M. C., Heller, E. A., Floyd, D. H., Dirksen, W. P., Shu, S., Tanaka, Y., Fernandez, S. A., Rosol, T. J. and Weilbaecher, K. N. (2009) 'Interferon-gamma targets cancer cells and osteoclasts to prevent tumor-associated bone loss and bone metastases', *J Biol Chem,* 284(7), pp. 4658-66.

Yang, J., Elias, J. J., Petrakis, N. L., Wellings, S. R. and Nandi, S. (1981) 'Effects of hormones and growth factors on human mammary epithelial cells in collagen gel culture', *Cancer Res,* 41(3), pp. 1021-7.

Yao, C., Lin, Y., Chua, M. S., Ye, C. S., Bi, J., Li, W., Zhu, Y. F. and Wang, S. M. (2007) 'Interleukin-8 modulates growth and invasiveness of estrogen receptor-negative breast cancer cells', *Int J Cancer,* 121(9), pp. 1949-57.

Yazdani, U. and Terman, J. R. (2006) 'The semaphorins', *Genome biology,* 7(3), pp. 211-211.

Yersal, O. and Barutca, S. (2014) 'Biological subtypes of breast cancer: Prognostic and therapeutic implications', *World J Clin Oncol,* 5(3), pp. 412-24.

Yu, E. Z., Burba, A. E. and Gerstein, M. (2007) 'PARE: a tool for comparing protein abundance and mRNA expression data', *BMC Bioinformatics,* 8, pp. 309.

Yu, S., Kim, T., Yoo, K. H. and Kang, K. (2017) 'The T47D cell line is an ideal experimental model to elucidate the progesterone-specific effects of a luminal A subtype of breast cancer', *Biochem Biophys Res Commun,* 486(3), pp. 752-758.

Zancan, P., Sola-Penna, M., Furtado, C. M. and Da Silva, D. (2010) 'Differential expression of phosphofructokinase-1 isoforms correlates with the glycolytic efficiency of breast cancer cells', *Mol Genet Metab,* 100(4), pp. 372-8.

Zhang, J. H., Zhou, D., You, J., Tang, B. S., Li, P. Y. and Tang, S. S. (2013) 'Differential processing of neuropeptide proprotein in human breast adenocarcinoma', *J Endocrinol Invest,* 36(9), pp. 745-52.

Zhao, X. Y., Chen, L., Li, Y. H. and Xu, Q. (2007) 'PlexinA1 expression in gastric carcinoma and its relationship with tumor angiogenesis and proliferation', *World J Gastroenterol,* 13(48), pp. 6558-61.

Zhao, Y., Kong, X., Li, X., Yan, S., Yuan, C., Hu, W. and Yang, Q. (2011) 'Metadherin mediates lipopolysaccharide-induced migration and invasion of breast cancer cells', *PLoS One,* 6(12), pp. e29363.

Zheng, W., Tayyari, F., Gowda, G. A., Raftery, D., McLamore, E. S., Porterfield, D. M., Donkin, S. S., Bequette, B. and Teegarden, D. (2015) 'Altered glucose metabolism in Harvey-ras transformed MCF10A cells', *Mol Carcinog,* 54(2), pp. 111-20.

Zheng, X., Wang, C., Xing, Y., Chen, S., Meng, T., You, H., Ojima, I. and Dong, Y. (2017) 'SB-T-121205, a next-generation taxane, enhances apoptosis and inhibits migration/invasion in MCF-7/PTX cells', *Int J Oncol,* 50(3), pp. 893-902.

Zhou, A., Webb, G., Zhu, X. and Steiner, D. F. (1999) 'Proteolytic processing in the secretory pathway', *J Biol Chem,* 274(30), pp. 20745-8.

Zhou, Y., Gormley, M. J., Hunkapiller, N. M., Kapidzic, M., Stolyarov, Y., Feng, V., Nishida, M., Drake, P. M., Bianco, K. and Wang, F. (2013) 'Reversal of gene dysregulation in cultured cytotrophoblasts reveals possible causes of preeclampsia', *The Journal of clinical investigation,* 123(123 (7)), pp. 2862-2872.

Zhou, Y. and Lindberg, I. (1994) 'Enzymatic properties of carboxyl-terminally truncated prohormone convertase 1 (PC1/SPC3) and evidence for autocatalytic conversion', *J Biol Chem,* 269(28), pp. 18408-13.

Zhu, X. and Lindberg, I. (1995) '7B2 facilitates the maturation of proPC2 in neuroendocrine cells and is required for the expression of enzymatic activity', *The Journal of cell biology,* 129(6), pp. 1641-1650.

Zou, Y., Stoeckli, E., Chen, H. and Tessier-Lavigne, M. (2000) 'Squeezing axons out of the gray matter: a role for slit and semaphorin proteins from midline and ventral spinal cord', *Cell,* 102(3), pp. 363-75.

Appendix

- **Positive control for SEMA3B (Western blot analysis)**

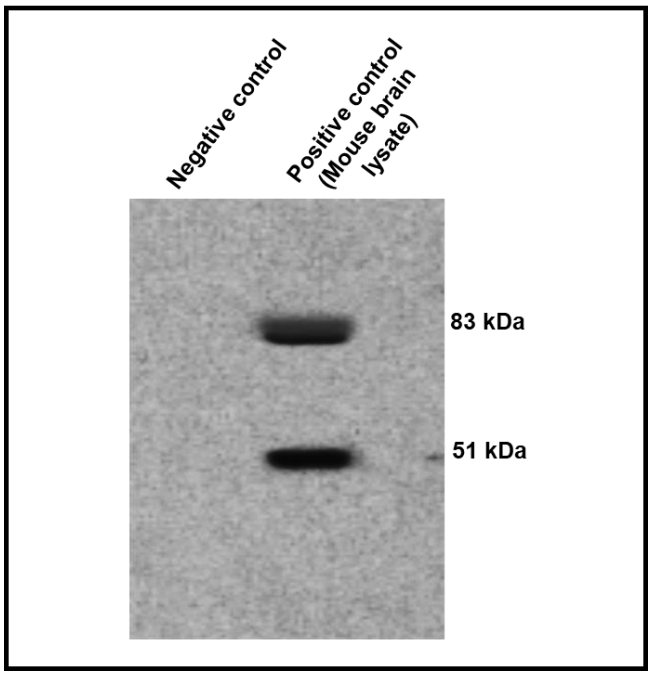

Figure 1: **SEMA3B protein expression in mouse brain lysate.** Mouse brain lysate was separated on a 10% SDS-PAGE gel, and then blotted onto PVDF and probed with the anti-SEMA3B antibody. It was used as a positive control for SEMA3B expression. Negative control is medium only. The size of molecular weight markers are indicated in kDa. Representative immunoblot shown of n=3.

- **Positive tissue controls for immunohistochemistry experiment.**

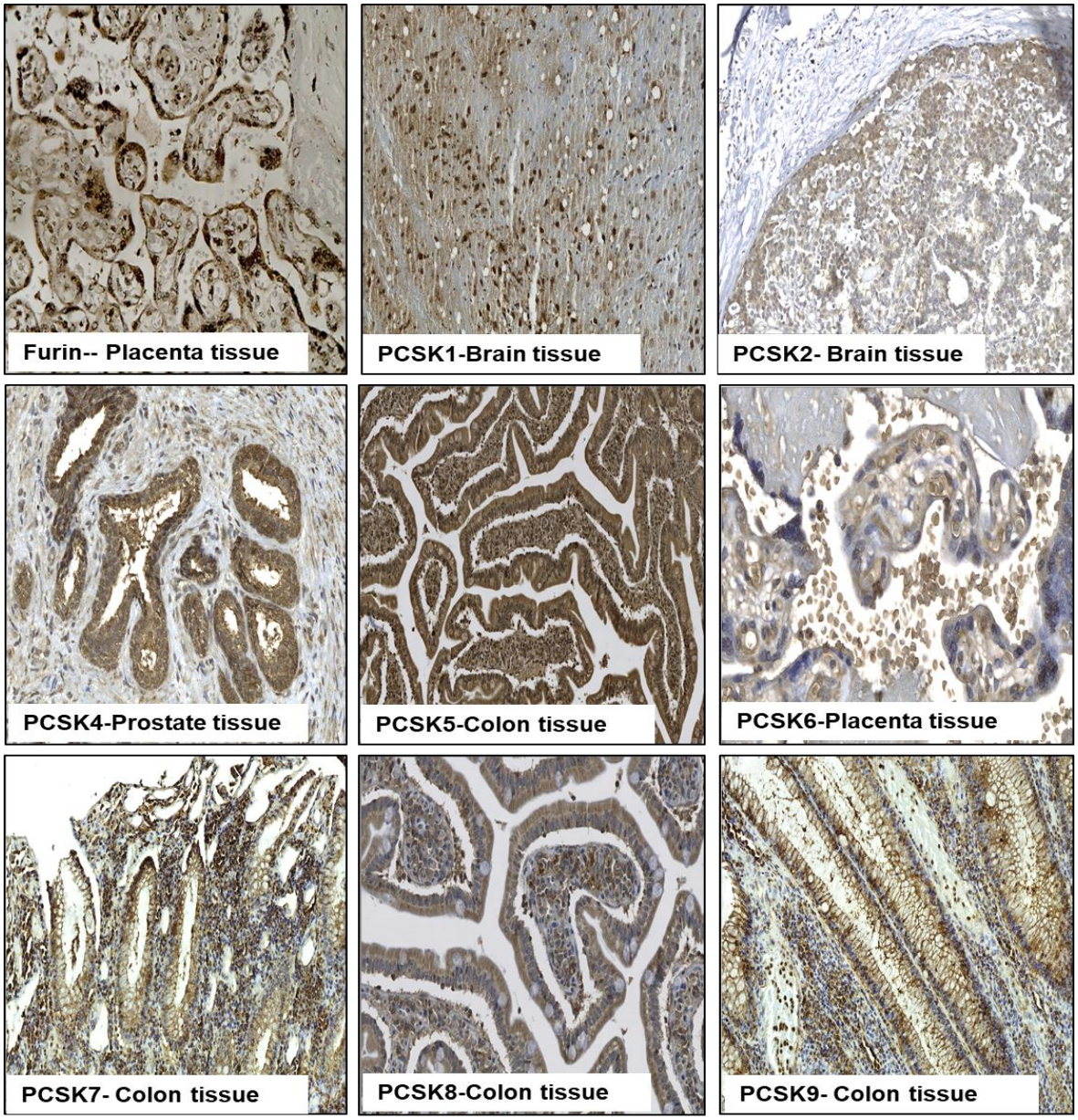

Figure 2: Positive tissue controls used for the IHC assay. The positive tissue controls were used at the same concentration as the experimental antibody for immunohistochemistry staining. Representative photographs of PPCs staining by immunohistochemistry in placenta tissue for furin, mouse brain tissue for PCSK1 and PCSK2, prostate tissue for PCSK4, colon tissue for PCSK5, plasenta tissue for PCSK6, colon tissue for PCSK7,PCSK8 and PCSK9. All images were taken using a x20 objective lens and the scale bar = 200 µm.

- **Isotype controls for immunohistochemistry experiment.**

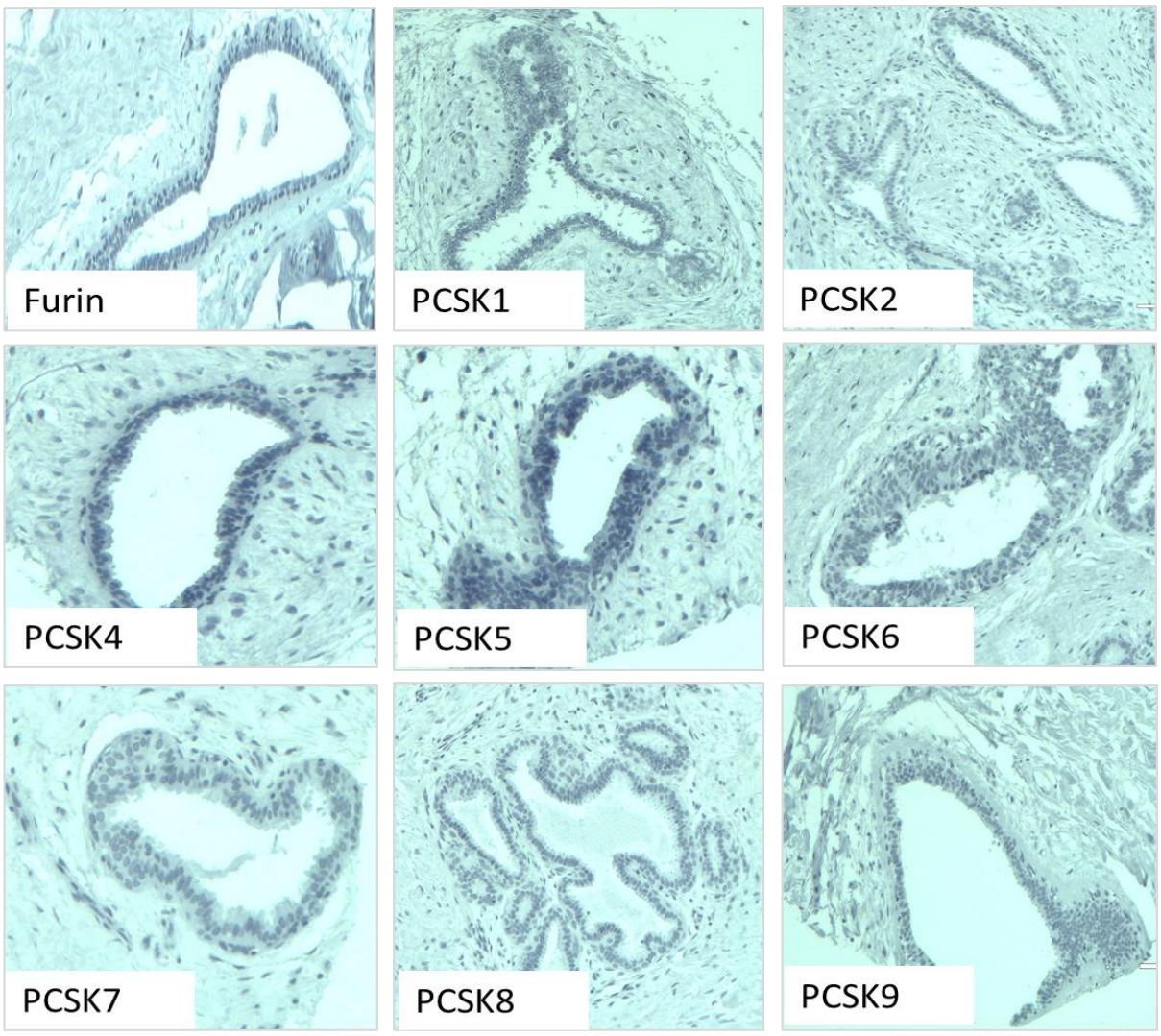

Figure 3: Isotype controls. The isotype controls were used at the same concentration as the experimental antibody for immunohistochemistry staining. Isotype controls did not bind non-specifically to breast tissues; demonstrating antibody binding was specific. Representative photographs of PPCs staining by immunohistochemistry in breast ducts tissues. All images were taken using a x20 objective lens and the scale bar = 200 µm.